

COVID ECONOMICS
VETTED AND REAL-TIME PAPERS

ISSUE 19
18 MAY 2020

SOCIAL DISTANCING BY SECTORS

Martin Bodenstein, Giancarlo Corsetti and
Luca Guerrieri

**THE EFFECT OF CONTAINMENT
MEASURES**

Pragyan Deb, Davide Furceri,
Jonathan D. Ostry and Nour Tawk

IS THE BCG VACCINE A PROTECTION?

Richard Bluhm and Maxim Pinkovskiy

CONSUMER PANIC

Michael Keane and Timothy Neal

CALLING FOR HELP

Marius Brühlhart and Rafael Lalive

**GLOBALIZATION IN THE TIME OF
COVID-19**

Alessandro Sforza and Marina Steininger

WORK FROM HOME: WHICH JOBS?

Maho Hatayama, Mariana Viollaz and
Hernan Winkler

LABOUR MARKET INEQUALITIES

Vincenzo Galasso

Covid Economics

Vetted and Real-Time Papers

Issue 19, 18 May 2020

Contents

Social distancing and supply disruptions in a pandemic <i>Martin Bodenstein, Giancarlo Corsetti and Luca Guerrieri</i>	1
The effect of containment measures on the COVID-19 pandemic <i>Pragyan Deb, Davide Furceri, Jonathan D. Ostry and Nour Tawk</i>	53
The spread of COVID-19 and the BCG vaccine: A natural experiment in reunified Germany <i>Richard Bluhm and Maxim Pinkovskiy</i>	87
Consumer panic in the Covid-19 pandemic <i>Michael Keane and Timothy Neal</i>	115
Daily suffering: Helpline calls during the Covid-19 crisis <i>Marius Brühlhart and Rafael Lalive</i>	143
Globalization in the time of COVID-19 <i>Alessandro Sforza and Marina Steininger</i>	159
Jobs' amenability to working from home: Evidence from skills surveys for 53 countries <i>Maho Hatayama, Mariana Viollaz and Hernan Winkler</i>	211
Covid: Not a great equaliser <i>Vincenzo Galasso</i>	241

Social distancing and supply disruptions in a pandemic¹

Martin Bodenstein,² Giancarlo Corsetti³ and Luca Guerrieri⁴

Date submitted: 13 May 2020; Date accepted: 14 May 2020

Drastic public health measures such as social distancing or lockdowns can reduce the loss of human life by keeping the number of infected individuals from exceeding the capacity of the health care system but are often criticized because of the social and economic costs they entail. We question this view by combining an epidemiological model, calibrated to capture the spread of the COVID-19 virus, with a multisector model, designed to capture key characteristics of the U.S. Input Output Tables. Our two-sector model features a core sector that produces intermediate inputs not easily replaced by inputs from the other sector, subject to minimum-scale requirements. We show that, by affecting workers in this core sector, the high peak of an infection not mitigated by social distancing may cause very large upfront economic costs in terms of output, consumption and investment. Social distancing measures can reduce these costs, especially if skewed towards non-core industries and occupations with tasks that can be performed from home, helping to smooth the surge in infections among workers in the core sector.

¹ The views expressed in this paper are solely the responsibility of the authors and should not be interpreted as reflecting the views of the Board of Governors of the Federal Reserve System or of any other person associated with the Federal Reserve System. We thank Jason Brown and Zeina Hasna for useful suggestions. Giancarlo Corsetti gratefully acknowledges support from Cambridge-INET.

² Chief, Global Modeling Studies, Board of Governors of the Federal Reserve System.

³ Professor of Macroeconomics, Cambridge University and CEPR Research Fellow.

⁴ Economist, Board of Governors of the Federal Reserve System.

Copyright: Martin Bodenstein, Giancarlo Corsetti and Luca Guerrieri

1 Introduction

By the end of March 2020, nearly four months after the first detection of significant coronavirus infections in China, most advanced economies have adopted measures restricting people's movements and activity on their territory, introduced tough controls at their borders, and mandated norms implementing social distancing. If only with some delay, governments have now converged on the idea that some restrictions are required to reduce the human cost of the disease.

The main motivation for public health measures that range from laxer social distancing to lockdowns is that our health care systems are capacity-constrained, and the stress of a surge in the number of infected people will cause mortality rates to rise steeply.¹ Among the many excellent papers articulating this point, [Eichenbaum, Rebelo, and Trabandt \(2020\)](#) shows that, if mortality rates were independent of the number of infected people, the “optimal” lockdown would be gradual and modulated to the spread of the disease. The optimal lockdown is front-loaded otherwise. Moreover, they show that, because of the spillovers of individual health safety decision, mandated measures are desirable even if households take consumption and labor supply decisions trading off economic benefits with the risk of contagion. In the same vein, [Jones, Philippon, and Venkateswaran \(2020\)](#) clarifies that a social planner would worry about two externalities, an infection externality and a healthcare congestion externality. Because of these externalities, the incentives for private agents to undertake action that could mitigate contagion are too weak from a social perspectives—motivating public interventions. In the presence of a constraint the health care sector, [Alvarez, Argente, and Lippi \(2020\)](#) shows that strong measures, which would be especially effective if implemented very early, remain optimal even at an advanced stage of diffusion of the disease. Despite the uncertainty surrounding the parameters driving the dynamic of the disease, discussed by, e.g., [Atkeson \(2020b\)](#), these results appear to be quite robust.²

We consider a different, complementary argument. Without some form of public health restrictions, the random spread of the disease may end up hitting industries and parts of the economy that, directly and indirectly, provide essential inputs to production and/or are essential

¹ A complementary argument from the medical profession is that understanding the effects of a new virus may take some time. It may be advisable to slow down the spread the disease to let medical and pharmaceutical research advance.

² The economic literature on the economic effects of the COVID-19 pandemic is growing very fast. A partial list of recent contributions includes [Alfaro, Chari, Greenland, and Schott \(2020\)](#), [Baker, Bloom, Davis, Kost, Sammon, and Viratyosin \(2020\)](#), [Guerrieri, Lorenzoni, Straub, and Werning \(2020\)](#), and [Koren and Petó \(2020\)](#).

for the economy to run. By incapacitating industries in this “core sector,” an unchecked spread of the disease would result in a steep fall in economic activity. While it may be difficult to identify precisely which specific industries and activities produce essential inputs and services and hence should be included in the core sector, there are some natural choices: distribution services, transportation, sanitation, energy supply, health care services, and food.³ With this list, even if only as a working hypothesis, we can use a macroeconomic model to quantify the implications of a pandemic for overall economic activity, when the disease impairs the core industries. We argue that, in this case, the economic recession can be greatly amplified, because, first, the output of the core sector is not easily substitutable, and, second, the production processes in many industries in this sector may be subject to a minimum-scale requirement for labor—i.e., they require a sufficient number of specialized and not easily substitutable employees to show up for work.

There are at least two key policy-relevant questions related to our argument. The first is whether and how differentiating public health restrictions by sector and occupational tasks could reduce the economic cost. As our baseline, we consider social distancing measures that in each sector require individuals who can continue working from home to do so, and be subject to a lockdown. This lockdown is extended to the non-working-age population in the same proportion as for the overall population. Combined, based on survey evidence for the United States, these measures would affect about one-third of the population. To avoid a resurgence of the epidemic, the policy would need to stay in place for 8 months. Using our model, we show how these restrictions can smooth out the trough in economic activity, as reduced contacts between the workers in the core sector and the rest of the population also smooth out the share of infected workers in the core sector. Intuitively, social distancing has an “infection externality”: it helps shield the core sector from surges in infection that could disproportionately reduce its output—thus undermining activity in the economy as a whole. Over time, with social distancing in place, workers in both the core and the non-core sectors are infected and develop immunity, but at a lower speed than without health measures, so that, at a later stage, the risk of a sharp reduction in activity due to shortage or disruption of core services remains contained. As a caveat, we should note that the peak of the infection implied by our baseline calibration would still well

³For an analysis of production structures and core sectors, see [Carvalho \(2014\)](#) and [Carvalho and Tahbaz-Salehi \(2018\)](#). [Barrot, Grassi, and Sauvagnat \(2020\)](#) offers a sectoral analysis of the effect of the COVID-19 pandemic.

exceed the capacity of health care systems to deal with the critically ill.

The second question concerns possibly consequential trade-offs between the length and the coverage of public health measures within and across sectors. According to our argument, smoothing the fall in economic activity requires pursuing a fine balance between avoiding supply shortages and allowing workers to acquire immunity. Strict and prolonged lockdowns do reduce the peak of the infection, but also tend to delay immunity, while constraining production. Moreover, absent a medical breakthrough on vaccination or treatment, lifting a strict lockdown may result in a reactivation of the epidemic. The dynamic of the epidemic when strict measures are relaxed may simply delay the economic damage from a sharp rise in the number of infected people—which could be expected to occur after a lengthy period in which policy already keeps economic activity at a very low level.⁴ We attempt to offer some ballpark estimates of the economic costs of waiting for a vaccine. If the wait lasted 18 months, at one end of the range, our calculations point to no reduction in labor supply, and hence no change in economic activity in our model, and at the other end of the range, costs as high as 40 percent of GDP for the duration of the wait. The wide range reflects that uncertainty from our imperfect understanding of the working of a complex economic system is compounded by uncertainty about basic characteristics of the disease.

To carry out our analysis, we develop a stylized “integrated assessment model for infectious diseases.”⁵ By combining a simple deterministic epidemiological model with a two-sector growth model our framework provides a map from the intensity of social distancing into the disease spread and the number of people able to work and, via this channel, into economic activity. The question we want to address is how much output can potentially be lost (via the mechanism we model in our paper) by letting the disease spread to its natural intensity, as opposed to trying to slow it down via social distancing. The epidemiological model tracks the progression of the infection across workers who provide labor inputs to the two production sectors. For our economic model, labor supply is exogenously driven by the epidemiological model. The labor supply, in turn, is reduced by the spread of the infection, as the symptomatic infective individuals cannot work, and by the social distancing measures put in place.

⁴ In this respect, our pessimistic scenario is in line with the conclusions by [Atkeson \(2020a\)](#).

⁵ We deliberately borrow the term “integrated assessment model” from the literature on climate change to emphasize the importance of linking economics to phenomena that are relevant for the well-being of humankind but that are outside the traditional focus of the economics profession. As in the case of climate change policies, public health policies may have consequences for economic activity that can influence the choices of policymakers.

In our framework, the infectious disease affects economic activity directly and indirectly: directly, through its negative impact on the labor force, as symptomatic infected workers become unable to work; and indirectly, as a contraction in the output of the core sector has nonlinear effects on aggregate activity. The epidemiological and economic models are also linked through health policy measures.⁶ Absent effective pharmacological instruments, isolating people through social distancing is the main tool of slowing the spread of the disease. Yet, such measures may come at direct economic costs if they result in a reduction of the number of workers, inefficient work arrangements and/or outright shut-downs of production facilities. Labor supply and productivity fall, causing total output to fall.

The key features of our model are as follows. For the epidemiological block of our framework, we expand the standard susceptible-infective-removed (SIR) model with a homogeneous population to a setting with multiple groups to account for the heterogeneous roles that individuals play in the economic production process.⁷ This setup gives us the flexibility to allow different lockdown coverage across groups, by sector and occupational task.

In the economic block of our framework, we assume a low degree of substitutability between core and non-core inputs in producing final output goods, as well as a realistically low degree of worker mobility across sectors (i.e., we set intersectoral mobility to zero). Most crucially, we posit that work in the core sector is subject to a minimum-scale requirement. This scale requirement captures the idea that technology in the industries in this sector is such that workers need to operate as members of a team. Close to the minimum scale, output falls more than proportionally to the labor input, reflecting that replacing team members with specialized skills could become more difficult. In addition, we allow for endogenous capacity utilization and put a lower bound on disinvestment, implying that accumulated capital cannot be consumed.

The key transmission channel between our epidemiological and our economic model is the change in the labor supply due to illness only—the disease incapacitates symptomatic workers. Via this channel, both the epidemic and the health policy response can have large effects on economic activity by reducing labor supply which, in turn, depresses aggregate consumption

⁶ To be clear, we abstract from other links, such as the ones related to the endogenous behavioral response of people to the spread of the disease, and the economic disruption from the “sudden stop”.

⁷ The origins of the SIR model and other closely related models of mathematical epidemiology trace back to the seminal contributions of Kermack and McKendrick (1927). Brauer, Driessche, and Wu (2008) offer an introduction to state-of-the-art mathematical epidemiology with numerous models that are more detailed about the dynamics of infectious diseases. However, most of these models feature the SIR model (or its close cousin the SIS model) at their core.

and investment. Relative to the existing literature our analysis of the dynamics of investment and capital utilization adds an important element to the picture of the macroeconomic risks associated with the current crisis. By no means is this the only relevant economic channel. We abstract from possible changes in consumption patterns, under an unfettered epidemic or a lockdown, that could intensify the economic contraction.⁸ We also abstract from the endogenous fall in demand due to financial frictions and nominal rigidities. Arguably, adding these realistic elements would exacerbate the shock amplification mechanism in spite of strong fiscal and monetary responses by national and international authorities.

The rest of the paper is organized as follows. Section 2 introduces the model, specifying both the epidemiological and the economic elements as well as the structure of social distancing. Section 3 discusses our calibration and solution methods. Section 4 discusses our results varying the type and intensity of social distancing measures. Section 5 considers how widespread testing would have to be to keep health outcomes unchanged while relaxing the intensity of social distancing measures. Section 6 concludes. Details on the model and sensitivity analysis are presented in the appendix.

2 The Integrated Model

Our integrated assessment model for infectious diseases combines a deterministic compartmental SIR model of epidemiology with a two-sector economic growth model. Epidemiological models attempt to map the complex transmission interactions of infectious diseases in a population into a formal mathematical structure that can describe the large scale dynamics. To integrate epidemiological and economic models, we have to make assumptions about the interaction of the spread of the disease with economic activity. In our framework, we allow for three channels. First, if at least some of the individuals who have fallen ill from the disease cannot work, the aggregate labor supply shrinks temporarily and reduces economic activity. Second, public health measures put in place to control the spreading of the infectious disease either prevent individuals from conducting their work altogether or limit their productivity (e.g., by imposing inefficient

⁸ For some early estimates of such changes for the COVID-19 epidemic, see [Baker, Farrokhnia, Meyer, Pagel, and Yannelis \(2020\)](#). [Jordà, Singh, and Taylor \(2020\)](#) provide estimates on how epidemics are different from other destructive episodes, such as wars, based on a dataset stretching back to the 14th century. For pandemics, they point to changes in consumption that they attribute to heightened precautionary behavior.

home-office arrangements). Again, the reduction in effective labor causes economic activity to fall and, if the health policy measures are implemented over a long time period, a decline in investment activity may cushion the near-term fall in consumption but add persistence to the economic repercussions. Third, in our two-sector economic growth model, it matters importantly for economic activity how the health measures affect the labor supply within and across sectors.

The SIR model captures how an infectious disease, such as COVID-19, spreads by direct person-to-person contact in a population. As an introduction to our variant of this model and the relevant terminology, in the next section we lay out a standard specification assuming that the population is homogeneous and has no distinguishing characteristics except for the health status. In the following section, we extend this one-group SIR model to a three-group SIR model in which the groups differ by the role of their members in the production process. The exposition of the one-group SIR model follows [Hethcote \(1989\)](#) and [Allen \(1994\)](#). Our three-group model borrows from work on epidemiological models with discrete spatial heterogeneity, see Chapter 7 in [Brauer, Driessche, and Wu \(2008\)](#).

2.1 Assumptions, Notation, and the One-Group SIR Model

Time is discrete and measured in days. In the one-group model, individuals only differ with regard to their health status. In particular, they have no distinguishing socioeconomic characteristics. At every instant in time, total population N is divided into three classes:

1. susceptible individuals of share S_t in population can incur the disease but are not yet infected;
2. infective individuals of share I_t in population transmit the disease;
3. removed individuals of share R_t in population are removed from the susceptible-infective interaction by recovery with immunity, isolation, or death.

We abstract from vital dynamics (births and natural deaths) and assume N to be constant and sufficiently large to treat each class as a continuous variable.

The population in the SIR model is homogeneously mixing and hence the “law of mass action” applies: the rate at which infective and susceptible individuals meet is proportional to their spatial density $S_t I_t$. The effective contact rate per period β is the average number of adequate

contacts per infective period. An adequate contact of an infective individual is an interaction that results in infection of the other individual if that person is susceptible. Thus, β can be expressed as the product of the average of all contacts and the probability of infection (transmission risk) given contact between an infectious and a susceptible individual. The parameter β is typically viewed to be constant over time, absent public health measures such as social distancing. In the rest of the paper, we will refer to this as the *basic* contact rate, as opposed to the *running* contact rate resulting from the imposition of social distancing measures. Infected individuals recover at the constant daily recovery rate γ , and receive permanent immunity as is often the case for viral diseases.⁹

Abstracting from the lethality of the viral disease, we write the discrete time SIR model as:

$$S_{t+1} = S_t - \beta I_t S_t, \quad (1)$$

$$I_{t+1} = I_t + \beta I_t S_t - \gamma I_t, \quad (2)$$

$$R_{t+1} = R_t + \gamma I_t, \quad (3)$$

$$1 = S_t + I_t + R_t, \quad (4)$$

with the initial conditions $S_0 > 0$ and $I_0 > 0$. In addition, $S_t \geq 0$, $I_t \geq 0$, and $S_t + I_t \leq 1$, and $N = 1$.

The basic reproduction number $R_0 = \frac{\beta}{\gamma} S_0$ determines whether the infectious disease becomes an epidemic, i.e., the disease goes through the population in a relatively short period of time, or not. This is the case for $\frac{\beta}{\gamma} S_0 > 1$; otherwise, the number of infective individuals decreases to zero as time passes, without an epidemic. If $R_0 \leq 1$ the number of infectives converges monotonically to zero (disease-free equilibrium).¹⁰

⁹ While it is widely presumed that recovery from COVID-19 yields at least temporary immunity, the jury is still out whether the immunity is permanent. If the recovery does not give permanent immunity, then the individual can be infected again and moves eventually back into the group of susceptible individuals, as captured in SIRS models or SIS models. SI(R)S models are the appropriate choice for a range of bacterial agent diseases. See also [Hethcote \(1989\)](#).

¹⁰ A closely related concept is the time-dependent running reproduction number, $R_t = \frac{\beta}{\gamma} S_t$, which measures the number of secondary infections in period t caused by a single infective individual. At the peak of the epidemic, when the number of currently infected individuals reaches its maximum, the running reproduction number drops below 1.

2.2 Three-Group SIR Model

Moving to the three-group SIR model, we assume that the total population N is split into three groups. The size of group $j \in \{1, 2, 3\}$ is denoted by N_j with $N_1 + N_2 + N_3 = 1$. The members of each group are homogeneous and share specific socioeconomic characteristics. More specifically, we assume that the members of the first two groups are in the labor force. In the two-sector economic model presented below, individuals of group j work in sector j with $j \in \{1, 2\}$. The members of Group 3 are not in the labor force; this group can be thought of as including individual outside the labor force, the young and the elderly.¹¹

As in the one-group model, $S_{j,t}$, $I_{j,t}$, $R_{j,t}$ denote the susceptible, infective, and removed subpopulations in each group with $S_{j,t} + I_{j,t} + R_{j,t} = N_j$.¹² As both the average number of contacts per person and the probability of transmission can differ between the members of the three groups, the effective contact rate transmission can be group-dependent.¹³ Let $\beta_{j,k,t}$ denote the group-dependent contact rate which measures the probability that a susceptible person in group j meets an infective person from group k and becomes infective. For convenience, we define the force of infection $\lambda_{j,t}$ for group j as

$$\lambda_{j,t} = \sum_{k=1}^3 \beta_{j,k,t} I_{k,t}. \quad (5)$$

The group-dependent recovery rate is denoted by γ_j and ϖ_j is the death rate.

With these definitions in place, the system of equations for the three-group SIR model is given by:

$$S_{j,t+1} - S_{j,t} = -\lambda_{j,t} S_{j,t}, \quad (6)$$

$$I_{j,t+1} - I_{j,t} = \lambda_{j,t} S_{j,t} - (\gamma_j + \varpi_j) I_{j,t}, \quad (7)$$

$$R_{j,t+1} - R_{j,t} = \gamma_j I_{j,t}, \quad (8)$$

with $j \in \{1, 2, 3\}$. Note that if $\beta_{j,k,t} = \beta_t$, then $\lambda_{j,t} = \beta_t I_t$ where $I_t = \sum_{j=1}^3 I_{j,t}$ denotes the

¹¹ It would be straightforward to model the young and the elderly as separate groups. Such an extension would allow for even more differentiated health policy measures than our stylized model affords.

¹² For a detailed mathematical analysis of a SIR model with two groups, see Magal, Seydi, and Webb (2016).

¹³ A straightforward example of two groups with different transmission coefficients are hospital patients and medical personnel.

number of total infectives and the dynamics of the three-group SIR model are identical with the one-group model. We return to the discussion of these parameters when describing social distancing measures in Section 2.4.2.

2.3 A Two-Sector Macroeconomic Model

Individuals live in identical households that pool consumption risk across the different household members, i.e., the composition of each household reflects the relative group sizes in the population. Absent social distancing, all susceptible and recovered individuals work. We allow for the possibility that infective individuals may be symptomatic or asymptomatic and assume that symptomatic individuals do not work. To be clear, ours is not a model that integrates strategic behavioral choices into an epidemiological framework, along the lines of [Kremer \(1996\)](#) and of [Greenwood, Kircher, Santos, and Tertilt \(2019\)](#). Nonetheless, the expected exogenous reduction in labor supply linked to the inability of the symptomatic ill individuals to work or to social distancing measures is integrated into the economic decisions we model.

Our model comprises two intermediate sectors, Sector 1 and Sector 2. Individuals in Group 1 provide labor services inelastically to firms in Sector 1. Individuals in Group 2 provide labor services inelastically to firms in Sector 2. Individuals in Group 3 are the young and the elderly who are not in the labor force. Final goods are produced with inputs from the two intermediate sectors with a constant elasticity of substitution function. These inputs are imperfect substitutes for each other.¹⁴ The two sectors differ by their production structure. In Sector 1, labor inputs are subject to a minimum scale requirement. This scale requirement is a simple way to capture the specialized skills of different workers, all of which are necessary to produce a certain product. Larger labor shortfalls make it more likely that production will be impaired by the absence of essential members of a team. We abstract from modeling the interaction of capital with the labor input in Sector 1. We have in mind production structures in which capital cannot easily compensate for shortfalls in the labor input. For example, if doctors and nurses do not show up for work, it seems unlikely that adjustments could be made to compensate for their absence. By contrast, with Sector 2, we are attempting to capture production processes in which the

¹⁴[Krueger, Uhlig, and Xie \(2020\)](#) also bridge an epidemiological model and a two-sector economic model, building on the setup of [Eichenbaum, Rebelo, and Trabandt \(2020\)](#). In the model of [Krueger, Uhlig, and Xie \(2020\)](#), different contact rates distinguish each sector. Furthermore, labor is the only input into production and labor mobility across sectors helps blunt the economic impact of the epidemic.

utilization of capital services can be more easily adapted, and in which labor inputs are more readily substitutable for capital services.

Households maximize consumption and supply two types of labor, $l_{1,t}$ and $l_{2,t}$ inelastically. Households also rent capital services $u_t k_{t-1}$ to firms in Sector 2, where u_t captures variable capacity utilization that can also be adjusted for those services. The utility function of households is:

$$U_t = E_t \sum_{i=0}^{\infty} \theta^i \log(c_{t+i} - \kappa c_{t+i-1}). \quad (9)$$

Households choose streams of consumption, investment, capital and utilization to maximize utility subject to the budget constraint

$$c_t + i_t = w_{1,t} l_{1,t} + w_{2,t} l_{2,t} + r_{k,t} u_t k_{t-1} - \nu_0 \frac{u_t^{1+\nu}}{1+\nu}, \quad (10)$$

where the term $-\nu_0 \frac{u_t^{1+\nu}}{1+\nu}$ captures costs from adjusting capital utilization. The parameter ν_0 allows us to normalize utilization to 1 in the steady state. Households' utility maximization is also subject to the law of motion for capital, given by

$$k_t = (1 - \delta) k_{t-1} + i_t, \quad (11)$$

and to a threshold level of investment,

$$i_t \geq \phi i, \quad (12)$$

where ϕi denotes a fraction of steady-state investment. Notice that when $\phi = 0$, Equation 12 implies the irreversibility of capital.

Moving to the description of the production sector, firms in Sector 1 use labor $l_{1,t}$ to produce the intermediate good $v_{1,t}$ and charge the price $p_{1,t}$. The production function is given by

$$v_{1,t} = \eta (l_{1,t} - \chi). \quad (13)$$

Firms in Sector 2 use capital k_{t-1} and labor $l_{2,t}$ to produce an intermediate good $v_{2,t}$,

$$v_{2,t} = (u_t k_{t-1}^\alpha) l_{2,t}^{1-\alpha}. \quad (14)$$

Sector 2 combines its intermediate good with the good produced in Sector 1 to produce the final output good:

$$y_t = \left((1 - \omega)^{\frac{\rho}{1+\rho}} (v_{1,t})^{\frac{1}{1+\rho}} + \omega^{\frac{\rho}{1+\rho}} (v_{2,t})^{\frac{1}{1+\rho}} \right)^{1+\rho}. \quad (15)$$

2.4 Integrating the Epidemiological and the Macroeconomic Model

The dynamics of the epidemiological and the macroeconomic models are tightly connected. As we assume that symptomatic infective individuals cannot work, the labor supply for each sector depends on the spread of the disease within the relevant population group. Moreover, social distancing measures can also affect economic activity if they reduce the labor supply.

2.4.1 Disease Spread and the Labor Supply

Without the disease, the labor supply in each sector is

$$l_{j,t} = N_j, \quad (16)$$

for $j \in [1, 2]$ for all t . As the disease starts spreading, assuming that symptomatic infective individuals cannot work, the labor supply in sector j is given by

$$l_{j,t} = N_j - (1 - \iota) I_{j,t}, \quad (17)$$

for $j \in [1, 2]$. We denote with ι the share of infective individuals who are asymptomatic, which is assumed to be constant in time and across the three groups.

2.4.2 Social Distancing and the Labor Supply

Social distancing and other non-pharmaceutical public health measures are modelled as a reduction in the effective contact rates, for the time span over which the measures are in place. Let $\bar{N}_{j,t}$ be the number of individuals in group j directly affected by social distancing during period t ; the share of group j individuals affected by the policy measure is therefore $\bar{N}_{j,t}/N_j$. The effectiveness of social distancing in reducing contact rates is controlled by the parameter $\vartheta \in [0, 1]$.¹⁵

¹⁵ This parameter accounts for the fact that even after closing down physical work places, individuals may continue to have close physical contacts in non-work settings.

If $\vartheta = 0$ social distancing has no effects on the contact rates. We model the group-dependent *running* contact rates in the presence of social distancing as

$$\beta_{j,k,t} = \beta^* \left(1 - \vartheta \frac{\bar{N}_{j,t}}{N_j}\right) \left(1 - \vartheta \frac{\bar{N}_{k,t}}{N_k}\right). \quad (18)$$

The parameter β^* is the *basic* contact rate that applies absent social distancing—assumed to be constant. The other two terms account for the reduction in the effective contact rates due to social distancing. As the intensity of social distancing can vary across groups, the effective contact rates $\beta_{j,k,t}$ vary across groups even if the basic contact rate does not.

Our approach to modeling social distancing embraces the key assumption of homogeneous mixing underlying the SIR model. Under the “law of mass action” the rate at which infective and susceptible individuals meet is proportional to their spatial density. For the case of $\vartheta = 1$, Equation 18 implies that the terms of the kind $\beta_{j,k,t} S_{j,t} I_{k,t}$ in Equation 6 can be written as

$$\beta^* \left(1 - \frac{\bar{N}_{j,t}}{N_j}\right) S_{j,t} \left(1 - \frac{\bar{N}_{k,t}}{N_k}\right) I_{k,t} = \beta^* \tilde{S}_{j,t} \tilde{I}_{k,t} \quad (19)$$

where $\tilde{S}_{j,t}$ and $\tilde{I}_{j,t}$ reflect the numbers of susceptible and infective individuals that are not affected by social distancing in this example. Hence, social distancing reduces the spatial density in our setting.

As we assume that social distancing applies to all group members regardless of their individual health status, the labor supply in sector j is given by

$$l_{j,t} = N_j - \max \left[\frac{\bar{N}_{j,t}}{N_j} - v_j, 0 \right] N_j - \min \left[\frac{\bar{N}_{j,t}}{N_j}, v_j \right] (1 - \iota) I_{j,t} - \left(1 - \frac{\bar{N}_{j,t}}{N_j}\right) (1 - \iota) I_{j,t}. \quad (20)$$

In Equation 20, the term $\max \left[\frac{\bar{N}_{j,t}}{N_j} - v_j, 0 \right] N_j$ is the number of individuals in group j under lockdown, where v_j is the share of individuals in group j who can continue working from home. The term $\min \left[\frac{\bar{N}_{j,t}}{N_j}, v_j \right] (1 - \iota) I_{j,t}$ is the number of sick and symptomatic individuals in group j who are under lockdown and are working from home. For the same group, the term $\left(1 - \frac{\bar{N}_{j,t}}{N_j}\right) (1 - \iota) I_{j,t}$ is the number of individuals who get sick and are symptomatic but are not under lockdown.

2.5 The Special Case of a One-Sector Macroeconomic Model

Our three-group/two-sector model nests a one-sector model that more closely resembles the setup that has been used in previous studies that considered the cost of social distancing measures. Trivially, the three-group SIR model readily collapses to a two-group model when we impose that all the shares pertaining to Group 1 are zero, i.e., $S_{1,t} = I_{1,t} = R_{1,t} = N_1 = 0$. For comparability of results across models, we continue to assume the presence of Group 3, the non-working-age population. Correspondingly the two-sector model collapses to a prototypical one-sector real business cycle model when we impose that the quasi-share parameter ω in Equation 15 is one.

3 Calibration and Solution

In this section, first we present our calibration, summarized in Table 1, distinguishing parameters relevant for the SIR model and for the two-sector economic model. Second, we discuss the solution method.

3.1 The Parameters of the SIR model

In calibrating the SIR model we need to set the values of the disease-specific parameters—the group-dependent contact rates $\beta_{j,k,t}$, recovery rates γ_j , and death rates ϖ_j —and the sizes of the three groups N_j . We assume that, absent social distancing measures, the three groups are identical from an epidemiological perspective. More specifically, the effective contact rates within and across groups are identical and constant over time, i.e., $\beta_{j,k,t} = \beta, \forall j, k$. Similarly, it is $\gamma_j = \gamma$ and $\varpi_j = \varpi$. In agreement with recent papers by economists on the spread of the COVID-19 disease, we set β equal to 0.2 and the recovery rate γ at $1/20$ implying a duration of illness of 20 days.¹⁶ We abstract from the lethality of the disease and highlight the direct implications of the pandemic for the economy. Hence, we set $\varpi = 0$ in our baseline calibration. The basic reproduction number R_0 implied by these parameter choices is equal to 4 meeting

¹⁶ The choices for β and γ are in line with those in Alvarez, Argente, and Lippi (2020) and are close to those in Eichenbaum, Rebelo, and Trabandt (2020). Under our parameterization, the one-group SIR model produces similar dynamics for the classes of susceptibles, infectives, and recovered as the slightly richer SEIR model (with the addition of an exposed class) discussed in Atkeson (2020b). There is considerable uncertainty about the exact values of these parameters that will likely persist into the future as non-pharmaceutical interventions and the possible emergence of herd immunity will complicate the econometric analysis.

the condition for the disease to spread as an epidemic. Finally, we set to 1 the parameter ϑ , which governs the effectiveness of social distancing measures and consider alternative values for robustness purposes.

It is worth reiterating that the calibration of our SIR model is daily. In order to link the results from the epidemiological model to the macroeconomic models, we average the results of the epidemiological model across thirty-day intervals.

3.2 The Parameters of the Economic Model

The relative sizes of the three groups are informed by the employment to population ratio, the age distribution of the U.S. population, and the employment share in the core sector. We set the combined size of Group 1 and Group 2, $N_1 + N_2$, at 0.65 or 65 percent of the total population, in line with data from the U.S. Bureau of Labor Statistics (BLS) for the employment-to-population ratio. Group 3 (the young and the elderly) accounts for 35 percent of the population, and thus $N_3 = 0.35$.

The individual group sizes N_1 and N_2 reflect the employment share of the group of industries in the economy that we deem essential and that are reported in Table 2. The data on value added come from the tables on GDP by Industry of the Bureau of Economic Analysis (BEA). The employment shares are based by matching the industries in the BEA table with data on hours worked by industry in the Productivity Release of the BLS. The shares reported in the table are for 2018, the latest year for which data are available at the time of writing. The total share of employment for the industries listed in the table is about 38 percent. Identifying the individuals working in the essential industries as the Group 1 individuals in the SIR model we set $N_1 = 0.65 \times 0.38 \approx 0.25$. Hence, Group 2 is of size $N_2 = 0.4$.

The total share of GDP for the industries listed in the table is about 27 percent. We fix the quasi-share parameter ω so that the value added of Sector 1 in the steady state is the same percent of total output in the model, i.e., denoting steady-state variables by omitting the time subscript, $\frac{p_1 v_1}{y_1} = 0.27$.

The unit of time for the economic model is set to 1 month. We set the discount factor θ to $1 - \frac{4}{100}/12$, implying an annualized interest rate of 4 percent in the steady state. The depreciation rate δ is set to $\frac{1}{10}/12$, implying an annual depreciation rate of 10 percent. The parameters governing consumption habits κ is set to 0.6, in line with estimates for medium-scale

macro models such as [Smets and Wouters \(2007\)](#). We set χ , the minimum scale parameter for the production function of Sector 1, to 0.5 times l_1 , implying that one-half of the steady state labor input for sector 1 is essential for production. The scaling parameter η is set to 2, offsetting the reduction in productivity implied by our choice of the minimum-scale parameter in the steady state. This choice for η leaves the steady state production level unchanged relative to a case without a minimum scale (i.e., when χ is 0). We set the parameter α governing the share of capital in the production function of Sector 2 to 0.3. The elasticity of substitution between factor inputs is $\frac{1}{3}$, implying a choice of $\rho = \frac{1}{1-\frac{1}{3}}$ as derived in the appendix. We set the parameter ν governing the elasticity of capacity utilization to 0.01, as in [Christiano, Eichenbaum, and Evans \(2005\)](#). Finally, the parameter ϕ is equal to 0, implying that investment, once installed as capital, is irreversible.

3.3 Cross-model Parameters

In our model, the macroeconomic cost of inaction is driven by the reduction in the labor supply caused by the inability of symptomatic infective individuals to work until recovered. To calculate the reduction in labor supply, we need to rely on an estimate of the asymptomatic infected individuals. A study of the passengers of the Diamond Princess cruise ship provides useful guidance. As reported in [Russell, Hellewell, Jarvis, Zandvoort, Abbott, Ratnayake, Flasche, Eggo, Edmunds, and Kucharski \(2020\)](#), about half of the passengers that tested positive for the virus were asymptomatic. The asymptomatic share was also found to be different by age group. We use a 40 percent estimate that applies to passengers of working age, i.e. $\iota = 0.4$. Given that labor supply is exogenous in our economic model, the fall in labor supply becomes more acute as the infective share increases.

When we study social distancing measures, we need to allow for the possibility that a fraction of the individuals subject to lockdown measures may still be able to work from home. To estimate the fraction of individuals who can do so, we use the American Time Use Survey of the BLS. According to survey data for 2018, the latest available at the time of writing, about 30 percent of American workers can work from home. The survey also provides differential rates by industry. Mapping the coarser industry categories onto our industry choices for Sector 1 as listed in [Table 2](#), we extrapolate that 15 percent of individuals in Group 1 can work from home, compared to 40 percent of individuals in Group 2. Thus, we set $v_1 = 0.15$ and $v_2 = 0.4$.

3.4 Solution Method

The solution method has three important characteristics: First, it allows for a solution of the SIR model that is exact up to numerical precision; second, it conveys the expected path of the labor supply in each group to the economic model as a set of predetermined conditions, following the numerical approach detailed in the appendix of [Bodenstein, Guerrieri, and Gust \(2013\)](#); and third, it resolves the complication of the occasionally binding constraints, implied by capital irreversibility, with a regime switching approach following [Guerrieri and Iacoviello \(2015\)](#). The modular solution approach has the advantage of allowing us to consider extensions of either module without complicating the solution of the other. The advantage of the regime-switching method of [Guerrieri and Iacoviello \(2015\)](#) is that it is remarkably resilient to the curse of dimensionality, while still accurate for the class of models we consider.¹⁷

4 Simulation Results

We are now ready to discuss our model predictions concerning the macroeconomic consequences of the spread of a contagious disease such as COVID-19. In a first exercise, we compare the results from our two-sector model relative to those from a model without sectoral differentiation—the special case of a one-sector model described in Section 2.5. In this exercise, we abstract from the effects of social distancing, hence we dub this case as policy *inaction*. In the following set of exercises, we compare the model under social distancing with the model under inaction, focusing on the macroeconomic effects of measures that successfully flatten the infective curve, at least for a time.

4.1 The Macroeconomic Costs of Inaction

The results from our first exercise, comparing the one-sector to the two-sector model in the absence of social distancing measures are shown in Figures 1 to 3. Figure 1 plots the evolution of susceptible, infective and removed individuals in the total population at the daily frequency. As we assume that the basic contact rates within and across groups are identical, the disease dynamics for each groups mirrors the evolution in the total population in this scenario without

¹⁷ [Guerrieri and Iacoviello \(2015\)](#) provide extensive comparisons of the performance of different solution methods for the same case of capital irreversibility considered here.

social distancing measures. With a slow start, the spread of the disease picks up momentum after 30 days. The population share of infective individuals peaks at 41 percent after 65 days. In the case plotted in the figure, almost all individuals will eventually have been infected by the virus.

Moving to the economic implications, we turn to Figure 2. The top two panels of this figure show the progression of the infection with the data now aggregated at the monthly frequency. For the one-sector model, we back out the reduction in the labor supply from the population share of infected individuals in groups 1 and 2 combined — adjusted by the proportion of asymptomatic sick individuals that, in the absence of widespread testing, could be expected to continue working. This combined share of infected individuals is shown on the top left panel. For the two-sector model, instead, we need to track the infected shares for groups 1 and 2 separately. These shares evolve as shown in the top right panel.¹⁸

In our model, the *direct* macroeconomic cost of inaction is driven by the reduction in the labor supply caused by the inability of symptomatic infective individuals to work until they recover. Using the estimates suggested by the case study of the Diamond Princess cruise ship discussed in the calibration section, we set the share of asymptomatic infective workers who can continue to work equal to 40 percent.

As shown in Figure 2, the reduction in total output tracks closely the share of infective individuals. However, the one- and two-sector models have very different quantitative implications. The trough in output is about 20 percent below steady state for the one-sector model, compared to about 30 percent for the two-sector model.¹⁹

Before discussing the other macro variables, it is useful to consider the infective shares and labor supplied by group, together with value added by sector, shown in Figure 3. The top two panels of this figure make it clear that the infection proceeds apace across the two groups, hence, the share of each group that is infective is the same. Given our assumptions, the decline in labor supply is also the same. What is not the same is the reduction in value added for the two sectors. The same reduction in labor supply results in a bigger contraction in value added for Sector 1,

¹⁸ Since in our baseline calibration the contact rates are the same within and across groups, in the absence of social distancing differentiated by group, we can aggregate the three-group SIR model into either a two-group SIR model or a one-group SIR model. There would be no loss of information from aggregation because group-specific paths could always be backed out from the aggregate path.

¹⁹ Using more common quarterly averages, the decline in output in the first quarter of the simulation is 13 percent for the one-sector model, versus 18 percent for the two-sector model.

given the minimum scale assumption in Equation 13.

Returning to Figure 2, the asymmetric sectoral contraction has key aggregate implications. Since the two sectoral inputs are imperfectly substitutable, there are reduced benefits from using them in proportions that deviate from the steady state share: it pays to reduce capacity utilization for Sector 2, amplifying the collapse in the output of Sector 2.

In the two-sector model, the consumption collapse mirrors the larger drop in output—both are V-shaped. The deeper and persistent contraction in consumption in turn reflects capital irreversibility—when this constraint becomes binding, investment cannot be reduced by an extent sufficient to smooth the consumption path as desirable. Note that wealth effects are so large that consumption plummets already in the first month, ahead of the drop in labor.²⁰

By contrast, consumption holds up much better in the one-sector model—mostly because, in this framework, households are able to finance their spending by reducing investment without running in supply and capital irreversibility constraints. To be clear: in comparison, investment (and capacity utilization) falls by more in the two-sector model. However, this contraction mostly reflects that the supply disruption in Sector 1 has a disproportionate effect on aggregate output.

The main takeaway from this first exercise is that the one-sector model may understate the collapse in output associated with an unchecked evolution of the disease predicted by our epidemiological model, with drastically different implications for aggregate consumption. In our two-sector model, the core sector operates subject to a minimum-production scale, hence it can respond sharply to a deep decline in labor supply as workers become ill in large numbers and stop working. On top of the direct negative effect of a falling workforce on production, activity is hit indirectly, but possibly strongly, by the supply disruption in essential production linkages among industries.

One may argue that the model overestimates the economic disruption because it does not account for the optimizing reaction by households, who may follow spontaneous, self-interested social distancing, reducing the contact rate and therefore the running reproduction number. However, we know from ongoing work on the subject that, even accounting for the spontaneous reaction by households, the initial rise in infections would remain rather steep (e.g., see [Farboodi, Jarosch, and Shimer \(2020\)](#)). Moreover, the optimizing decision by rational agents may consist

²⁰ As output is predetermined in the first period, investment turns positive before falling.

of not going to work, even when the individual is not infected—a reaction that may be quite strong if one accounts for the considerable uncertainty about the nature and the effects of the disease. Finally, in sensitivity analysis, we show that results are quite insensitive to the basic reproduction number, unless this number falls very close to 1. If only loosely, this sensitivity exercise accounts for the potential aggregate effects of different spontaneous reactions to the spread of the disease.

4.2 Comparing the Macroeconomic Consequences of Inaction and Social Distancing

Using our two-sector model, the following analysis considers the macroeconomic consequences of social distancing measures designed to smooth out the infection curve. We compare these consequences with those of the inaction case studied in the previous section. We stress from the start that our exercises are only meant to provide insight on how the dynamics of the disease and of the economy are interconnected. An exercise in optimal policy design would require a much more articulated model. Yet we may note here that a lockdown has a straightforward motivation as a policy action that internalizes the infection externality from individual interactions—that would not be internalized even if individuals optimally trade-off consumption and labor supply decisions with the risk of being infected (see, e.g., [Eichenbaum, Rebelo, and Trabandt \(2020\)](#)).

4.2.1 A Baseline

In our analysis, we consider the possibility that social distancing measures could be targeting first and foremost workers who are able to continue supplying their labor services from home. In line with the American Time Use Survey, conducted by the Bureau of Labor Statistics, the share of the labor force that can work from home is 15 percent of workers in Group 1 (the group that supplies labor to the core sector), and 40 percent of workers in Group 2 (the group that supplies labor to the other sector). Requiring this subset of workers to work from home and observe a strict lockdown produces benefits for the rest of the population and other workers, for instance, by reducing the chance of contagion during commuting to the workplace. With regard to individuals not in the labor force, Group 3, we consider strict social distancing measures applied to about 30 percent of group members, the same proportion as for the overall

population. Under this policy setup, keeping all the above measures in place for 8 months can avoid a resurgence of the epidemic once these measures are lifted.

The health consequences of this policy in the three-group SIR model are illustrated by Figure 4. The top panels in this figure show the effects at a daily frequency for the aggregate population, first for the inaction scenario, then with social distancing in place. It is apparent that the policy successfully flattens the infection curve. The peak of the infection share drops from about 40 percent to about 15 percent—unfortunately still very high relative to the capacity constraint of health care systems, even when taking account for the fact that not all infected individuals experience symptoms. However, note that about 10 percent of the population never becomes infected. The bottom three panels of the figure show group-specific health outcomes. Strikingly, the health outcomes of workers in Group 1, who continue working in higher proportion, are analogous to those of individuals in Group 2 and Group 3. This is because the higher degree of social distancing in the latter groups also helps shield individuals in Group 1.

The economic consequences of social distancing and inaction are shown at the monthly frequency in Figure 5. Recall that, in our setup, the economic costs of the disease arise directly from the inability of the symptomatic ill to continue working, and indirectly from possible supply constraints on the economy due to a large contraction of the core sector. Having said so, the figure suggests that smoothing out the peak of the infection curve does benefit economic activity. The peak contraction in output is less than one half relative to the case of inaction (at monthly rates, 15 percent as opposed to about 30 percent). Disinvestment for consumption smoothing purposes never runs into the irreversibility constraint. Consumption is not V-shaped, but holds up rather well (at the cost of a lower capital stock over time). As apparent from Figure 6, key to this result is that the social distancing policy in this exercise compresses the trough for value added in both sectors, but particularly in Sector 1, which contracts only 20 percent, as opposed to 40 percent in the scenario without intervention.

In sum, apart from containing the loss of life, social distancing can significantly smooth the output and consumption costs of the disease.²¹ This economically beneficial effect stems from lockdown policies skewed towards the non-active population and workers in the non-core sector, and is targeted at the share of workers who could reasonably keep performing their occupational

²¹ Correia, Luck, and Verner (2020) finds empirical evidence for beneficial effects of health policies for the case of the 1918 influenza epidemic.

tasks from home. This combination of measures is successful to the extent that, through a positive health externality from the share of individuals at home, it keeps the infection rate among the workers in core industries low. A key implication highlighted by our two-sector model is that the contraction in value added in the two sectors remains roughly comparable, which helps contain the aggregate decline in activity.

4.2.2 Trading Off Coverage and Duration of Social Distancing

The measures we considered so far limit social distancing to individuals who can work from home—assuming that, unless ill with symptoms, all other workers go to the workplace.²² We now consider whether, based on the same mechanism, there are economic gains from taking stricter health measures that cover a greater share of the population.

Figure 7 shows the effect of a lockdown that is extended to a share of individuals equal to 18 percent in Group 1 and 45 percent in Group 2. This alternative policy implies an increase of 3 and 5 percentage points, respectively, relative to the previous policy. Individuals in Group 3 continue to be locked down in the same proportion as for groups 1 and 2 combined (about 35 percent in this case as opposed to about 30 percent in the previous case). Since these changes slow down the build-up of herd immunity, the implementation of these new measures for eight months (as above) would not be sufficient to avoid a resurgence of the share of infected individuals once social distancing is ended. For consistency with our previous exercise, we set the duration of the lockdown to 9 months.

The stricter and longer measures significantly flatten the infection curve, whose peak is now at about 11 percent. All else equal, a lower infection peak shields better the core sector, resulting in economic gains (while reducing the strain on the national health care systems). However, these gains now imply some economic losses from reducing the labor supply and some economic gains from smoothing out the infection peak. Still, Figure 7, suggests that, on balance, the cumulative decline in consumption over 24 months is smaller than the cumulative decline without intervention.

²² This is likely an upper bound: as discussed by [Eichenbaum, Rebelo, and Trabandt \(2020\)](#) it is individually rational to cut on labor supply.

4.2.3 Sensitivity

Underlying our analysis is the concern that a precipitous decline in employment brought about by infectious diseases may expose links in the production chain that are hard to predict. In our model, we capture this possibility by conjecturing that a critical mass of workers is needed for the core sector (Sector 1) to produce value added. The higher this critical mass is, the larger the effect of an infection spike among individuals in Group 1. We study the sensitivity of our results to this parameter in the appendix.

Among the parameters governing the disease dynamics, the highest uncertainty is probably about the value of the contact rate β . As shown in the appendix, the economic costs of COVID-19 in the two-sector model are sizeable and exceed those in the one-sector model as long as β does not drop below 0.075, a level that would also greatly curtail the spread of the disease.

Finally, we also analyze the trade-off in differentiating social distancing measures across groups. Namely, these measures can be made more stringent for Group 3, and less stringent for the groups in the labor force, improving economic outcomes without a significant deterioration in health outcomes, as shown in the appendix.²³

4.3 Extensions and Discussion

The rest of this section presents an exploratory analysis of lockdowns that do not prevent the resurgence of the epidemic when lifted, or are put in place in view of the availability of a vaccine, and a discussion of open issues, raised by the considerable uncertainty surrounding the parameters of the model.

4.3.1 Lockdowns that “Go Wrong.”

Figure 8 reports results for implementing a social distancing policy that is stricter relative to our baseline but is kept in place for a shorter time period. Namely, we posit that the lockdown is extended to 40 percent of individuals in Group 1 and 90 percent of individuals in both Group 2 and Group 3, for a period of 3 months, after which, all measures are removed.

²³ The reduction in economic cost will be apparent by comparing Figure 9, discussed in Section 4.3.3, and Figure A.4, in the appendix. A higher share of individuals under lockdown in Group 3 for Figure A.4, allows a reduction of the lockdown shares in Group 1 and Group 2. Accordingly, the lockdowns considered for those figures obtain comparable peak infection shares, while resulting in very different economic costs.

In this scenario, at the time in which the lockdown is lifted, the disease has not had a chance to reduce the size of the susceptible population, implying insufficient herd immunity to smooth out the peak of the infection share relative to the case of inaction. As a result, the economic costs grow. A strict lockdown produces staggering economic costs upfront, through the reduction in labor supply. In addition, the economy suffers a second-round drop in activity, when the infection peaks, that is, by itself, comparable to the case of inaction.

4.3.2 Waiting for a Vaccine

All of the policies considered thus far smooth out the infection curve but do not go insofar as preventing the infective share from surging for a prolonged period of time—which in all likelihood remains well above the level consistent with the response capacity of the health care system. The question we now address concerns the output loss associated with strict measures undertaken to keep the share of infected individuals low enough for the health care system to cope, and long enough to benefit from a vaccine at some point in the (not so near) future. Namely, we focus on measures able to keep the population share of infected individuals below 1.5 percent for 18 months, which, based on estimates cited in press reports at the time of writing, is the timespan required for a safe vaccine to be developed.²⁴

In our model economy, the cost of keeping down the population share of the infected is reduced by policies that strive to equalize the reduction in value added across Sectors 1 and 2. Given the sectoral differences in the ability to work remotely, and given the minimum scale requirement for the labor inputs of the core sector, we set lockdown shares of 25, 60, and 47 percent for Groups 1, 2, and 3, respectively (note that the lockdown share for Group 3 is the same as the share for Group 1 and 2 combined). Results for this scenario are shown in Figure 9, where we assume that the immunization program can be completed before lifting the lockdown. The figure shows that the economy suffers a sustained reduction in output, about 20 percent, throughout the time-span in which the social distancing measures are in place. Note that the reduction in consumption would persist beyond the arrival of the vaccine, as investment would have to rise for some time, to rebuild the lost (consumed) capital stock.

The figure is generated under the assumption that the vaccine is successfully deployed after

²⁴ We use the 1.5 percent share for illustrative purposes and offer sensitivity analysis. One way to set the target peak incidence of the disease is to link it explicitly to the capacity of the health care sector as in [Moghadas, Shoukat, Fitzpatrick, Wells, Sah, Pandey, Sachs, Wang, Meyers, Singer, and Galvani \(2020\)](#).

the development period and immunizes the entire susceptible population. As can be extrapolated from Figure 8, should the vaccine development fail, the epidemic spreads again at the end of the lockdown, causing additional economic costs similar to a scenario of inaction.

4.3.3 Discussion

The economic consequences of waiting for a vaccine can vary drastically depend on characteristics of the COVID-19 virus and the related effectiveness of lockdowns. To date, the parameters of the epidemiological models for the spread of this corona virus are still a topic of intense debate.

In all the cases presented, we have assumed that the social distancing measures would be completely effective at mitigating the contagion rate—we set the parameter ϑ in Equation 19 equal to 1. Alvarez, Argente, and Lippi (2020) consider a lower effectiveness of social distancing, and set ϑ to 0.8. In this case, without a stricter social distancing measure, the peak of the population share of infective individuals would rise from about 1.5 percent to about 8 percent. Attempting to bring the infective share back down to 1.5 percent requires tightening the lockdown. While reiterating that optimal policies are beyond our goals, we note that in this case raising the share of individuals in groups 1, 2 and 3 to 32, 75, and 59 percent, respectively can achieve the goal of keeping the infective share below 1.5 percent.²⁵ With this policy in place, our model points to an output drop of about 40 percent for the duration of the wait for a vaccine.²⁶

On a more “hopeful” note, other changes to the design of the lockdown policy could reduce its economic cost without devaluing its beneficial effect on public health. One such change would consist of adopting stricter measures towards individuals outside the labor force—for instance, by bringing the share of Group 3 under lockdown to 80 percent (with an effectiveness parameter ϑ equal to 1). This change would allow policymakers to achieve the 1.5 percent target peak share of infected individuals while reducing the shares of individuals in groups 1 and 2 under lockdown to 17 and 44 percent, respectively. With these shares close to the shares of individuals that could be expected to work from home for both groups, the output cost would be compressed to an average of about 5 percent for the 18 month wait.²⁷

There is still general uncertainty about the relevant value of R_0 in the absence of policy

²⁵ We still constrain the share of individuals under lockdown in Group 3 to match the share for groups 1 and 2 combined.

²⁶ See Figure A.3 in the appendix

²⁷ See Figure A.4 in the appendix.

interventions. The challenges are considerable. At the time of the writing, testing is skewed towards symptomatic infected individuals.²⁸ Furthermore, health measures also influence the spread of the disease, complicating the measurement issues. In our baseline calibration, choices for β and γ imply a value of R_0 equal to 4. The cost of waiting for a vaccine would be lower if the relevant R_0 were lower. Following the estimates by [Moghadas, Shoukat, Fitzpatrick, Wells, Sah, Pandey, Sachs, Wang, Meyers, Singer, and Galvani \(2020\)](#), we consider the effect of lowering β from 0.2 to 0.1, which brings R_0 to 2. With this change, if all individuals who can work from home did so, i.e. 15 percent of Group 1 and 40 percent of Group 2, and if an additional 30 percent share of the young and the elderly were under lockdown (under the assumption that the lockdown is perfectly effective), the peak infection share would drop to 0.3 percent of the population. Halving the values for β and R_0 relative to our baseline, the lockdown would not entail a reduction in labor supply due to the infection. And the much lower peak infection share would relieve the strain on the health care sector.²⁹

5 Widespread Randomized Testing

The economic costs of a lockdown preventing a high peak of infections over the timespan required to develop and administer a vaccine could be staggeringly high. Widespread randomized testing has been proposed as an additional health measure that could help reduce the population under a lockdown, thereby containing the economic costs of prolonged social distancing measures, see [Romer and Shah \(2020\)](#).

In what follows, we offer a quantitative assessment of this measure integrating it in the context of our model. We do so under three simplifying, “best scenario” hypotheses: (a) tests are perfectly accurate, (b) the test results are available quickly, and (c) it is possible to isolate any infected individual who tests positive quickly and effectively. Under these assumptions, we can model the effects of random testing by extending the baseline three-group SIR model to

²⁸ [Stock \(2020\)](#) cites alternative estimates and quantifies the importance of an asymptomatic infective group, more likely to be subjected to testing, to influence the available (non-randomized) data and affect the estimates of the parameter β in the SIR model.

²⁹ [Moghadas, Shoukat, Fitzpatrick, Wells, Sah, Pandey, Sachs, Wang, Meyers, Singer, and Galvani \(2020\)](#) show that with $R_0 = 2$, the peak incidence share associated with not exceeding ICU capacity in the United States is roughly 0.4 percent of the population. See Figure 2, Panel E and related discussion in their study.

include within each group a subpopulation of individuals with positive test results:

$$S_{j,t+1} - S_{j,t} = -\lambda_{j,t} S_{j,t}, \quad (21)$$

$$I_{j,t+1} - I_{j,t} = \lambda_{j,t} S_{j,t} - (\gamma_j + \varpi_j) I_{j,t} - \varphi_{j,t} \left(1 - \frac{\bar{N}_j}{N_j}\right) I_{j,t}, \quad (22)$$

$$\hat{I}_{j,t+1} - \hat{I}_{j,t} = \varphi_{j,t} \left(1 - \frac{\bar{N}_j}{N_j}\right) I_{j,t} - (\gamma_j + \varpi_j) \hat{I}_{j,t} \quad (23)$$

$$R_{j,t+1} - R_{j,t} = \gamma_j \left(I_{j,t} + \hat{I}_{j,t}\right), \quad (24)$$

with $j \in \{1, 2, 3\}$ and where $\lambda_{j,t} = \sum_{k=1}^3 \beta_{j,k,t} I_{k,t}$. As before $\beta_{j,k,t}$ is influenced by social distancing measures, as in Equation 18. The term $\hat{I}_{j,t}$ denotes the new subpopulation of infected individuals, within Group j . They are identified as infected by testing individuals in Group j not under the lockdown at the daily rate $\varphi_{j,t}$.³⁰ Randomized testing identifies infected individuals regardless of whether or not they are symptomatic, so they can be isolated, thereby reducing the spread of the disease. It should be intuitive that, technology and budget permitting, repeating the testing daily at a sufficiently high rate could suppress the spread of the disease altogether.

We carry out our analysis of testing building on simulations in the previous section, where we considered measures able to keep the population share of infected individuals below 1.5 percent over the course of 18 months. There, we showed that lockdown shares of 25, 60, and 47 percent for groups 1, 2, and 3, respectively, would achieve this goal at the cost of a 20 percent drop in output. Relative to this scenario, reducing the lockdown shares to 20, 50, and 39 percent for groups 1, 2, and 3, respectively, would halve the drop in output to about 10 percent but push up the peak for the share of infected individual to about 7 percent of the population.³¹

Starting from the latter, milder scenario, we ask: how much randomized testing would be necessary to bring the peak share of infected individuals down from 7 to 1.5 percent? In addressing this question, following the logic of our model, we skew the testing towards individuals in Group 1. This would be the most efficient way to achieve the goal of lowering the peak, given that individuals in Group 1, being subject to the lowest lockdown share, have the highest contact rates. Our simulation suggests that bringing the peak of total infections down would require setting the parameter φ_1 to 0.09; i.e., 9 percent of individuals in Group 1 not under lockdown

³⁰ We assume that all infected individuals in Group j recover or die at the same rate whether they are in isolation or not.

³¹ We have imposed again that the individuals in Group 3 are under lockdown in the same proportion as the entire population.

would have to be randomly selected for testing every day to compensate for the relaxation in the lockdown described above.

To put this result in perspective recall that Group 1 accounts for about 25 percent of the population and that 20 percent of this group would be under lockdown; it follows that the share of the population that would need to be randomly tested daily is $0.25 \times (1 - 0.20) * 0.09 \approx 0.018$. With the current U.S. population at around 330 million, about 6 million people would have to be randomly selected to be tested each day. This may sound like a staggering goal. Yet, if the cost of a test were to be pegged at \$100 per person, with U.S. GDP at about \$20.5 trillion, the annual cost of testing would amount to a little over 1% of GDP.³² According to our model, this alternative would be about ten times cheaper than the additional cost of a stricter lockdown required to achieve the same health-related goal.

While widespread randomized testing could, in principle, be a cheaper alternative to a strict lockdown vis-à-vis the goal of reducing contact rates, current capacity is far from the scale of testing required to relax substantially social distancing measures without compromising health outcomes. At the time of writing, newspaper reports point to roughly 150 thousand tests per day in the United States. Additional health measures, such as capillary contact tracing could enhance the effectiveness of testing even if the wide scale implied by our calculations could not be achieved.

6 Conclusion

A precipitous decline in employment brought about by the spread of an infectious disease can increase economic costs non-linearly if it ends up compromising linkages in the production structure that are critical for the working of the economy as a whole. To explore the economics of this scenario, we specify a two-sector model featuring a set of industries that produce core inputs used by all the other industries. Essential to our result is that these core inputs are both poorly substitutable with other inputs, and produced subject to a minimum scale of production.

Once combined with an epidemiological model, our integrated assessment framework suggests that the way an unchecked spread of an epidemic can create vast damage to the economy is by

³² The cost estimate of \$100 in our calculations is based on the Medicare reimbursement rate for Covid-19 tests in force at the time of writing.

bringing the core industries to operate at their minimum scale—with the result of undermining efficient production in other sectors and thus aggregate economic activity. This is an argument for social distancing, on top of the argument stressing the need to reduce the loss of human life resulting from congestion overwhelming hospitals and health care systems.

In our model, the direct economic cost of the disease stems from the inability of symptomatic infected individuals to continue working. The indirect costs come from the constraint that malfunctioning core industries may place on other industries via input-output linkages. Social distancing measures modulated to shield essential economic linkages can buffet the fall in aggregate economic activity effectively and without compromising the primary goal of flattening the infection curve. The experiments we consider in this paper consist of applying social distancing measures to the non-working-age population, and to parts of the labor force—proportionately more to workers in non-core industries and to occupations that involve tasks that can be performed from home. These measures work through a key epidemiological externality that ends up protecting workers in the core industries.

Simulations of our integrated assessment model for infectious diseases suggest that even moderate public health restrictions may actually improve economic outcomes relative to inaction. Nonetheless, we reiterate that the goals of our analysis are specific and modest. There are many missing elements that would be required for a precise quantification and/or the assessment and design of optimal policy, and we shy away from the difficult task of assigning an economic value to the loss of life.

In particular, our stylized model abstracts from the endogenous fall in demand due to financial frictions and nominal rigidities. We also stress that we do not explicitly take into account issues in the congestion of the health care system. Given the range of current estimates for the parameters governing the epidemiological model, the least costly public health measures we consider in our baseline—keeping at home workers that can continue working from home, and extending a lockdown of the young and elderly in the same proportion as for the working population—seems unlikely to reduce the share of infected individuals to an extent sufficient to avoid overwhelming the health care system.

We attempt to offer some rough estimates of the cost of imposing lockdowns that can bring down the infection peak from the level implied by our baseline without intervention. We focus on measures that could keep the peak population share of infected individuals below 1.5 percent for

18 months. Our calculations point to a wide range of possible costs stemming from the reduction in labor supply. Depending on which parameters we use for the epidemiological segment of the model, the least costly social distancing measures we consider could avoid a reduction in labor supply altogether—but could also cause GDP losses as high as 40 percent of GDP for the duration of the wait. Because of the lingering uncertainty on the way the disease spreads, these estimates cannot be but useful blueprints for further analysis.

References

- Alfaro, L., A. Chari, A. N. Greenland, and P. K. Schott (2020). Aggregate and firm-level stock returns during pandemics, in real time. *Covid Economics, Vetted and Real Time Papers* 4, 2–24. [1]
- Allen, L. (1994). Some discrete-time SI, SIR, and SIS epidemic models. *Mathematical Bioscience* 124(1), 83–105. [6]
- Alvarez, F., D. Argente, and F. Lippi (2020). A Simple Planning Problem for COVID-19 Lockdown. Technical report, NBER working paper 26981. [1, 13, 24]
- Atkeson, A. (2020a). Lockdowns and gdp is there a tradeoff? Technical report. [3]
- Atkeson, A. (2020b). What Will be the Economic Impact of COVID-19 in the US? Rough Estimates of Disease Scenarios. Staff Report 595, Federal Reserve Bank of Minneapolis. [1, 13]
- Baker, S. R., N. Bloom, S. J. Davis, K. J. Kost, M. C. Sammon, and T. Viratyosin (2020). The unprecedented stock market impact of covid-19. Technical report, NBER Working Paper No. 26945. [1]
- Baker, S. R., R. Farrokhnia, S. Meyer, M. Pagel, and C. Yannelis (2020). How does household spending respond to an epidemic? consumption during the 2020 covid-19 pandemic. Technical report, NBER Working Paper No. 26949. [5]
- Barrot, J., B. Grassi, and J. Sauvagnat (2020). Sectoral Effects of Social Distancing. *Covid Economics* 1(3), 85–102. [2]
- Bodenstein, M., L. Guerrieri, and C. J. Gust (2013). Oil shocks and the zero bound on nominal interest rates. *Journal of International Money and Finance* 32(C), 941–967. [16]
- Brauer, F., P. Driessche, and J. Wu (2008). *Mathematical Epidemiology*. Number 1945 in Lecture Notes in Mathematics,. Springer, Berlin, Heidelberg. [4, 6]
- Carvalho, V. M. (2014). From Micro to Macro via Production Networks. *Journal of Economic Perspectives* 28(4), 23–48. [2]
- Carvalho, V. M. and A. Tahbaz-Salehi (2018). Production Networks: A Primer. Cambridge Working Papers in Economics 1856, Faculty of Economics, University of Cambridge. [2]
- Christiano, L. J., M. Eichenbaum, and C. L. Evans (2005). Nominal Rigidities and the Dynamic Effects of a Shock to Monetary Policy. *Journal of Political Economy* 113(1), 1–45. [15]
- Correia, S., S. Luck, and E. Verner (2020). Pandemics depress the economy, public health interventions do not: Evidence from the 1918 flu. Technical report, available at SSRN. [20]
- Eichenbaum, M. S., S. Rebelo, and M. Trabandt (2020). The Macroeconomics of Epidemics. NBER Working Papers 26882, National Bureau of Economic Research, Inc. [1, 9, 13, 19, 21]
- Farboodi, M., G. Jarosch, and R. Shimer (2020). Internal and external effects of social distancing in a pandemic. *Covid Economics, Vetted and Real-Time Papers* (9), 22–58. [18]

- Greenwood, J., P. Kircher, C. Santos, and M. Tertilt (2019). An equilibrium model of the african hiv/aids epidemic. *Econometrica* 87(4), 1081–1113. [9]
- Guerrieri, L. and M. Iacoviello (2015). OccBin: A toolkit for solving dynamic models with occasionally binding constraints easily. *Journal of Monetary Economics* 70(C), 22–38. [16]
- Guerrieri, V., G. Lorenzoni, L. Straub, and I. Werning (2020). Macroeconomic implications of covid-19: Can negative supply shocks cause demand shortages? Technical report, NBER Working Paper No. 26918. [1]
- Hethcote, H. (1989). Three Basic Epidemiological Models. In S. Levin, T. Hallam, and L. G. (eds) (Eds.), *Applied Mathematical Ecology. Biomathematics*. Springer, Berlin, Heidelberg. [6, 7]
- Jones, C., T. Philippon, and V. Venkateswaran (2020). Optimal Mitigation Policies in a Pandemic: Social Distancing and Working from Home . Technical report, NBER working paper 26984. [1]
- Jordà, O., S. R. Singh, and A. M. Taylor (2020). Longer-run economic consequences of pandemics. *Covid Economics, Vetted and Real-Time Papers* (1), 1–15. [5]
- Kermack, W. O. and A. G. McKendrick (1927). A contribution to the mathematical theory of epidemics. *Proceedings of the Royal Society A*(115), 700–721. [4]
- Koren, M. and R. Petó (2020). Business disruptions from social distancing. *Covid Economics, Vetted and Real-Time Papers* (2), 13–31. [1]
- Kremer, M. (1996). Integrating Behavioral Choice into Epidemiological Models of AIDS. *The Quarterly Journal of Economics* 111(2), 549–573. [9]
- Krueger, D., H. Uhlig, and T. Xie (2020). Macroeconomic dynamics and reallocation in an epidemic. *Covid Economics, Vetted and Real-Time Papers* (5), 21–55. [9]
- Magal, P., O. Seydi, and G. Webb (2016). Final size of an epidemic for a two-group sir model. *SIAM Journal on Applied Mathematics* 76(5), 2042–2059. [8]
- Moghadas, S. M., A. Shoukat, M. C. Fitzpatrick, C. R. Wells, P. Sah, A. Pandey, J. D. Sachs, Z. Wang, L. A. Meyers, B. H. Singer, and A. P. Galvani (2020). Projecting hospital utilization during the covid-19 outbreaks in the united states. Technical report, Proceedings of the National Academy of Sciences of the United States of America. [23, 25]
- Romer, P. and R. Shah (2020, April). Testing is our way out. The Wall Street Journal. [25]
- Russell, T. W., J. Hellewell, C. I. Jarvis, K. V. Zandvoort, S. Abbott, R. Ratnayake, S. Flasche, R. M. Eggo, W. J. Edmunds, and A. J. Kucharski (2020). Estimating the infection and case fatality ratio for covid-19 using age-adjusted data from the outbreak on the diamond princess cruise ship. Technical report, MedRxiv. [15]
- Smets, F. and R. Wouters (2007). Shocks and Frictions in US Business Cycles: A Bayesian DSGE Approach. *American Economic Review* 97(3), 586–606. [15]
- Stock, J. H. (2020). Data gaps and the policy response to the novel coronavirus. *Covid Economics, Vetted and Real-Time Papers* (3), 1–11. [25]

Table 1: Parameters for the Integrated Assessment Model

Parameter	Used to Determine	Parameter	Used to Determine
$\beta = 0.2$	contact rate (daily)	$\gamma = 1/20$	removal rate (daily)
$\varpi = 0$	death rate (daily)	$\vartheta = 1$	effectiveness social distancing
$\iota = 0.40$	share of symptomatic infectives	$N_1 = 0.25$	size Group 1
$N_2 = 0.40$	size Group 2	$N_3 = 0.35$	size Group 3
$v_1 = 0.15$	share working from home Sector/Group 1	$v_2 = 0.40$	share working from home Sector/Group 2
$\theta = 1 - \frac{4}{100}/12$	discount factor (monthly)	$\delta = \frac{1}{10}/12$	capital depreciation rate (monthly)
$\kappa = 0.6$	habit persistence	$\nu = 0.001$	elasticity capacity utilization
$\phi = 0$	degree of capital reversibility	$1 - \omega = 0.27$	quasi-share value added Sector 1
$\eta = 2$	scaling parameter Sector 1	$\chi = \frac{1}{2}N_1$	minimum scale Sector 1
$\rho = \frac{1}{1-1/3}$	substitution elasticity Sectors 1 and 2	$\alpha = 0.3$	share capital in production Sector 2

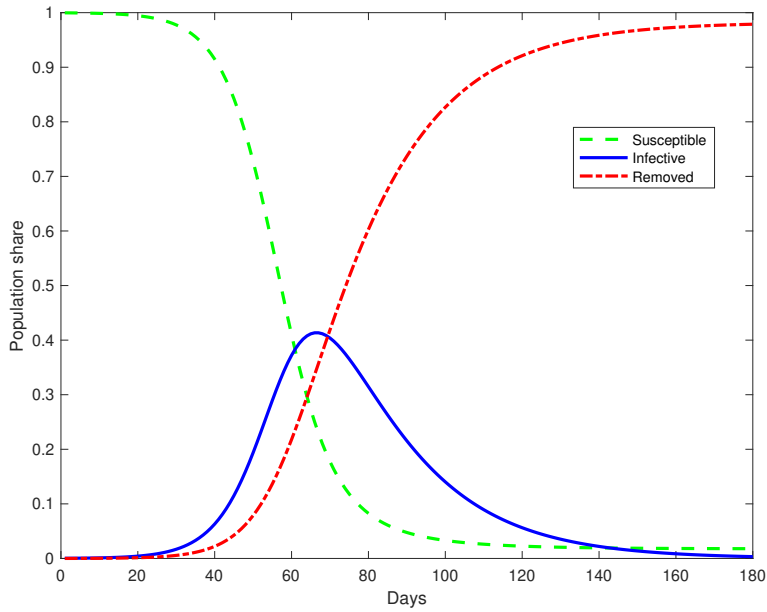
Note: This table summarizes the parameterization of the baseline integrated assessment model.

Table 2: The Core Sector: Share of GDP and of Employment

Line	Sector	Value Added,\$ bn.	Percent of GDP	Percent of Employment
3	Agriculture, forestry, fishing, and hunting	166.5	0.81	2.65
10	Utilities	325.9	1.58	0.52
26	Food and beverage and tobacco products	268.9	1.31	1.86
31	Petroleum and coal products	172.2	0.84	0.12
37	Food and beverage stores	156.4	0.76	2.2
40	Transportation and warehousing	658.1	3.2	5.27
76	Health care and social assistance	1536.9	7.47	8.66
91	Federal government, general services	729.0	3.54	0.88
96	State government, general services	1600.5	7.78	15.38
	Total	5614.4	27.29	37.56

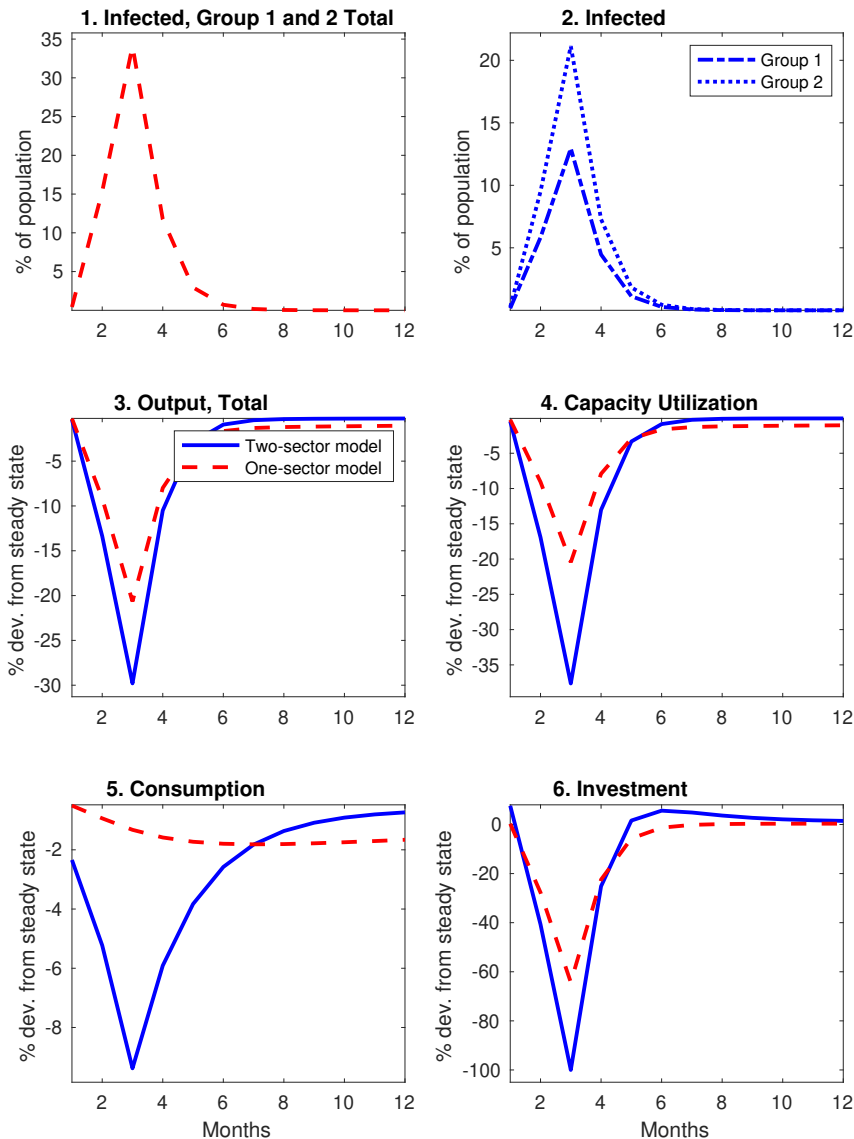
Source: Authors' calculations based on Bureau of Economic Analysis, GDP by Industry, and Bureau of Labor Statistics, Productivity Release.

Figure 1: Dynamics in the SIR Model



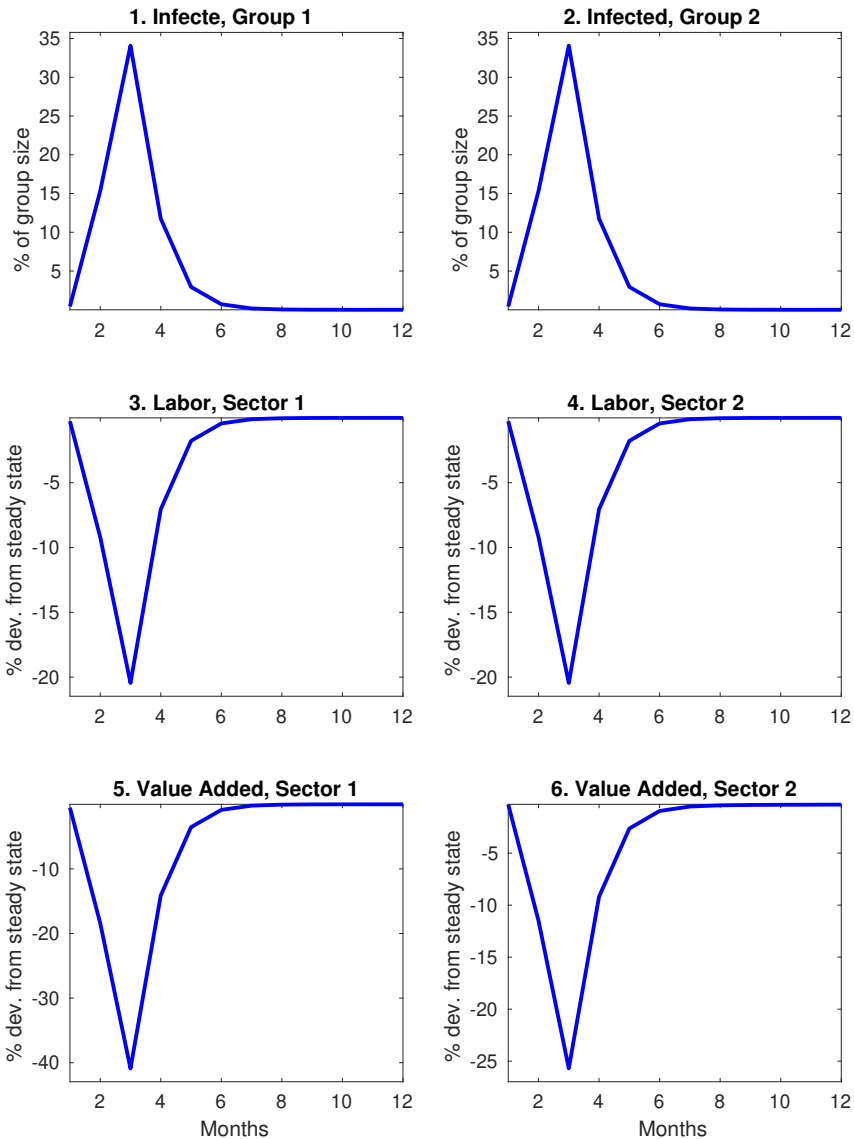
Note: The paths shown are for the total population. The parameters β and γ are 0.2 and 1/20, respectively, implying that R_0 is 4. The contact rates are assumed to be identical across groups.

Figure 2: Aggregate Economic Consequences of COVID-19 Without Social Distancing: Comparing One-Sector and Two-Sector Modeling Approaches



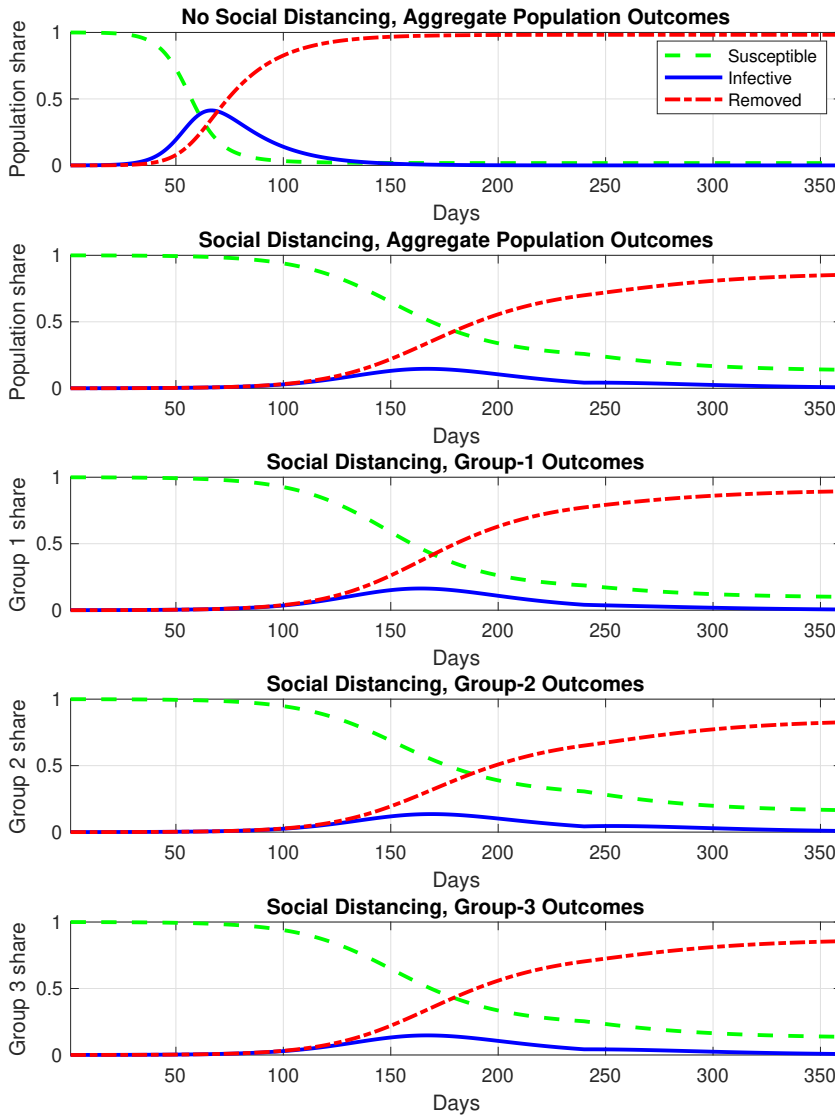
Note: In this figure, we assume that no social distancing measures are taken to reduce the spread of the disease. The economic costs stem from the reduction in labor supply from symptomatic infected individuals. Based on the case study for the Diamond Princess cruise ship, we assume that 40 percent of individuals of working age would be asymptomatic when infected and, in the absence of widespread testing, would continue working.

Figure 3: Sectoral Economic Consequences of COVID-19 Without Social Distancing



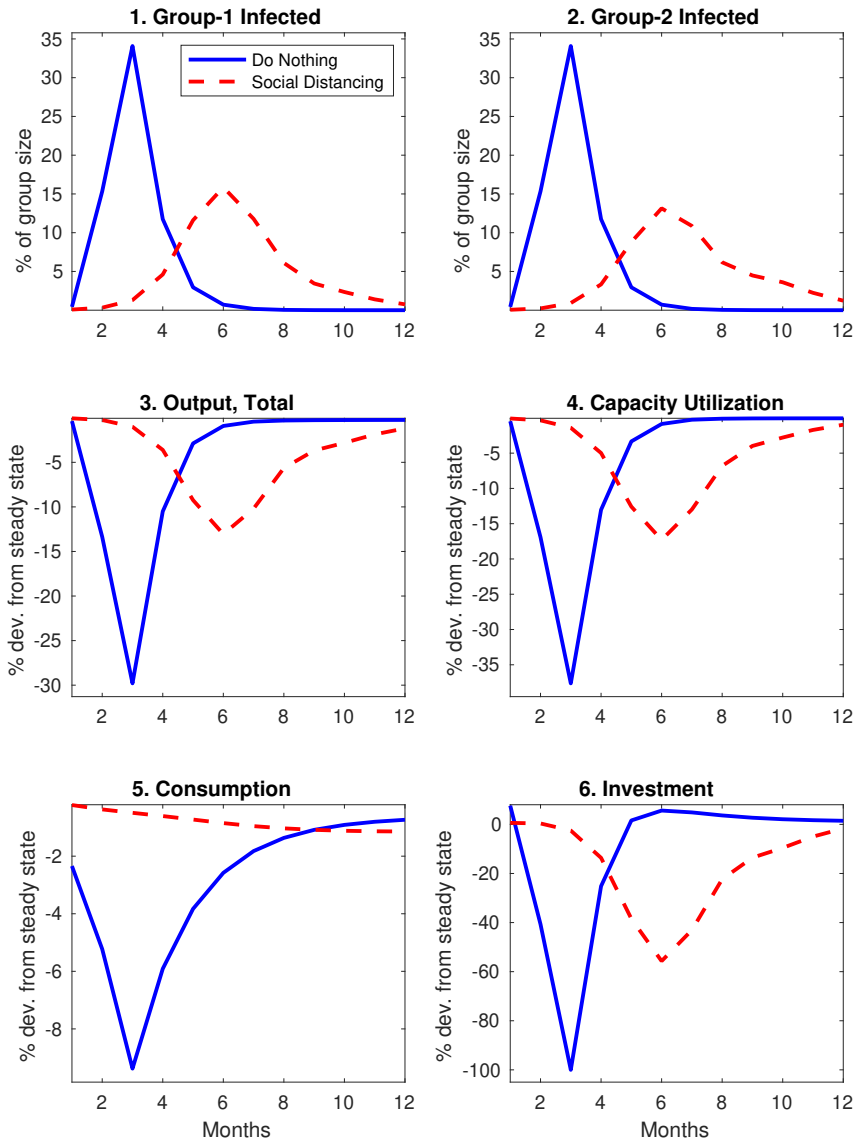
Note: This figure provides additional sectoral details for the two-sector model, complementing the paths for aggregate variables shown in Figure 2.

Figure 4: Dynamics in the Three-Group SIR Model



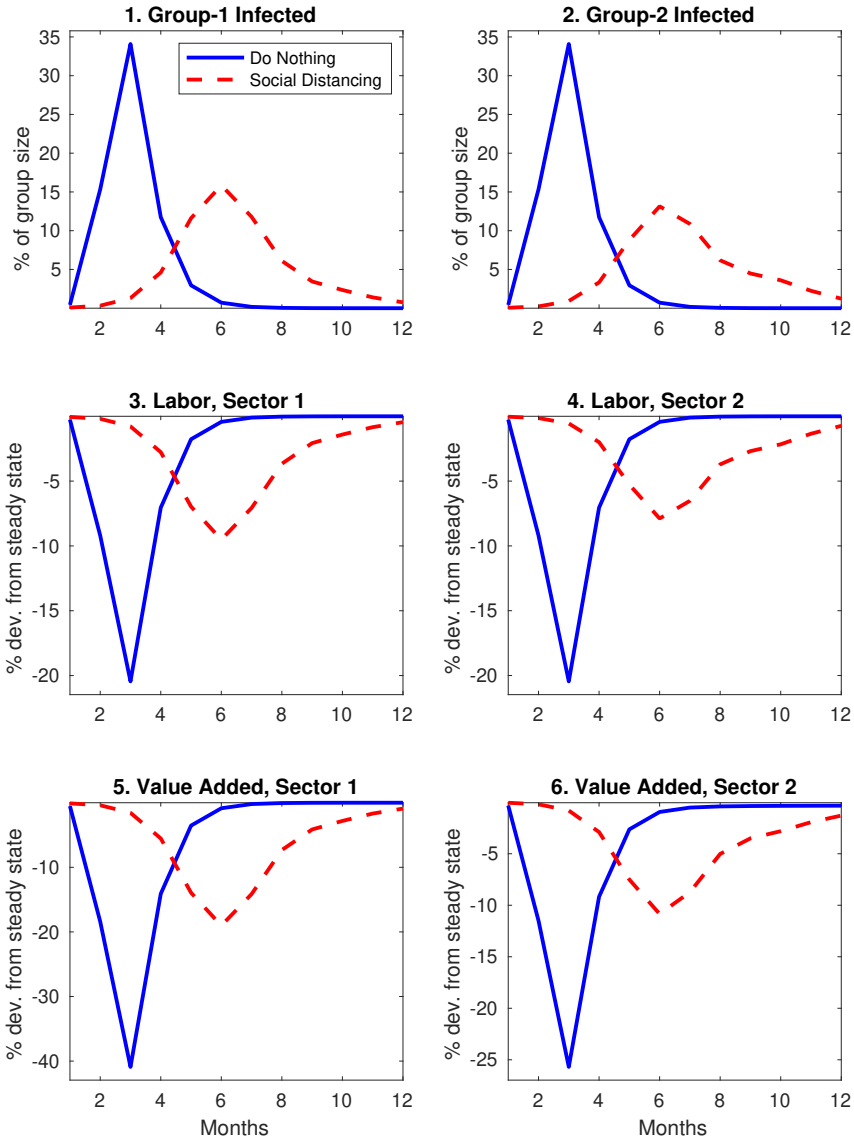
Note: The top panel presents the aggregate output of our three-group SIR model for the case of no intervention. The other panels pertain to a health policy that locks down individuals in Group 1 and Group 2 who can continue working from home (15 and 40 percent, respectively), and individuals in Group 3, who are not in the labor force, in the same proportion as for the overall population (about 30 percent). To avoid a resurgence of the disease, the lockdowns last 8 months.

Figure 5: Comparing the Aggregate Economic Consequences of COVID-19 with and Without Social Distancing: A Two-Sector Approach



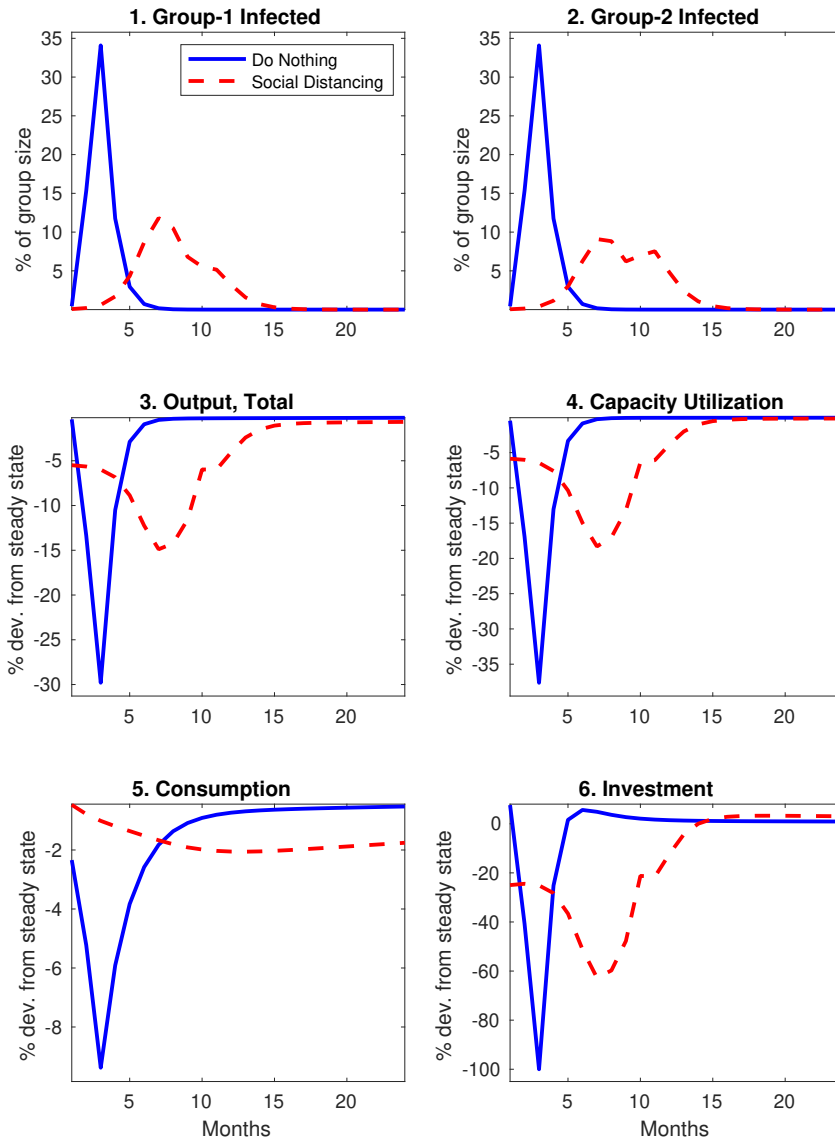
Note: This figure compares the economic consequences of no health policy intervention and of the social distancing policy whose health outcomes are more fully illustrated in Figure 4. The health policy considered here locks down individuals in groups 1 and 2 who can continue working from home (15 and 40 percent, respectively) and are assumed to be equally productive at home. Individuals in Group 3, those who are not in the labor force, are locked down in the same proportion as for the overall population (about 30 percent). To avoid a resurgence of the disease, the lockdowns last 8 months.

Figure 6: Comparing the Sectoral Economic Consequences of COVID-19 with and Without Social Distancing



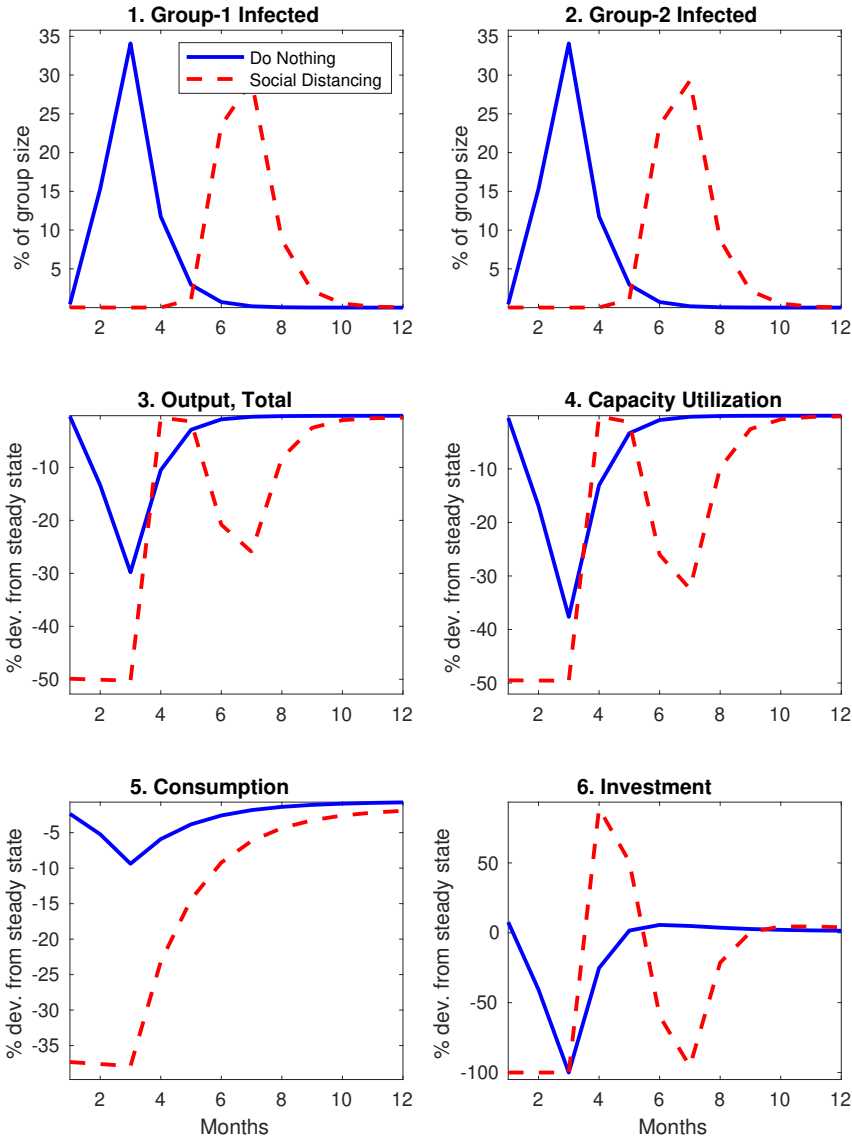
Note: This figure provides additional sectoral details for the two-sector model, complementing the paths for aggregate variables shown in Figure 5

Figure 7: More Aggressive Social Distancing Measures



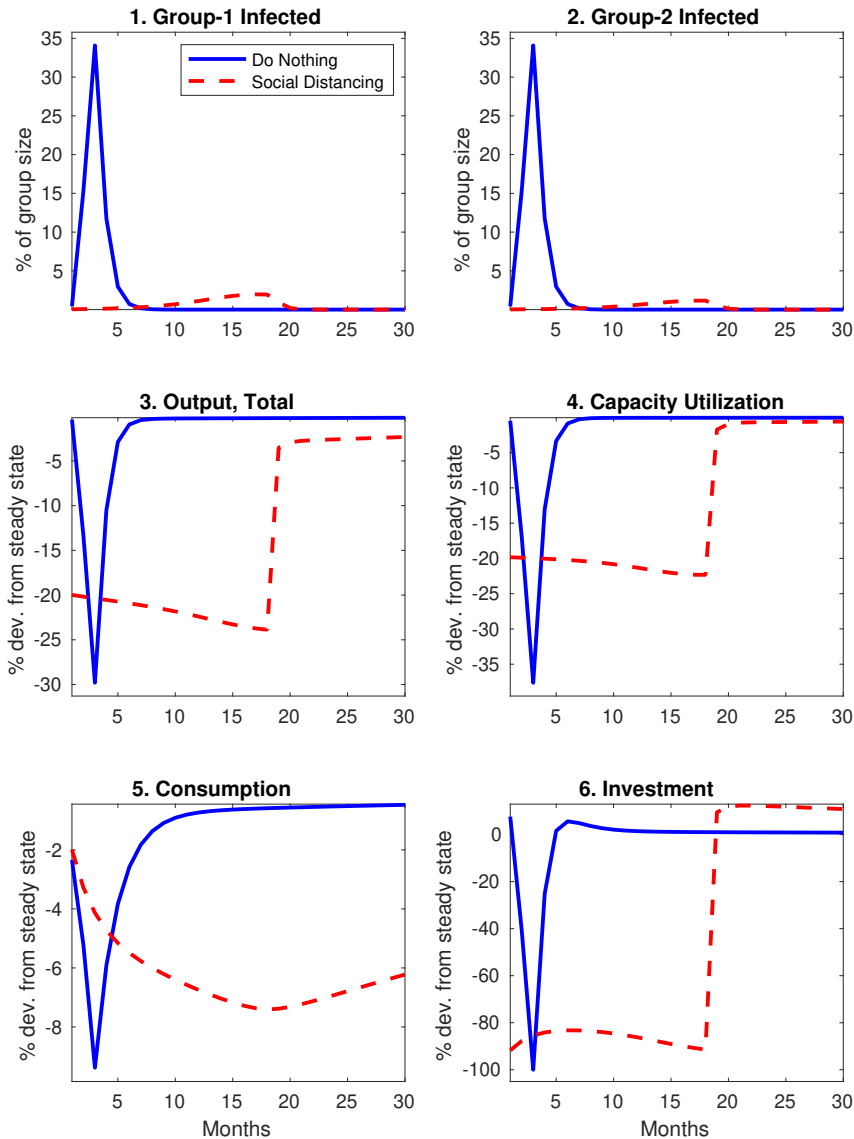
Note: The health policy considered locks down 18 percent of individuals in Group 1 and 45 percent in Group 2, increases of 3 and 5 percentage points, respectively, relative to the case of Figure 5. Individuals in Group 3, who are not in the labor force, continue to be locked down in the same proportion as for Groups 1 and 2 combined (about 35 percent, compared with 30 percent for the previous case). To avoid a resurgence of the disease, the lockdowns last 9 months, one month longer than for the previous case.

Figure 8: Social Distancing Gone Wrong



Note: Under the health policy considered, 40 percent of individuals in Group 1 and 90 percent of individuals in both Group 2 and Group 3 are locked down for a period of 3 months, after which, all measures are lifted.

Figure 9: Waiting for a Vaccine



Note: To keep the peak share of infected individuals below 1.5 percent of the population, we set lockdown shares of 25, 60, and 47 percent for Groups 1, 2, and 3, respectively (note that the lockdown share for Group 3 is the same as for the overall population). The lockdown shares in Groups 1 and 2 were chosen to align the reduction in value added across the two economic sectors, compressing the decline in aggregate output. A vaccine that is perfectly effective is assumed to become available after 18 months.

A Additional Details for the Two-Sector Model

This appendix derives the equilibrium conditions for the two-sector model and the steady-state condition. Finally, it also shows the derivation of the elasticity of substitution between the two factor inputs in the production function for final output goods.

A.1 Equilibrium conditions

Households maximize

$$\begin{aligned} & \max_{c_t, \lambda_{c,t}, i_t, k_t, \lambda_{k,t}, u_t, \lambda_{i,t}} E_t \sum_{i=0}^{\infty} \beta^i [\log(c_{t+i} - \kappa c_{t+i-1}) \\ & + \lambda_{c,t+i} (-c_{t+i} - i_{t+i} + w_{1,t+i} l_{1,t+i} + w_{2,t+i} l_{2,t+i} + r_{k,t+i} u_t k_{t+i-1} - \nu_0 \frac{u_t^{1+\nu}}{1+\nu}) \\ & + \lambda_{k,t+i} (-k_{t+i} + (1-\delta)k_{t+i-1} + i_{t+i}) + \lambda_{i,t+i} (i_t - \phi i)] . \end{aligned}$$

These are the first-order conditions from the households' problem:

$$\frac{1}{c_t - \kappa c_{t-1}} - \theta \kappa E_t \frac{1}{c_{t+1} - \kappa c_t} = \lambda_{c,t}, \quad (25)$$

$$c_t + i_t = w_{1,t} l_{1,t} + w_{2,t} l_{2,t} + r_{k,t} k_{t-1}, \quad (26)$$

$$\lambda_{c,t} = \lambda_{k,t} + \lambda_{i,t+i}, \quad (27)$$

$$E_t \lambda_{c,t+1} r_{k,t+1} u_{t+1} - \lambda_{k,t} + \theta(1-\delta) E_t \lambda_{k,t+1} = 0, \quad (28)$$

$$k_t = (1-\delta)k_{t-1} + i_t, \quad (29)$$

$$\lambda_{c,t} r_{k,t} k_{t-1} = \lambda_{c,t} \nu_0 u_t^\nu, \quad (30)$$

and the complementary slackness condition

$$\lambda_{i,t+i} (i_t - \phi i) = 0. \quad (31)$$

Firms in Sector 1 solve this cost-minimization problem

$$\min_{l_t^1} w_t l_t^1 + p_t^1 [v^1 - \eta (l_t^1 - \nu)]$$

And from the production function, we also have that

$$v_{1,t} = \max [\eta (l_{1,t} - \chi), 0] \quad (32)$$

and that

$$w_t = \eta p_{1,t}. \quad (33)$$

Firms in Sector 2 solve this cost-minimization problem

$$\begin{aligned} & \min_{u_t k_{t-1}, l_{2,t}, v_{1,t}} r_{k,t} u_t k_{t-1} + w_{2,t} l_{2,t} + p_{1,t} v_{1,t} \\ & + \left[y_t - \left((1-\omega)^{\frac{\rho}{1+\rho}} (v_{1,t})^{\frac{1}{1+\rho}} + \omega^{\frac{\rho}{1+\rho}} ((u_t k_{t-1})^\alpha (l_{2,t})^{1-\alpha})^{\frac{1}{1+\rho}} \right)^{1+\rho} \right] \end{aligned}$$

Appendix

Notice that firms choose $u_t k_{t-1}$ as if it were a single input, representing capital services. The first-order conditions for this problem are:

$$r_{k,t} - (1 + \rho) \left((1 - \omega)^{\frac{\rho}{1+\rho}} (v_{1,t})^{\frac{1}{1+\rho}} + \omega^{\frac{\rho}{1+\rho}} (k_{t-1}^\alpha l_{2,t}^{1-\alpha})^{\frac{1}{1+\rho}} \right)^\rho \\ \frac{1}{1+\rho} \omega^{\frac{\rho}{1+\rho}} ((u_t k_{t-1})^\alpha l_{2,t}^{1-\alpha})^{\frac{1}{1+\rho}-1} \alpha (u_t k_{t-1})^{\alpha-1} l_{2,t}^{1-\alpha} = 0.$$

Notice that $y^x = \left((1 - \omega)^{\frac{\rho}{1+\rho}} (v_{1,t})^{\frac{1}{1+\rho}} + \omega^{\frac{\rho}{1+\rho}} ((u_t k_{t-1})^\alpha l_{2,t}^{1-\alpha})^{\frac{1}{1+\rho}} \right)^{(1+\rho)x}$. Find x , such that $x(1 + \rho) = \rho$. That is $x = \frac{\rho}{1+\rho}$. Accordingly,

$$r_{k,t} - y^{\frac{\rho}{1+\rho}} \omega^{\frac{\rho}{1+\rho}} (v_{2,t})^{-\frac{\rho}{1+\rho}} \alpha \frac{v_{2,t}}{u_t k_{t-1}} = 0.$$

Which can be further simplified as

$$r_{k,t} = \alpha \left(\omega \frac{y_t}{v_{2,t}} \right)^{\frac{\rho}{1+\rho}} \frac{v_{2,t}}{u_t k_{t-1}}. \quad (34)$$

$$w_{2,t} = (1 - \alpha) \left(\omega \frac{y_t}{v_{2,t}} \right)^{\frac{\rho}{1+\rho}} \frac{v_{2,t}}{l_{2,t}}. \quad (35)$$

$$p_{1,t} - (1 + \rho) \left((1 - \omega)^{\frac{\rho}{1+\rho}} (v_{1,t})^{\frac{1}{1+\rho}} + \omega^{\frac{\rho}{1+\rho}} ((u_t k_{t-1})^\alpha l_{2,t}^{1-\alpha})^{\frac{1}{1+\rho}} \right)^\rho \frac{1}{1 + \rho} (1 - \omega)^{\frac{\rho}{1+\rho}} (v_{1,t})^{\frac{1}{1+\rho}-1} = 0.$$

Simplifying

$$p_{1,t} - y^{\frac{\rho}{1+\rho}} (1 - \omega)^{\frac{\rho}{1+\rho}} (v_{1,t})^{-\frac{\rho}{1+\rho}} = 0. \\ p_{1,t} = \left(\frac{(1 - \omega) y}{v_{1,t}} \right)^{\frac{\rho}{1+\rho}}. \quad (36)$$

And from the production function,

$$y_t = \left((1 - \omega)^{\frac{\rho}{1+\rho}} (v_{1,t})^{\frac{1}{1+\rho}} + \omega^{\frac{\rho}{1+\rho}} (v_{2,t})^{\frac{1}{1+\rho}} \right)^{1+\rho} \quad (37)$$

and where

$$v_{2,t} = (u_t k_{t-1})^\alpha l_{2,t}^{1-\alpha}. \quad (38)$$

And from the budget constraint we can derive that the goods market must clear

$$y_t = c_t + i_t + \nu_0 \frac{u_t^{1+\nu}}{1 + \nu}.$$

The 13 equations above allow us to determine 14 variables y_t , $v_{1,t}$, $v_{2,t}$, c_t , i_t , k_t , u_t , $\lambda_{c,t}$, $\lambda_{i,t}$, $\lambda_{k,t}$, $p_{1,t}$, $w_{1,t}$, $w_{2,t}$, $r_{k,t}$, with $l_{1,t}$ and $l_{2,t}$ determined by exogenous processes.

A.2 Steady-State Conditions

Set $u_t = 1$ and later set ν_0 to support this choice. Notice that the investment constraint must be slack in the steady state, so

Appendix

$$\lambda_i = 0. \quad (39)$$

Using

$$\lambda_{c,t} = \lambda_{k,t} + \lambda_{i,t},$$

and $\lambda_{c,t}r_{k,t} - \lambda_{k,t} + \theta(1 - \delta)E_t\lambda_{i,t+1} = 0$, we can see that

$$r_k = 1 - \theta(1 - \delta). \quad (40)$$

Using

$$r_k = \alpha \left(\omega \frac{y}{v_2} \right)^{\frac{\rho}{1+\rho}} \frac{v_2}{k} \quad (41)$$

and combining it with $r_k = 1 - \theta(1 - \delta)$, we can use a numerical solver to get k , given l_1 and l_2 .

Knowing k , and with

$$v_1 = \eta(l_1 - \chi), \quad (42)$$

we can solve for y using the production function

$$y = \left((1 - \omega)^{\frac{\rho}{1+\rho}} (v_1)^{\frac{1}{1+\rho}} + \omega^{\frac{\rho}{1+\rho}} (k^\alpha (l_2)^{1-\alpha})^{\frac{1}{1+\rho}} \right)^{1+\rho} \quad (43)$$

From $k_t = (1 - \delta)k_{t-1} + i_t$, we have that

$$i = \delta k \quad (44)$$

Using $\lambda_{c,t}r_{k,t}k_{t-1} = \lambda_{c,t}\nu_0 u'_t$, find the value of ν_0 that ensures $u = 1$. Accordingly

$$\nu_0 = r_k k \quad (45)$$

And using the resource constraint, we can solve for c

$$c = y - i - \nu_0 \frac{u_t^{1+\nu}}{1 + \nu} \quad (46)$$

$$\lambda_c = \frac{1}{(1 - \kappa)c} - \theta\kappa \frac{1}{(1 - \kappa)c}. \quad (47)$$

$$\lambda_k = \lambda_c \quad (48)$$

$$p_1 = \left(\frac{(1 - \omega)y}{l_1} \right)^{\frac{\rho}{1+\rho}} \quad (49)$$

$$w_1 = \eta p_1 \quad (50)$$

$$v_2 = k^\alpha (l_2)^{1-\alpha} \quad (51)$$

$$w_2 = (1 - \alpha) \left(\omega \frac{y}{v_2} \right)^{\frac{\rho}{1+\rho}} \frac{v_2}{l_2} \quad (52)$$

A.3 Deriving the Elasticity of Substitution for the Production Function of Sector 2

$$y_t = \left((1 - \omega)^{\frac{\rho}{1+\rho}} (v_{1,t})^{\frac{1}{1+\rho}} + \omega^{\frac{\rho}{1+\rho}} (v_{2,t})^{\frac{1}{1+\rho}} \right)^{1+\rho}$$

$$\frac{\partial y_t}{\partial v_{1,t}} = (1 + \rho) \left((1 - \omega)^{\frac{\rho}{1+\rho}} (\eta(l_{1,t} - \nu))^{\frac{1}{1+\rho}} + \omega^{\frac{\rho}{1+\rho}} (v_{2,t})^{\frac{1}{1+\rho}} \right)^{\rho} \frac{1}{1 + \rho} (1 - \omega)^{\frac{\rho}{1+\rho}} (v_{1,t})^{\frac{1}{1+\rho} - 1}$$

Notice again that $y^x = \left((1 - \omega)^{\frac{\rho}{1+\rho}} (\eta(l_{1,t} - \nu))^{\frac{1}{1+\rho}} + \omega^{\frac{\rho}{1+\rho}} (v_{2,t})^{\frac{1}{1+\rho}} \right)^{(1+\rho)x}$. Find x , such that $x(1 + \rho) = \rho$. That is $x = \frac{\rho}{1+\rho}$. Accordingly,

$$\frac{\partial y_t}{\partial v_{1,t}} = y^{\frac{\rho}{1+\rho}} (1 - \omega)^{\frac{\rho}{1+\rho}} \eta (v_{1,t})^{-\frac{\rho}{1+\rho}}$$

$$\frac{\partial y_t}{\partial v_{2,t}} = y^{\frac{\rho}{1+\rho}} (\omega)^{\frac{\rho}{1+\rho}} (v_{2,t})^{-\frac{\rho}{1+\rho}}$$

$$\frac{\frac{\partial y_t}{\partial v_{1,t}}}{\frac{\partial y_t}{\partial v_{2,t}}} = \frac{(1 - \omega)^{\frac{\rho}{1+\rho}} (v_{1,t})^{-\frac{\rho}{1+\rho}}}{(\omega)^{\frac{\rho}{1+\rho}} (v_{2,t})^{-\frac{\rho}{1+\rho}}}$$

$$\log \frac{\frac{\partial y_t}{\partial v_{1,t}}}{\frac{\partial y_t}{\partial v_{2,t}}} = \log \left(\frac{(1 - \omega)^{\frac{\rho}{1+\rho}} (v_{1,t})^{-\frac{\rho}{1+\rho}}}{(\omega)^{\frac{\rho}{1+\rho}} (v_{2,t})^{-\frac{\rho}{1+\rho}}} \right) = \log \left(\frac{(1 - \omega)^{\frac{\rho}{1+\rho}}}{(\omega)^{\frac{\rho}{1+\rho}}} \right) + \frac{\rho}{1 + \rho} \log \frac{v_{2,t}}{v_{1,t}}$$

The elasticity is given by

$$Elast = \frac{d \log(v_{2,t}/v_{1,t})}{d \log(\frac{\partial y_t}{\partial v_{1,t}} / \frac{\partial y_t}{\partial v_{2,t}})} = \frac{1 + \rho}{\rho}$$

Therefore to hit a desired elasticity set ρ as

$$\rho Elast - \rho = 1$$

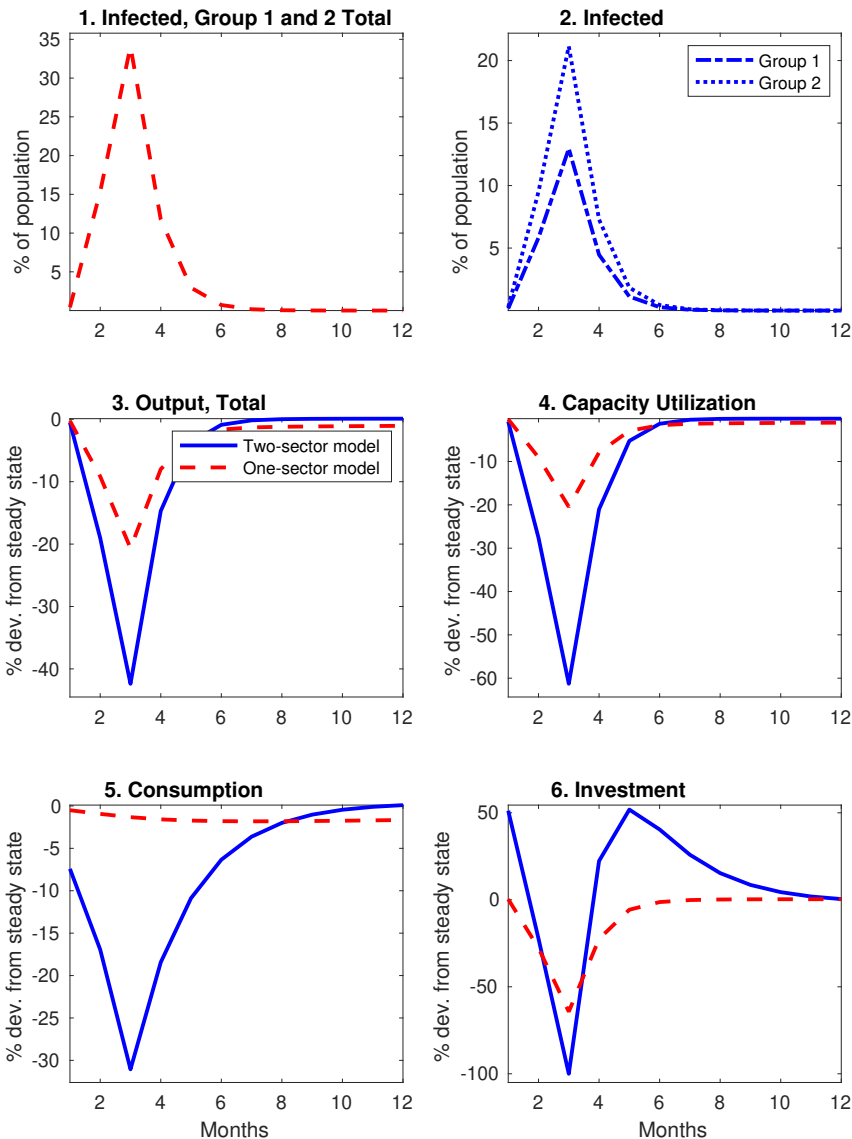
$$\rho = \frac{1}{Elast - 1}.$$

B Additional Sensitivity Analysis

Figures A.1 and A.2 offer sensitivity analysis pertaining to the comparison on the economic effects of the Spread of COVID-19 without any social distancing measures. The compare the economic effects using one- and two-sector models. Figure A.1 shows dynamic responses analogous to those in Figure 2, but increases the minimum scale parameter χ from one-half of the steady state labor supply to six-tenths. Figure A.2 considers sensitivity to a range of values of the contact rate parameter, β . It shows that the differences between the one- and two-sector models persist as long as the contact rate does not drop below about 0.075, a level that would also curtail the spread of the disease.

Figures A.3 and A.4 complement the discussion of the cost of waiting for a vaccine offered in Section 4.3.3. They pertain, respectively, to sensitivity analysis to the effectiveness of the lockdown and to the share to of the population to which the lockdown applies.

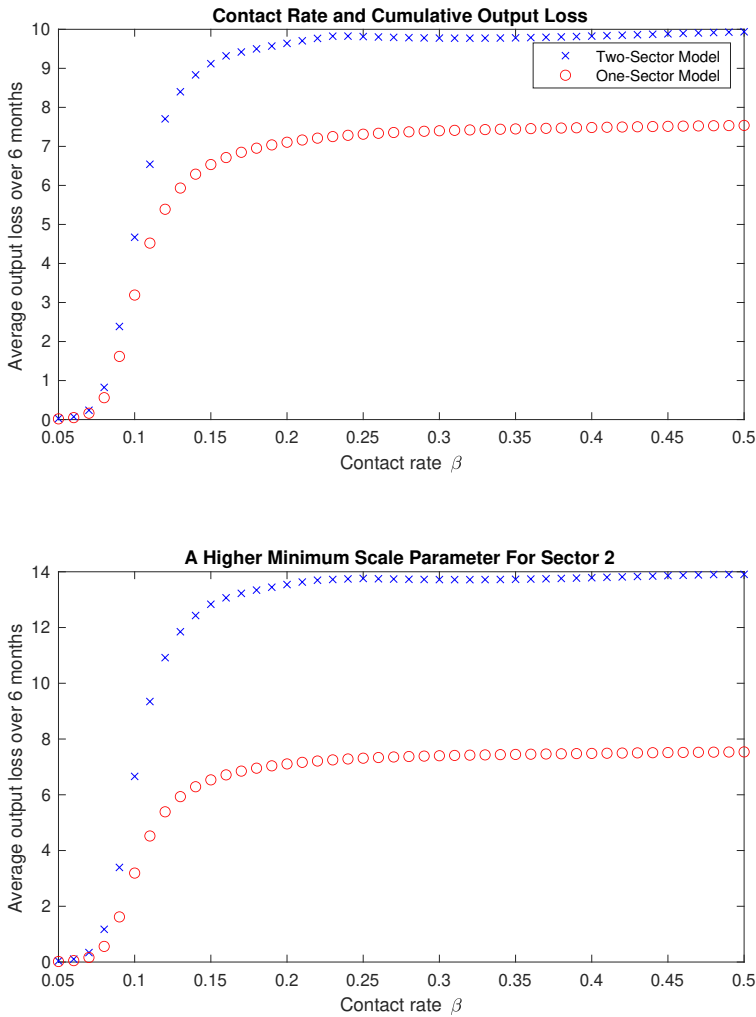
Figure A.1: Aggregate Economic Consequences of COVID-19 Without Social Distancing: An Increase in the Minimum Scale of Sector 1



Note: We assume that no social distancing measures are taken to reduce the spread of the disease. The output loss stems from the reduction in labor supply from symptomatic infected individuals. For the case shown here, we have increased the minimum scale parameter for Sector 1, χ , to five-sixths of the steady state labor input, as opposed to one-half in the baseline calibration.

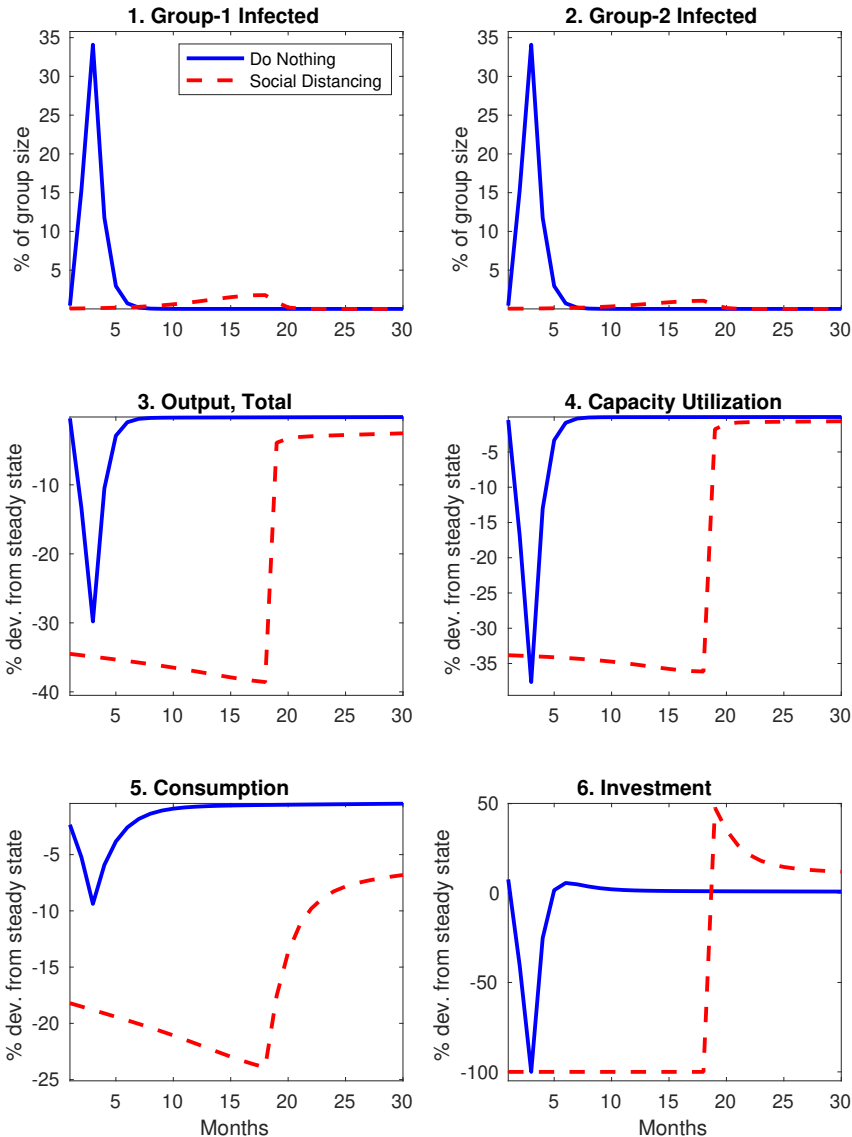
Appendix

Figure A.2: Comparing the Aggregate Economic Consequences of COVID-19 Without Social Distancing in One- and Two-Sector Models: Sensitivity to the Contact Rate



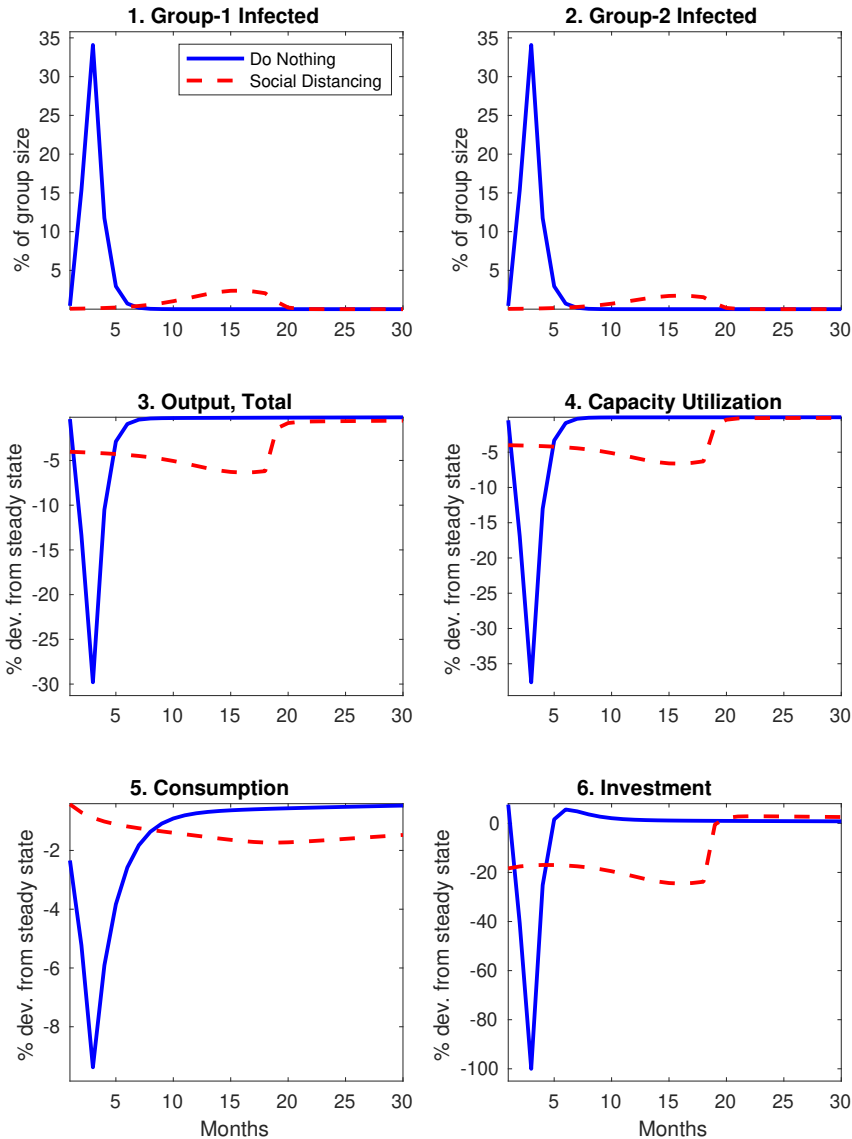
Note: We assume that no social distancing measures are taken to reduce the spread of the disease. The output loss stems from the reduction in labor supply from symptomatic infected individuals. The figure shows the cumulative output loss over six months alternatively based on one- and two-sector models for different values of β (set at 0.2 in our baseline). The top panel keeps all other parameters at their baseline values. For the bottom panel, we have increased the minimum scale parameter for Sector 1, χ , to five-sixths of the steady state labor input, as opposed to one-half in the baseline calibration.

Figure A.3: Waiting for a Vaccine: Assuming a Lower Effectiveness of the Lockdown at Reducing Contact Rates



Note: We model the reduction in effectiveness by setting ϑ to 0.8. Raising the share of individuals in Groups 1, 2 and 3 to 32, 75, and 59 percent, respectively, as considered here, can keep the share of infective individuals below 1.5 percent while waiting for a vaccine for 18 months.

Figure A.4: Waiting for a Vaccine



Note: The alternative policy considered extends the lockdown to 80 percent of individuals outside the labor force, those in Group 3 (with an effectiveness parameter ϑ equal to 1). This change would achieve the target of a 1.5 percent share of infected individuals even with a reduction of the shares of individuals in Groups 1 and 2 under lockdown to 17 and 44 percent, respectively.

The effect of containment measures on the COVID-19 pandemic¹

Pragyan Deb,² Davide Furceri,³ Jonathan D. Ostry⁴
and Nour Tawk⁵

Date submitted: 10 May 2020; Date accepted: 14 May 2020

Since the first outbreak was reported in Wuhan, China in late-December 2019, the 2019 coronavirus disease (COVID-19) has spread to over 200 countries/territories globally. In response, many countries have implemented several containment measures to halt the spread of the virus and limit the number of fatalities. It remains unclear the extent to which these unprecedented measures have been successful. The paper examines this question using daily data on the number of COVID-19 cases and deaths as well as on real-time containment measures implemented by countries around the world. Results suggest that containment measures have been, on average, very effective in flattening the “pandemic curve” and reducing the number of fatalities. These effects have been stronger in countries where containment measures have been implemented faster and have resulted in less mobility—de facto, more social distancing—and in those with lower temperatures, lower population density, a larger share of an elderly population and stronger health systems. Among different types of containment measures, stay-at-home orders seems to have been more effective in reducing the number of deaths.

¹ The views expressed in this paper are those of the authors and do not necessarily represent those of the IMF or its member countries. We would like to thank Naihan Yang for excellent research assistance.

² Economist, IMF.

³ Deputy Division Chief, IMF and University of Palermo.

⁴ Deputy Director, IMF and CEPR.

⁵ Economist, IMF.

Copyright: Pragyan Deb, Davide Furceri, Jonathan D. Ostry and Nour Tawk

I. INTRODUCTION

Since the outbreak was first reported in Wuhan, China in late-December 2019, the corona virus disease (COVID-19) has spread to over 200 countries and territories globally (Figure 1, panel A). As of May 11, more than 4 million cases have been confirmed, resulting in nearly 300 thousand deaths.

In the absence of a vaccine or effective treatments, many countries have responded by implementing several non-pharmaceutical interventions to halt the spread of the virus and limit the number of fatalities. Interventions included improved diagnostic testing and contact tracing, isolation and quarantine for infected people, and most notably measures aimed at reducing mobility and creating social distancing (containment measures, hereafter). While the extent and type of containment measures introduced varies across countries, most countries have introduced a combination of: (i) school closures; (ii) workplace closures; (iii) cancellation of public events; (iv) restrictions on size of gatherings ; (v) closures of public transport; (vi) stay-at-home orders; (vii) restrictions on internal movement; (viii) restrictions on international travel. Figure 1 (panel B) presents the broad patterns of containment measures across time and country groups, based on a composite index of these measures (see next section for detail).

To date, it remains unclear the extent to which these unprecedented measures have been successful and what would have been the number of cases and fatalities in the absence of these interventions. Indeed, despite significant theoretical contributions on the topic, to the best of our knowledge, the quantitative effect of these measures has not yet been examined, beyond China (see next section for a brief review). We try to address this gap by using daily data on the number of COVID-19 cases and deaths as well as on real-time containment measures implemented by 129 countries around the world.

Establishing causality is difficult in this context because, as illustrated in Figure 1, countries have introduced containment measures in response to the spread of the virus. This implies that addressing causality requires the researcher to effectively control for this endogenous response. Failure to control for possible reverse causality would result in estimates of the effect of containment measures on infections and deaths being upward biased—that is, toward *not* finding significant effectiveness.

We address this issue by controlling for the change in the number of infected cases (or deaths) occurring in the day before the implementation of containment measures. Given lags in the implementation of interventions at daily frequency, this allows one to effectively control for the endogenous response of containment measures to the spread of the virus. To further account for expectations about the country-specific evolution of the pandemic, we also control for country-specific linear, quadratic, and cubic time trends.

Results suggest that containment measures have been, on average, very effective in flattening the “pandemic curve” and reducing the number of fatalities. These effects have been stronger in countries where containment measures have been implemented faster and have resulted in more “de facto” social distancing and in those with lower temperatures, lower population density, a larger share of elderly population, and stronger health systems. Across different types of containment measure, stay-at-home orders seem to have been most effective in limiting the number of deaths.

The remainder of the paper is structured as follows. Section II provides a brief review of the rapidly growing literature on the effect on containment measures on the COVID-19 pandemic. Section III describes the data and econometric methodology. Section IV presents our results on the effect of containment measures on COVID-19 cases and fatalities, and how these

effects vary across countries (depending on country-specific characteristics) and type of containment measure. The last section concludes.

II. RELATED LITERATURE

The literature on the effectiveness of containment measures is rapidly expanding. The empirical strand of these studies focuses on the impact of measures in China. Kraemer *et al.* (2020) match real-time mobility data from Wuhan with detailed case data of travel history to showcase the role of mobility in the transmission of COVID-19 across cities in China, as well as the impact of control measures on the spread of the epidemic. They find that while mobility played a large role in the spread of the virus initially, after the implementation of control measures, the correlation between infection growth rates and mobility dropped significantly.

Chinazzi *et al.* (2020) use a global metapopulation disease model to project the impact of travel restrictions on the spread of COVID-19. The model estimates that while travel restrictions reduced case importations outside China significantly, they would not impact the trajectory of the pandemic if they are not combined with a reduction in the transmissibility of the disease.

H. Tian *et al.* (2020) investigate the role of the Wuhan travel ban and public health non-pharmaceutical interventions (NPI) in China on the reproduction number (R_0) of COVID-19, using a geocoded repository of COVID-19 data. They find that the reproduction number fell significantly after travel restrictions and public health interventions were implemented.

Cowling *et al.* (2020) use cross-sectional telephone surveys to model social behavior towards COVID-19 in Hong Kong SAR, and then examine the impact of NPIs and social behavior on COVID-19 transmission. They find that social distancing measures and behavioral

changes coincided with a substantial drop in influenza transmission in February 2020, which suggests a similar impact on COVID-19 transmission rates.

Modelling approaches have also been used to understand the impact of containment measures. Eichenbaum, Rebelo and Trabandt (2020) extend the classic SIR model by Kermack and McKendrick (1927) to study the equilibrium interactions between economic decisions and the dynamics of epidemics. Their model finds that, while people's decisions to cut back on work and consumption reduce fatalities, they exacerbate the recession during an epidemic.

Forslid and Herzing (2020) use a basic epidemiologic model calibrated to resemble COVID-19 dynamics to study the implications of quarantines. They find that the implementation of early quarantine can delay but not alter the course of a pandemic, while delaying quarantine reduces both deaths and economic costs but results in a higher peak infection.

Brotherhood et al. (2020) calibrate a standard SIR epidemiological model to investigate the role of testing and quarantine measures. They find that imposing restrictions for the young (given limited mobility of the elderly) can prolong the epidemic as herd immunity is delayed and expose the elderly to extended periods of risk. They also find that testing and quarantine would significantly reduce infections, even if only targeted to the young, who are highly mobile. Finally, their results suggest that quarantines are most efficient close to when a vaccine is in place, so that the disease has a lower chance of rebounding.

III. DATA AND METHODOLOGY

A. Data

We assemble a comprehensive daily database across many areas.

COVID-19 infections and deaths

Data on infections and deaths are collected from the COVID-19 Dashboard¹, which is sourced by the Coronavirus Resource Center of Johns Hopkins University. Coverage begins from January 22, 2020 and provides the location and number of confirmed cases, deaths, and recoveries for 208 affected countries and regions. For this paper, the data cut-off is May 11, 2020.

Containment measures

We use data Oxford's COVID-19 Government Response Tracker² (OxCGRT) for containment measures. OxCGRT collects information on government policy responses, scores the stringency of the measures, and aggregates the data into a common Stringency Index. In addition to the Stringency Index, this paper uses eight containment measures from the database, namely: (i) school closures; (ii) workplace closures; (iii) public event cancellations; (iv) gathering restrictions; (v) public transportation closures; (vi) stay-at-home orders; (vii) restrictions on internal movement; and (viii) international travel bans. This database starts on January 1, 2020 and covers 151 countries/regions.

¹ COVID-19 Map, JHU Coronavirus Resource Center, Accessed May 11, 2020
<https://coronavirus.jhu.edu/map.html>.

² "Coronavirus Government Response Tracker." Blavatnik School of Government. Accessed May 11, 2020.
<https://www.bsg.ox.ac.uk/research/research-projects/coronavirus-government-response-tracker>.

Additional controls used are:

Temperature and humidity

We include daily data on mean temperature and humidity for 95 countries. The data are collected from the Air Quality Open Data Platform and include humidity and temperature for each major city, based on the median of several stations, in 95 countries from January 1, 2020.³

Tests conducted

We use daily data on COVID-19 tests from Our World in Data, an open source platform drawn from countries' Ministry of Health.⁴ The dataset covers total tests conducted and tests per thousand people in 84 countries from January 1, 2020 onwards. Given limited data coverage on testing, this variable is not used in the baseline specification and but in the robustness check analysis.

Population density and age structure

We use indicators which are relevant to the COVID-19 pandemic, such as population density and age structure. Indicators are sourced from The World Development Indicators database,⁵ which is developed by the World Bank Group and compiled from official international sources. Data coverage includes 189 member countries, with the latest available data.

³ COVID-19 Worldwide Air Quality Data. Accessed May 11, 2020. <https://aqicn.org/data-platform/COVID-19/report/>

⁴ Hasell, Joe, COVID-19 Testing - Statistics and Research." <https://ourworldindata.org/coronavirus-testing>.

⁵ "World Development Indicators." Washington, D.C.: The World Bank. Accessed May 11, 2020.

Health robustness indices

We use two different indices for health robustness. The first is the Global Health Security index, published by the Johns Hopkins Center for Health Security, which provides a comprehensive assessment of health security across 195 countries.⁶ It generates an index based on countries' health scores for the following six categories: (i) prevention of the emergence or release of pathogens; (ii) early detection and reporting for epidemics of potential international concern; (iii) rapid response to and mitigation of the spread of an epidemic; (iv) sufficient and robust health system to treat the sick and protect health workers; (v) commitments to improving national capacity, financing plans to address gaps, and adhering to global norms; and (vi) overall risk environment and country vulnerability to biological threats.

We also use the Health Index, which measures the overall health condition of economies on a 0-7 scale. It is sourced from the 2019 Global Competitiveness Report by the World Economic Forum and covers 114 economies.⁷

Mobility Trends

We use data provided by Apple Map's Mobility Trends Report and Google Mobility Reports.⁸ Apple's daily report produces walking and driving indices for 66 countries, sent from user's devices to the Apple map server. Specifically, it measures the relative volume of direction requests. Data are available both for walking as well as driving directions. The report started from January 13, 2020. Google Mobility reports show how visits and lengths of stay have

⁶ "The Global Health Security Index." GHS Index. Accessed May 11, 2020. <https://www.ghsindex.org>.

⁷ Schwab, Klaus; Sala i Martin, Xavier; World Economic Forum, "Global Competitiveness Report 2019", World Economic Forum, 10/2019. Accessed May 11, 2020.

⁸ Apple Maps Mobility Trends Report, Accessed May 11, 2020. <https://www.apple.com/covid19/mobility>.

changed since containment measures have begun. Daily data is available for 89 countries in our dataset, with coverage beginning from February 15th 2020.

B. Methodology

This section describes the empirical methodology used to examine the causal effect of containment measures on flattening the pandemic curve—that is, reducing the number of people infected—and reducing the number of deaths.

Establishing causality is difficult in this context because, as illustrated in the previous sections, countries have introduced containment measures in response to the spread of the virus. This implies that addressing causality requires effectively controlling for this endogenous response.

We address the reverse-causality issue by controlling for the change in the number of infected cases (or deaths) the day before the implementation of containment measures. Given lags in the implementation of containment measures at daily frequency, this allows the researcher to effectively control for the endogenous response of containment measures to the spread of the virus. To further account for expectations about the country-specific (exponential) evolution of the pandemic, we also control for country specific linear, quadratic and cubic time trends.

Two econometric specifications are used to estimate the effect of containment measures on the number of confirmed COVID-19 cases and deaths. The first establishes whether containment had, on average, significant effects on infections and deaths. The second assesses whether these effects vary across countries depending on country-specific characteristics, such as the capacity of the health system, average temperature, the share of vulnerable (or elderly) persons in the population, etc.

We follow the approach proposed by Jordà (2005) to estimate the dynamic cumulative effect of containment measures on the number of confirmed COVID-19 cases and deaths, a methodology used also by Auerbach and Gorodnichenko (2013), Ramey and Zubairy (2018), and Alesina et al. (2019) among others. This procedure does not impose the dynamic restrictions embedded in vector autoregressions and is particularly suited to estimating nonlinearities in the dynamic response. The first regression we estimate is:

$$\Delta d_{i,t+h} = u_i + \theta_h c_{i,t} + X'_{i,t} \Gamma_h + \sum_{\ell=1}^L \psi_{h,\ell} \Delta d_{i,t-\ell} + \varepsilon_{i,t+h} \quad (1)$$

where $\Delta d_{i,t+h} = d_{i,t+h} - d_{i,t+h-1}$ and $d_{i,t}$ is the logarithm of the number of deaths (infections), in country i observed at date t . $c_{i,t}$ denotes the OxCGRT Stringency Index. u_i are country-fixed effects to account for time-invariant country-specific characteristics (for example, population density, age profile of the population, health capacity, average temperature, etc.). X is a vector of control variables which includes daily temperature and humidity levels, in addition to country-specific linear, quadratic and cubic time trends.

The second specification allows the response to vary with countries characteristics. It is estimated as follows:

$$\begin{aligned} \Delta d_{i,t+h} = & u_i + \theta_h^L F(z_{i,t}) c_{i,t} + \theta_h^H (1 - F(z_{i,t})) c_{i,t} + X'_{i,t} \Gamma_h + \sum_{\ell=1}^L F(z_{i,t}) \psi_{h,\ell} \Delta d_{i,t-\ell} + \\ & \sum_{\ell=1}^L (1 - F(z_{i,t})) \psi_{h,\ell} \Delta d_{i,t-\ell} + \varepsilon_{i,t+h} \end{aligned}$$

with $F(z_{it}) = \exp^{-\gamma z_{it}} / (1 - \exp^{-\gamma z_{it}})$, $\gamma > 0$ (2)

where z is a country-specific characteristic normalized to have zero mean and a unit variance.

The weights assigned to each regime vary between 0 and 1 according to the weighting function $F(\cdot)$, so that $F(z_{it})$ can be interpreted as the probability of being in a given state of the economy. The coefficients β_L^k and β_H^k capture the impact of containment measures at each horizon h in cases of very low levels of z ($F(z_{it}) \approx 1$ when z goes to minus infinity) and very high levels of z ($1 - F(z_{it}) \approx 1$ when z goes to plus infinity), respectively. $F(z_{it})=0.5$ is the cutoff between low and high country-specific characteristics—that is, for example, low and high health capacity.

This approach is equivalent to the smooth transition autoregressive model developed by Granger and Teräsvirta (1993). The advantage of this approach is twofold. First, compared with a model in which each dependent variable would be interacted with a measure of country-specific characteristics, it permits a direct test of whether the effect of containment measures varies across different country-specific “regimes”. Second, compared with estimating structural vector autoregressions for each regime, it allows the effect of containment measures to vary smoothly across regimes by considering a continuum of states to compute impulse responses, thus making the functions more stable and precise.

Equations (1 and 2) are estimated for each day $h=0,\dots,30$. Impulse response functions are computed using the estimated coefficients θ_h , and the 95 percent confidence bands associated with the estimated impulse-response functions are obtained using the estimated standard errors of the coefficients θ_h , based on robust standard errors clustered at the country level.

Our sample consists of a balanced sample of 129 economies with at least 30 observation days after a significant outbreak (100 cases).⁹

⁹ Similar results are obtained when using alternative thresholds.

IV. RESULTS

A. Baseline

Figure 2 shows the estimated dynamic cumulative response of the number of confirmed COVID-19 cases and death to a unitary change in the aggregate containment stringency index over the 30-day period following the implementation of the containment measure, together with the 95 percent confidence interval around the point estimate. Given the potentially large measurement errors in the number of cases and deaths, the precision of the estimated effects is remarkable. This is also overserved in the results for daily infections and deaths and not just the cumulative impacts shown in the impulse responses (Figure A1).

The results provide strong evidence that containment measures, by reducing mobility (Figure A2), have significantly reduced the number of infections and the number of deaths. In particular, they suggest that countries that have put in place stringent measures, for example those implemented in Wuhan or in countries such as New Zealand (where the stringency index has moved from about 0 to 1), may have reduced the number of confirmed cases and deaths by around 200 percent relative to the underlying country-specific path in the absence of interventions. In addition, we find that lagged values of daily temperature and humidity affect significantly the number of cases and deaths, with cold and dry conditions facilitating the spread of the virus.

We also find evidence to support the hypothesis that early intervention and containment have had a significant impact on infections and ultimate on mortality. For each country, we compute the public health response time (PHRT) as the number of days it takes for the country to implement containment measures after a significant outbreak (defined as 100 confirmed cases). For calculating the PHRT, we include all non-pharmaceutical

interventions other than international travel restrictions, since these were often implemented before confirmed domestic outbreaks and as an effort to reduce exposure from people that had traveled to China. We find that containment measures in countries with low PHRT—that is, countries that put in place containment measures faster—reduced the average number of infections and deaths by 300 and 400 percent respectively, while the impact was not statistically significant at a 95 percent confidence interval for countries where the PHRT was relatively high (Figure 3).

B. Robustness checks

We have carried out several robustness checks of these findings. Here, we discuss the main ones. First, since containment measures have been introduced first in China, there is the risk that the longer-term (30 days) results may simply reflect the observed flattening of the pandemic curve in China. To address this issue, we repeated the analysis excluding China from the sample. Second, we checked whether the results are driven by the inclusion of the United States, which as of now is the country with the largest number of confirmed cases and deaths. Third, we included additional controls in the regressions that could be correlated with the number of cases and deaths, such as the daily change in the number of tests and daily time fixed effects. Fourth, instead of using an index of containment measures, which attempts to quantify the severity of the measures, we used a simple dummy variable to identify the start and end of containment and mitigation measures—this is similar to treating the containment measures as a shock. Another concern is that containment measures were announced before being implemented and, therefore, were anticipated. This may have resulted in reduced mobility ahead of the implementation of the containment measures and to an upward bias in the estimates. To check

for this possibility, we repeated the analysis adding changes in mobility as controls, for a more limited set of countries for which data are available. Finally, we experimented with the lag structure of the regressions, the horizon for the local projections and alternative specifications for the standard errors (e.g. Driscoll-Kraay standard errors). In all cases, the results are very similar to, and not statistically different from, the baseline—we report some of these results in Figure 4.

C. Role of country characteristics and health infrastructure

This section examines whether the average effect of containment measures presented in the previous section varies across countries depending on country characteristics. It focuses on characteristics that are thought to influence the spread of the virus and its associated fatalities.

Temperature

While no strong consensus has been reached on the role of temperature in the transmission of the virus, emerging data as well as results discussed in the previous section suggest that cold and dry conditions may facilitate the spread of the novel coronavirus.¹⁰ To test for the role of temperature in affecting the effect of containment measures on infections and deaths, we estimated equation (2) using as an interaction variable the average country temperature in the first 4 months of 2020. The results in Figure 5 suggest that the effect of containment measures is stronger in countries with lower average temperatures. While stringent containment measures may have reduced the number of confirmed cases and deaths by more about 400 percent in countries with very low average temperature, they did not have

¹⁰ <https://www.cebm.net/covid-19/do-weather-conditions-influence-the-transmission-of-the-coronavirus-sars-cov-2/>

statistically significant effects in countries with very high average temperate measures.

Similar results are obtained for humidity.

Age

Information available on the virus suggests that people over the age of 65 are particularly vulnerable to its effects. For example, in the United States about 80 percent of total deaths are concentrated in this age group.¹¹ To examine the role of age, we estimated equation (2) with an interaction variable that measures the share of the population above 65. The results presented in Figure 6 suggest that containment measures have had a large impact, both in terms of confirmed cases as well as lives saved, in countries with a relatively high share of the elderly population. In contrast, the impact is not statistically significantly different from zero in countries with a very young population. The result for cases may appear puzzling—COVID-19 is known to have a higher mortality rate for the elderly, but not necessarily a higher infection rate—but the results are an artefact of the data. Most countries in our sample have not tested for COVID-19 universally; instead testing has been mostly restricted to people who are most sick or hospitalized. And since the elderly predominantly fall into this category, the number of cases confirmed with COVID-19 is disproportionately high in countries with a greater share of elderly.

Population density

The spread of the virus is likely to be more difficult to control in countries with higher population density, where keeping social distancing is more difficult, all else equal. The results obtained by estimating equation (2) using population density as an interaction term confirm this hypothesis. In particular, we find that while stringent containment measures have been associated

¹¹ https://www.cdc.gov/nchs/nvss/vsrr/covid_weekly/index.htm

with a reduction of about 400 percent of COVID-19 cases 30 days after implementation of the measures in countries with a low population density (Figure 7). In contrast, we do not find statistically significant differences between the effects of the measures on the number of deaths between low- and high-density population countries.

Health preparedness

Health preparedness is of paramount importance to detect the spread of the virus and contain it, as well as to cure those that get infected. To examine whether the effect of containment measures varies across countries based on their health security and capabilities, we estimate equation (2) using two alternative indicators of health preparedness: (i) the Global Health Security Index from John Hopkins; and (ii) the Health Index compiled by the World Economic Forum. The results obtained for both indicators paint a similar picture: containment measures are more effective in countries with higher health security and a better health index (Figure 8).¹² In particular, while stringent containment measures may have reduced the number of confirmed cases and deaths by more about 400 percent in countries with very strong health systems, they did not have statistically significant effects in countries with weak health capabilities.

Mobility and *de facto* social distancing

The analysis so far has relied on *de jure* measures of containment. However, the actual outcomes in terms of infections and deaths are likely to be determined by compliance with these

¹² Similar results are obtained for the individual sub-indices of the Global Health Security Index.

de jure measures. In order to assess the *de facto* impact of social distancing, we interacted the containment measures with data on mobility available from Apple mobility trends reports. The results suggest that containment measures have been more effective in countries where these measures resulted in lower mobility and greater social distancing in practice (Figure 9).

D. Types of containment measures

In this section, we examine whether the effect of containment varies across types of measure: (i) school closures; (ii) workplace closures; (iii) cancellation of public events; (iv) restrictions on size of gathering; (v) closures of public transport; (vi) stay-at-home requirements; (vii) restrictions on internal movement; and (viii) restrictions on international travel.

Estimating the overall effect of each measure is challenging, because many of these measures were often introduced simultaneously as part of the country's response to limit the spread of the virus. Here, we use two alternative approaches to gauge the potential magnitude of the effect of each of these measures and highlight which type has been the most effective. In the first approach, we introduce each measure one at a time in equation (1). Clearly, the problem with this approach is that the estimates suffer from omitted variable bias. In the second approach, we include them all together. While this approach addresses omitted variable bias, given the high correlation across measures, the effects are likely to be less precisely estimated due to multicollinearity.

The results from the two exercises are reported in Figure 10 and 11. They suggest that all measures have contributed to significantly reduce the number of COVID-19 cases and deaths, with stay-at-home orders appearing to have been more effective in reducing the number of

deaths. The results are similar when we use dummy variables for the date of implementation or removal of the various measures (instead of the indices that quantify also the severity).

V. CONCLUSIONS

In the absence of a vaccine or effective treatments, containment measures are key to halting the spread of the virus and limiting the number of fatalities. In this paper, we have provided a first empirical assessment which quantifies the effectiveness of containment measures on the number of COVID-19 infections and deaths.

While the approach is not based on controlled experiments, our approach based on daily data and real-time observations of containment measures should limit concerns about reverse causality (from the spread of the virus to the nature of containment policies). We thus consider our empirical estimates to provide a reasonable assessment of the causal effect of containment policies on infections and deaths. Specifically, we find that containment measures have significantly reduced the number of infections, and more importantly, the number of deaths. Our results suggest that countries that have put in place stringent measures, such as those implemented in Wuhan, China or in countries like New Zealand (where the stringency index has moved from about 0 to 1), may have reduced the number of confirmed cases and deaths by more than 200 percent relative to the underlying country-specific path in the absence of measures. This is particularly true for countries that put in place containment measures quickly.

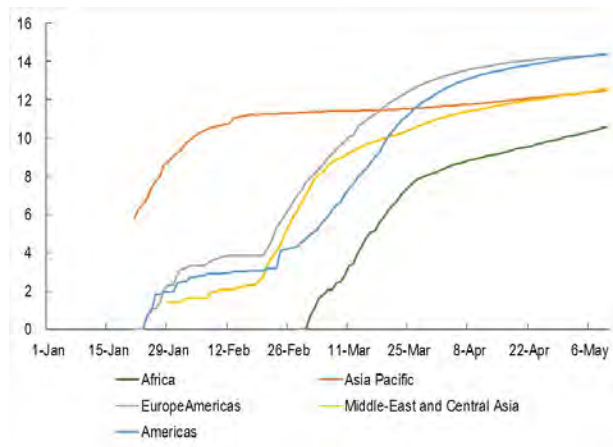
Containment measures have had stronger effects in countries where the measures were implemented faster and resulted in less mobility—*de facto*, more social distancing—and in countries with lower temperatures, lower population density, a larger share of older population, and stronger health systems. Among different types of containment measures, stay-at-home orders seems to have been more effective in reducing the number of deaths.

References

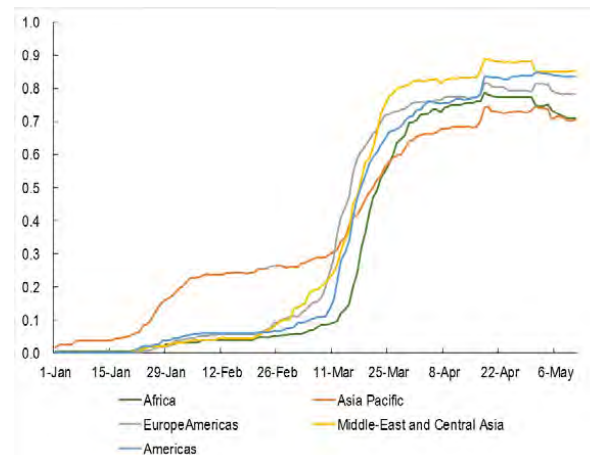
- Alesina, A.F., Furceri, D., Ostry, J.D., Papageorgiou, C. and Quinn, D.P., 2019. Structural Reforms and Elections: Evidence from a World-Wide New Dataset (No. w26720). National Bureau of Economic Research.
- Auerbach, A.J. and Gorodnichenko, Y., 2013. Output spillovers from fiscal policy. *American Economic Review*, 103(3), pp.141-46.
- Brotherhood L., Kircher P., Santos C., Tertilt M., 2020. An economic model of the COVID-19 epidemic: the importance of testing and age-specific policies. CEPR Discussion Paper DP14695, Centre for Economic Policy Research.
- Chinazzi et al., 2020. The effect of travel restrictions on the spread of the 2019 novel coronavirus (COVID-19) outbreak. *Science*, 368, 395-400.
- Cowling et al., 2020. Impact assessment of non-pharmaceutical interventions against coronavirus disease 2019 and influenza in Hong Kong: an observational study. *Lancet Public Health* 2020; 5: e279–88.
- Eichenbaum M., Rebelo S., Trabandt M., 2020. The Macroeconomics of Epidemics. NBER Working Papers 26882, National Bureau of Economic Research, Inc.
- Forslid R., Herzing M., 2020. Assessing the consequences of quarantines during a pandemic. CEPR Discussion Paper DP14699, Centre for Economic Policy Research.
- Granger, C.W.J. and Teräsvirta, T., 1993. *Modelling Nonlinear Economic Relationships* Oxford University Press. New York.
- Jordà, Ò., 2005. Estimation and inference of impulse responses by local projections. *American economic review*, 95(1), pp.161-182.
- Kraemer et al., 2020. The effect of human mobility and control measures on the COVID-19 epidemic in China. *Science*, 368, 493–497.
- H. Tian et al., 2020. An investigation of transmission control measures during the first 50 days of the COVID-19 epidemic in China. *Science* 10.1126/science.abb6105 (2020).
- Ramey, V.A. and Zubairy, S., 2018. Government spending multipliers in good times and in bad: evidence from US historical data. *Journal of Political Economy*, 126(2), pp.850-901.

Figure 1: Evolution of Total Infection and Containment Measures

Panel A. Total cases (log scale)



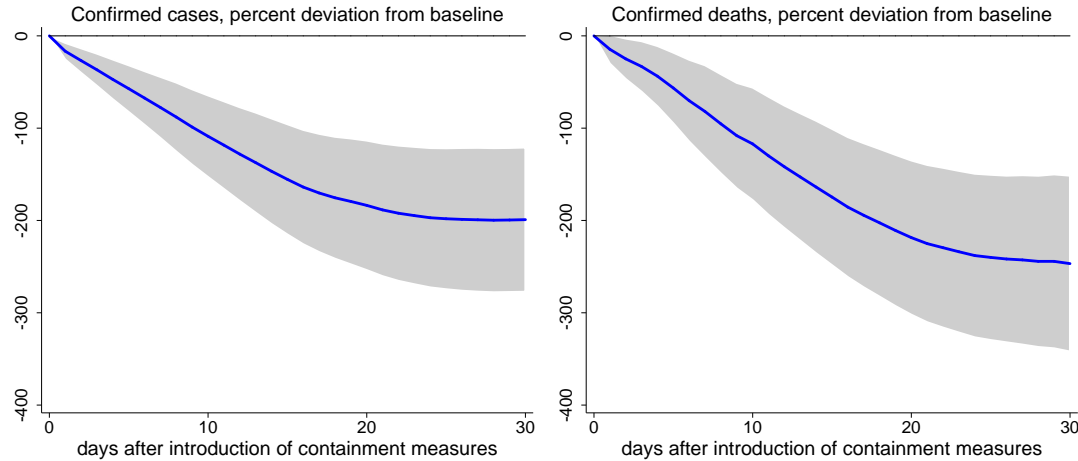
Panel B. Stringency of containment measure



Source: Haver, OxCGR Stringency Index and IMF Staff calculations.

Note: The index is scaled to vary between zero (least stringent) to 1 (most stringent) containment measures. It is comprised of the following categories: (i) School closing; (ii) Workplace closing; (iii) Cancel public events; (iv) Restrictions on gathering size; (v) Close public transport; (vi) Stay at home requirements; (vii) Restrictions on internal movement; (viii) Restrictions on international travel.

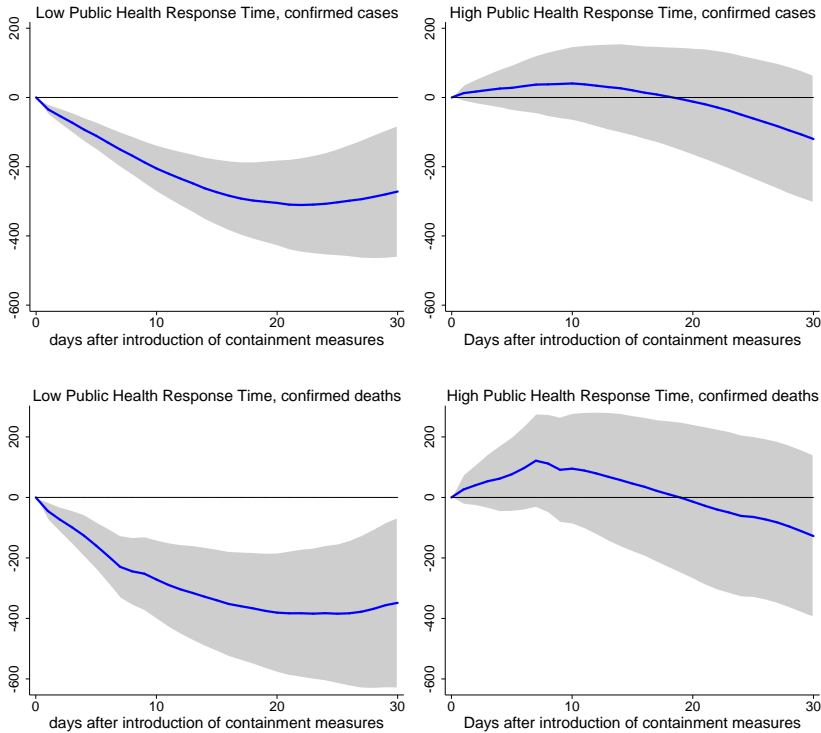
Figure 2: Effect of Containment Measures on Total Confirmed COVID-19 Cases and Deaths



Note: Impulse response functions are estimated using a sample of 129 countries using daily data from the start of the outbreak. The analysis is restricted to countries with a significant outbreak that has lasted at least 30 days. $t = 0$ is the date when the outbreak becomes significant (100 cases) in each country. The graph shows the response and confidence bands at 95 percent. The horizontal axis shows the response x days after the containment measures. Estimates based on $\Delta d_{i,t+h} = u_i + \theta_h c_{i,t} + X'_{i,t} \Gamma_h + \sum_{\ell=1}^L \psi_{h,\ell} \Delta d_{i,t-\ell} + \varepsilon_{i,t+h}$ where $\Delta d_{i,t+h} = d_{i,t+h} - d_{i,t+h-1}$ and $d_{i,t}$ is the logarithm of the number of COVID-19 cases or deaths (depending on specification) in country i observed at date t . The model is estimated at each horizon $h = 0, 1, \dots, H$, with a lag structure $\ell = 1, 2, \dots, L$; $c_{i,t}$ is the index capturing the level of containment and mitigation measures; X is a matrix of time varying control variables and country specific linear, quadratic and cubic time trend. Results are based on May 11 data.

Figure 3: Interaction with Public Health Response Time

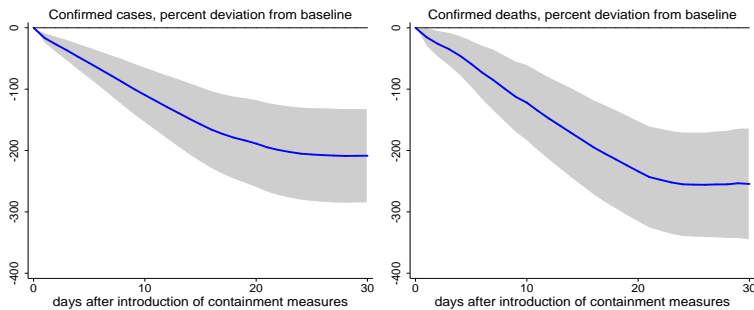
(percent deviation from baseline)



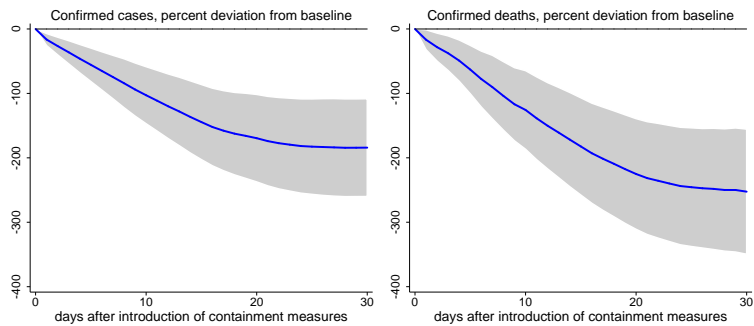
Note: Impulse response functions are estimated using a sample of 129 countries using daily data from the start of the outbreak. The analysis is restricted to countries with a significant outbreak that has lasted at least 30 days. The graph shows the response and confidence bands at 95 percent. The horizontal axis shows the response x days after the containment measures. Estimates based on $\Delta d_{i,t+h} = u_i + u_t + \theta_h^H F(z_{i,t}) c_{i,t} + \theta_h^H (1 - F(z_{i,t})) c_{i,t} + X'_{i,t} \Gamma_h + \sum_{\ell=1}^L F(z_{i,t}) \psi_{h,\ell} \Delta d_{i,t-\ell} + \sum_{\ell=1}^L (1 - F(z_{i,t})) \psi_{h,\ell} \Delta d_{i,t-\ell} + \varepsilon_{i,t+h}$ with $F(z_{i,t}) = \frac{\exp(-\gamma z_{i,t})}{(1 - \exp(-\gamma z_{i,t}))}$, $\gamma > 0$ where $\Delta d_{i,t+h} = d_{i,t+h} - d_{i,t+h-1}$ and $d_{i,t}$ is the logarithm of the number of COVID-19 cases or deaths (depending on specification) in country i observed at date t and z is the country-specific characteristics normalized to have zero mean and a unit variance. The model is estimated at each horizon $h = 0, 1, \dots, H$, with a lag structure $\ell = 1, 2, \dots, L$; $c_{i,t}$ is the index capturing the level of containment and mitigation measures; X is a matrix of time varying control variables and country specific linear, quadratic and cubic time trend. Results are based on May 11 data.

Figure 4: Robustness Checks

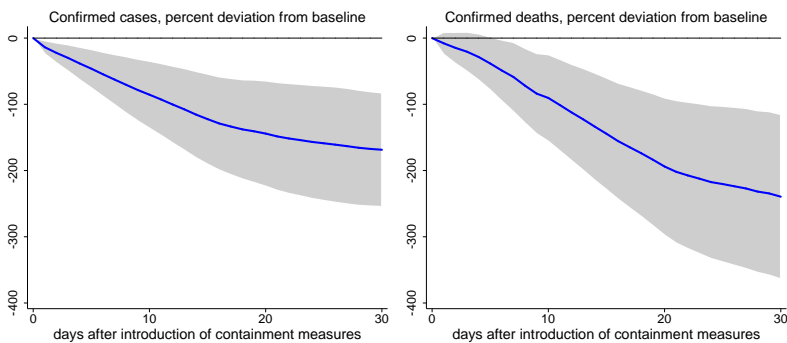
Response to stringency of containment measures: ex China



Response to stringency of containment measures: ex United States



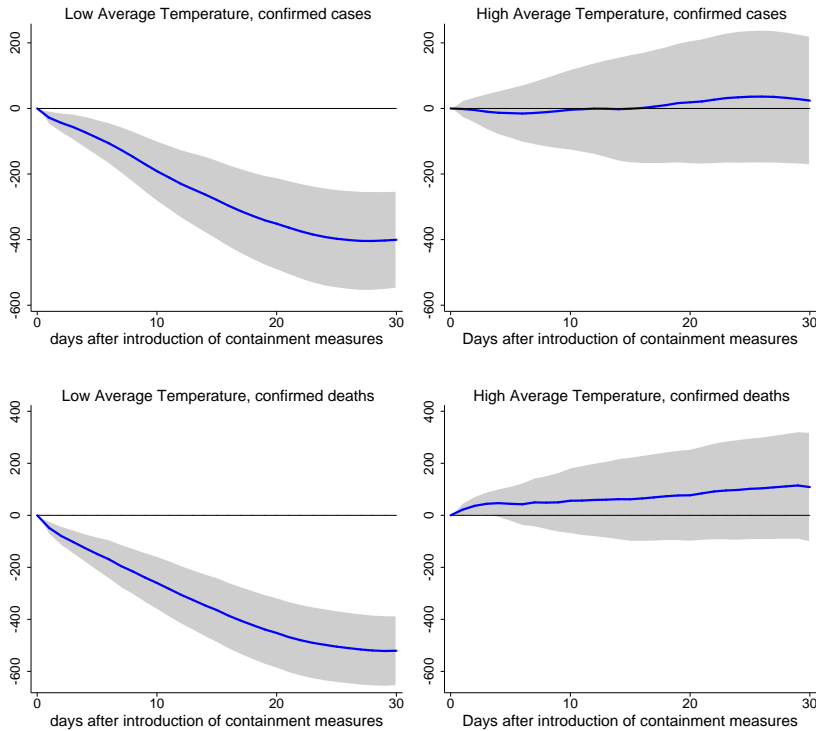
Response to stringency of containment measures: with time fixed-effects



Note: Impulse response functions are estimated using a sample of 129 countries using daily data from the start of the outbreak. The analysis is restricted to countries with a significant outbreak that has lasted at least 30 days. $t = 0$ is the date when the outbreak becomes significant (100 cases) in each country. The graph shows the response and confidence bands at 95 percent. The horizontal axis shows the response x days after the containment measures. Estimates based on $\Delta d_{i,t+h} = u_i + \theta_h c_{i,t} + X'_{i,t} \Gamma_h + \sum_{\ell=1}^L \psi_{h,\ell} \Delta d_{i,t-\ell} + \varepsilon_{i,t+h}$ where $\Delta d_{i,t+h} = d_{i,t+h} - d_{i,t+h-1}$ and $d_{i,t}$ is the logarithm of the number of COVID-19 cases or deaths (depending on specification) in country i observed at date t . The model is estimated at each horizon $h = 0, 1, \dots, H$, with a lag structure $\ell = 1, 2, \dots, L$; $c_{i,t}$ is the index capturing the level of containment and mitigation measures; X is a matrix of time varying control variables and country specific linear, quadratic and cubic time trend. Results are based on May 11 data.

Figure 5: Interaction with Average Air Temperature

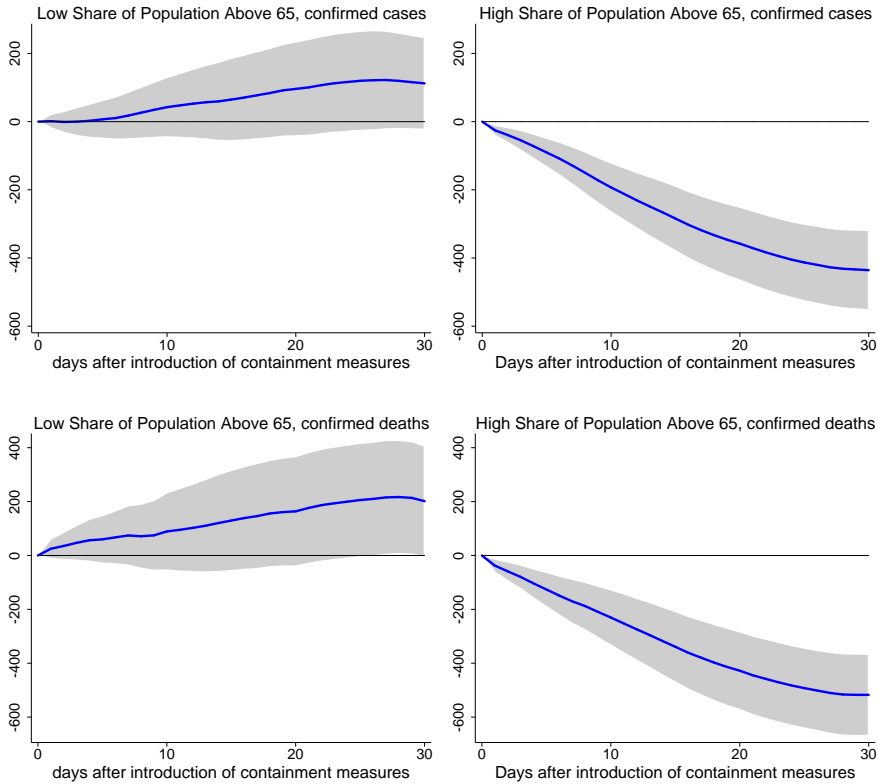
(percent deviation from baseline)



Note: Impulse response functions are estimated using a sample of 129 countries using daily data from the start of the outbreak. The analysis is restricted to countries with a significant outbreak that has lasted at least 30 days. The graph shows the response and confidence bands at 95 percent. The horizontal axis shows the response x days after the containment measures. Estimates based on $\Delta d_{i,t+h} = u_i + u_t + \theta_h^H F(z_{i,t}) c_{i,t} + \theta_h^H (1 - F(z_{i,t})) c_{i,t} + X'_{i,t} \Gamma_h + \sum_{\ell=1}^L F(z_{i,t}) \psi_{h,\ell} \Delta d_{i,t-\ell} + \sum_{\ell=1}^L (1 - F(z_{i,t})) \psi_{h,\ell} \Delta d_{i,t-\ell} + \varepsilon_{i,t+h}$ with $F(z_{i,t}) = \frac{\exp^{-\gamma z_{i,t}}}{(1 - \exp^{-\gamma z_{i,t}})}$, $\gamma > 0$ where $\Delta d_{i,t+h} = d_{i,t+h} - d_{i,t+h-1}$ and $d_{i,t}$ is the logarithm of the number of COVID-19 cases or deaths (depending on specification) in country i observed at date t and z is the country-specific characteristics normalized to have zero mean and a unit variance. The model is estimated at each horizon $h = 0, 1, \dots, H$, with a lag structure $\ell = 1, 2, \dots, L$; $c_{i,t}$ is the index capturing the level of containment and mitigation measures; X is a matrix of time varying control variables and country specific linear, quadratic and cubic time trend. Results are based on May 11 data.

Figure 6: Interaction with Share of Population above 65 years

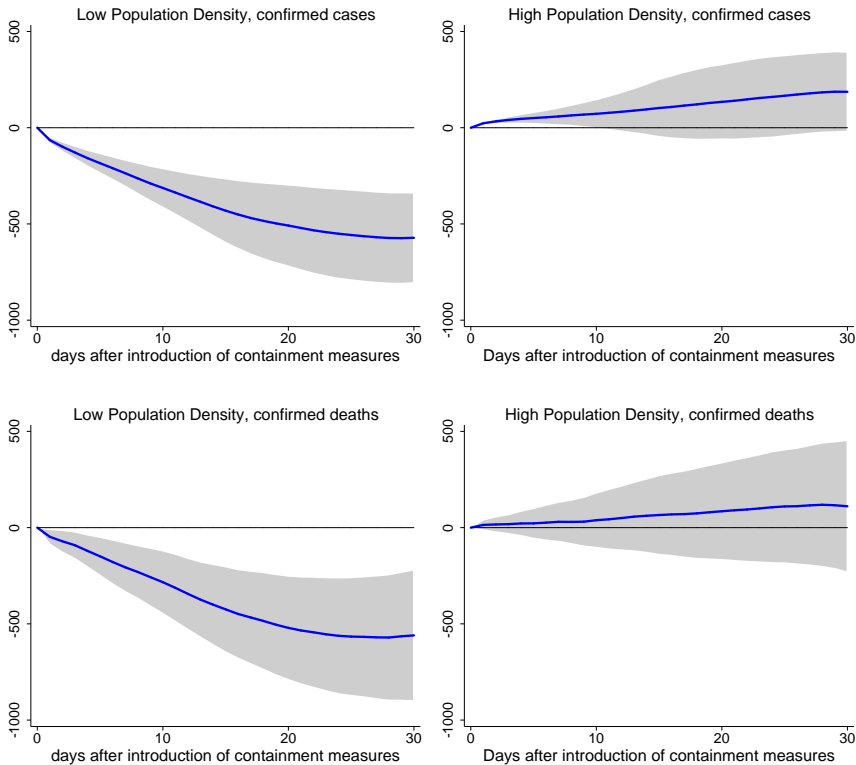
(percent deviation from baseline)



Note: Impulse response functions are estimated using a sample of 129 countries using daily data from the start of the outbreak. The analysis is restricted to countries with a significant outbreak that has lasted at least 30 days. The graph shows the response and confidence bands at 95 percent. The horizontal axis shows the response x days after the containment measures. Estimates based on $\Delta d_{i,t+h} = u_i + u_t + \theta_h^t F(z_{i,t}) c_{i,t} + \theta_h^H (1 - F(z_{i,t})) c_{i,t} + X'_{i,t} \Gamma_h + \sum_{\ell=1}^L F(z_{i,t}) \psi_{h,\ell} \Delta d_{i,t-\ell} + \sum_{\ell=1}^L (1 - F(z_{i,t})) \psi_{h,\ell} \Delta d_{i,t-\ell} + \varepsilon_{i,t+h}$ with $F(z_{i,t}) = \frac{\exp^{-\gamma z_{i,t}}}{(1 - \exp^{-\gamma z_{i,t}})}$, $\gamma > 0$ where $\Delta d_{i,t+h} = d_{i,t+h} - d_{i,t+h-1}$ and $d_{i,t}$ is the logarithm of the number of COVID-19 cases or deaths (depending on specification) in country i observed at date t and z is the country-specific characteristics normalized to have zero mean and a unit variance. The model is estimated at each horizon $h = 0, 1, \dots, H$, with a lag structure $\ell = 1, 2, \dots, L$; $c_{i,t}$ is the index capturing the level of containment and mitigation measures; X is a matrix of time varying control variables and country specific linear, quadratic and cubic time trend. Results are based on May 11 data.

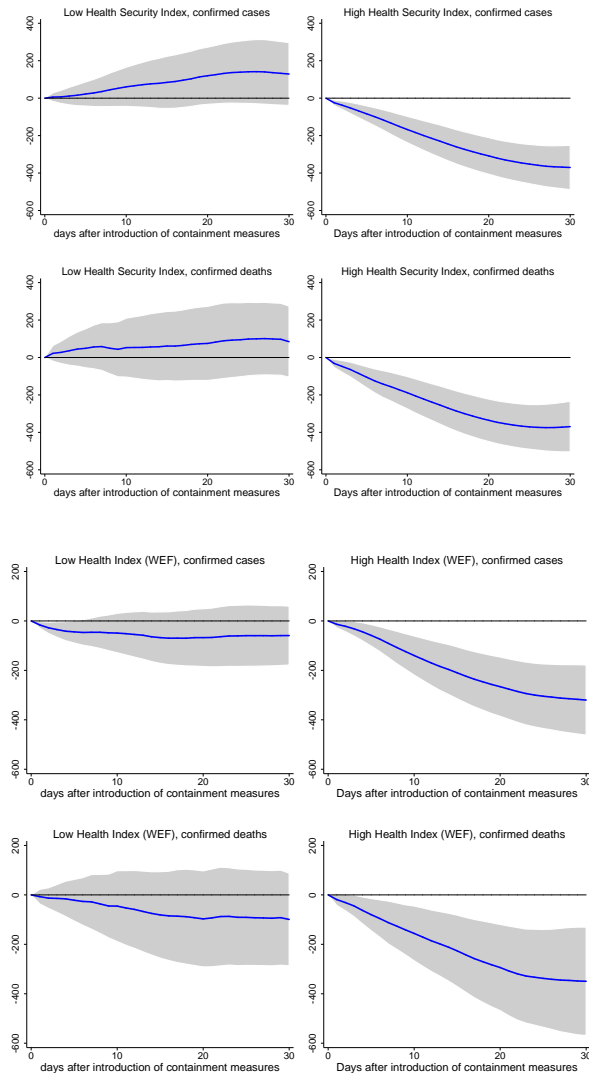
Figure 7: Interaction with Population Density

(percent deviation from baseline)



Note: Impulse response functions are estimated using a sample of 129 countries using daily data from the start of the outbreak. The analysis is restricted to countries with a significant outbreak that has lasted at least 30 days. The graph shows the response and confidence bands at 95 percent. The horizontal axis shows the response x days after the containment measures. Estimates based on $\Delta d_{i,t+h} = u_i + u_t + \theta_h^c F(z_{i,t})c_{i,t} + \theta_h^d (1 - F(z_{i,t}))c_{i,t} + X'_{i,t}\Gamma_h + \sum_{\ell=1}^L F(z_{i,t})\psi_{h,\ell}\Delta d_{i,t-\ell} + \sum_{\ell=1}^L (1 - F(z_{i,t}))\psi_{h,\ell}\Delta d_{i,t-\ell} + \varepsilon_{i,t+h}$ with $F(z_{i,t}) = \frac{\exp^{-\gamma z_{i,t}}}{(1 - \exp^{-\gamma z_{i,t}})}$, $\gamma > 0$ where $\Delta d_{i,t+h} = d_{i,t+h} - d_{i,t+h-1}$ and $d_{i,t}$ is the logarithm of the number of COVID-19 cases or deaths (depending on specification) in country i observed at date t and z is the country-specific characteristics normalized to have zero mean and a unit variance. The model is estimated at each horizon $h = 0, 1, \dots, H$, with a lag structure $\ell = 1, 2, \dots, L$; $c_{i,t}$ is the index capturing the level of containment and mitigation measures; X is a matrix of time varying control variables and country specific linear, quadratic and cubic time trend. Results are based on May 11 data.

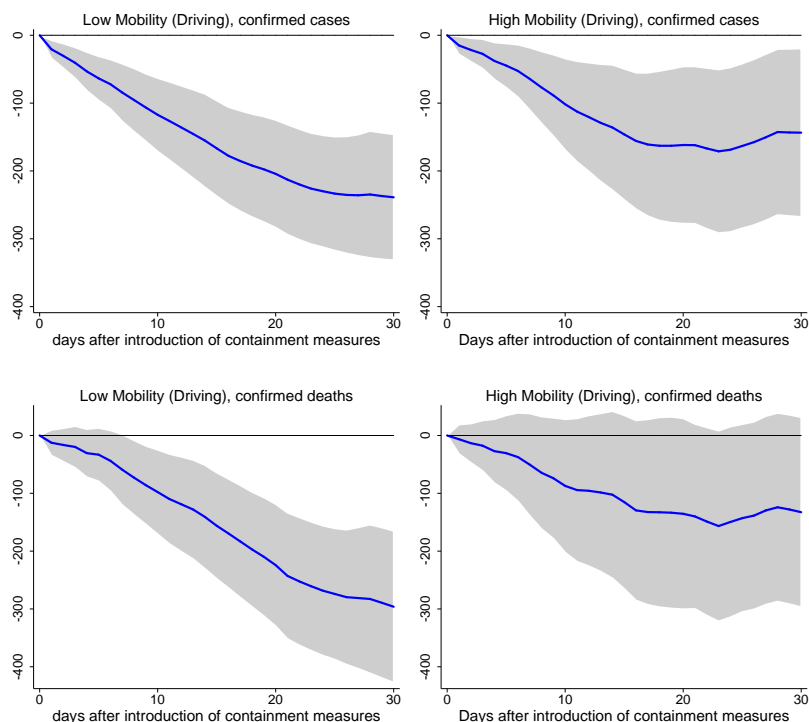
Figure 8: Interaction with Health Security Index and Health Infrastructure
(percent deviation from baseline)



Note: Impulse response functions are estimated using a sample of 129 countries using daily data from the start of the outbreak. The analysis is restricted to countries with a significant outbreak that has lasted at least 30 days. The graph shows the response and confidence bands at 95 percent. The horizontal axis shows the response x days after the containment measures. Estimates based on $\Delta d_{i,t+h} = u_i + u_t + \theta_h^H F(z_{i,t}) c_{i,t} + \theta_h^H (1 - F(z_{i,t})) c_{i,t} + X'_{i,t} \Gamma_h + \sum_{\ell=1}^{\ell} F(z_{i,t}) \psi_{h,\ell} \Delta d_{i,t-\ell} + \sum_{\ell=1}^{\ell} (1 - F(z_{i,t})) \psi_{h,\ell} \Delta d_{i,t-\ell} + \varepsilon_{i,t+h}$ with $F(z_{i,t}) = \frac{\exp^{-\gamma z_{i,t}}}{(1 - \exp^{-\gamma z_{i,t}})}$, $\gamma > 0$ where $\Delta d_{i,t+h} = d_{i,t+h} - d_{i,t+h-1}$ and $d_{i,t}$ is the logarithm of the number of COVID-19 cases or deaths (depending on specification) in country i observed at date t and z is the country-specific characteristics normalized to have zero mean and a unit variance. The model is estimated at each horizon $h = 0, 1, \dots, H$, with a lag structure $\ell = 1, 2, \dots, L$; $c_{i,t}$ is the index capturing the level of containment and mitigation measures; X is a matrix of time varying control variables and country specific linear, quadratic and cubic time trend. Results are based on May 11 data.

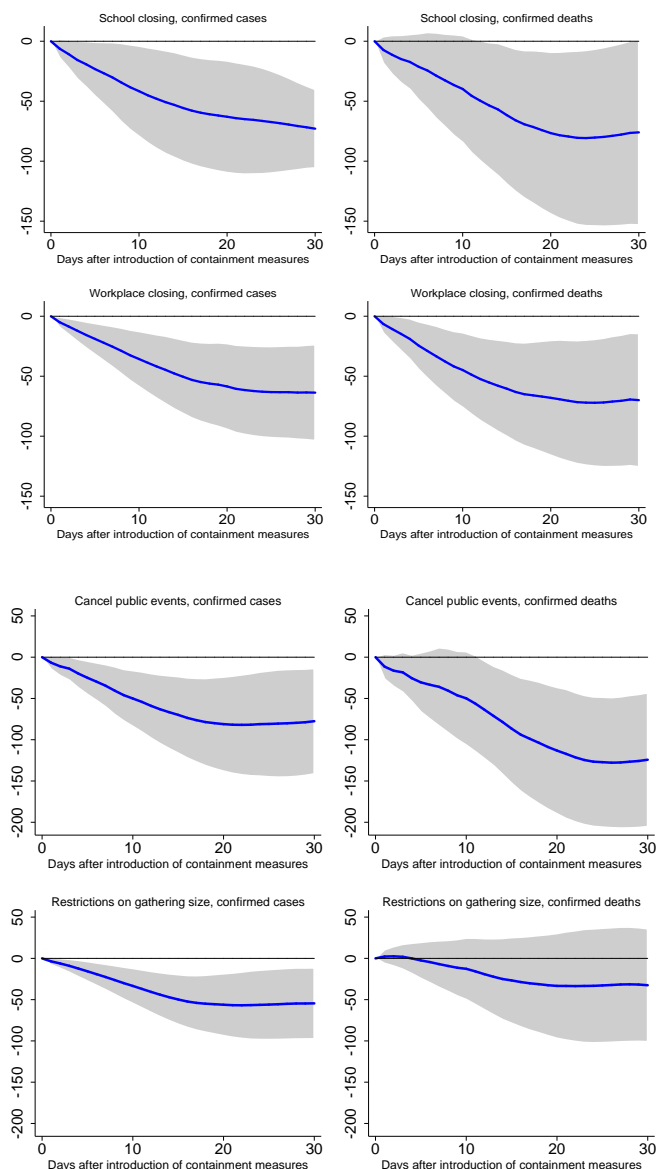
Figure 9: Interaction with Mobility (Driving)

(percent deviation from baseline)



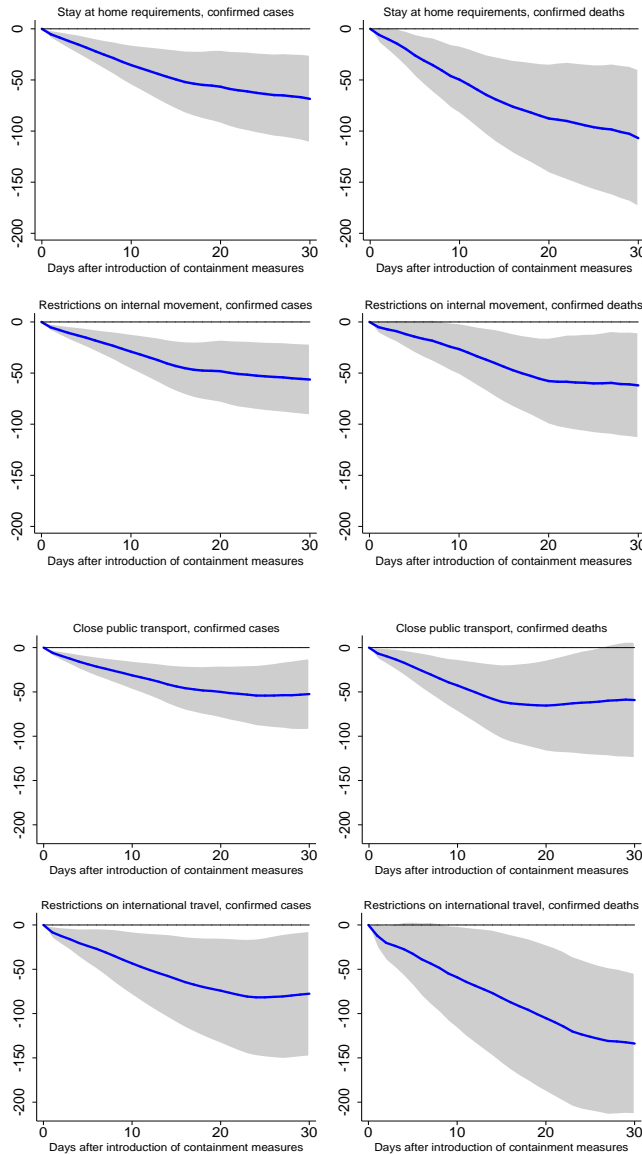
Note: Impulse response functions are estimated using a sample of 129 countries using daily data from the start of the outbreak. The analysis is restricted to countries with a significant outbreak that has lasted at least 30 days. The graph shows the response and confidence bands at 95 percent. The horizontal axis shows the response x days after the containment measures. Estimates based on $\Delta d_{i,t+h} = u_i + u_t + \theta_h^d F(z_{i,t})c_{i,t} + \theta_h^d (1 - F(z_{i,t}))c_{i,t} + X'_{i,t}\Gamma_h + \sum_{\ell=1}^L F(z_{i,t})\psi_{h,\ell}\Delta d_{i,t-\ell} + \sum_{\ell=1}^L (1 - F(z_{i,t}))\psi_{h,\ell}\Delta d_{i,t-\ell} + \varepsilon_{i,t+h}$ with $F(z_{i,t}) = \frac{\exp^{-\gamma z_{i,t}}}{(1 - \exp^{-\gamma z_{i,t}})}$, $\gamma > 0$ where $\Delta d_{i,t+h} = d_{i,t+h} - d_{i,t+h-1}$ and $d_{i,t}$ is the logarithm of the number of COVID-19 cases or deaths (depending on specification) in country i observed at date t and z is the country-specific characteristics normalized to have zero mean and a unit variance. The model is estimated at each horizon $h = 0, 1, \dots, H$, with a lag structure $\ell = 1, 2, \dots, L$; $c_{i,t}$ is the index capturing the level of containment and mitigation measures; X is a matrix of time varying control variables and country specific linear, quadratic and cubic time trend. Results are based on May 11 data.

Figure 10a: Local projection response to different containment measures
(percent deviation from baseline)



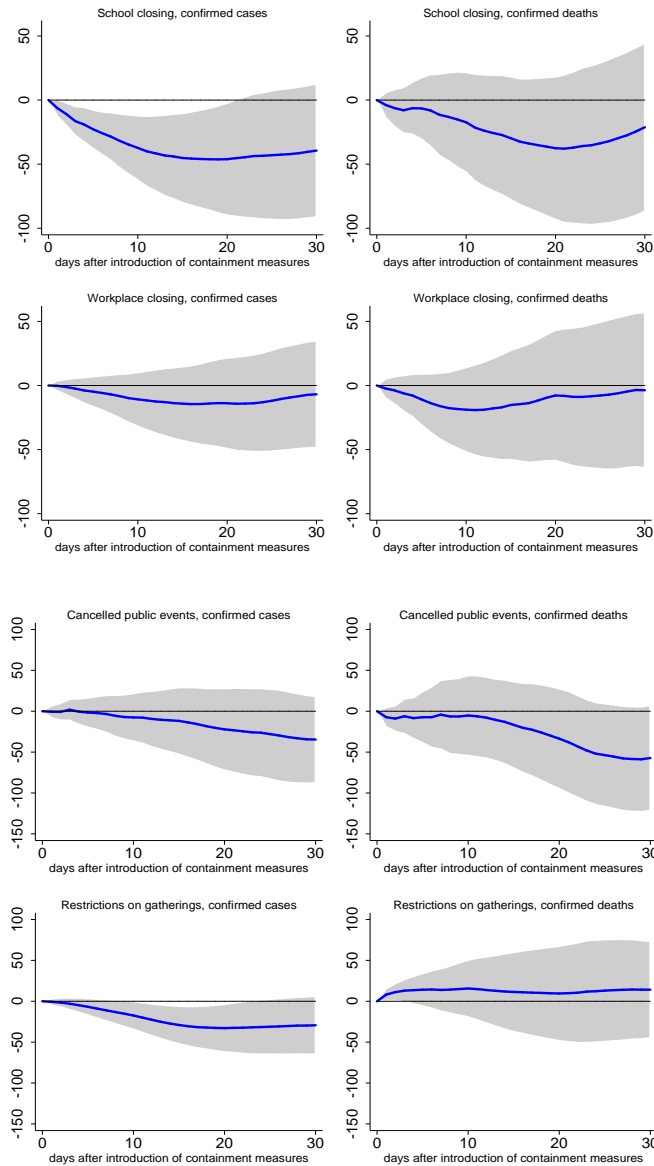
Note: Impulse response functions are estimated using a sample of 129 countries using daily data from the start of the outbreak. The analysis is restricted to countries with a significant outbreak that has lasted at least 30 days. $t = 0$ is the date when the outbreak becomes significant (100 cases) in each country. The graph shows the response and confidence bands at 95 percent. The horizontal axis shows the response x days after the containment measures. Estimates based on $\Delta d_{i,t+h} = u_i + \theta_h c_{i,t} + X'_{i,t} \Gamma_h + \sum_{\ell=1}^L \psi_{h,\ell} \Delta d_{i,t-\ell} + \varepsilon_{i,t+h}$ where $\Delta d_{i,t+h} = d_{i,t+h} - d_{i,t+h-1}$ and $d_{i,t}$ is the logarithm of the number of COVID-19 cases or deaths (depending on specification) in country i observed at date t . The model is estimated at each horizon $h = 0, 1, \dots, H$, with a lag structure $\ell = 1, 2, \dots, L$; $c_{i,t}$ is the index capturing different types containment and mitigation measures, introduced one at a time; X is a matrix of time varying control variables and country specific linear, quadratic and cubic time trend. Results are based on May 11 data.

Figure 10b: Local projection response to different containment measures
(percent deviation from baseline)



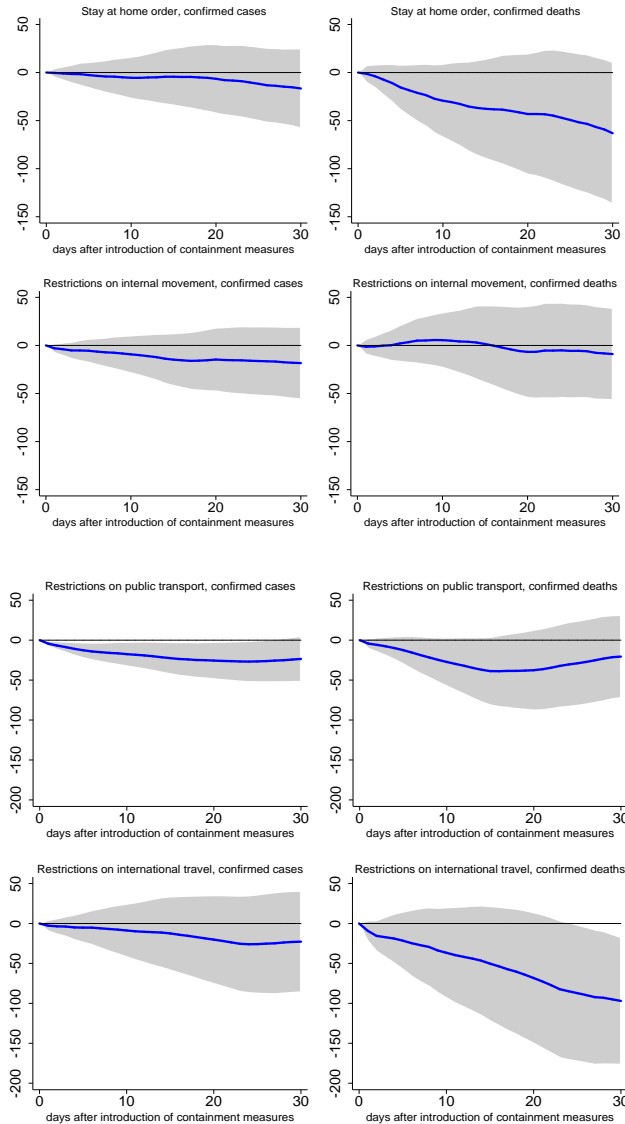
Note: Impulse response functions are estimated using a sample of 129 countries using daily data from the start of the outbreak. The analysis is restricted to countries with a significant outbreak that has lasted at least 30 days. $t = 0$ is the date when the outbreak becomes significant (100 cases) in each country. The graph shows the response and confidence bands at 95 percent. The horizontal axis shows the response x days after the containment measures. Estimates based on $\Delta d_{it+h} = u_i + \theta_h c_{it} + X'_{it} \Gamma_h + \sum_{\ell=1}^L \psi_{h,\ell} \Delta d_{it-\ell} + \varepsilon_{it+h}$ where $\Delta d_{it+h} = d_{it+h} - d_{it+h-1}$ and d_{it} is the logarithm of the number of COVID-19 cases or deaths (depending on specification) in country i observed at date t . The model is estimated at each horizon $h = 0, 1, \dots, H$, with a lag structure $\ell = 1, 2, \dots, L$. c_{it} is the index capturing different types containment and mitigation measures, introduced one at a time. X is a matrix of time varying control variables and country specific linear, quadratic and cubic time trend. Results are based on May 11 data.

Figure 11a: Local projection response to different containment measures (together)
(percent deviation from baseline)



Note: Impulse response functions are estimated using a sample of 129 countries using daily data from the start of the outbreak. The analysis is restricted to countries with a significant outbreak that has lasted at least 30 days. $t = 0$ is the date when the outbreak becomes significant (100 cases) in each country. The graph shows the response and confidence bands at 95 percent. The horizontal axis shows the response x days after the containment measures. Estimates based on $\Delta d_{i,t+h} = u_i + \theta_h c_{i,t} + X'_{i,t} \Gamma + \sum_{\ell=1}^L \psi_{h,\ell} \Delta d_{i,t-\ell} + \varepsilon_{i,t+h}$ where $\Delta d_{i,t+h} = d_{i,t+h} - d_{i,t+h-1}$ and $d_{i,t}$ is the logarithm of the number of COVID-19 cases or deaths (depending on specification) in country i observed at date t . The model is estimated at each horizon $h = 0, 1, \dots, H$, with a lag structure $\ell = 1, 2, \dots, L$. $c_{i,t}$ are indices capturing different types containment and mitigation measures, introduced simultaneously in the regression; X is a matrix of time varying control variables and country specific linear, quadratic and cubic time trend. Results are based on May 11 data.

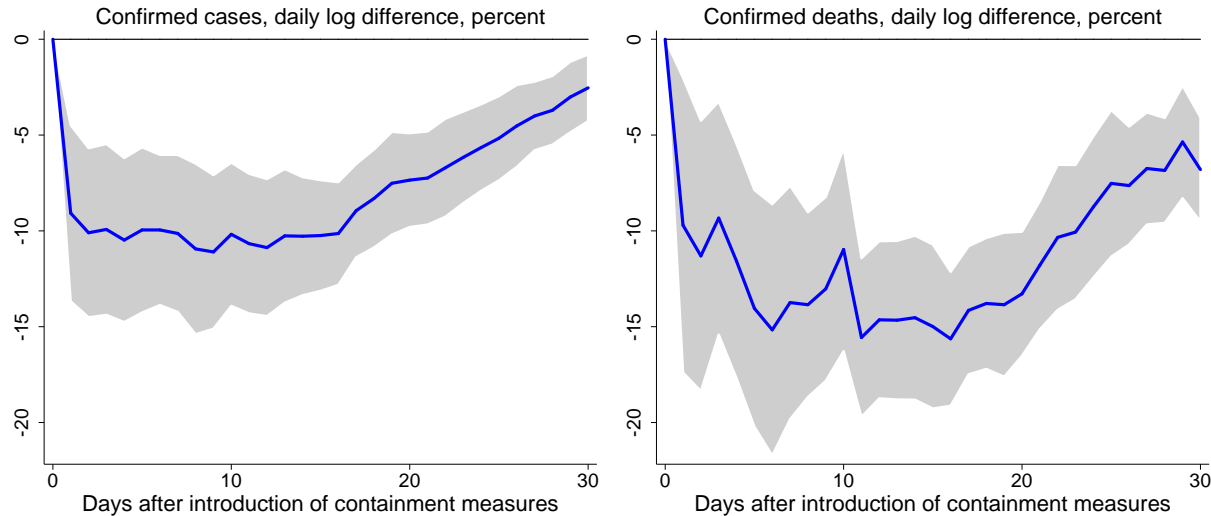
Figure 11b: Local projection response to different containment measures (together)
(percent deviation from baseline)



Note: Impulse response functions are estimated using a sample of 129 countries using daily data from the start of the outbreak. The analysis is restricted to countries with a significant outbreak that has lasted at least 30 days. $t = 0$ is the date when the outbreak becomes significant (100 cases) in each country. The graph shows the response and confidence bands at 95 percent. The horizontal axis shows the response x days after the containment measures. Estimates based on $\Delta d_{i,t+h} = \ln(d_{i,t+h}) - \ln(d_{i,t})$ and $\Delta d_{i,t} = \ln(d_{i,t}) - \ln(d_{i,t-1})$ where $\Delta d_{i,t+h} = d_{i,t+h} - d_{i,t}$ and $d_{i,t}$ is the logarithm of the number of COVID-19 cases or deaths (depending on specification) in country i observed at date t . The model is estimated at each horizon $h = 0, 1, \dots, H$, with a lag structure $\ell = 1, 2, \dots, L$; $c_{i,t}$ are indices capturing different types containment and mitigation measures, introduced simultaneously in the regression; X is a matrix of time varying control variables and country specific linear, quadratic and cubic time trend. Results are based on May 11 data.

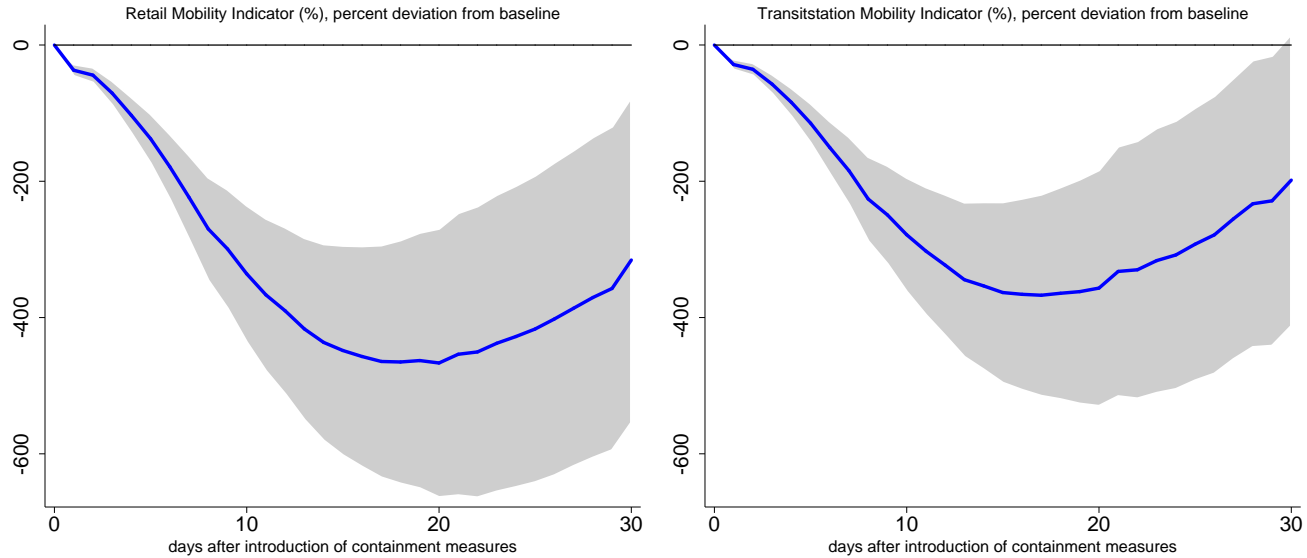
ANNEX

Figure A1: Effect of Containment Measures on New Daily COVID-19 Cases and Deaths



Note: Impulse response functions are estimated using a sample of 129 countries using daily data from the start of the outbreak. The analysis is restricted to countries with a significant outbreak that has lasted at least 30 days. $t = 0$ is the date when the outbreak becomes significant (100 cases) in each country. The graph shows the response and confidence bands at 95 percent. The horizontal axis shows the response x days after the containment measures. Estimates based on $\Delta d_{i,t+h} = u_i + \theta_h c_{i,t} + X'_{i,t} \Gamma_h + \sum_{\ell=1}^L \psi_{h,\ell} \Delta d_{i,t-\ell} + \varepsilon_{i,t+h}$ where $\Delta d_{i,t+h} = d_{i,t+h} - d_{i,t+h-1}$ and $d_{i,t}$ is the logarithm of the number of COVID-19 cases or deaths (depending on specification) in country i observed at date t . The model is estimated at each horizon $h = 0, 1, \dots, H$, with a lag structure $\ell = 1, 2, \dots, L$; $c_{i,t}$ is the index capturing the level of containment and mitigation measures; X is a matrix of time varying control variables and country specific linear, quadratic and cubic time trend. Results are based on May 11 data.

Figure A2: Effect of Containment Measures on Mobility



Note: Impulse response functions are estimated using a sample of 70 countries using daily data from the start of the outbreak. Google mobility and retail indices are reported as percent deviations for each day of the week to that corresponding day of the week in the baseline. They are smoothed out over 7 days to estimate the average deviation from the baseline, and then cumulated to report the total deviation from the baseline. The analysis is restricted to countries with a significant outbreak that has lasted at least 30 days. $t = 0$ is the date when the outbreak becomes significant (100 cases) in each country. The graph shows the response and confidence bands at 95 percent. The horizontal axis shows the response x days after the containment measures. Estimates based on $\Delta d_{i,t+h} = u_i + \theta_h c_{i,t} + X'_{i,t} \Gamma_h + \sum_{\ell=1}^L \psi_{h,\ell} \Delta d_{i,t-\ell} + \varepsilon_{i,t+h}$ where $\Delta d_{i,t+h} = d_{i,t+h} - d_{i,t+h-1}$ and $d_{i,t}$ is the logarithm mobility in country i observed at date t . The model is estimated at each horizon $h = 0, 1, \dots, H$, with a lag structure $\ell = 1, 2, \dots, L$; $c_{i,t}$ is the index capturing the level of containment and mitigation measures; X is a matrix of time varying control variables and country specific linear, quadratic and cubic time trend. Results are based on May 11 data.

The spread of COVID-19 and the BCG vaccine: A natural experiment in reunified Germany¹

Richard Bluhm² and Maxim Pinkovskiy³

Date submitted: 12 May 2020; Date accepted: 13 May 2020

As COVID-19 has spread across the globe, several observers noticed that countries still administering an old vaccine against tuberculosis—the BCG vaccine—have had fewer COVID-19 cases and deaths per capita in the early stages of the outbreak. This paper uses a geographic regression discontinuity analysis to study whether and how COVID-19 prevalence changes discontinuously at the old border between West Germany and East Germany. The border used to separate two countries with very different vaccination policies during the Cold War era. We provide formal evidence that there is indeed a sizable discontinuity in COVID-19 cases at the border. However, we also find that the difference in novel coronavirus prevalence is uniform across age groups and show that this discontinuity disappears when commuter flows and demographics are accounted for. These findings are not in line with the BCG hypothesis. We then offer an alternative explanation for the East-West divide. We simulate a canonical SIR model of the epidemic in each German county, allowing infections to spread along commuting patterns. We find that in the simulated data, the number of cases also discontinuously declines as one crosses from west to east over the former border.

1 The views expressed in this paper are those of the authors and do not necessarily reflect the position of the Federal Reserve Bank of New York or the Federal Reserve System. We are grateful to Gerda Asmus, Melanie Krause and the seminar participants of the Omni-Method Group at UCSD for providing very helpful comments. Any errors or omissions are the responsibility of the authors.

2 Leibniz University Hannover, Institute of Macroeconomics, and University of California San Diego, Department of Political Science.

3 Federal Reserve Bank of New York.

Copyright: Richard Bluhm and Maxim Pinkovskiy

1 Introduction

As COVID-19 has spread across the globe, there is an intense search for treatments and vaccines, with numerous trials running in multiple countries. In light of this, there is now a lively controversy over whether the *Bacillus Calmette-Guérin* (BCG) vaccine against tuberculosis may somehow protect individuals against COVID-19 or limit its severity. Multiple studies (see, e.g., Miller et al., 2020, Berg et al., 2020) pointed out that countries with mandatory BCG vaccination tend to have substantially fewer coronavirus cases and deaths per capita than countries without mandatory vaccination, and that the intensity of the epidemic is lower for countries that began vaccinating earlier.¹ At least eight clinical trials are taking place across the globe² in which some medical workers or volunteers receive the BCG vaccine to test its effectiveness against COVID-19. These trials are likely to take at least a year and the virus is still spreading globally at a rapid pace. As of now, the WHO cautions that there is no evidence that the vaccine protects against the novel coronavirus.³

In this paper we propose a different way to test the hypothesis that BCG protects a large share of vaccinated populations against coronavirus: a regression discontinuity analysis of coronavirus cases at the former border between East Germany and West Germany. This border separated capitalist West Germany from communist East Germany from 1949 to 1990 until the two countries were reunified as the current Federal Republic of Germany. In line with many other Western European countries, West Germany discontinued a policy of de facto universal BCG vaccination (which began in the 1950s) for the general population in 1975, while, equally in line with other former Soviet Bloc countries, East Germany strictly enforced a policy of mandatory BCG vaccination at birth from 1953 until 1990. Although it is known that other characteristics change discontinuously at the old East German border (even before it existed, see Becker et al., 2020, Fuchs-Schündeln and Hassan, 2015, Alesina and Fuchs-Schündeln, 2007), these differences are considerably smaller than if different countries or regions are compared. Moreover, areas of Germany on both sides of the discontinuity have been subject to the same state response to the COVID-19 pandemic. Other discontinuities

¹This started a lively debate in the community on the fallacies of cross-country regressions. As our approach differs from these studies, we only note that other studies which are not based on cross-country data find no such effects, for example when looking at passengers on the Diamond Princess or when controlling for countries' intensity of testing for COVID-19 (Asahara, 2020).

²For example, the BRACE trial in Australia (NCT04327206), the BCG-CORONA trial in the Netherlands (NCT04328441), and more recent trials in Brazil (NCT04369794), Columbia (NCT04362124), Denmark (NCT04373291), Egypt (NCT04350931) and the United States (NCT04348370). ClinicalTrials.gov registry codes are provided in parentheses.

³This warning was based on a review of the available evidence from three cross-country studies. The scientific briefing is published here ([www.who.int/publications-detail/bacille-calmette-gu%C3%A9rin-\(bcg\)-vaccination-and-covid-19](http://www.who.int/publications-detail/bacille-calmette-gu%C3%A9rin-(bcg)-vaccination-and-covid-19)) and explained further in Curtis et al. (2020).

are also less of a concern since we can exploit variation both in space and across age groups to improve identification.

We find a strong discontinuity in cumulative COVID-19 cases across the old East German border, with cases per million roughly halving at the border as of April 26 2020. This discontinuity is robust to controlling for other variables that change discontinuously at the border, such as population density, disposable income, average age and the fraction of the population over 65, as well as age-adjusted death rates from all causes and from infectious diseases.⁴ Importantly, while these control variables are discontinuous at the border, the discontinuities typically go the “wrong way” in terms of their correlations with characteristics that usually indicate more vulnerable populations. Counties on the eastern side of the border are poorer, older and have higher death rates, although they have lower population density, than counties just to the west of the border. We document that the initial geography of the outbreak in wealthier and well-connected places implies that these correlations are reversed from what intuition would suggest. For example, the outbreak is currently stronger in richer, younger and generally healthier places of Germany.

Evidence from discontinuities in COVID-19 confirmed cases by age group suggests that this discontinuity does not come from people on the eastern side of the border being protected by the BCG vaccine. The timing of the adoption and the cessation of mandatory vaccination in East and West Germany implies that the only age groups for which discontinuities should be observed should be individuals between ages 30 and 45, as well as people between ages 59 and 69. For other age groups, there should be no direct effect of the BCG vaccine since they were either unvaccinated or vaccinated on both sides of the border. However, there is a discontinuous decrease in COVID-19 confirmed cases of approximately the same size as one crosses the border into the east for every age group for which we have data, starting with individuals who are 15 years old (people younger than 15 rarely manifest strong enough COVID-19 symptoms to get tested).⁵

We provide further evidence on what could be giving rise to the discontinuity in coronavirus cases at the old border to East Germany by considering the matrix of commuter

⁴Prominent newspapers in Germany have noticed that there is much lower COVID-19 prevalence in the former East than in the West but offer only suggestive explanations (e.g., *Die Zeit*, a German weekly, www.zeit.de/2020/13/coronavirus-ausbreitung-osten-westen-faktoren, or *Der Tagesspiegel*, a Berlin-based German daily, www.tagesspiegel.de/politik/mehr-flaeche-mehr-alte-warum-der-osten-weniger-unter-corona-leidet/25796940.html). Moreover, low COVID-19 mortality in Germany as a whole has been the subject of media interest.

⁵One could expect that vaccinated individuals in a population offer some degree of protection to the unvaccinated. In fact, medical research (Curtis et al., 2020) suggests that there may be a countervailing effect as BCG-vaccinated places may have more asymptomatic individuals with a greater propensity to spread the virus. Even if the overall spillover did offer protection to unvaccinated individuals, the resulting discontinuity for such individuals should be smaller than for the population affected directly by the vaccine.

flows across German counties. Apart from strong connections between major cities in the West and Berlin, these flows still generally proceed within the former West or within the former East rather than between both sides. Since the epidemic started in the West, these flows imply that it was more likely that it would be transmitted more rapidly and widely there than in the East. We simulate a SIR model with mobility flows between counties to assess how mobility patterns shaped the geography of the pre-lockdown outbreak. In line with our empirical evidence, we find that the model also generates a discontinuity at the border, with more cases per capita on the western side relative to the eastern side, without any reference to the BCG hypothesis.

An important caveat is that our study looks only at whether or not there is a long-run effect of the BCG vaccine (roughly decades after it was administered). The BCG hypothesis essentially comes in two variants. The broad version suggested by cross-country correlations hypothesizes that people who have received this vaccine in the past (perhaps with refreshers) develop no or comparatively milder symptoms of COVID-19 than those who have not, enough for this to show up in the incidence of novel coronavirus cases around the world. If this were true, the BCG vaccine would provide a respite to the developing world as the virus spreads globally, which is why prominent news outlets have reported this correlation.⁶ This is the question we address in this paper. However, the BCG vaccine's positive effect on other viral infections, such as yellow fever (Arts et al., 2018), is a trained response of the immune system typically occurring within one to twelve months after it has been administered. The evidence of such trained responses is mixed (for a review see Kandasamy et al., 2016) although recently a consensus seems to have emerged that the protective effects on other diseases occur via epigenetic reprogramming (Kleinnijenhuis et al., 2015, Covián et al., 2019). The narrow version of the hypothesis suggests that the vaccine might have a short-run effect which could offer some protection to health workers and other risk groups. Our research design cannot test this aspect as the vaccine has been discontinued in both parts of Germany for 30 years. Only the results from randomized trials can answer that question.

The remainder of the paper is organized as follows. Section 2 describes the county-level data on cases, covariates, and commuter flows. Section 3 discusses the temporal differences in BCG policies in Germany from partition to reunification and describes our empirical strategy. Section 4 presents the results for discontinuities in overall cases, the most relevant covariates, cases by age-groups, and the placebo test with cases simulated from a county-level SIR model with mobility. Section 5 concludes.

⁶See, for example, *The New York Times* (www.nytimes.com/2020/04/03/health/coronavirus-bcg-vaccine.html) or *Bloomberg News* (www.bloomberg.com/news/articles/2020-04-02/fewer-coronavirus-deaths-seen-in-countries-that-mandate-tb-vaccine).

2 Data

COVID-19 spread in Germany: We obtain counts of cumulative cases of and deaths from COVID-19 by German county (*Kreis*) and by age group for every date since February 29 2020 from the Robert Koch Institute's Coronavirus Dashboard.⁷ Germany has one of the most comprehensive testing regimes among the heavily affected countries.⁸ Nevertheless, given the difficulties in recording asymptomatic cases of COVID-19 that may still be contagious, it is very likely that the case counts we employ in this paper are a lower bound for novel coronavirus infections in Germany.⁹ Streeck et al. (2020) study a large sample of the city of Heinsberg—a community with an early a super-spreading event—and estimate that the true case count is about five times larger than officially registered cases. We proceed on the necessary assumption that the cumulative reported case count is a valid measure of COVID-19 intensity in a given subpopulation, and that undercounting errors are uniform across age groups and locations.

We start our analysis with a map of COVID-19 cases in Germany by county as of April 26 (see Figure 1). The former border between East and West Germany is outlined in red. The darker the shading of a county, the more novel coronavirus cases per million inhabitants it has. Several counties with high concentrations stand out (such as Heinsberg, bordering the Netherlands, and much of Bavaria, both places where the epidemic was first recorded). It is also clear that there is a greater density of COVID-19 cases around major cities (Berlin, Hamburg or Stuttgart), similar to the United States. However, we immediately see that counties just to the west of the former border are a much darker shade of blue than counties just to its east.

County-level covariates: We collect four groups of county-level characteristics: income and demographics, historical mortality, and commuting flows. Baseline characteristics of each county (shapes, names and areas) are from the Federal Agency for Cartography and Geodesy (*Bundesamt für Kartographie und Geodäsie*).

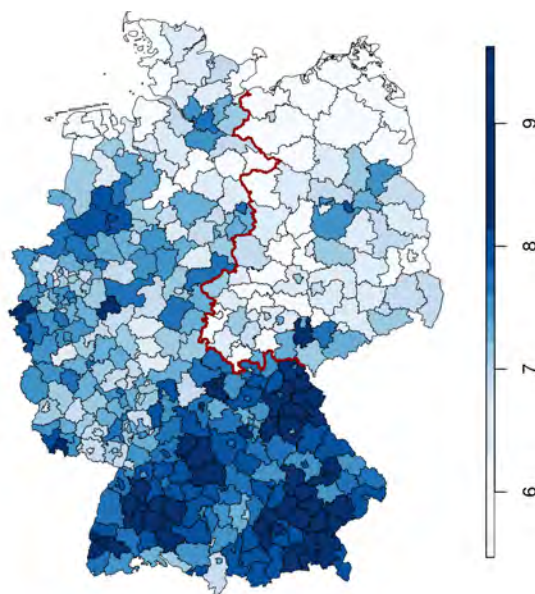
Measures of disposable income in 2017, the age distribution in 2018 (aggregated to different age groups or shares), and population density in 2018 are taken from official

⁷The data are publicly available at corona.rki.de.

⁸By April 21 2020, Germany had conducted 2,072,669 tests or about 24,966 tests per million people (Robert Koch-Institut, 2020). This is almost double the testing rate in the United States, United Kingdom or South Korea, see www.businessinsider.com/coronavirus-testing-per-capita-us-italy-south-korea-2020-4.

⁹These considerations may make it reasonable to treat cumulative case counts as an indication of the severity rather than of the incidence of COVID-19, since very mild cases, which may account for the majority of COVID-19 infections, typically do not lead to testing.

Figure 1 – Covid-19 cases in Germany, April 26 2020, $\log(1 + \text{cases}/\text{million})$



Notes: Illustration of the spatial distribution of COVID-19 cases in Germany as of April 26, 2020. The map shows the $\log(1 + \text{cases}/\text{million people})$ in each county using population data from 2018.

statistics published by the federal statistical office and the statistical offices of each state.¹⁰

We also collect data on overall mortality (in 2017), mortality from selected infectious diseases and mortality from respiratory diseases (both in 2016) from the same source. Germany does not publish age-adjusted mortality figures. Given that the age-profile of the population varies significantly across counties in Germany, we manually age-adjust all mortality figures using the corresponding age distribution of the entire country in 2017 or 2016, respectively.¹¹ This allows us to analyze regional mortality differences net of local demographics.

Last but not least, we use the latest available data on commuting flows published by the Federal Employment Agency (*Bundesagentur für Arbeit*). The agency regularly releases an origin-destination matrix of commuting flows across German counties. These flows capture about 33 million officially registered jobs (all jobs with social security contributions). Approximately 39%, or 13 million, of the jobs are in a different county than the primary

¹⁰The data are available at www.regionalstatistik.de/genesis.

¹¹The age-adjustment re-weights local mortality with the age profile of the entire country. We follow the direct method used by the U.S. Centers for Disease Control (Klein and Schoenborn, 2001).

tax residence of the employee. We use the county-to-county data from December 2019 to capture connections between western and eastern counties just before the outbreak of the novel coronavirus. While this cannot account for all travel flows around the outbreak perfectly, we assume that such unobserved flows follow the dominant pattern of employees returning home.¹²

3 Empirical Strategy

Our study exploits a discontinuous change in vaccination policies across the former border dividing East and West Germany from 1949 until 1990.

Germany had a non-vaccination policy until the end of World War II and did not join Red Cross-led vaccination campaigns in the early post-war years, even though tuberculosis was widespread among the war-ravaged population.¹³ BCG policies then diverged quickly when the country was divided. In 1953, the German Democratic Republic (GDR) introduced mandatory vaccination for a variety of diseases, including the BCG vaccine against tuberculosis.¹⁴ The policy lasted until the collapse of the GDR in 1990. The Federal Republic of Germany only required mandatory vaccination for smallpox from 1949 until the end of 1975. The BCG vaccine was highly recommended but administered on a voluntary basis. In practice, vaccination of newborns was near universal by the mid-1960s.¹⁵ In 1974, the policy was changed to vaccinate only children in risk groups and, in 1975, the BCG vaccine was temporarily withdrawn from the market in the West. Neo-natal vaccination practically ceased for two years (Genz, 1977). Voluntary vaccination of risk groups continued thereafter until 1998 (Robert Koch-Institut, 1976, 1998) but few people were vaccinated in West Germany from 1975 onward or in reunified Germany after 1990. Currently, no BCG vaccine is licensed in Germany. We summarize these political changes in Table 1. We use precisely these differences in vaccination policies across the former East and West, as well as

¹²A suitable alternative would be an origin-destination matrix derived from mobile phone movements through the early months of 2020. However, Germany's strong privacy protection laws have the side-effect that such products are rarely produced by private companies.

¹³This decision was in part due to the "Lübeck vaccination disaster" in which 251 infants were vaccinated with a BCG vaccine contaminated with live tuberculosis bacteria. Almost all children fell ill with tuberculosis and 72 died, leading the Interior Ministry to reject BCG vaccination as unsafe in 1930 (Loddenkemper and Konietzko, 2018).

¹⁴Enforcement in the GDR was strict. "From 1954 on, school children who had not yet been vaccinated had to present a letter of exemption not only from their parents but also from a physician" (Harsch, 2012, p. 420). Vaccinations substantially outstripped newborns in the early 1950s, suggesting that young adults born before the GDR existed where also vaccinated ex post.

¹⁵Due to the decentralized nature of the West German health care system, the initial roll out of the vaccination policy varied strongly by state in the 1950s. However, by 1964, practically all newborns in West Germany were BCG vaccinated shortly after birth (Kreuser, 1967).

across cohorts, to identify the effect of historical BCG vaccination on the spread of COVID-19 cases.

Table 1 – Timeline of vaccination policies in both parts of Germany, 1949 until today

Year	West Germany (FRG)	East Germany (GDR)
1949		First BCG vaccinations
1951-52		Extended program with GDR manufactured BCG vaccine
1953	BCG vaccine is licensed	Mandatory vaccination (with refresher), target rate at least 95%
1955	Recommendation to vaccinate all newborn children	
Mid 1960s	Near universal vaccination of newborns	Near universal vaccination of newborns
1974	Recommendation to only vaccinate children in risk groups	
1975	BCG vaccination temporarily halted	
1983	Further restriction to only those children that have TB in the family	
1988	Vaccine recommended only for children that tested negative for tuberculin and are risk groups	
1990	Reunification, policies of FRG continue	Reunification, policies of FRG apply
1998	Vaccination no longer recommended	

Notes: Based on Klein (2013) and various sources cited in the text.

We employ two related techniques to exploit these policy discontinuities. For our baseline estimates, we specify a spatial regression discontinuity (RD) design of the form

$$y_c = \alpha + \beta \text{EAST}_c + \delta_1 d_c + \delta_2 (d_c \times \text{EAST}_c) + \lambda_{s(c)} + \varepsilon_c \quad \text{if } |d_c| < b \quad (1)$$

where c indexes counties (*Kreise*), y_c is the outcome variable, EAST_c indicates whether the county was part of East Germany before reunification, d_c is the distance of county c from the former East German border (it is negative if $\text{EAST}_c = 0$ and positive if $\text{EAST}_c = 1$), and $\lambda_{s(c)}$ is a fixed effect for the border segment associated with county c . Border segments are defined as pairs of bordering states (*Bundesländer*). Note that we drop Berlin throughout the analysis and focus on the border separating the two larger countries, as Berlin in its entirety cannot be cleanly assigned to either East or West. Following Gelman and Imbens (2019), our specification uses an interacted local linear RD polynomial at a variety of plausible bandwidths b , ranging from 50 km to 200 km. We select this range by computing optimal bandwidths for the specification without border segment fixed effects according to various criteria developed in the literature (Imbens and Kalyanaraman, 2011, Calonico et al., 2014).

They vary by outcome but generally fall somewhere in the range between 80–200 km.

Spatial RD designs identify the causal effect directly at the border if three crucial assumptions hold (see, e.g., [Dell, 2010](#)). First, all other factors besides our treatment variable (BCG vaccination) should vary smoothly from counties just to the east and just to the west of the border at the time it was drawn. The strength of the RD approach is that it non-parametrically controls for these confounders, even if they are unobserved. Second, there should be no compound treatment, so that counties belonging to the West or East of the former border vary only according to the BCG regime. Third, there should be no selective sorting at the border at the time of the treatment. The first and second assumption are likely to be violated in our setting. As [Becker et al. \(2020\)](#) document, the post-war border is already visible in many economic variables before World War II and East Germany differed from West Germany in many more ways than its BCG vaccination policy. Selective sorting is unlikely during the Cold War years and was probably not motivated by the different BCG regimes, but selective migration did occur prior to the closing of the border in 1961. Hence, the simple discontinuity design presented in eq. (1) has a number of flaws.

We address these concerns by additionally exploiting the temporal discontinuity across cohorts. The RKI data reports COVID-19 cases for several cohorts, including those that are currently 15–34 or 35–59 years old. [Table 1](#) shows that most members of the first age group did not get the vaccine anywhere. In the second group, everyone was vaccinated in the East but only those above 45 years old could have received the vaccine in the West if they were not part of the small risk group. The effect of pre-World War II confounders does not vary specifically across these two age groups and any compound treatment mostly affects the older cohort. We can therefore identify whether BCG vaccinations have an effect on the COVID-19 cases by simply comparing the regression coefficients across these two groups. Following [Deshpande \(2016\)](#), we can formalize this comparison by estimating a regression discontinuity differences-in-differences (RD-DD) specification

$$y_{c,a} = \alpha_a + \beta \text{EAST}_c + \gamma \text{EAST}_c \times \text{OLD}_a + \delta_1 d_c + \delta_2 d_c \times \text{EAST}_c + \delta_3 d_c \times \text{OLD}_a + \delta_4 d_c \times \text{EAST}_c \times \text{OLD}_a + \lambda_{s(c),a} + \varepsilon_{c,a} \quad \text{if } |d_c| < b \quad (2)$$

where a indexes age groups (15–34 and 35–59), OLD_a is an indicator for the age group 35–59, and the intercept and the border segment fixed effects are allowed to vary by age group. The coefficient of interest, γ , delivers an estimate of the difference in discontinuities across cohorts. The identification assumptions for this specification are less stringent than for the original RD design because we now allow discontinuities in other controls as long as they are the same across age groups. In particular, any compound treatment effects are differenced

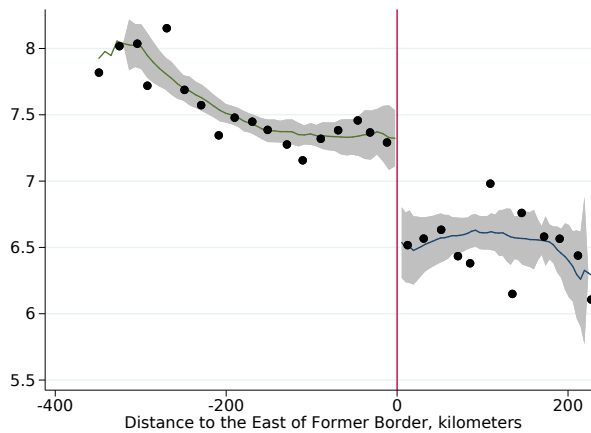
out if they are the same at ages 15–34 and 35–59, and selective sorting at the border is allowed insofar as both age groups are sorting in the same way.

If the BCG hypothesis is true, then we would expect to see a negative discontinuity in cases for the older cohorts but no discontinuity or a much smaller discrepancy in the younger cohort. Finding a sizable discontinuity in both cohorts, or no differences in the discontinuity across cohorts, would be direct evidence against the broad version of the BCG hypothesis and an indication that something else is driving these results. As our data does not contain any age group which was recently vaccinated, we cannot assess whether the BCG vaccine has a short-run effect on those that were vaccinated within the last year.

4 Results

Baseline regression discontinuity results: To formalize the intuition of [Figure 1](#), we use a regression discontinuity design, in which we nonparametrically estimate coronavirus prevalence as a function of the distance to the border and compare the estimates just to the east and just to the west of the border. Our main dependent variable is the logarithm of unity plus the number of cumulative COVID-19 cases per million in a German county as of April 26, 2020. As the average German county (*Kreis*) has about 200,000 inhabitants and nearly every *Kreis* has at least one confirmed COVID-19 case, this function behaves very similarly to the logarithm of cumulative cases per million. [Figure 2](#) presents nonparametric estimates of the mean of the dependent variable by distance to the border of the former GDR, with positive distances indicating locations in former East Germany and negative distances corresponding to locations in former West Germany. We use a bandwidth of 100 km, which corresponds well to the optimal bandwidth (following [Imbens and Kalyanaraman, 2011](#)). We observe that while the nonparametric estimates are continuous to the left and to the right of zero, they are very discontinuous at zero with a downward jump of approximately 0.7 log points as one moves from west to east. This implies that there are half as many cases per capita in a former East German county relative to a West German county just across the border. This halving of cases dominates the variation in coronavirus prevalence among counties in the East (where it is uniformly low) and is sizable relative to the average prevalence in the West. Faraway counties in Bavaria (close to the early outbreaks in Italy) or near the borders with France and the Benelux countries have the highest cases.

The first row of [Table 2](#) further formalizes our results by estimating [eq. \(1\)](#) for 5 different bandwidths—50 km, 75 km, 100 km, 150 km and 200 km. The smallest of these bandwidths entails running the regression on 77 German counties closest to the former border, whereas the largest of these bandwidths runs the regression on 287 of the 401 counties in Germany.

Figure 2 – Discontinuity in $\log(1 + \text{cases}/\text{million})$ at former border

Notes: Illustration of the discontinuity $\log(1 + \text{cases}/\text{million people})$ across the former border between West and East Germany. The figure shows non-parametric local polynomial estimates for bins of the dependent variable, where each bin is 20 km wide. 95% confidence intervals are shaded in grey.

The latter three correspond to the range of the optimal bandwidths discussed in [Section 3](#).¹⁶ Different bandwidths alter the variance-bias trade-off in the RD point estimate. The degree of misspecification error is essentially controlled by the choice of bandwidth. Smaller than optimal, or undersmoothed, bandwidths create less bias in conventional confidence intervals than large bandwidths ([Calonico et al., 2014](#)), which is why we emphasize the results for 100 km or less. We see that the estimate for a 100 km bandwidth is a drop of -0.83 log points, or 57% of the cumulative COVID-19 case count as one crosses the border from West to East. This estimate is robust and statistically significant at 99% across bandwidths, ranging from -0.71 for a bandwidth of 75 km to -0.89 for a bandwidth of 200 km.¹⁷

The second row of [Table 2](#) shows that there is also a discontinuity in COVID-19 deaths per million residents, which is larger in size than the discontinuity in the cumulative COVID-19 cases (although the estimates are noisier and the confidence intervals overlap because deaths are a small fraction of cases). For a 100 km bandwidth, crossing the border from west to east entails a 1.05 log point (65% decrease) in the number of deaths per million residents, with estimates for wider bandwidths showing a 50% larger drop.

¹⁶These bandwidths were computed for specifications without border segment fixed effects, whereas [eq. \(1\)](#) always includes border segment fixed effects.

¹⁷We present additional robustness of the discontinuity in cumulative COVID-19 cases to alternative functional forms of the local polynomial in [Table B-1](#) of the Appendix.

Table 2 – Discontinuities in cases, deaths and other variables

	<i>The dependent variable varies by panel</i>				
	<i>The bandwidth is</i>				
	50 km (1)	75 km (2)	100 km (3)	150 km (4)	200 km (5)
<i>Panel A. Log(1+cases/million)</i>					
EAST	-.787*** (.240)	-.710*** (.149)	-.830*** (.154)	-.987*** (.196)	-.890*** (.143)
<i>Panel B. Log(1+deaths/million)</i>					
EAST	-.963** (.488)	-.860*** (.308)	-1.05*** (.290)	-1.48*** (.423)	-1.59*** (.201)
<i>Panel C. Disposable income p.c.</i>					
EAST	-.084*** (.026)	-.100*** (.014)	-.104*** (.005)	-.128*** (.015)	-.134*** (.014)
<i>Panel D. Population density</i>					
EAST	-.692** (.279)	-.584*** (.097)	-.659*** (.230)	-.474*** (.154)	-.102 (.193)
<i>Panel E. Percent older than 64</i>					
EAST	2.585*** (.889)	2.175*** (.830)	2.424*** (.658)	3.132*** (.616)	3.109*** (.613)
<i>Panel F. Percent older than 45 and younger than 65</i>					
EAST	2.251*** (.778)	1.653*** (.567)	2.105*** (.546)	1.714*** (.478)	.992** (.445)
<i>Panel G. Age-adjusted overall death rate per million</i>					
EAST	.057*** (.018)	.048** (.020)	.045** (.020)	.059*** (.016)	.041* (.023)
<i>Panel H. Age-adjusted infectious diseases death rate per million</i>					
EAST	2.048** (.841)	1.723* (.998)	2.190** (1.087)	2.630** (1.146)	2.688** (1.119)
<i>Panel I. Age-adjusted respiratory diseases death rate per million</i>					
EAST	2.613** (1.109)	2.191* (1.258)	2.785** (1.372)	3.216** (1.457)	3.310** (1.437)
Observations	77	106	138	203	287

Notes: The table reports results from a regression discontinuity specification with an interacted local linear RD polynomial and border segment fixed effects. Disposable income per capita and population density are measured in logs. Standard errors clustered on the state (*Bundesländer*) level are reported in parentheses.

Discontinuities in control variables: It is well known that while West and East Germany have been reunified for 30 years, there are still considerable differences between the two territories. Alesina and Fuchs-Schündeln (2007) document persistent differences in trust, and Fuchs-Schündeln and Hassan (2015) show that many important economic variables are still discontinuous at the border.

In the remainder of Table 2 we investigate these additional discontinuities to assess whether they may explain the discontinuity in COVID-19 intensity that we have observed in the previous subsection. We see that regardless of the bandwidth used in the 50 km–200 km range, log population density, log disposable income, the share of the population aged 45 to 64 and the share older than 64, the date that the first COVID-19 case was recorded, and age-adjusted mortality from all causes, infectious diseases and respiratory diseases all show discontinuities at the old border. This fact alone complicates the interpretation of the discontinuity in cumulative COVID-19 cases as causal, and raises the possibility that it may be driven by some of these variables and not by an inherent characteristic of East Germans, such as BCG vaccination.

It is noteworthy that the signs of the discontinuities indicate that counties just to the east of the border have lower population density, lower consumption, an older population, a later introduction of COVID-19 and higher age-adjusted mortality rates than counties just to the west of the border. Intuitively, all of these factors, except for population density, should lead one to expect that counties just to the east should have a higher COVID-19 prevalence than counties just to the west. However, as we show in Table B-2 in the Appendix, both within the former East Germany and within the former West Germany, the raw correlations between cumulative COVID-19 cases and consumption per capita, population age and age-adjusted mortality rates all point in the “wrong” direction. For example, the correlation between log consumption per capita and log cumulative COVID-19 cases per capita is positive, while the correlations between log cumulative cases and age or mortality variables are generally negative. This suggests that the geography of the early outbreak in Germany was very particular. Indeed, some of the first cases in Bavaria were imported during the winter sports season from Italy and Austria, while early cases in the southwest can be linked to carnival celebrations. The virus then spread quickly through comparatively young and affluent counties—an issue to which we return below. While a similar pattern currently holds across US counties (where affluent and urban areas were exposed first), there are first signs that these correlations may ultimately reverse. The highest case counts per capita within New York City, for example, are in the poorer zip codes of Brooklyn, Queens and the Bronx, while upper-class zip codes have fewer cases.¹⁸

¹⁸See www.time.com/5815820/data-new-york-low-income-neighborhoods-coronavirus/.

Table 3 – Regression discontinuity results with controls

	<i>The dependent variable is $\log(1+\text{cases}/\text{million})$</i>				
	<i>The bandwidth is</i>				
	50 km (1)	75 km (2)	100 km (3)	150 km (4)	200 km (5)
<i>Panel A. No Controls</i>					
EAST	-.787*** (.240)	-.710*** (.149)	-.830*** (.154)	-.987*** (.196)	-.890*** (.143)
<i>Panel B. Population density</i>					
EAST	-.750*** (.220)	-.673*** (.155)	-.807*** (.183)	-.979*** (.203)	-.887*** (.144)
<i>Panel C. Disposable income p.c.</i>					
EAST	-.675*** (.256)	-.605*** (.189)	-.661*** (.171)	-.814*** (.200)	-.682*** (.177)
<i>Panel D. Disposable income p.c. and population density</i>					
EAST	-.606** (.243)	-.537** (.232)	-.602** (.242)	-.782*** (.238)	-.654*** (.193)
<i>Panel E. Percent older than 45 but younger than 65 and percent older than 64</i>					
EAST	-.582*** (.159)	-.530*** (.104)	-.717*** (.158)	-.804*** (.175)	-.694*** (.165)
<i>Panel F. Controls from panels D and E</i>					
EAST	-.411** (.181)	-.384** (.160)	-.442** (.183)	-.591*** (.212)	-.498** (.199)
<i>Panel G. Days since first case</i>					
EAST	-.777*** (.241)	-.698*** (.153)	-.813*** (.156)	-.972*** (.198)	-.858*** (.148)
<i>Panel H. Age-adjusted overall death rate per million</i>					
EAST	-.717*** (.216)	-.646*** (.143)	-.740*** (.151)	-.875*** (.205)	-.798*** (.160)
<i>Panel I. Age-adjusted infectious diseases death rate per million</i>					
EAST	-.673** (.274)	-.607*** (.142)	-.640*** (.135)	-.786*** (.157)	-.740*** (.134)
<i>Panel J. Age-adjusted respiratory diseases death rate per million</i>					
EAST	-.648** (.268)	-.591*** (.140)	-.614*** (.125)	-.757*** (.151)	-.708*** (.128)
Observations	77	106	138	203	287

Notes: The table reports results from a regression discontinuity specification with an interacted local linear RD polynomial and border segment fixed effects. Disposable income per capita and population density are measured in logs. Standard errors clustered on the state (*Bundesländer*) level are reported in parentheses.

For each of the control variables analyzed in Table 2, we present evidence that the discontinuity in cumulative COVID-19 cases remains after adding the control variable in eq. (1). Table 3 presents the results. Panel A replicates the estimates without controls for reference. We see that irrespective of which additional variable is controlled for and regardless of the bandwidth used the estimate of the discontinuity in cumulative COVID-19 cases—the coefficient β in eq. (1)—remains negative and statistically significant at least at 5%. Only the magnitude declines somewhat across the different specifications. Even including multiple controls in the same regression—as in Panel F, where we include log disposable income per capita, log population density and percentages of the population above 45 and above 65—does not render the discontinuity in cumulative COVID-19 cases statistically insignificant. However, the magnitude of the RD coefficient falls by half, suggesting that these variables might play some role in explaining the East-West differential.

On balance, the evidence so far shows that there is a discontinuity in the intensity of COVID-19 across the former border separating East and West Germany, which is not primarily mediated by many of the channels one might have anticipated *ex ante* (or which were suggested by the German news media). We now turn to investigating potential explanations for this discontinuity, and specifically to the question of whether the discontinuity could be coming from greater BCG vaccination in former East Germany.

Age-specific regression discontinuity and RD-DD results: We now leverage the fact that different cohorts were vaccinated in the different parts of Germany to assess whether the BCG vaccine plays any role in this robust discontinuity for overall cases. The Robert Koch Institute provides age category breakdowns for county-level data on COVID-19 cases and deaths allowing us to obtain county-specific case and death totals for individuals aged 15–34 and individuals aged 35–59. As discussed earlier, if the discontinuity in COVID-19 cases is caused by the direct long-term effect of BCG vaccination, then we would expect that discontinuities in detected cases among people aged 15–34 should be close to zero (as most of them were never vaccinated in either part of Germany) while discontinuities among people aged 35–59 should be nonzero (since all of whom were vaccinated in the East but only those above 45 in the West). Given assessments in the medical community, we do not presume that spillovers to unvaccinated parts of the population would play a large role.¹⁹

Table 4 presents estimates of the discontinuity in cumulative COVID-19 cases per capita by age group. Panel A reproduces the baseline estimates. The next two rows present

¹⁹In the best case, having received the BCG vaccine bolsters the immune response to COVID-19 so that individuals display fewer symptoms (Curtis et al., 2020). Whether this implies that their viral load is lower so that they would infect fewer people, or whether the exact opposite would happen because they are more likely to be asymptomatic and feel “safe” is not clear at this point.

discontinuities for age groups 0–4 and 5–14. Individuals in both of these groups are unvaccinated on both sides of the former border, so that we should expect no discontinuity if BCG vaccination were to drive the difference. Instead, we observe statistically significant negative discontinuities in COVID-19 cases per capita for each of these groups. Moreover, these discontinuities are much larger in magnitude than the baseline discontinuity shown in Panel A. This evidence does not align with the BCG hypothesis. However, we are reluctant to place a lot of weight on them, since there are few COVID-19 cases in children younger than 15.

Panel D of Table 4 presents discontinuity estimates for individuals aged between 15 and 34. Roughly a quarter of COVID-19 cases in Germany involve people in this age group, so that the concern about drawing conclusions from too few data points does not apply. Once again, there are statistically significant negative discontinuities in cases per capita as one crosses the old border from west to east. Moreover, the magnitudes of these discontinuities are larger than the magnitudes of these discontinuities for the population as a whole (in Panel A). Panel E presents estimates for individuals between 35 and 59. Half of these individuals were vaccinated in West Germany while all of them were vaccinated in East Germany. Accordingly, we would expect this population to exhibit the largest discontinuity in COVID-19 cases per capita if the broad BCG hypothesis were true. However, while the discontinuities are large, statistically significant and negative, they are slightly smaller than the discontinuities for the whole population, let alone the 15–34 and 5–14 age groups. We present graphical illustrations of these discontinuities in Figure 3.

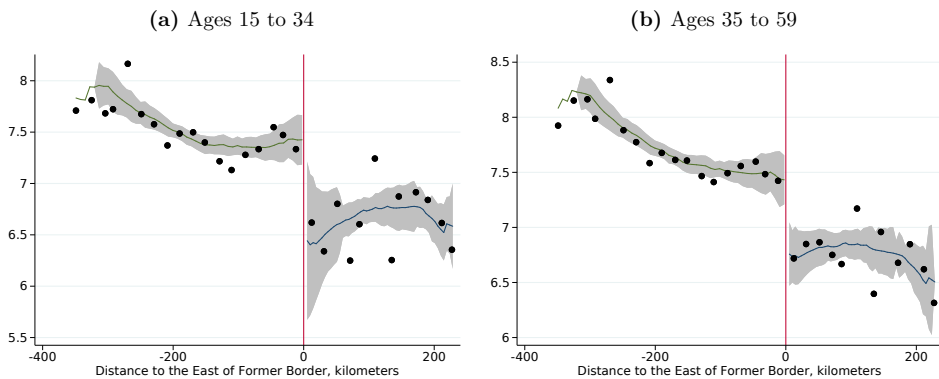
The results for the RD-DD specification which formalizes this comparison are presented in Panel H of Table 4. Recall that the coefficient of interest is γ . It captures the additional effect of being in the East on cumulative cases per million among the 35–59 population compared to the 15–34 cohort. This specification underlines that there is no statistically significant difference in COVID-19 prevalence across these two cohorts in spite of the abrupt change in BCG vaccination. Instead, the estimated effect is positive and equal to approximately a third of the baseline effect for the 15–34 population. Hence it appears that, if anything, the 35–59 year old population in the East is more vulnerable to infections with the novel coronavirus relative to their peers in the West. All of the available evidence points in the direction of a larger discontinuity in COVID-19 cases per capita for populations that were unvaccinated on both sides of the former border. Again, this fact is inconsistent with the empirical predictions of the BCG hypothesis.

Placebo simulation with commuting patterns: If the BCG vaccine does not explain the East-West differential in coronavirus cases, then what does? A potential answer can

Table 4 – Regression discontinuity by age group and RD-DD

	<i>The dependent variable varies by panel</i>				
	<i>The bandwidth is</i>				
	50 km (1)	75 km (2)	100 km (3)	150 km (4)	200 km (5)
<i>Panel A. All cases</i>					
EAST	-.787*** (.240)	-.710*** (.149)	-.830*** (.154)	-.987*** (.196)	-.890*** (.143)
<i>Panel B. Cases for ages 00-04</i>					
EAST	-1.59 (1.049)	-1.81** (.831)	-2.11*** (.606)	-2.44*** (.637)	-1.49*** (.511)
<i>Panel C. Cases for ages 05-14</i>					
EAST	-3.42*** (.582)	-2.53*** (.605)	-2.72*** (.783)	-2.83*** (.776)	-2.04** (.814)
<i>Panel D. Cases for ages 15-34</i>					
EAST	-1.04** (.464)	-.937* (.496)	-1.10* (.570)	-1.18** (.461)	-.993*** (.278)
<i>Panel E. Cases for ages 35-59</i>					
EAST	-.685*** (.166)	-.610*** (.104)	-.732*** (.128)	-.848*** (.181)	-.770*** (.151)
<i>Panel F. Cases for ages 60-79</i>					
EAST	-.678** (.302)	-.719*** (.125)	-.858*** (.093)	-1.07*** (.189)	-1.06*** (.113)
<i>Panel G. Cases for ages 80p</i>					
EAST	-.984** (.434)	-.928* (.535)	-1.33** (.533)	-1.72*** (.412)	-1.63*** (.276)
<i>Panel H. RD-DD on age 15-34 and 35-59</i>					
EAST × OLD	.363 (.391)	.327 (.426)	.370 (.486)	.337 (.349)	.223 (.246)
Observations	77	106	138	203	287

Notes: The table reports results from a regression discontinuity specification with an interacted local linear RD polynomial and border segment fixed effects. Standard errors clustered on the state (*Bundesländer*) level are reported in parentheses.

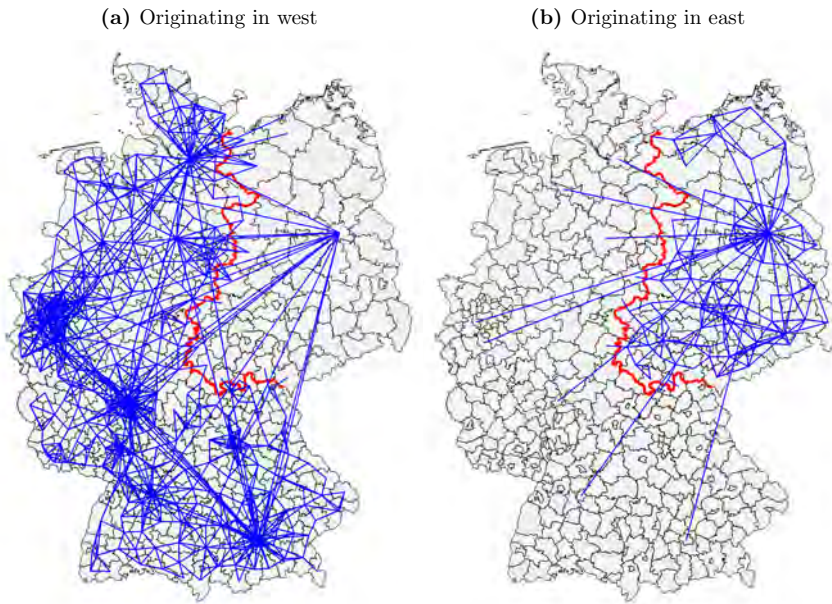
Figure 3 – Age-specific discontinuity in $\log(1 + \text{cases}/\text{million})$ at former border

Notes: Illustration of the discontinuity $\log(1 + \text{cases}/\text{million people})$ across the former border between West and East Germany for different age groups. Panel a) shows results for ages 15 to 34 and panel b) shows results for ages 35 to 59. Both figures show non-parametric local polynomial estimates for bins of the dependent variable, where each bin is 20 km wide. 95% confidence intervals are shaded in grey.

be found in Germany's regional connectedness. If those who live in the west work in the west and those who live in the east work in the east, it may be the case that travel flows have not readjusted completely since reunification. In other words, western counties along the former border may be disproportionately disconnected to their eastern neighbors than if there never would have been a national border dividing them. Although commuting over long distances is very common in Germany—almost 40% of jobs were in a different county than the primary residence—decades of partition meant that its infrastructure was re-oriented to connect counties within the west or east (Santamaria, 2020), with lasting effects on the spatial equilibrium in Germany.²⁰ As the epidemic started in the west, it may have had a harder time spreading eastward because relatively fewer people commute from west to east than commute across comparable distances within the west. The eastward spread was then further interrupted by the nation-wide lock-down on March 22 2020.

Figure 4a presents major outgoing commuter flows (more than 1,000 commuters per county) originating in what used to be West Germany. We see that our expectation is confirmed: almost all of them also go to the West. The only major destination in former East Germany is Berlin (neither Dresden nor Leipzig receive significant inflows from the west

²⁰Large infrastructure projects try to overcome this pattern since reunification but it is, for example, still difficult to reach Dresden from Cologne (or anywhere in the Ruhrgebiet) by public transport. Similarly, the Berlin–Munich high-speed rail connection was under construction since 1996 and only achieved modern speeds close to 4 hours in December 2017. Both distances are slightly less than 600 km.

Figure 4 – Major commuting flows (at least 1,000 people) by origin

Notes: Illustration of major commuter flows origination in the former FRG and former GDR based on the December 2019 commuting flows published by the Federal Employment Agency (*Bundesagentur für Arbeit*). For the purposes of this map, Berlin is geographically considered to be a part of the East.

but some counties on the eastern side of the old border receive some non-negligible flows). Similarly, in [Figure 4b](#) we see that major outgoing commuter flows originating in former East Germany also generally terminate in the East, again with the exception of significant flows from the capital to other western major cities. This holds in spite of a large wave of migration from East to West post-reunification. In fact, some of these flows are government workers who officially commute between Bonn, the old capital of the FRG which retained some government functions, and Berlin.

[Table 5](#) puts these figures into our RD framework and presents discontinuity estimates for the fraction of incoming commuter flows that originate in West Germany at the county-level. Panel A shows that counties just to the east of the border receive between 32 and 72 percentage points more of their commuter flows from East Germany than do counties just to the west of the border. The standard errors are relatively small, so that these estimates are significant at all conventional levels. In Panel B of [Table 5](#) we add this fraction of commuters from the West to our baseline regression for COVID-19 cases per capita across all age groups. This has a comparatively strong effect on the results. The RD coefficient at the reference

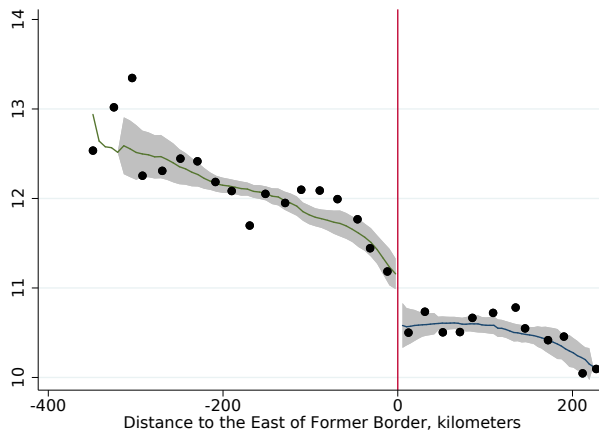
Table 5 – Regression discontinuity results with commuting and simulated results

	<i>The dependent variable is $\log(1+\text{cases}/\text{million})$</i>				
	<i>The bandwidth is</i>				
	50 km (1)	75 km (2)	100 km (3)	150 km (4)	200 km (5)
<i>Panel A. Fraction of incoming flows from West</i>					
EAST	-.354*** (.027)	-.475*** (.026)	-.555*** (.022)	-.669*** (.020)	-.720*** (.021)
<i>Panel B. $\log(1+\text{cases}/\text{million})$, controlling for flows from West</i>					
EAST	-.544*** (.187)	-.363** (.166)	-.349* (.202)	-.322 (.200)	-.350 (.224)
<i>Panel C. $\log(1+\text{cases}/\text{million})$, controlling for income, demographics and flows from West</i>					
EAST	-.320 (.220)	-.171 (.166)	-.075 (.231)	-.160 (.252)	-.242 (.248)
<i>Panel D. $\log(1+\text{simulated cases}/\text{million})$</i>					
EAST	-.438* (.227)	-.493* (.254)	-.588** (.235)	-.866*** (.245)	-.862*** (.222)
Observations	77	106	138	203	287

Notes: The table reports results from a regression discontinuity specification with an interacted local linear RD polynomial and border segment fixed effects. Standard errors clustered on the state (*Bundesländer*) level are reported in parentheses.

bandwidth of 100 km falls by almost 0.5 log points and is only marginally significant at 10%. At higher bandwidths, the effect is no longer significant at conventional levels. This is a larger impact than controlling for log disposable income per capita, log population density and the age distribution at the same time. In Panel C we also add log population density, the age distribution as well as log disposable income (the controls from Panel E of Table 3). Now the effect becomes numerically small at the reference bandwidth and insignificant for the entire range of bandwidths. In other words, accounting for only differences in mobility and demographics is enough for the discontinuity in cases to disappear.

Our final exercise demonstrates that mobility patterns, population differences and the geography of the initial outbreaks can create a counterfactual discontinuity just like the one we observe in the actual data. We simulate a canonical SIR model of the coronavirus epidemic in each German county with mobility flows following [Wesolowski et al. \(2017\)](#) and [Bjørnstad and Grenfell \(2008\)](#). In the model, we allow infections to spread along commuting patterns starting from the distribution of coronavirus cases on February 29 2020 and use the approximate epidemiological characteristics of the outbreak in Germany (e.g., a reproduction number, R_0 of 2.5). We use the observed commuting flows from December 2019 together with

Figure 5 – Discontinuity in $\log(1 + \text{simulated cases}/\text{million})$ at former border

Notes: Illustration of the discontinuity $\log(1 + \text{simulated cases}/\text{million people})$ across the former border between West and East Germany. The simulation and its underlying parameters are described in [Appendix A](#). The figure shows non-parametric local polynomial estimates for bins of the dependent variable, where each bin is 20 km wide. 95% confidence intervals are shaded in grey.

county population data to proxy for actual mobility around the time of the outbreak. We simulate the model for 60 periods (days) but stop all commuting flows after 22 days to reflect the nation-wide shutdown. The details of the simulation are provided in [Appendix A](#).²¹

Panel D of Table 5 presents the discontinuity estimates for the simulated log cumulative cases per capita. We find that in the simulated data, the number of cases also discontinuously declines as one crosses from west to east over the former border. The decline is somewhat smaller, but close in magnitude, to the decline observed in the actual data. This confirms the results of the RD design with controls for commuter flows and strongly suggests that mobility is a key driver of the geography of the early outbreak. Our methodology cannot exclude other alternative explanations, and officially registered commuter flows likely do not represent person-to-person movement across Germany perfectly. However, our simulation constructs a situation that shares some essential features of the data, and that explains the discontinuously lower novel coronavirus prevalence across the border into the former East without reference to the (broad) BCG hypothesis. This fact together with the pattern in the discontinuities across cohorts, leaves us very skeptical that the BCG vaccine plays a role in explaining the geography of the outbreak in Germany.

²¹The simulation overpredicts the overall case count because we do not explicitly model social distancing (apart from the lack of commuting). In the observed data, the reproduction number declined toward unity over the same period.

5 Conclusion

Our paper provides a cautionary tale of potentially misleading correlations, which appear early in the outbreak of an epidemic. Using the modern applied econometrics toolkit, we show that there is a stark break in cumulative COVID-19 cases at the former border which used to separate East and West Germany. However, our analysis strongly suggests that an appealing explanation—the variation in BCG vaccination status for large populations across the border—cannot account for this discontinuity. Instead, more mundane factors appear to be behind this East-West differences. Accounting for commuter flows, income and demographics is sufficient for the difference to vanish. These results help to address the identification problems encountered in the scientific and journalistic debate on the merits of the BCG hypothesis.

Our findings have several important limitations. First, they are derived from the context of Germany, the health profile of its population, and the specific strains of COVID-19 circulating there, and therefore may not be as applicable to other parts of the world. Second, they cannot speak to the possibility of a short-run boost to the immune system coming from the BCG vaccine that may offer individuals some “trained immunity” against COVID-19. In particular, our results should not be taken to anticipate the outcomes of the clinical trials that are currently taking place. Third, our study looks at a summary measure of the intensity of the epidemic—cumulative case counts per capita—and does not consider in detail other dimensions, such as the lethality of infections or the speed of transmission from the infected to the susceptible.

While it is disappointing to find evidence against a partial remedy, we believe that negative results are necessary for the world to redeploy resources in the right direction. They also help guard against a false sense of security that countries with a current BCG vaccination policy might feel. To the extent that current case counts around the globe are a product of the early geography of the pandemic rather than of immutable features of populations, less affected countries and regions should take their reprieve as a time to prepare rather than as a time for complacency. It is not unimaginable that the raw discontinuity we documented will eventually disappear or even turn around if the infection spreads to a poorer, older and more disease-prone population in the East.

References

- Alesina, A. and N. Fuchs-Schündeln (2007). Goodbye Lenin (or not?): The effect of communism on people's preferences. *American Economic Review* 97(4), 1507–1528.
- Arts, R. J., S. J. Moorlag, B. Novakovic, Y. Li, S.-Y. Wang, M. Oosting, V. Kumar, R. J. Xavier, C. Wijmenga, L. A. Joosten, et al. (2018). BCG vaccination protects against experimental viral infection in humans through the induction of cytokines associated with trained immunity. *Cell Host & Microbe* 23(1), 89–100.
- Asahara, M. (2020). The effect of BCG vaccination on COVID-19 examined by a statistical approach: no positive results from the Diamond Princess and cross-national differences previously reported by world-wide comparisons are flawed in several ways. *medRxiv*. DOI: 10.1101/2020.04.17.20068601.
- Becker, S. O., L. Mergele, and L. Woessmann (2020). The separation and reunification of Germany: Rethinking a natural experiment interpretation of the enduring effects of communism. *Journal of Economic Perspectives* 34(2), 71–143.
- Berg, M. K., Q. Yu, C. E. Salvador, I. Melani, and S. Kitayama (2020). Mandated Bacillus Calmette-Guérin (BCG) vaccination predicts flattened curves for the spread of COVID-19. *medRxiv*. DOI: 10.1101/2020.04.05.20054163.
- Bjørnstad, O. N. and B. T. Grenfell (2008). Hazards, spatial transmission and timing of outbreaks in epidemic metapopulations. *Environmental and Ecological Statistics* 15(3), 265–277.
- Calonico, S., M. D. Cattaneo, and R. Titiunik (2014). Robust nonparametric confidence intervals for regression-discontinuity designs. *Econometrica* 82(6), 2295–2326.
- Covián, C., A. Fernández-Fierro, A. Retamal-Díaz, F. E. Díaz, A. E. Vasquez, M. K.-L. Lay, C. A. Riedel, P. A. González, S. M. Bueno, and A. M. Kalergis (2019). BCG-induced cross-protection and development of trained immunity. implication for vaccine design. *Frontiers in Immunology* 10, 1–14.
- Curtis, N., A. Sparrow, T. A. Ghebreyesus, and M. G. Netea (2020). Considering BCG vaccination to reduce the impact of COVID-19. *The Lancet*.
- Dell, M. (2010). The persistent effects of Peru's mining Mita. *Econometrica* 78(6), 1863–1903.
- Deshpande, M. (2016). Does welfare inhibit success? The long-term effects of removing low-income youth from the disability rolls. *American Economic Review* 106(11), 3300–3330.
- Fuchs-Schündeln, N. and T. A. Hassan (2015, June). Natural experiments in macroeconomics. Working Paper 21228, National Bureau of Economic Research.
- Gelman, A. and G. Imbens (2019). Why high-order polynomials should not be used in regression discontinuity designs. *Journal of Business & Economic Statistics* 37(3), 447–456.
- Genz, H. (1977). Entwicklung der Säuglingstuberkulose in Deutschland im ersten Jahr nach Aussetzen der ungezielten BCG-Impfung. *DMW-Deutsche Medizinische Wochenschrift* 102(36), 1271–1273.
- Harsch, D. (2012). Medicalized social hygiene? Tuberculosis policy in the German Democratic Republic. *Bulletin of the History of Medicine* 86(3), 394–423.
- Imbens, G. and K. Kalyanaraman (2011). Optimal Bandwidth Choice for the Regression

- Discontinuity Estimator. *Review of Economic Studies* 79(3), 933–959.
- Kandasamy, R., M. Voysey, F. McQuaid, K. de Nie, R. Ryan, O. Orr, U. Uhlig, C. Sande, D. O'Connor, and A. J. Pollard (2016). Non-specific immunological effects of selected routine childhood immunisations: systematic review. *BMJ* 355, i5225.
- Klein, R. J. and C. A. Schoenborn (2001). Age adjustment using the 2000 projected US population. *Healthy People 2010 Statistical Notes*, 1–10.
- Klein, S. (2013). *Zusammenhang zwischen Impfungen und Inzidenz und Mortalität von Infektionskrankheiten: Zeitreihenanalysen mit Meldedaten zu Diphtherie, Pertussis, Poliomyelitis und Tetanus von 1892 bis 2011 in Deutschland*. Ph. D. thesis, Freie Universität Berlin.
- Kleinnijenhuis, J., R. van Crevel, and M. G. Netea (2015, 01). Trained immunity: consequences for the heterologous effects of BCG vaccination. *Transactions of The Royal Society of Tropical Medicine and Hygiene* 109(1), 29–35.
- Kreuser, F. (1967). *Stand der Tuberkulose-Bekämpfung im Bundesgebiet, in West-Berlin und in Mitteldeutschland*, pp. 33–147. Berlin, Heidelberg: Springer Berlin Heidelberg.
- Loddenkemper, R. and N. Konietzko (2018). Tuberculosis in Germany before, during and after World War II. In *Tuberculosis and War*, Volume 43, pp. 64–85. Karger Publishers.
- Miller, A., M. J. Reandelar, K. Fasciglione, V. Roumenova, Y. Li, and G. H. Otazu (2020). Correlation between universal BCG vaccination policy and reduced morbidity and mortality for COVID-19: An epidemiological study. *medRxiv*. DOI: 10.1101/2020.03.24.20042937.
- Robert Koch-Institut (1976). *Impfempfehlungen der Ständigen Impfkommission*. Robert Koch-Institut.
- Robert Koch-Institut (1998). *Impfempfehlungen der Ständigen Impfkommission*. In *Epidemiologisches Bulletin* 1998, Number 31. Robert Koch-Institut.
- Robert Koch-Institut (2020). *Epidemiologisches Bulletin* 17 / 2020.
- Santamaria, M. (2020, February). Reshaping Infrastructure: Evidence from the division of Germany. The Warwick Economics Research Paper Series (TWERPS) 1244, University of Warwick, Department of Economics.
- Streeck, H., B. Schulte, B. Kuemmerer, E. Richter, T. Hoeller, C. Fuhrmann, E. Bartok, R. Dolscheid, M. Berger, L. Wessendorf, M. Eschbach-Bludau, A. Kellings, A. Schwaiger, M. Coenen, P. Hoffmann, M. Noethen, A.-M. Eis-Huebinger, M. Exner, R. Schmithausen, M. Schmid, and B. Kuemmerer (2020). Infection fatality rate of SARS-CoV-2 infection in a German community with a super-spreading event. *medRxiv*. DOI: 10.1101/2020.05.04.20090076.
- Wesolowski, A., E. zu Erbach-Schoenberg, A. J. Tatem, C. Lourenço, C. Viboud, V. Charu, N. Eagle, K. Engø-Monsen, T. Qureshi, C. O. Buckee, and C. J. E. Metcalf (2017). Multinational patterns of seasonal asymmetry in human movement influence infectious disease dynamics. *Nature Communications* 8(1), 1–9.

A SIR Model with commuter flows

We simulate a SIR model with multiple locations and exogenous migration flows between locations. This model has been used in [Wesolowski et al. \(2017\)](#) and [Bjørnstad and Grenfell \(2008\)](#). Let

$$\tilde{I}_{i,t} = I_{i,t} + \frac{N_i \sum_j m_{j,i} \frac{I_{j,t}}{N_j}}{N_i + \sum_j m_{j,i}} \quad (\text{A-1})$$

$$S_{i,t+1} = S_{i,t} - \beta S_{i,t} \frac{\tilde{I}_{i,t}}{N_i} \quad (\text{A-2})$$

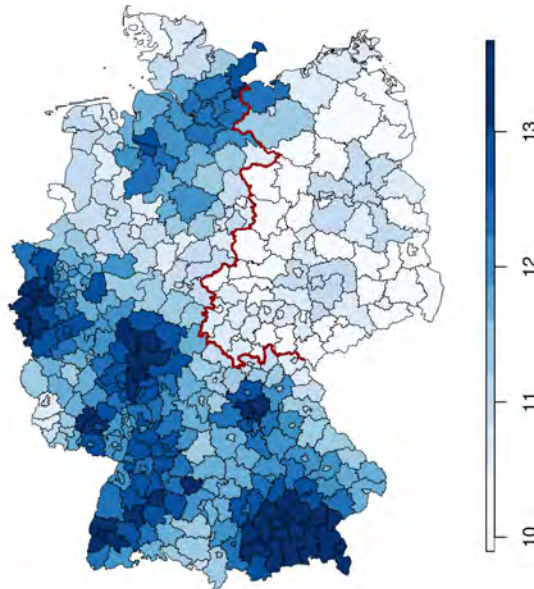
$$I_{i,t+1} = I_{i,t} + \beta S_{i,t} \frac{\tilde{I}_{i,t}}{N_i} - \gamma I_{i,t} \quad (\text{A-3})$$

$$R_{i,t+1} = R_{i,t} + \gamma I_{i,t} \quad (\text{A-4})$$

where $m_{j,i}$ is the number of commuters going from location j to location i each period and all other variables are as in the classical SIR model. We take German counties as the locations in our models. We assume $\gamma = 1/7$ (because the incubation period is 7 days on average, and much of the transmission is pre-symptomatic) and $R_0 = \beta/\gamma = 2.5$. We assume the initial counts of infected to correspond to the reported cases by county on February 29. We simulate the model for 60 time periods, assuming that after time period 22, all cross-county commuting flows are shut down to simulate measures taken by the German government.

We have tried other parametrizations of the SIR model and we get similar results provided that the epidemic is not allowed to evolve too close to the long-run equilibrium (which, when migration flows are eventually shut down, is the same for each county and hence, would not generate a discontinuity). The magnitude of the case counts resulting from the epidemic vary widely between parametrizations. We view this exercise not as an attempt to model the COVID-19 epidemic in Germany but to provide an illustration that mobility patterns can generate discontinuities in the spread of an epidemic without there being essential discontinuities in the underlying epidemic resistance of the population.

Figure A-1 – Counterfactual COVID-19 cases in Germany, end of April



Notes: Illustration of the simulated spatial distribution of an epidemic with the parameters described in the Appendix, the same starting distribution across German counties as cumulative COVID-19 cases on Feb. 29, 2020; and following the December 2019 commuting flows published by the Federal Employment Agency (*Bundesagentur für Arbeit*). The map shows the $\log(1 + \text{simulated cases/million people})$ in each county using population data from 2018.

B Appendix Tables

Table B-1 – Regression discontinuity estimates for various approximating polynomials

	<i>The dependent variable is $\log(1+\text{cases}/\text{million})$</i>				
	<i>The bandwidth is</i>				
	50 km (1)	75 km (2)	100 km (3)	150 km (4)	200 km (5)
<i>Panel A. Interacted linear polynomial in distance to the border</i>					
EAST	-.787*** (.240)	-.710*** (.149)	-.830*** (.154)	-.987*** (.196)	-.890*** (.143)
<i>Panel B. Linear polynomial in distance to the border</i>					
EAST	-.670* (.357)	-.718*** (.119)	-.889*** (.128)	-.985*** (.145)	-.898*** (.168)
<i>Panel C. Linear polynomial in latitude and longitude</i>					
EAST	-.805*** (.112)	-.911*** (.092)	-1.03*** (.102)	-1.00*** (.088)	-.928*** (.077)
<i>Panel D. Interacted cubic polynomial in distance to the border</i>					
EAST	-.432 (.540)	-1.09** (.528)	-1.44*** (.216)	-.708** (.306)	-.776*** (.231)
<i>Panel D. Cubic polynomial in distance to the border</i>					
EAST	-1.15*** (.395)	-.767** (.378)	-.614** (.259)	-.880*** (.141)	-.975*** (.133)
<i>Panel E. Cubic polynomial in latitude and longitude</i>					
EAST	-.768*** (.206)	-.822*** (.100)	-.999*** (.091)	-1.21*** (.131)	-1.20*** (.113)
Observations	77	106	138	203	287

Notes: The table reports results from a regression discontinuity specification with an interacted local linear RD polynomial and border segment fixed effects. Standard errors clustered on the state (*Bundesländer*) level are reported in parentheses.

Table B-2 – OLS Correlations between COVID-19 cases and control variables

	<i>The dependent variable is $\log(1+\text{cases}/\text{million})$</i>		
	<i>The sample is</i>		
	West (1)	East (2)	All (3)
Disposable income p.c.	2.38*** (.74)	3.43* (1.99)	3.38*** (.60)
Population density	-.03 (.08)	.15*** (.02)	.08 (.07)
Percent older than 64	-.08*** (.03)	-.01 (.06)	-.12*** (.02)
Percent older than 45 and younger than 65	-.01 (.01)	-.04*** (.00)	-.06*** (.02)
Age-adjusted overall death rate	-2.56** (1.10)	-2.96*** (.87)	-3.38*** (.87)
Age-adjusted infectious diseases death rate	-20.33** (8.88)	-2.55 (14.19)	-23.04* (13.34)
Age-adjusted respiratory death rate	-8.79*** (1.77)	-3.14 (5.17)	-9.88*** (1.90)
Observations	324	76	400

Notes: The table reports results from ordinary least squares regressions for the samples indicated in the column headers. Standard errors clustered on the state (*Bundesländer*) level are reported in parentheses.

Consumer panic in the Covid-19 pandemic¹

Michael Keane² and Timothy Neal³

Date submitted: 13 May 2020; Date accepted: 14 May 2020

We develop an econometric model of consumer panic (or panic buying) during the COVID-19 pandemic. Using Google search data on relevant keywords, we construct a daily index of consumer panic for 54 countries from January to late April 2020. We also assemble data on government policy announcements and daily COVID-19 cases for all countries. Our panic index reveals widespread consumer panic in most countries, primarily during March, but with significant variation in the timing and severity of panic between countries. Our model implies that both domestic and world virus transmission contribute significantly to consumer panic. But government policy is also important: Internal movement restrictions - whether announced by domestic or foreign governments - generate substantial short run panic that largely vanishes in a week to ten days. Internal movement restrictions announced early in the pandemic generated more panic than those announced later. In contrast, travel restrictions and stimulus announcements had little impact on consumer panic.

1 This research was supported by Australian Research Council grants FL110100247 and CE170100005. The authors acknowledge Yuanyuan Deng, Inka Eberhardt, Katja Hanewald, Heloise Labit Hardy, Shahin Kiaei, George Kurdna, Sejeong Lee, Shiko Maruyama, Peyman Firouzi Naeim, Miguel Olivo-Villabril, Thanh Phan, Olena Stavrunova, and Nada Wasi for assistance with translations.

2 Professor of Economics, University of New South Wales & ARC Centre of Excellence in Population Ageing Research (CEPAR).

3 Postdoctoral Research Fellow, University of New South Wales & ARC Centre of Excellence in Population Ageing Research (CEPAR).

Copyright: Michael Keane and Timothy Neal

1. INTRODUCTION

In this paper we present a model of consumer panic during the COVID-19 pandemic. Panic buying of storable consumer goods is a common phenomenon during natural disasters and man-made crises. Examples include both World Wars (Hughes 1988), the Great East Japan Earthquake in 2011,¹ and the recent hyperinflation in Zimbabwe (Musvanhiri 2017). Panic may be provoked by much less, such as in the United States in 1973 when Johnny Carson joked about a shortage of toilet paper on *The Tonight Show*, causing the *Great Toilet Paper Scare* that led to panic buying and actual shortages (Malcolm 1974). Thus, it is not surprising that the COVID-19 pandemic has caused consumers in many countries to engage in panic buying of storable consumer goods like toilet paper, rice and pasta - see e.g. Knoll (2020) and Rieder (2020). In this paper we develop a predictive model of how government policies such as social distancing, lockdowns and travel restrictions, as well as growth in COVID-19 cases, generate such behavior.

To clarify the discussion, it is necessary to define what we mean by “panic buying.” First, we need to understand why consumers hold inventories of storable consumer goods in normal times. Erdem, Imai, and Keane (2003) - henceforth EIK - estimated a structural model of optimal consumer demand for storable goods in a stationary environment. In a stationary environment, consumers have two motives for building up inventories of storable goods in excess of current consumption needs: (i) as a buffer stock to protect against stock outs given uncertainty about future usage needs, and (ii) because it is optimal to stock up on storable goods when confronted with a “deal” (i.e., an instance when the good is offered by retailers at a relatively low price).

In the event of natural disasters or crises, however, consumers are commonly observed to stock up on consumer goods to an extent that greatly exceeds levels observed in normal times. During the COVID-19 pandemic, IRI (2020) document a sharp spike in grocery spending, and increases in stockpiling, in several countries. For example, for the week ending March 15, spending on paper products (including toilet paper) was up 50% (year-on-year) in Italy, 108% in France, 109% in Germany, 134% in the UK, and 217% in the US. There are both psychological and economic explanations for such stockpiling behavior in a crisis. For example, a standard psychological explanation is that stocking up on storable goods helps consumers gain a sense of control over the uncertain/risky situation created by a crisis (e.g. Grohol 2020).

On the other hand, as noted by Hansman et al. (2020), there is nothing intrinsically irrational or “panicky” about stocking up on storable consumer goods in a crisis. There are two main economic explanations for a jump in optimal inventory holdings in a crisis situation. First, in the EIK inventory model, any potential supply disruption that increases stock out risk, or any restriction on movement that increases the cost of store visits, will have the effect of increasing optimal inventory holdings.² Second, as emphasized by Hansman et al. (2020), a crisis often leads to higher expected future prices,

¹See Hori and Iwamoto (2014), Ishida et al. (2013), and Kurihara et al. (2012) for research into the consumer reaction to the earthquake.

²In the EIK inventory model the cost of a store visit and the stock-out risk are two key parameters that drive optimal inventory holdings: Optimal inventory is increasing in the cost of a store visit (i.e., if store visits were costless, one could buy consumer goods on a just-in-time basis, keeping inventories near zero). The COVID-19 pandemic increased the cost of a store visit in three ways: (i) One may wish to avoid stores to avoid contact with potentially infected customers, (ii) if a consumer becomes infected they must quarantine at home, making store visits impossible for a time, (iii) government policies like lockdowns may make going to the store more difficult. Optimal inventory is also increasing in the risk of

making the current price look like a “deal” that calls for stocking up.³ Again, this is optimal behavior in an inventory model.

Our primary goal in this paper is to develop a predictive model of how government policies impact on panic buying, so we do not need to take a stand on the extent to which the phenomenon is driven by psychological or economic factors. Regardless of the underlying cause, the phenomenon of panic buying is socially costly for several reasons. A sudden crisis induced jump in consumer demand above expected historical levels may often lead to retail store stocks outs in the short run. This is especially true in the case of just-in-time supply chains where little inventory is available to handle sudden jumps in demand. During the COVID-19 pandemic, serious stock out situations have been observed in many countries for consumer staples like toilet paper, rice and pasta. Such retail stocks outs are costly for consumers who are unable to obtain enough of the desired product to meet their usage needs, and particularly costly for vulnerable groups like the elderly and the disabled for whom shopping can be challenging.

Shortages created by panic buying also force consumers to devote extra time and effort to shopping, diverting time away from welfare-improving activities like work, leisure, and sleep, as well as generating psychological costs by inducing anxiety and stress. Shortages may heighten anxiety about the pandemic - and the government's response - among the general population. Furthermore, as stressed by Hansman et al. (2020), reputable retailers avoid price increases during crises, both due to legal constraints and long run reputational concerns. This can lead to speculative buying and the emergence of black markets. Moreover, consumer panic may directly promote virus transmission, by causing people to flock to the supermarket before the onset of a lockdown.

We develop a measure of consumer panic for 54 countries over the first four months of 2020 using Google search data. The measure shows that consumers in most of the large economies of the world experienced panic in response to the COVID-19 pandemic. Much of the panic occurring in March, consistent with IRI (2020) data showing sharp increases in March grocery sales. We find strong heterogeneity in the timing and severity of consumer panic across countries in the sample. Some countries experienced more panic than others (such as Australia and the United States), and some panicked earlier while others much later. Generally speaking, panic appeared earlier in the Asian region than the rest of the world, and richer countries tended to panic more than poorer ones.

Given that consumer panic is a common response to crises and socially costly, it is useful to consider how government policy may contribute to - or alleviate - the phenomenon. Government policy as it relates to COVID-19 has focused on either the containment of viral transmission or efforts to prop up the economy. To that end, we construct three daily measures of government policy during the pandemic: ‘internal restrictions’ which curtail the freedom of movement and association within a city or greater region, ‘travel restrictions’ which limit or prevent people from entering the country, and ‘stimulus announcements’ which are announcements of a significant fiscal or monetary policy measures. The measures show that the majority of policy change occurred between the 13th and 24th of March, which is around the time that many of the world governments learnt that COVID-19 would severely affect their country.

stock outs. If a crisis raises stock-out risk - either due to supply disruptions or due to a lagged response of supply to the crisis-induced increase in demand - it also leads to higher optimal inventory.

³The expectation of future price increases may even lead to speculative buying, where some people attempt to buy up inventory for subsequent resale at a higher price.

There is substantial heterogeneity across countries in the timing, severity, and incrementalism of the policy response. Some countries, such as Brazil and South Korea, did not impose severe restrictions on movement, while others such as Spain and Peru imposed strict lockdowns. Countries such as Italy and Norway imposed internal restrictions ‘early’ (relative to other countries), while others like Singapore, Mexico and India imposed restrictions quite late. Some countries such as the United States and Canada allowed states/provinces to gradually implement restrictions (or not), while many others such as France and Argentina announced lockdowns at the federal level.

Using this data, we investigate a number of interesting questions related to consumer panic during the COVID-19 pandemic. For instance, why did some countries panic more than others, and why did some countries panic earlier and others later? One possibility is that differences in the extent and timing of the spread of COVID-19 explain differences in consumer panic. But heterogeneity in the severity and timing of government policy to contain the virus may also play a role. With many countries experiencing outbreaks of COVID-19 simultaneously, it is worth considering whether panic is driven primarily by policy change and virus transmission at the domestic level, or if consumers respond to events in other countries as well? (Perhaps because they serve as a signal of what is likely to occur in their own country.) If the activity of other countries also drive panic, does the impact of domestic policy announcements depend on what other countries have done? - i.e. does it matter for panic if governments implement lockdowns early or late relative to other countries?

If government policy has an impact on consumer panic, and if that impact is context dependent, then we need to learn these lessons so that it can factor into the decision making of policymakers during the next pandemic/crisis, or even during subsequent waves or strains of COVID-19. To address this issue, we develop a dynamic model of panic as a function of policy change and the spread of COVID-19. It features domestic policy changes, the average change of policy in other countries, a nonlinear specification of domestic and overseas COVID-19 case increases, and interaction terms that allow for the effect of domestic policy changes to vary by the average state of policy overseas.

We find evidence for several conclusions about the spread of consumer panic during the COVID-19 pandemic: First, the announcement of internal movement restrictions clearly generates increased consumer panic, and the magnitude of the effect is large. This is in contrast to travel restrictions and stimulus announcements, where we find no evidence that either systematically leads to higher consumer panic. Second, consumers are also sensitive to the announcement of internal restrictions overseas, which explains why panic surged in some countries prior to domestic policy change. We also find strong evidence that the context of policy announcement matters: if the policy is announced early (relative to other countries) it has more of an effect on panic than policy announced later. The last conclusion of note is that the spread of the virus matters significantly too, although only if it is entered in the specification nonlinearly.

One policy implication of these results is that implementation of internal movement restrictions can be expected to induce panic buying in the short-run, particularly if the policy is announced before similar measures in other countries. The data suggests that the panic response is sudden, strong, and dissipates in a week to ten days. As the main objective of implementing internal movement restrictions is to contain virus transmission, early implementation of such a policy may still be optimal despite negative short-run

consequences.⁴ Nevertheless, the speed of the panic response suggests that measures to prevent shortages in the face of consumer panic, such as rationing or priority access for vulnerable groups to essential goods, need to be implemented prior to (or simultaneously with) the announcement of policy change and not after the fact.

The second policy implication is that the announcement of strong travel restrictions appears to have very little effect on consumer panic. Thus, presuming travel restrictions are effective in suppressing virus transmission, implementing them early would appear to have been a very good policy strategy for governments in the current pandemic. Unlike internal restrictions, there is also no benefit in waiting to implement them. Further research is needed on the effects of policy change on unemployment and virus transmission to determine the optimal policy mix that balances the desire to suppress virus transmission with minimizing economic disruption and consumer panic.⁵

The outline of the paper is as follows. Section 2 describes how we construct measures of panic and government policy during the COVID-19 pandemic, and describes key features of the data. Section 3 describes the econometric methods we use to model consumer panic. Section 4 presents our estimation results, including impulse response functions for policy changes. Section 5 draws conclusions from the analysis.

2. MEASURING PANIC AND POLICY DURING THE COVID-19 PANDEMIC

2.1. *Measuring Consumer Panic*

A good measure of consumer panic must satisfy several criteria. Panic by its very nature is subject to sudden daily changes. The factors that drive panic - government policy and virus transmission - have also been subject to sudden changes during the pandemic. Thus, to model the dynamics of the panic process, we need a daily measure of consumer panic. The COVID-19 pandemic is a very recent event that has just reached its fifth month, so we also need a measure of panic that is available as close to the present day as possible. Lastly, we require a measure that is available for many countries, in order to exploit heterogeneity in virus transmission and policy response. While supermarket scanner data on grocery sales is available on a daily basis, it is not available for many of the countries we wish to include in the analysis. Accordingly, in this article we construct a high frequency measure of consumer panic using Google search data.

Google search data was shown by Choi and Varian (2012) to be useful in “now-casting” current values of economic indicators such as unemployment claims and consumer confidence. Da et al. (2011) use Google search data to obtain a useful measure of investor attention that predicts demand for stocks, while Goel et al. (2010) demonstrate that present search activity on Google can be useful in predicting near-future consumer behavior.⁶ Underlying all of this research is the idea that Google search data is a useful

⁴Since virus transmission leads to higher consumer panic as well, the early implementation of the policy could even be optimal in regards to the minimization of consumer panic over the long term.

⁵Chinazzi et al. (2020) study the effect of travel restrictions on virus transmission, while Fang et al. (2020) study the effect of internal movement restrictions. The former paper argues that travel restrictions have only modest effects unless combined with transmission-reduction interventions (e.g., internal movement restrictions).

⁶Google search data has also been used extensively in other sciences, including Ginsberg et al. (2009) who use it to predict outbreaks of influenza. And most recently, Lampos et al. (2020) use it to estimate underlying numbers of COVID-19 cases in a country.

indicator of consumer demand. Using Google search data to measure the degree of consumer panic in an economy is a simple extension of this idea, and it allows us to capture sudden surges in panic as they occur across the world in reaction to the virus.

The Google Health Trends API provides data on the proportion of searches undertaken on their search engine within a jurisdiction and time period matching any specified word or phrase. For example, for the word ‘panic’, the API will return the probability that a short search-session, which is defined as a few consecutive searches by a single user, includes a search for ‘panic’ within a particular jurisdiction during a day. The data is provided in the form of a probability, thus adjusting for differences in population and Google usage between countries. The numbers are obtained from a uniformly distributed random sample of Google web searches, and are available for daily search activity (using the UTC timezone) in most countries of the world.

To construct an index of panic during the COVID-19 pandemic, we use a set of keywords or phrases that attempt to track a sudden proclivity for abnormal patterns of consumer behavior indicative of ‘panic buying.’ It is crucial to not only find words that people in English-speaking countries are likely to search, but also ones that can be translated into many other languages and receive search activity across the globe. We collected data for the following five words or phrases: ‘toilet paper’, ‘panic buying’, ‘hoarding’, ‘panic’, and ‘supermarket’ (and their translations).⁷

Only the term ‘toilet paper’ relates to a specific good, while the remainder track search interest in specific concepts. Of course, there are other products that experienced a surge in demand following the onset of the pandemic, including face masks and hand sanitizer. We choose not to include these products as their utility arguably increases dramatically during a pandemic, and a surge in demand could be seen as a perceived need for immediate use. Toilet paper, on the other hand, does not provide more utility during this pandemic as Diarrhoea is a very rare symptom of COVID-19. Any increase in demand for toilet paper is therefore due to reasons other than immediate use.

Our index for panic is the sum of the probabilities of the first five terms:

$$P_{ct} = (ToiletPaper_{ct} + PanicBuying_{ct} + Hoarding_{ct} + Panic_{ct} + Supermarket_{ct}) * 100$$

where $ToiletPaper_{ct}$ is the search probability for that keyword in country c on day t , and likewise for the other search terms. Probabilities of individual search terms are inherently small, so the sum is multiplied by 100 to make it more readable.

For countries that are not majority English-speaking, we translated these terms into 23 languages in consultation with native speaking colleagues. If a country has a non-trivial number of speakers of a certain language, we add the search probabilities of the translated term to the probability of the English term. For instance, in the case of Switzerland, we add the German, French, and Italian translations to the English search probabilities. Example translations can be found in the Appendix.

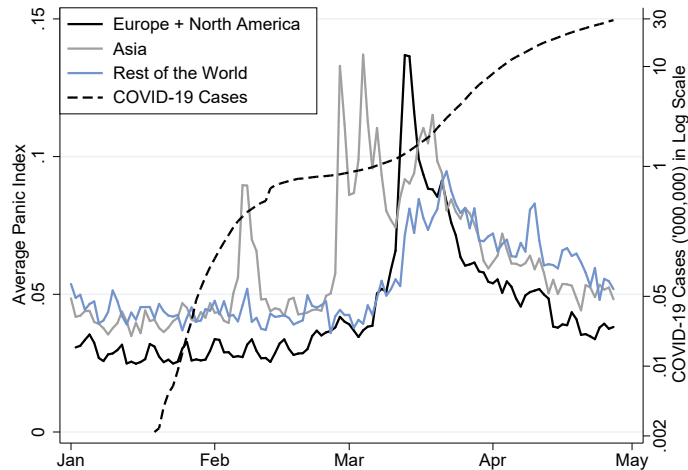
The result is a balanced panel dataset that contains 54 countries ($N = 54$), including all of the major economies in the world save for Mainland China,⁸ and daily measures of panic from the 1st of January this year to the 27th of April ($T = 118$).⁹

⁷For privacy reasons Google censor the probability of a search term if it did not get enough distinct searches. A country must have enough Google searches for each keyword for its data to be usable.

⁸We cannot include Mainland China as the government restricts the use of the Google search engine.

⁹The complete list of countries/jurisdictions in the dataset are as follows: Argentina, Australia, Austria, Belgium, Bolivia, Brazil, Canada, Chile, Colombia, Denmark, the Dominican Republic, Ecuador, Egypt, Finland, France, Germany, Greece, Guatemala, Hong Kong SAR, India, Iran, Ireland, Italy,

Figure 1. Average Panic and Worldwide Cases of COVID-19



Note: This figure plots the average panic across North America and European Countries, Asian countries (including Oceania), and the Rest of the World which includes Southern and Central America, Africa, and the Middle East. Also presented in log scale is the global confirmed cases of COVID-19 on the secondary y-axis.

Figure 1 plots the panic index against global COVID-19 cases in log scale. For the purpose of illustration, we group the countries into three regions: Europe and North America, Asia (including Oceania), and the Rest of the World, which includes Southern and Central America, Africa, and the Middle East. The first panic occurred in Singapore and Taiwan from February 6th to 10th, which increased the panic index for Asia to double its normal level (i.e., from about .04 to about .08). During this time COVID-19 cases in China climbed from 20,000 to over 40,000, and cases were starting to spread in other East Asian countries. Panic quickly returned to normal levels in Asia until February 28th, when it surged to an average of 0.14 and remained high during the first week of March. By this point COVID-19 cases in China had plateaued above 80,000, but cases outside China were growing very quickly. This was particularly true in Italy, who over this period grew from 650 confirmed cases to 6,000.

It wasn't until the 11th of March that North America and Europe began to experience high levels of panic, with the index increasing from about 0.05 to a peak of almost triple that amount at 0.14. Consistent with this, the IRI (2020) supermarket sales data show a massive spike in demand for paper products in the week ending March 15. It was in the first week of March that many governments around the world began to appreciate that

Japan, Kenya, Malaysia, Mexico, Morocco, the Netherlands, New Zealand, Norway, Panama, Peru, the Philippines, Poland, Portugal, Qatar, Romania, Russia, Saudi Arabia, Singapore, South Africa, South Korea, Spain, Sweden, Switzerland, Taiwan, Thailand, Turkey, the United Arab Emirates, the United Kingdom, the United States, Uruguay, and Vietnam.

COVID-19 would severely affect their country. In the second and third weeks of March, reported COVID-19 cases were growing exponentially in many countries of the world, and unprecedented legislation was being announced in attempts to contain the spread of the virus. The remainder of the countries in the sample, which include Central and South America, Africa, and the Middle East, also experienced a surge in panic in the middle of March. By April, the panic index subsided as people adapted to a new normal and fears of imminent food shortages subsided in most advanced economies.

Figure 1 shows significant heterogeneity between regions in the timing and severity of the panic over the past four months. There was also significant heterogeneity across countries within regions.¹⁰ This leads to the question of why some countries panicked much more than other countries, and why some countries panicked earlier and others later. The differential spread of COVID-19 across countries, and their diverse range of policy responses, provide an excellent opportunity to study how different factors drive the spread of consumer panic.

Table 1. Descriptive Statistics of Google Trends Keywords and Panic Index

	Mean	Median	Std. Dev.	CV
Keyword Searches:				
<i>Toilet Paper</i>	0.008	0.003	0.027	3.320
<i>Panic</i>	0.010	0.007	0.011	1.150
<i>Panic Buying</i>	0.002	0.000	0.005	2.591
<i>Hoarding</i>	0.002	0.001	0.003	1.573
<i>Supermarket</i>	0.027	0.018	0.028	1.012
Panic Index	0.049	0.039	0.044	0.894

Note: CV refers to the Coefficient of Variation.

Table 1 presents descriptive statistics of the individual search terms and the overall panic index. Among the five search terms present in the panic index P_{ct} , ‘Supermarket’ is the most often searched term, followed by ‘panic’ and then ‘toilet paper.’ Looking at the coefficient of variation, ‘toilet paper’ has the most variability of all the search terms, due to its very small probability of being searched in normal times and very large spikes during the COVID-19 pandemic.

2.2. Measuring Government Policy

A remarkable effect of the pandemic has been the dramatic response from governments: Drastic changes to the functioning of society have often been formulated in under a week and announced only one or a few days before implementation. Government policy has focused on containment of viral transmission, along with fiscal and monetary policy

¹⁰An Appendix with graphs of the panic index for every country is available on request.

devised to prop up the economy while containment measures are given time to work. As our outcome of interest is panic, which as we have seen is subject to high frequency changes, it is important to track the evolution of government policy in a precise manner that captures the timing of any sudden changes. Because of this we measure policy changes at their announcement rather than at their implementation.

We categorize policy announcements into three broad types: (1) ‘internal restrictions’ which curtail freedom of movement and association within a city or greater region, (2) ‘travel restrictions’ which limit or prevent people from entering the country, and (3) ‘stimulus announcements’ which are changes in fiscal or monetary policy. We now discuss how we code the policy announcement variables, recognizing that this must involve some degree of subjectivity:

The index for ‘internal restrictions’ is defined as follows:

$$Internal_{ct} = Schools_{ct} + Gatherings_{ct} + Movement_{ct} \quad (2.1)$$

where $Schools_{ct} = 1$ if there is a federal closure of primary and secondary schools in country c on day t , and 0 otherwise. $Gatherings_{ct} = 1$ if there is a ban on very large gatherings (more than 500 to 2000 people), 2 if there is also a ban on smaller gatherings (more than 50 to 200 people), and 0 otherwise. $Movement_{ct} = 1$ if the government strongly encourages work from home where feasible, there are heavy restrictions on the use of public spaces, and most retail and entertainment businesses are closed. $Movement_{ct} = 2$ if, in addition to the above, many non-essential industries are shut down and a majority of individuals are prevented from working, and 0 otherwise. Occasionally a half point will be assigned to a policy position when it is difficult to categorize (such as State governments adopting a policy but not the federal government). $Internal_{ct}$ can range from 0 to 5.

The index for ‘travel restrictions’ is defined as follows:

$$Travel_{ct} = (ChinaBan_{ct} + IranBan_{ct} + ItalyBan_{ct} + SouthKoreaBan_{ct})/2 + Noncitizens_{ct} + Citizens_{ct} \quad (2.2)$$

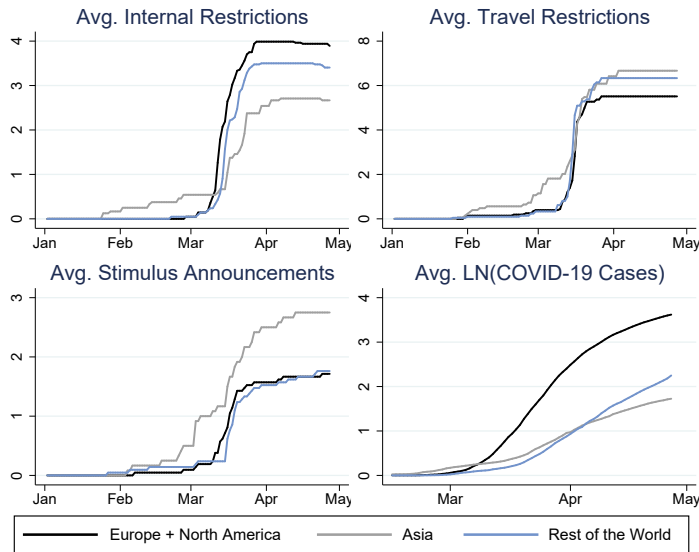
where $ChinaBan_{ct} = 1$ if all travellers arriving from China must self-isolate for 14 days, 2 if all travellers from China are banned from entering the country, and 0 otherwise. Likewise for $IranBan_{ct}$, $ItalyBan_{ct}$, and $SouthKoreaBan_{ct}$, which were chosen along with China as they were the four countries to be most affected from COVID-19 early in the Pandemic. $Noncitizens_{ct} = 1$ if non-citizens arriving in the country must self-isolate for 14 days, 2 if non-citizens are banned from entering the country, and 0 otherwise. Likewise, $Citizens_{ct} = 1$ if all citizen entrants must self-isolate for 14 days, 2 if citizens are effectively prevented from entering the country, and 0 otherwise.¹¹

Lastly, the variable for stimulus announcements $Stimulus_{ct}$ is the sum of all government policy announcements that signal significant changes in fiscal or monetary policy. We collected these from an array of media websites.

Figure 2 describes the evolution of our three policy measures over the sample period and across 54 countries, measured as a simple average across the three regions defined above. Looking at internal restrictions in the top-left panel, it is clear that most policy change occurs between the 13th and 24th of March, when the average index increased from one to over three. Europe and North America behave similarly to the rest of the

¹¹As far as we know, no countries in the sample officially stated that its own citizens were not allowed to re-enter the country, but there were several instances when borders were so tightly closed it was virtually impossible for citizens to obtain transport back into the country.

Figure 2. Average Policy and COVID19 Cases by Region



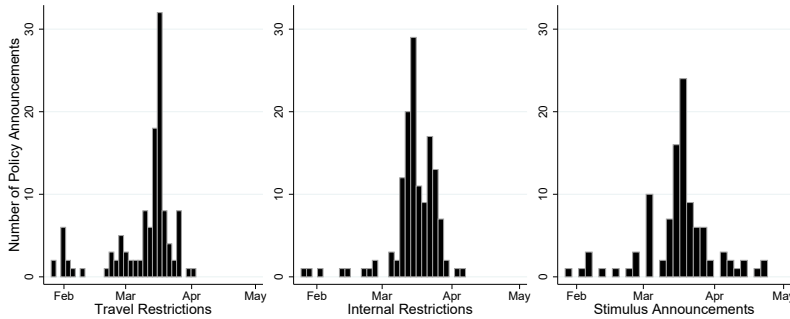
Note: This figure plots the average value of the three policy variables constructed in this article and log of COVID-19 cases across three regions in the sample of 54 countries.

world, while the Asian countries imposed some internal restrictions much earlier but settled at a lower average level. Travel Restrictions behave similarly, with many countries in the sample completely closing their borders around mid-March, and Asian and Oceanic countries again implementing policy change sooner than the other regions. The Asian region adopted an incrementalist approach to Stimulus announcements of frequent announcements of small policy changes, while the other regions tended to announce large stimulus packages in Mid-March.

The above discussion masks significant heterogeneity in policy within regions. Figure 3 plots the number of policy announcements made in each category between February and May. The peak of the distribution sits firmly within early-to-mid March, for internal restrictions, and the middle of March for travel restrictions. Nevertheless, more than a few internal restriction announcements were made in early and late March (with some even in early April and February). And for travel restrictions there were a number of countries such as Australia and New Zealand who were gradually ramping up entrant restrictions throughout the end of January to early March.

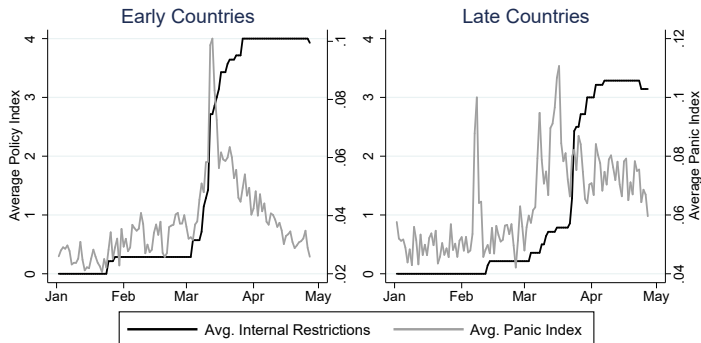
It is worth considering whether countries that announced strong containment policies earlier than most others, which we'll call the 'early countries,' had different consumer panic patterns than those who announced their policies late, which we'll call the 'late countries.' Figure 4 considers average internal restrictions and average panic across seven notably early countries and seven notably late countries. The early countries had moved to tight internal restrictions by early March, and average panic seems to track the policy

Figure 3. The Timing of Policy Announcements



Note: This figure graphs the distribution of new policy announcements by date across the three categories.

Figure 4. Average Panic and Internal Restrictions by Group

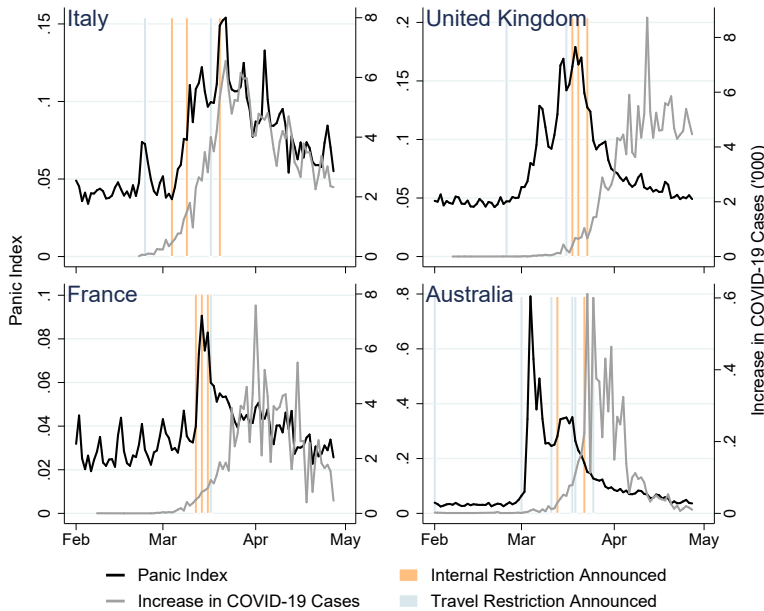


Note: 'Early Countries' include Austria, Belgium, Ireland, Italy, Hong Kong, Norway, and Romania. 'Late Countries' include India, Mexico, Qatar, Singapore, Sweden, the United Arab Emirates, and Vietnam.

index very closely for these countries until the panic decays in late March and April. The late countries had a very different experience, where tight restrictions on movement did not occur until late in March. In the late countries panic peaks well prior to the implementation of tight policy measures, and panic also dissipates much more slowly. This suggests two hypotheses about the relationship between internal restrictions and panic: First, that individuals in a country not only react to domestic policy change but also overseas policy change. Second, that the effect of announcing internal restrictions on panic may depend crucially on the international context in which it is announced, with late implementation leading to less consumer panic in the short-run.

Finally, Figure 5 presents the experience of four countries in detail: Italy, the United Kingdom, France, and Australia. The subgraphs for each country feature the panic

Figure 5. Panic, COVID-19, and Government Policy in Select Countries



index from February to May, the daily increase in COVID-19 cases (in thousands), and announcements of internal and travel restrictions which are shaded in two colors.

In Italy there was a brief spike in panic on Feb. 23-24, around the time that outbreaks were reported in northern Italy and several governors imposed interstate travel restrictions. The real surge in panic began in the second week of March, and it continued to climb until March 22, when our panic index peaked at three times its normal level. In early March the government began implementing restrictions on medium and large sized gatherings, including restrictions on movement in the worst affected parts of the country. On March 20 a nationwide lockdown was announced, and soon after that panic reached its peak of 0.15. Since then, panic has trended down in a way entirely consistent with declines in the number of new cases per day from about 6,000 to about 2,000.

France offers an interesting comparison as the panic surges and subsides much quicker than in Italy, akin to the rapid speed in which containment policy escalates. A nationwide lockdown was announced in France on the 16th of March, which is the same day that panic reaches its peak of 0.083. Comparing the trends in daily COVID-19 cases, it's also clear France implemented its lockdown sooner in the life of viral transmission.

In the United Kingdom panic peaks roughly the same time as in Italy even though the virus started spreading much later. The peak of panic occurs simultaneously with the announcement of internal restrictions, with a school closing announcement on the 18th

of March and restrictions on gatherings and movement being announced on the 20th and the 23rd of March. Unlike Italy and France, the number of new COVID-19 cases has not declined by the end of the sample period.

The experience of Australia is notable for the incredible speed and scale with which panic took hold in early March. On March 2nd the panic index was at 0.08, already double its typical level. Two days later it increased to 0.79, which is exceeded only by a value of 1.03 in Japan on Feb. 28th. Unlike in other countries, the escalation in panic does not appear to correspond with any significant increase in domestic COVID-19 cases. Indeed, it is important to note that axes in Figure 5 are scaled differently for Australia: It has an order of magnitude higher peak panic index and lower peak caseload than the other three countries! Nor does any important policy announcement seem to explain the panic: While a travel ban from Iran was announced on the 1st of March, it seems unlikely that this was important enough to be the direct cause. Restrictions on gatherings were announced on March 13th, along with a series of escalating travel restrictions, which coincides with a secondary minor peak in the middle of March.

Looking at these four examples, we see a great deal of heterogeneity in the timing and severity of consumer panic, the timing of COVID-19 transmission across countries, and finally the timing and severity of containment policy. It would be exceedingly difficult to make conclusions on the likely causes of panic surges without a multivariate statistical model of panic, to which we now turn.

3. METHODOLOGY

3.1. Conceptual Framework

It is useful to first present a simple conceptual framework to motivate our empirical specification. To set ideas, let P_{ct} denote the level of consumer panic for a typical consumer in country c on day t of the pandemic. Let S_{ct} denote the severity of the pandemic, and let R_{ct} denote the policy regime in place in country c on day t . Then we may write:

$$P_{ct} = F(E(S_{ct}|I_{ct}), E(S_{ct+1}, \dots | I_{ct}), R_{ct}, E(R_{ct+1}, \dots | I_{ct}), \mu_c) \quad (3.3)$$

Here $E(S_{ct}|I_{ct})$ denotes the *perceived* severity of the pandemic on day t , conditional on the available information set I_{ct} . Similarly, $E(S_{ct+1}, \dots | I_{ct})$ denotes the expected severity of the pandemic in future periods. μ_c is a range of country-specific factors that affect the propensity to panic (e.g., cultural factors, strength of the social safety net).

The information set has the form:

$$I_{ct} = (C_{ct}, C_{c,t-1}, \dots, C_{ft}, C_{f,t-1}, \dots, R_{ct}, R_{c,t-1}, \dots, R_{ft}, R_{f,t-1}) \quad (3.4)$$

where C_{ct} denotes the COVID-19 caseload in country c on day t , and C_{ft} denotes a vector of caseloads in foreign countries. Similarly, R_{ct} denotes the policy regime in country c on day t , and R_{ft} denotes a vector of policy regimes in foreign countries. Thus, the information set includes current and lagged caseloads both domestic and foreign, as well as current and lagged policies, both domestic and foreign.

In writing (3.3)-(3.4) we assume that consumers have incomplete information about the severity of the crisis, which seems obvious given that even epidemiologists have great uncertainty on the virulence and transmissibility of COVID-19 at this stage of the pandemic. We assume consumers use COVID-19 caseloads, both domestic and foreign, to

infer the severity of the pandemic. Consumers also use government policy as a signal of the severity of the pandemic, under the reasonable assumption that governments and the experts they consult have information about the pandemic exceeding that of the typical consumer.¹²

We may consider equation (3.3) the “structural” equation for consumer panic. The “reduced form” equation for consumer panic is obtained by substituting out for the unobserved expectation terms in (3.3) using the information set in (3.4) to obtain:

$$P_{ct} = f(C_{ct}, C_{c,t-1}, \dots, C_{ft}, C_{f,t-1}, \dots, R_{ct}, R_{c,t-1}, \dots, R_{ft}, R_{f,t-1}, \dots, \mu_c) \quad (3.5)$$

In this framework the policy regime R_{ct} affects consumer panic through four channels. First, there is the direct effect of the policy. Second, there is the effect of the policy on expected future policy. Third, there is the effect operating through the impact of policy on the perceived current severity of the pandemic $E(S_{ct}|I_{ct})$. Fourth, there is the impact of policy on the expected severity of the pandemic in the future $E(S_{ct+1}, \dots|I_{ct})$.

As a simple example, consider an internal movement restriction that makes it more difficult for consumers to leave home and visit the store. First, as discussed in the introduction, anything that raises the cost of store visits will cause consumers to desire higher inventories. Thus, a new internal restriction may generate “panic” buying (i.e., heavy stockpiling) in the short run. Second, if the policy leads consumers to expect even tighter restrictions in the future, it will encourage even more demand today. Third, if consumers have incomplete information about the severity of the crisis and use government policy as a signal, it is plausible that a new internal movement restriction may cause panic by causing consumers to infer that the crisis is worse than previously thought. Fourth, stronger government action may increase confidence about the future course of the pandemic, reducing fears of future shortages. Through this channel, a new internal movement restriction may reduce consumer panic.¹³

The overall impact of any policy move on consumer panic will depend on the balance of these four forces. The first key point we wish to make is that this balance is likely to depend on the consumer information set, and in particular the time since the start of the crisis. Early in the pandemic, when there is a great deal of uncertainty about its severity, the third channel is likely to be very strong, so we would not be surprised if strong policy action induces consumer panic. Later in the crisis, when consumers have better information, we hypothesize that this third channel is weaker, so that policy actions will be less likely to induce panic.

The number of COVID-19 cases reported in foreign countries provide signals about the current and likely future severity of the pandemic in one’s own country. Policy actions of foreign governments are also likely to be a key source of consumer information about the potential severity of the pandemic in their home country. They may also provide signals about the likely future policies one’s own government will adopt. Thus, foreign

¹²See Avery et al. (2020) for a discussion of alternative epidemiological models, as well the uncertainty about the inputs to those models. Their paper discusses how the caseload projections of the Imperial College model in Ferguson et al. (2020) significantly influenced several leading countries, such as the US and UK, to impose strict social distancing rules after an initial response that was more moderate.

¹³The severity of the pandemic at time t will be some function of past severity and past containment policy $S_{ct} = g(S_{ct-1}, R_{ct-1})$. In Section 2.2 we defined the internal restriction policy measure R_{ct} so larger values imply stricter constraints on movement. So it is reasonable to assume that $\partial S_{ct} / \partial R_{ct-1} < 0$. A similar assumption makes sense for travel restrictions. But in the case of stimulus announcements it is not clear why they would affect virus transmission, a point we return to when interpreting the results.

government policies R_{ft} and foreign caseloads C_{ft} may also affect domestic panic through channels two through four described above.

A key issue we wish to address is whether the level of panic induced by domestic policy action depends on the timing of that action relative to other countries. We hypothesize that if a country acts early the second channel (i.e., policy action signals a more severe crisis) is likely to dominate, so that early strong policy actions will induce short run panic. We also hypothesize that if a country acts relatively late, then the severity of the pandemic will already be fairly well understood, so this signalling mechanism will be less strong. Thus, we expect later action to induce less consumer panic. To capture these type of effects, it is important that when we specify the reduced form model in (3.5) we allow the policy regime in foreign countries to moderate the impact of domestic policy.

3.2. Reduced Form Model of Consumer Panic

Guided by the above conceptual framework, we proceed to specify a reduced form model of consumer panic. A priori, we decided to model consumer panic as a dynamic process in which the level of panic in country c on day t depends on its own lagged level, as well as changes in the forcing variables (i.e., domestic and foreign policy regimes, domestic and foreign cases) from day $t-1$ to day t . This was because we expected that changes in policy and COVID-19 cases would have strong short-run effects on panic, but that these effects would die off rather quickly. After some experimentation with functional form, we arrived at the following model as our main specification:

$$\begin{aligned} \ln P_{ct} = & \mu_c + \sum_{\ell=0}^1 (\beta_{\ell} \Delta \mathbf{R}_{c,t-\ell} + \gamma_{\ell} \Delta \mathbf{R}_{f,t-\ell} + \lambda_{\ell} (\Delta \mathbf{R}_{c,t-\ell} * \mathbf{R}_{f,t-\ell})) \\ & + \theta_1 \Delta \ln C_{ct} + \theta_2 \Delta C_{ct} + \theta_3 (\Delta \ln C_{ct} \cdot \Delta C_{ct}) + \theta_4 \Delta \ln C_{ct}^* + \theta_5 \Delta C_{ct}^* \\ & + \theta_6 \Delta \ln C_{ft} + \theta_7 \Delta C_{ft} + \theta_8 \Delta C_{CN,t} + \theta_9 C_{CN,t} \cdot I_{c \in Asia} \\ & + \sum_{\ell=1}^2 \rho_{\ell} \ln P_{c,t-\ell} + \psi \text{day}_t + e_{ct} \end{aligned} \quad (3.6)$$

Here $\ln P_{ct}$ is the log of the panic index for country c on day t , and the model includes two lags of the dependent variable. $\mathbf{R}_{ct} = [\text{Internal}_{ct}, \text{Travel}_{ct}, \text{Stimulus}_{ct}]$ is a vector of our three policy variables: Internal Restrictions, Travel Restrictions, and Stimulus Announcements. These enter the model in first difference form ($\Delta \mathbf{R}_{ct}$) and we include both the current and first lagged daily difference. \mathbf{R}_{ft} is a vector of the same three policy variables for foreign countries, measured as the simple average across countries outside of country c .¹⁴ We also enter this variable in first-differenced form, including one lag.

The term $\lambda_{\ell} (\Delta \mathbf{R}_{c,t-\ell} * \mathbf{R}_{f,t-\ell})$ allows the effect of domestic policy changes to vary depending on the international context in which they are announced, where the international context is captured by \mathbf{R}_{ft} , the average level of the policy variables in countries outside of c . If $\lambda_{p\ell} < 0$ then the effect of announced changes in policy $\Delta \mathbf{R}_{c,t-\ell}$ on panic is reduced the more governments overseas have already announced that change in policy. We hypothesize that $\lambda_{p\ell} < 0$ based on the discussion in Section 3.1.

¹⁴We experimented with weighted averages based on criteria such as distance, GDP, population, and the incremental R^2 when panic in country c is regressed on measures for each foreign country separately. But these refinements had little impact on the results.

We let changes in the number of confirmed COVID-19 cases enter the model in several different ways. First, we enter the daily percentage change in domestic cases, $\Delta \ln C_{ct}$, the daily absolute change in domestic cases, ΔC_{ct} , and the product of these two terms. Early in the pandemic, when caseloads are low, large daily percentage increases are sometimes observed. Later in the pandemic, when caseloads are higher, the daily percentage changes are typically small, but the absolute changes can be large. We included both percentage and absolute changes, as well as their interaction, as this allows the model to be quite flexible in terms of how caseloads affect consumer panic.

Second, we were interested to see if surprise changes in caseloads had larger effects than predictable changes. To test this, we built predictive models for both percentage and absolute changes in caseloads (available on request). We defined the surprise changes in caseloads as the residuals from these models. These are denoted by $\Delta \ln C_{ct}^*$ and ΔC_{ct}^* in equation (3.6). Third, we also allow foreign reported cases to influence domestic panic. We include both the daily percentage change in foreign cases, $\Delta \ln C_{ft}$, and the daily absolute change in foreign cases, ΔC_{ft} .

Fourth, we cannot include mainland China directly in our model as it restricts access to Google. However, as the pandemic originated in China, we include the number of confirmed changes in mainland China as a driver of consumer panic in other countries $C_{CN,t}$. We also included an interaction between the number of Chinese cases and an indicator for whether country c is in East or Southeast Asia, to allow for the possibility that Chinese cases have a larger effect on consumers in nearby countries. Finally, day_t is a vector of day-of-the-week dummies to capture daily differences in search activity.

The term μ_c is a country specific fixed effect meant to capture differences across countries in the baseline level of Google search activity for panic related terms. We estimate the model by fixed effects, relying on the fact that we have a long panel ($T=116$) so that the so-called Nickell (1981) bias that arises from applying a fixed effects estimator to a lagged dependent variable model in a panel with small T is rendered negligible.

We assume the error e_{it} satisfies usual assumptions: serially uncorrelated, homoskedastic, independent in the cross-section and independent from the regressors. We found evidence of conditional heteroskedasticity, and applied a weighted least squares procedure described below. Given this, we show in Section 4 that the model passes a stringent set of specification tests, so the testable assumptions on the errors are not rejected.

Before turning to the results, there are two additional details of the specification. First, to avoid having the log of the panic index be too sensitive to days with exceptionally low levels of search activity, we add .01 to the index before taking the log, so that we actually work with $\ln(P_{ct} + .01)$. The value .01 corresponds to roughly the first decile of the distribution of P_{ct} across all countries and days in the sample (Recall from Table 1 that P_{ct} has a mean of .049). Second, to mitigate extremely large percentage increases in number of cases starting from very low levels, we added 50 to the number of cases before taking the log, so we actually work with $\Delta \log(C_{ct} + 50)$. The value of 50 was obtained after a grid search to determine which value gave the best fit to the data.

4. RESULTS

Here we present empirical results from estimating the consumer panic model of equation (3.6) on the panel data set described in Section 2. First we present results from a simplified model that includes only domestic policy and COVID-19 case data. Then we present results from our full model that also includes international variables.

Table 2. Regression Models of Panic during the COVID-19 Pandemic

Models of $\ln(\text{panic}_{ct})$:	Model 1		Model 2	
	β	S.E.	β	S.E.
Internal Restrictions:				
$\Delta \text{Internal}_{ct}$	0.083	0.016	0.123	0.027
$\Delta \text{Internal}_{ct-1}$	0.069	0.016	0.144	0.031
$\Delta \text{Internal}_{ft}$			0.292	0.087
$\Delta \text{Internal}_{ft-1}$			0.234	0.110
$\Delta \text{Internal}_{ct} * \text{Internal}_{ft}$			-0.032	0.013
$\Delta \text{Internal}_{ct-1} * \text{Internal}_{ft-1}$			-0.046	0.014
Stimulus Announcements:				
$\Delta \text{Stimulus}_{ct}$	0.052	0.022	0.102	0.044
$\Delta \text{Stimulus}_{ct-1}$	0.020	0.024	0.041	0.047
$\Delta \text{Stimulus}_{ft}$			0.068	0.138
$\Delta \text{Stimulus}_{ft-1}$			0.134	0.132
$\Delta \text{Stimulus}_{ct} * \text{Stimulus}_{ft}$			-0.082	0.035
$\Delta \text{Stimulus}_{ct-1} * \text{Stimulus}_{ft-1}$			-0.038	0.037
Travel Restrictions:				
$\Delta \text{Travel}_{ct}$	0.010	0.008	0.024	0.017
$\Delta \text{Travel}_{ct-1}$	0.008	0.008	0.015	0.019
$\Delta \text{Travel}_{ft}$			-0.068	0.049
$\Delta \text{Travel}_{ft-1}$			-0.064	0.042
$\Delta \text{Travel}_{ct} * \text{Travel}_{ft}$			-0.007	0.004
$\Delta \text{Travel}_{ct-1} * \text{Travel}_{ft-1}$			-0.004	0.005
Domestic COVID-19 Cases:				
$\Delta \ln(C_{ct})$	0.848	0.062	0.356	0.071
ΔC_{ct}	0.004	0.002	0.004	0.002
$\Delta C_{ct} * \Delta \ln(C_{ct})$	0.022	0.023	0.032	0.017
$\Delta \ln(C_{ct}^*)$	-0.462	0.087	-0.142	0.086
ΔC_{ct}^*	-0.004	0.005	-0.006	0.004
International COVID-19 Cases:				
$\Delta \ln(C_{ft})$			0.689	0.136
ΔC_{ft}			0.013	0.007
$\Delta C_{CN,t}$			-0.001	0.003
$\Delta C_{CN,t} * \text{Asia}_i$			0.018	0.009
Autoregressive Terms:				
$\ln(\text{panic}_{ct-1})$	0.447	0.012	0.392	0.012
$\ln(\text{panic}_{ct-2})$	0.251	0.012	0.235	0.012
Diagnostics:				
AR1 Term of \hat{e}_{ct}	-0.014	0.013	0.021	0.013
CD Test p-value		0.000		0.152
Sims Test p-value		0.000		0.128
R^2 – Within units		0.625		0.636

Note: Estimation is performed by WLS. Both models have 6,264 observations, with $N = 54$ and $T = 116$. The models also include country and day of the week effects. The CD Test refers to the Pesaran (2015) test with a null of weak cross-sectional dependence. The Sims Non-Causality Test refers to a F-test on the significance of three leads of all the regressors as suggested by Sims (1972).

4.1. Domestic Model

The first two columns of Table 2, labelled “Model 1,” report results from a restricted model that includes only domestic COVID-19 cases and domestic policy variables, omitting the foreign variables from equation (3.6). In this model both the current and lagged change in internal restrictions are highly significant. The point estimates imply that if a government increases internal restrictions by 1 on a 0-5 scale (e.g. closing schools or restricting gatherings) this causes the panic index to increase by approximately 8.3% on the same day. (Subsequent changes are more difficult to interpret as the model contains the lagged policy change and two lags of the panic index, so we present impulse response functions later.) The current period stimulus is also significant, but with a smaller effect size, while travel restrictions are insignificant.

Both the percentage and absolute changes in COVID-19 cases are significant determinants of panic, but their interaction is not significant. The point estimates imply that a 10% increase in confirmed COVID-19 cases increases the panic index by 8.5%, which is similar to the effect of the one unit increase in our internal restriction measure.

The results from this simplified model are suspect however, as the specification tests point to a number of severe problems. On the plus side, we do not find evidence of serial correlation in the residuals, suggesting our lag structure is adequate. Additional lags of the dependent and independent variables were not significant in this model or in the specifications discussed below. However, the Pesaran (2015) test overwhelmingly rejects the null hypothesis of “weak” cross sectional dependence. The implication is that the residuals contain important shocks that are correlated across countries. And a Sims (1972) non-causality test finds that leads of the policy variables are highly significant in the panic equation, thus rejecting the hypothesis that the policy variables are predetermined with respect to consumer panic.

4.2. Main Specification

We report results from the full model of (3.6) in the right two columns of Table 2, labelled “Model 2.” This model adds international COVID-19 cases and policy variables. Our full model easily passes the Pesaran CD Test and Sim’s non-causality test, implying that the international caseload and policy variables account for the non-weak cross-sectional dependence found in Model 1, as well as the error component that predicts future policy.¹⁵

These results are intuitive in the pandemic context for two reasons: First, it seems clear that foreign caseload and policy changes influence domestic consumer panic. Indeed, quite a few countries experience spikes in the panic index prior to having substantial numbers of confirmed domestic cases. Hence, controlling for the international variables purges the residuals of the component that induces cross-sectional dependence. Both foreign caseload and policy changes clearly have strong influences on future domestic policy decisions. Hence, controlling for the international variables purges the residuals of the component that predicts future domestic policy.

In the full model both the current and lagged change in internal restrictions are again

¹⁵If we estimate the full model of equation (3.6) by applying a within transformation and running OLS (thus obtaining the fixed effects estimator via the Frisch-Waugh theorem) there is evidence of conditional heteroskedasticity. We model this heteroskedasticity (results available on request) and then apply weighted least squares.

highly significant. As we see in Table 2, the average level of internal restrictions in *foreign* countries is also a significant positive determinant of domestic consumer panic, suggesting that domestic consumers use foreign government policy as a signal of the severity of the pandemic and/or to predict their own government's future policy. The magnitude of the coefficients on the foreign averages is roughly double those on domestic restrictions, but note that changes in the international averages tend to be smaller from day to day.

Furthermore, the interactions between domestic internal restrictions and the average level of restrictions in foreign countries are negative and significant. This supports our key hypothesis that internal restrictions tend to cause less domestic consumer panic if they are introduced relatively late in the pandemic compared to other countries.

Figure 6 shows impulse response functions for domestic internal movement restrictions, evaluated at the average international level of internal restrictions on three different dates: Feb 21 (early), March 13 (middle) and April 1 (late). If a government increases internal restrictions by one unit (e.g. closing schools or restricting gatherings) on Feb 21 it causes the panic index to increase by approximately 12% on the same day. The effect peaks at about 18% on day 2, and then gradually vanishes after about a week to ten days. But if a government delays until March 13 the peak is only about 13% on day 2, and if the government delays until April 1st the impulse response function shows no significant effects (although the short-run impact is imprecisely estimated and the confidence interval covers a range of about +10% to -10% on the first and second day).

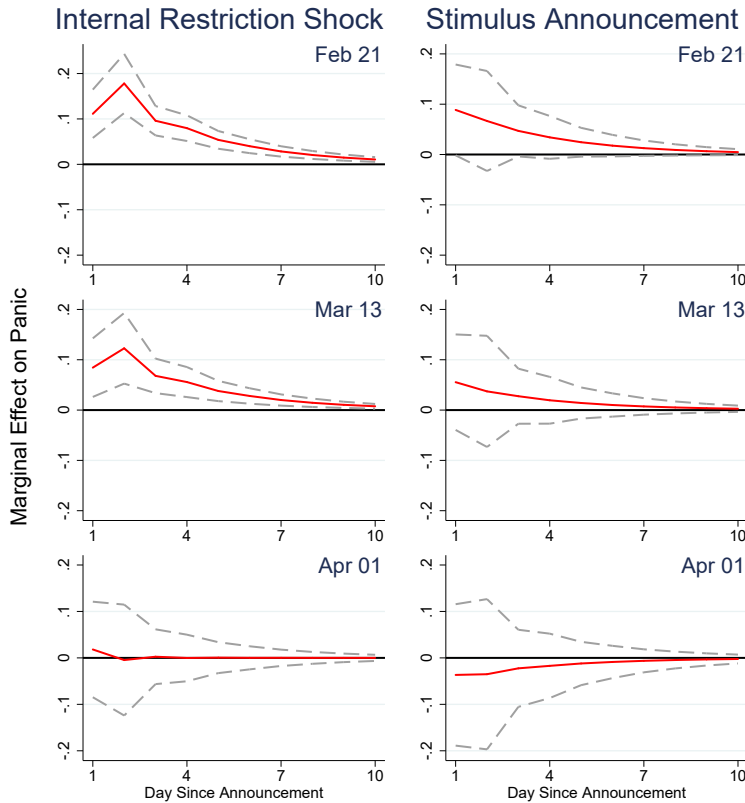
Our point estimates imply that stimulus announcements also have a positive short-run effect on consumer panic. Again, the interaction with the international average of stimulus announcements is also significant, implying the effect is lessened if the announcement comes "late" relative to other countries. But the impulse response functions on the right side of Figure 6 show the effects of stimulus announcements are both weaker and less precisely estimated than those of internal movement restrictions. As was the case with internal restrictions, we find the effect of stimulus announcements on panic diminishes if they come later in the pandemic. We find no statistically or quantitatively significant effects of travel restrictions (impulse response not shown).

Finally, we consider the role of COVID-19 caseloads. Both percentage and absolute changes in domestic COVID-19 cases are significant and positive drivers of panic, as is the interaction between the two. Given our flexible specification, the overall effect of a given increase in cases depends on both the percentage and absolute change. The impulse response functions in the left panel of Figure 7 show the effects of average increases of COVID-19 cases in February, March and April. The average (across all countries) of the daily increases were 1% on a base of 15 cases in February, 11% on 2,900 cases in March, and 7.3% on 18,600 cases in April. Thus, both percentage and absolute changes tend to be small in February. The largest percentage increases tend to be in March, and the largest absolute increases tend to be in April.

Our model implies the typical March daily increase in caseloads would have increased the panic index by about 4% immediately, with an effect that dies off over time, becoming negligible after about a week. Effects of typical April changes in caseloads are about 25% smaller. This combined with the fact that most policy announcements were concentrated in March (see Figure 3) is consistent with the fact that most countries saw very low levels of the panic index in February, following by peaks of the panic index during March, with the index declining through April (see Figures 1, 4, 5).

Interestingly, we find that surprise changes in domestic cases have no greater effect on

Figure 6. Impulse Response Functions For Policy Change

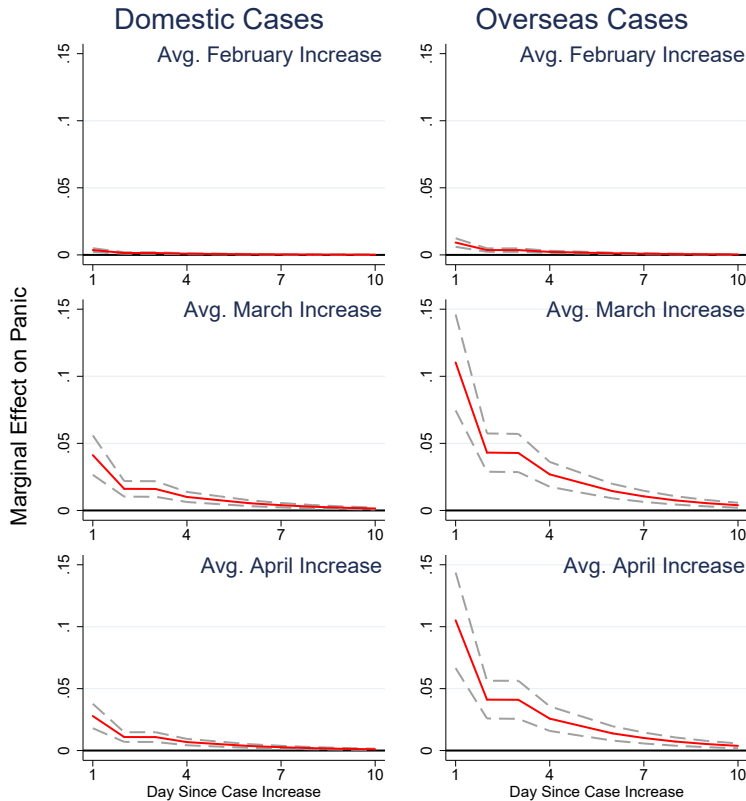


panic that absolute changes. Thus, it seems that consumers react to the total changes in cases, rather than reacting to the surprise component *per se*.

International COVID-19 cases are very significant determinants of domestic panic, both statistically and quantitatively. Impulse response functions in the right panel of Figure 7 show effects of average increases in worldwide COVID-19 cases in February, March and April.¹⁶ Our model implies the typical March daily increase in caseloads increased the panic index by about 11% immediately, with an effect that dies off over time, becoming

¹⁶As we noted earlier, the average (across all countries) of the daily increases are 1% on a base of 15 cases in February, 11% on 2,900 cases in March, and 7.3% on 18,600 cases in April. The international average

Figure 7. Impulse Response Functions For COVID-19 Case Increases



Note: The average daily increase in February is a percentage increase of 1% and absolute increase of 2, in March it is a percentage increase of 11% and absolute increase of 314, and in April it is a percentage increase of 5.5% and absolute increase of 1,564.

negligible after about a week. Effects of typical April changes in caseloads are similar. Comparing these impulse response functions to those for domestic cases in the left panel of Figure 7, we see that international cases have substantially larger effects on domestic panic than domestic cases. This makes sense, given that large caseloads were concentrated in a relatively few countries, while panic was widespread across many countries.

caseload changes used to construct the right panel of Figure 7 are the same as the average domestic changes used to construct the left panel.

Finally, we find that cases in China are a significant determinant of panic in East and Southeast Asian countries, but not elsewhere. Overall, we have found that both international policy regimes and international cases are important drivers of domestic panic, suggesting that consumers do pay attention to international conditions.

4.3. Model Fit

Figure 8 illustrates how the model fits the time series of the panic index data for selected countries. The figure presents fitted values of the daily panic index based on current and lagged values of the forcing variables (i.e., policy variables and COVID-19 cases). We present both conditional predictions, where the two lags of the panic index in equation (3.6) are always set at their true values, and unconditional predictions, where we plug in the two previous day's predicted panic indices from the model. Italy and France are examples of countries where the model provides very good predictions of the path of the panic index based on the forcing variables.

Our model fits the UK somewhat less well, as the conditional predictions only generate about half to two-thirds of the increase in panic. This is largely due to the fact that UK panic index rises to substantially higher levels than those of Italy and France, and the large UK increase is not easy to explain based on the forcing variables. Also, referring back to Figure 5, one can see that in Italy and France domestic cases began to rise and internal restrictions were announced prior to the large spike in panic in early to mid-March. But in the UK panic increased substantially prior to the emergence of substantial domestic cases or internal restrictions. So the increase in panic in the UK in early March is driven largely by international cases and policies.

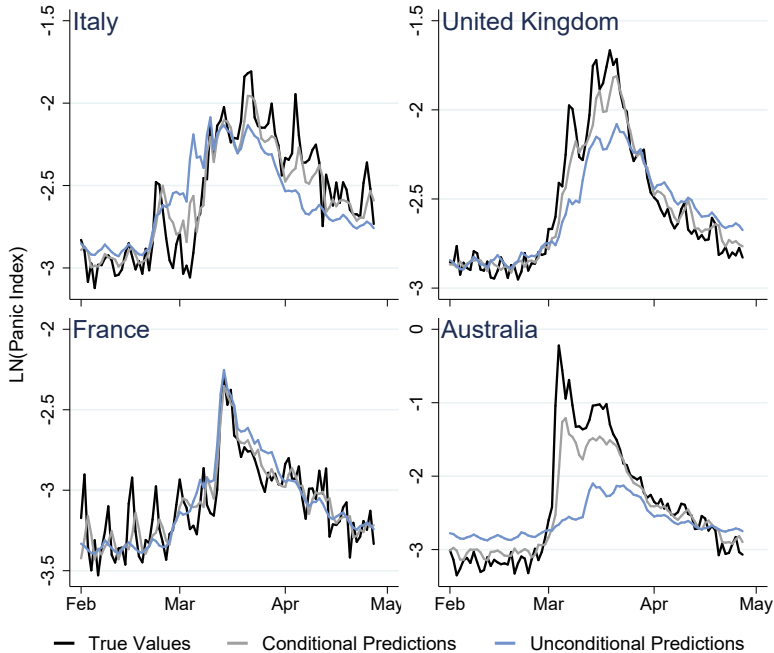
Australia is an example of a country where the panic index had a massive spike on a particular day (March 2) and the model is not able to explain why this occurred. As we noted in Section 2, the increase in the panic index in Australia was an order of magnitude greater than we observe in almost any other country, so it is not at all surprising that our model cannot explain it. The other countries with similar hard to explain massive spikes are Japan, Taiwan and Singapore.¹⁷ It is of course not surprising that a variable like “panic” is sometimes hard to predict based only on observed forcing variables, so we would argue that - with the exception of this set of countries - the model generally fits quite well. (An Appendix showing the fit for all 54 countries is available on request).

4.4. Discussion

As we discussed in Section 3.1, there are four channels through which internal restrictions may plausibly affect consumer panic, and the overall effect depends on the balance of these four. Recall that internal restrictions: (i) increase the cost of store visits, which increases desired inventories, leading to a short-run spike in demand, (ii) increase expected future costs of store visits, with a similar effect, (iii) increase perceived severity of the pandemic, which may increase consumer panic, and (iv) reduce expected future severity of the pandemic, which may reduce consumer panic. Estimates from a reduced

¹⁷In addition, the model under-predicts the magnitude of early panic spikes in the US, Canada, Mexico and Germany. But, unlike Australia, Japan, Taiwan and Singapore, it underestimates the magnitude of the spikes rather than missing them altogether (similar to the case of the UK).

Figure 8. Conditional and Unconditional Predictions of Log Panic from Model 2



form model cannot disentangle these different channels, but our model implies that the three panic increasing effects dominate until very late March and early April.

Our model also implies that stimulus announcements have a significant positive effect on consumer panic in the short-run, but the point estimates imply this is much weaker than the effect of internal restrictions. A weaker effect seems plausible, as stimulus announcements do not have any plausible effects on the cost of store visits, so channels (i)-(ii) are not operative. Their only positive effect on consumer panic would seem to operate through channel (iii), as they may signal greater severity of the pandemic.

Our model implies that travel restrictions have no significant effect on consumer panic. Again, travel restrictions have no plausible effects on costs of store visits, so channels (i)-(ii) are not operative. Our results suggest that the signalling effect of travel restrictions, operating through channel (iii), is fully counter-balanced by channel (iv), whereby consumers expect that travel restrictions will help mitigate the severity of the pandemic in the future, thus reducing panic.

Another key finding is that both foreign cases and the policy decisions of foreign governments contribute to domestic panic. A model that fails to account for this was found to be seriously misspecified, as it suffered from meaningful cross-sectional dependence

and a failure of the predetermination assumption for the domestic policy variables. This is because the foreign caseload and policy variables contribute not only to domestic consumer panic in the short run, but also to future domestic policy decisions.

5. CONCLUSION

Panic buying of storable consumer goods is a common phenomenon during natural disasters and man-made crises. But consumer panic has been little studied from an econometric point of view (A notable exception being Hansman et al. 2020). This is because of the difficulty of obtaining suitable data, and the lack of variation in the determinants of panic. Typical panics are one-off events where consumers in a particular location react to news of a crisis (e.g., an approaching hurricane) by stockpiling consumer goods. The nature of such a panic makes it difficult to study using conventional econometric methods: First, relevant high frequency data on consumer response is difficult to obtain because of the very suddenness of the event. Second, panic events (like a hurricane) typically affect a particular group of consumers in a particular location at about the same time. Thus it is hard to find variation in the forcing variables that drive the a panic.

The COVID-19 pandemic provides a unique opportunity to study consumer panic for two reasons: First, the panic has affected nearly every country on earth, but at different times and to different degrees. Thus, there is a great deal of variation across locations in the timing and severity of the panic-inducing event. Furthermore, governments have responded to the pandemic with a variety of different policies implemented at different times and with differing strictness, generating variation in the policy drivers of panic.

The first contribution of this article is to construct a daily index of consumer panic for 54 countries, covering the key period from January 1st to late April 2020. Spikes in the index align well with the timing of stockpiling as measured in the IRI (2020) data for the subset of countries where IRI data is available. We also construct daily data on government policy announcements in response to the pandemic, including internal movement restrictions, travel restrictions and economic stimulus. And we collect daily data on COVID-19 cases for all 54 countries.

The result is a high-frequency panel dataset on consumer panic, government policy and COVID-19 cases that covers many countries over a key four month period of the pandemic. By exploiting the heterogeneity in the timing and severity of panic, along with the heterogeneity in governmental policy response and virus transmission, a panel data model is better placed to overcome issues of spurious regression that would inevitably arise from a time series or cross-sectional study of the same problem.

The second contribution of this article is to build a dynamic model that allows for panic to respond to domestic and international policy change, and domestic and international virus transmission. Importantly, our model allows the effect of domestic policy to depend on the international context. We show that a model that attempts to predict panic based only on domestic events is seriously misspecified, but that a model that incorporates the international context passes a stringent set of specification tests.

Our results show that the announcement of internal movement restrictions generates considerable consumer panic in the short-run, but the effect largely vanishes after a week to ten days. Consumer panic also responds to announcements of internal movement restrictions in foreign countries, suggesting that consumers take these as a signal of the severity of the pandemic and/or likely future policy in their home country. Furthermore, internal movement restrictions generate less panic if they are implemented relatively late

compared to other countries. The other two policies we consider, travel restrictions and stimulus announcements, do not appear to generate significant consumer panic.

Consumer panic is also sensitive to both domestic and worldwide COVID-19 cases. We find that consumers are most sensitive to changes in COVID-19 cases that are large in *both* percentage and absolute terms. They are less responsive to large percentage increases from a small base, or large absolute changes from a large base. This emphasises the midway point of the curve of new COVID-19 cases.

It is important for governments to better understand how to minimize consumer panic while pursuing their policy goals in a pandemic environment. For example, one possible lesson for government is that, in the early stages of a pandemic, when internal restrictions are first being contemplated, large retailers could be advised to carry extra stock of key consumer goods. Given that the panic induced by internal restrictions is sudden but short lived, having extra stock to handle and an initial surge in demand could prevent shortages and hence prevent consumer panic from taking hold in the first place.

It is particularly important to learn lessons from the COVID-19 pandemic given that future pandemics are essentially inevitable, whether in the near term from a second wave or new strain of COVID-19, or longer term as new virus strains emerge. This article is the first attempt to model the determinants of consumer panic in a pandemic environment, but there is significant scope for this to be an area of active future research.

References

- Avery, C., W. Bossert, A. Clark, G. Ellison, and S. F. Ellison (2020). Policy implications of models of the spread of Coronavirus: Perspectives and opportunities for economists. *NBER Working Paper No. 27007*.
- Chinazzi, M., J. T. Davis, M. Ajelli, C. Gioannini, M. Litvinova, S. Merler, A. P. y Piontti, K. Mu, L. Rossi, K. Sun, et al. (2020). The effect of travel restrictions on the spread of the 2019 novel coronavirus (COVID-19) outbreak. *Science* 368(6489), 395–400.
- Choi, H. and H. Varian (2012). Predicting the present with Google trends. *Economic record* 88, 2–9.
- Da, Z., J. Engelberg, and P. Gao (2011). In search of attention. *The Journal of Finance* 66(5), 1461–1499.
- Erdem, T., S. Imai, and M. P. Keane (2003). Brand and quantity choice dynamics under price uncertainty. *Quantitative Marketing and economics* 1(1), 5–64.
- Fang, H., L. Wang, and Y. Yang (2020). Human mobility restrictions and the spread of the novel coronavirus (2019-ncov) in China. *NBER Working Paper No. 26906*.
- Ferguson, N., D. Laydon, G. Nedjati Gilani, N. Imai, K. Ainslie, M. Baguelin, S. Bhatia, A. Boonyasiri, Z. Cucunuba Perez, G. Cuomo-Dannenburg, et al. (2020). Report 9: Impact of non-pharmaceutical interventions (NPIs) to reduce COVID19 mortality and healthcare demand. Imperial College London.
- Ginsberg, J., M. H. Mohebbi, R. S. Patel, L. Brammer, M. S. Smolinski, and L. Brilliant (2009). Detecting influenza epidemics using search engine query data. *Nature* 457(7232), 1012–1014.
- Goel, S., J. M. Hofman, S. Lahaie, D. M. Pennock, and D. J. Watts (2010). Predicting consumer behavior with web search. *Proceedings of the National academy of sciences* 107(41), 17486–17490.
- Grohol, J. (2020). Panic buying: The psychology of hoarding toilet paper, beans

- and soup. *PsychCentral*. Available online: <https://psychcentral.com/blog/panic-buying-the-psychology-of-hoarding-toilet-paper-beans-soup/>.
- Hansman, C., H. Hong, A. de Paula, and V. Singh (2020). A sticky-price view of hoarding. *NBER Working Paper No. 27051*.
- Hori, M. and K. Iwamoto (2014). The run on daily foods and goods after the 2011 Tohoku earthquake: a fact finding analysis based on homescan data. *The Japanese Political Economy* 40(1), 69–113.
- Hughes, W. T. (1988). A tribute to toilet paper. *Reviews of infectious diseases* 10(1), 218–222.
- IRI (2020). Covid-19 impact: Consumer spending tracker for measured channels. Information Resources Inc. Available online at: <https://www.iriworldwide.com/IRI/media/Library/2020-04-30-IRI-BCG-COVID-Global-Consumer-Spend-Tracker.pdf>.
- Ishida, T., A. Maruyama, and S. Kurihara (2013). Consumer reaction to the Great East Japan Earthquake. *Journal of Life Sciences* 7(8), 883.
- Knoll, C. (2020). Panicked shoppers empty shelves as coronavirus anxiety rises. *The New York Times*. Available online: <https://www.nytimes.com/2020/03/13/nyregion/coronavirus-panic-buying.html>.
- Kurihara, S., A. Maruyama, and A. Luloff (2012). Analysis of consumer behavior in the Tokyo metropolitan area after the Great East Japan Earthquake. *Journal of Food System Research* 18(4), 415–426.
- Lampos, V., S. Moura, E. Yom-Tov, I. J. Cox, R. McKendry, and M. Edelstein (2020). Tracking COVID-19 using online search. *arXiv preprint arXiv:2003.08086*.
- Malcolm, A. (1974). The ‘shortage’ of bathroom tissue: Classic study in rumor. *The New York Times*. Available online: <https://www.nytimes.com/1974/02/03/archives/the-shortage-of-bathroom-tissue-a-classic-study-in-rumor-shortage.html>.
- Musvanhiri, P. (2017). Zimbabweans stock up on essentials amid fears of hyperinflation. *Deutsche Welles*. Available online: <https://www.dw.com/en/zimbabweans-stock-up-on-essentials-amid-fears-of-hyperinflation/a-40724529>.
- Nickell, S. (1981). Biases in dynamic models with fixed effects. *Econometrica: Journal of the Econometric Society*, 1417–1426.
- Pesaran, M. H. (2015). Testing weak cross-sectional dependence in large panels. *Econometric Reviews* 34(6–10), 1089–1117.
- Rieder, K. (2020). What we may learn from historical financial crises to understand and mitigate COVID-19 panic buying. *VOXeu*. <https://voxeu.org/article/mitigating-covid-19-panic-buying-lessons-historical-financial-crisis>.
- Sims, C. A. (1972). Money, income, and causality. *The American economic review* 62(4), 540–552.

APPENDIX: TRANSLATING THE ENGLISH SEARCH TERMS

Table 3 contains an extensive list of translations of the English keywords that we used to derive the panic index. The priority was to obtain translations that were being actively searched in the relevant countries over the last four months. If a literal or strict translation did not yield sufficient google search activity, a loose translation or even a translation of a related concept that had more activity would be chosen instead (e.g. a translation of ‘stockpiling’ instead of ‘hoarding’). In our acknowledgements we mention the native speakers that helped us by looking at the translations and suggesting possible alternatives. Translations for the remaining languages, which are Russian, Vietnamese, Arabic, Persian, Turkish, Hindi, Greek, and Thai can be found in the files of the online replication package released alongside this article.

Table 3. Example Translations of the English Google Search Terms

English Keywords:	Toilet Paper	Panic	Panic Buying	Hoarding	Supermarket	Recession	Unemployment
French	papier toilette	panique	pénurie	palissade	super-marché	récession	chômage
German	Toilettenpapier	Panik	Hamsterkäufe	Vorrat	Supermarkt	Rezession	Arbeitslosigkeit
Spanish	papel higiénico	panico + incertidumbre	desabastecimiento + compras de panico	acopio	supermercado	recesión	desempleo
Portuguese	papel higienico	histeria	escassez	aglomeração	supermercado	recessão	desemprego
Italian	carta igienica	panico	coronavirus supermercato	scorta	supermercato	recessione	disoccupazione
Dutch	toiletpapier	paniek	hamsteren	voorraad	supermarkt	recessie	werkloosheid
Polish	papier toaletowy	panika	składowanie	skarb		recesja	bezrobocie
Danish	toiletpapir	panik	lager	hamstring	supermarked		arbejdsløshed
Finnish	vessapaperi	paniikki	hamstraus	aita		lama	työttömyys
Swedish	toalettpapper	panik	hamstra	hamstring	mataffär	lågkonjunktur	arbetslöshet
Norwegian	toalettpapir	panikk	hamstre	samler	dagligvarebutikk	resesjon	arbeidsløshet
Japanese	トイレットペーパー	パニック	買いだめ	買いだめ	スーパーマーケット	不況	失業
Korean	화장지	공황	사재기	비축	마트	경기	실업
Chinese	衛生紙	恐慌	搶購	囤	超級市場	經濟蕭條	失業

Note: This table outlines some of the translations of the English keywords that we used for other languages. The translations for the remaining languages, which are Russian, Vietnamese, Arabic, Persian, Turkish, Hindi, Greek, and Thai can be found in the online replication package released alongside this article.

Daily suffering: Helpline calls during the Covid-19 crisis¹

Marius Brühlhart² and Rafael Lalive³

Date submitted: 12 May 2020; Date accepted: 13 May 2020

We use helpline calls to measure psychological and social suffering in the population at a daily frequency. Our data are from Switzerland's most popular free anonymous helpline, focusing on the Covid-19 crisis period. We compare calls (a) between the pandemic period of 2020 and the corresponding period of 2019 and (b) along the timeline of the lockdown. We find the total volume of calls to have grown in line with the long-run trend. To the extent that calls did increase, this was mainly explained by worries linked directly to the pandemic: calls by persons over 65 and calls about fear of infection. Encouragingly, calls about violence were down on the previous year. Calls about addiction and suicidality increased during the initial phase of the lockdown, plateaued, and returned to their 2019 levels once gradual opening started. Calls about relationship problems decreased in the early phase of the lockdown, and gradually increased, again reaching 2019 levels once opening up started. Overall, these results suggest that psychological and social strain is of second-order importance relative to the medical anxieties generated by the pandemic.

1 We are grateful to the board of the Swiss helpline "Die Dargebotene Hand (143)", and especially to Sabine Basler and Ursula Stahel, for providing us with the high-quality data for this analysis. Their professionalism and generosity are much appreciated.

2 Professor of Economics, HEC Lausanne, University of Lausanne and member of the Swiss National COVID-19 Science Task Force.

3 Professor of Economics, HEC Lausanne, University of Lausanne and member of the Swiss National COVID-19 Science Task Force.

Copyright: Marius Brühlhart and Rafael Lalive

1. Introduction

How can one monitor the prevalence of psychological and social distress in the population at high frequency and in real time? And specifically now: how well are populations coping with the Covid-19 crisis? While medical and economic costs are being quantified and tracked at regular intervals, few measurements exist as yet on the concomitant psychological and social costs.

Previous literature in public health has found quarantine to damage mental health and to increase loneliness (Brooks *et al.* 2020), and to be perceived negatively (Blendon, 2006). Implementing a generalised lockdown is built on solidarity, as the non-infected are restricting their movements to reduce the risk of transmission for everyone, and adherence to it is a public good (Dayrit and Mendoza, 2020). And quarantine is often the only option as isolation becomes increasingly ineffective in a situation of rapid increase in infections (Day *et al.* 2006).

Switzerland adopted a partial lockdown of the country to tackle Covid-19. The government recommended staying at home as much as possibly, a mild form of isolation, and much less strict than quarantine. Nonetheless, individuals were much less in contact with other individuals, so the repercussions of the lockdown on psychological health could be substantial.

We investigate helpline calls as a way of monitoring suffering in real time. We analyse call logs of the main Swiss telephone and online helpline, “Die Dargebotene Hand”.⁴ This is a very well-known nationwide free service, funded through charitable donations. The helpline allows people in various situations of mental or social distress to speak anonymously to a friendly and well trained volunteer.⁵

Analysing calls to a helpline to gauge psychological and social strain is appealing for two main reasons. First, unlike survey answers, helpline calls can serve as a measure of “revealed anxiety” – given common inhibition thresholds, most people need to experience genuine distress before calling the helpline.⁶ In that sense, helpline calls might be a more reliable gauge of the prevalence of severe psychological and social strain than survey responses. Second, helpline calls are logged on a daily basis and therefore allow for monitoring at high frequency and in real time.

An additional advantage in the Covid-19 crisis is that helpline calls can be expected to attain particular relevance during a lockdown, when face-to-face contacts are severely limited.

Switzerland has been in partial lockdown since Monday, 16 March 2020, after an announcement by the federal government on Friday, 13 March 2020. The plan for lifting the

⁴ See <https://www.143.ch/>.

⁵ Volunteers adhere to the standards of the International Federation of Telephone Emergency Services (www.ifotes.org). The fact that interlocutors are not professionals has been found to lower callers’ inhibitions towards contacting such helplines.

⁶ Hoax calls are explicitly dropped from the call counts used in our data.

lockdown was announced on April 16, 2020: restrictions on a small number of sectors in retail trade were to be relaxed on April 27, 2020, while schools and the remainder of retail trade were announced to reopen on May 11. We therefore analyse time-averaged effects of the lockdown as well as their evolution since the start of the lockdown by comparing daily helpline calls before and after March 13, 2020 to the number of calls over the corresponding period in the previous year.

2. Data and Estimation

We have obtained daily counts of calls to the helpline “Die Dargebotene Hand” (DDH) for the period 28 February to 6 May in 2019 and 2020, resulting in a total of 136 daily observations covering 63,639 calls.⁷ The helpline answers some 470 calls per day, or 14,000 calls per month (30 days). Approximately 95% of “calls” are made by phone, with the remainder being lodged online (email and chat function).

Callers remain anonymous, but helpline operators fill in call reports featuring their best guess of the gender and age category of the caller, as well as up to three problem types per call. For the purpose of this analysis, we distinguish the following nine “problem categories”:⁸

1. Fear of infection (available in 2020, not in 2019)
2. Economic worries
3. Physical health
4. Struggle with everyday life
5. Psychological suffering
6. Problems with relationships, family
7. Loneliness
8. Violence
9. Addiction, suicidality

Operators can log up to three problem types per call. On average in our data, 1.32 of those problem categories are recorded per call.

We use the daily counts of calls by caller type and problem category to track the evolution of revealed anxiety before and after the announcement of the Covid-19-lockdown in Switzerland on Friday 13 March 2020. The Swiss lockdown implied closure of schools and non-essential services. The lockdown was only partial insofar as people were still allowed to move around freely and some economic activities, mainly in the primary and secondary

⁷ This is not the universe of calls nationwide, as DHH has a decentralised structure and not all regional call centres report their data. The data underlying this study cover mainly calls in German from the following nine cantons: Aargau, Basel-Land, Basel-Stadt, Bern, Fribourg, Jura, Neuchâtel, Solothurn and Valais. These cantons together account for some 40% of the Swiss population. The fact that helpline volunteers only operate in the three main national languages, German, French and Italian, could imply a certain selection effect in so far as immigrant populations with limited local language proficiency may not be able to avail of the service. As 2020 is a leap year, we average the call counts for 28 and 29 February 2020 so as to have the same number of observations in both years.

⁸ In the raw data, 17 problem types are distinguished. We aggregate them to obtain meaningful groups and to avoid cases with too few observations. We do not consider the problem type “miscellaneous” of the raw data.

sectors, continued. First steps towards lifting the lockdown were announced on 16 April, which is why we also highlight that date in some of our graphs.

As a “control period”, we compare the evolution during the Covid-19 crisis to the corresponding counts of calls on the same dates in 2019. As daily call counts fluctuate greatly, we show

- mean daily call counts in the sample periods for 2020 and 2019 (Figures 1 and 2),
- moving averages with a two-week window (Figures 2 and 4), and
- third-order polynomial fits allowing us to gauge the statistical significance of differences over time, within 2020 as well as between 2020 and 2019 (Figures 5 and 6).

We also report OLS regressions of call counts on various time measures, in Tables 1 and 2. Call counts are expressed in natural logarithms, in order for estimated coefficients to be interpretable as percentage effects. This allows us to control for weekend effects and for the fact that Easter fell nine days earlier in 2020 than in 2019. By allowing for square time trends, these regressions moreover allow us to test for possibly non-linear evolutions of certain call types. In this specification, the evolution of the number of problems would grow proportionally to calendar time, along the exponential trajectory of viral infection rates in the absence of social distancing. A quadratic specification allows testing whether calls grow first but decrease after the lockdown reduces the spread of the virus.

3. Results

Rather than discussing each graph and regression table individually, we present results by focusing straight away on what we consider the most important findings.

***Result 1:** The volume of total calls is 5.7% higher in our 2020 sample period than in the corresponding 2019 period, in line with trend growth of previous years.*

The volume of calls between 28 February and 6 May 2020 was 32,694 (daily average 481), and it had been 30,945 in the corresponding 2019 period (daily average 455; see also the first panel of Figure 1). A joint test on the 2020-specific effects in the first column of Table 1 shows this increase to be statistically significant. However, the average annual growth rate in total calls over the 2016–2019 period had been 5.3%. The Covid-19-crisis therefore does not seem to have triggered an unusual increase in the total number of calls.⁹

⁹ The definition of a “call” in our data is a call that is answered by a volunteer and results in a conversation. Sometimes, calls cannot be answered because lines are busy or because of technical issues. We are assured by the data providers that the relatively modest year-on-year increase in “calls” is not due to capacity constraints (in fact capacity was expanded at the outset of the crisis, but demand growth has remained below expectations).

Result 2: The strongest increases in call numbers in the 2020 lockdown relative to the corresponding 2019 period are observed for persons aged >65 (+29%).

This can be gleaned from Table 1, and it is illustrated in Figure 1.

Given the greater health risks posed by Covid-19 to the elderly, it is unsurprising to see their revealed anxiety increasing the most. We see no significant difference in the increase of calls by men and women.

Result 3: The problem categories that increased most in the 2020 lockdown relative to the corresponding 2019 period were “fear of infection” (new category), “loneliness” (+20%), and “struggle with everyday life” (+19%).

This can be gleaned from Tables 2a and 2b, and it is illustrated in Figure 2.

These findings suggest that the direct effects of the pandemic and the lockdown were the main sources of revealed anxiety.

Result 4: The problem categories that decreased most in the 2020 lockdown relative to the corresponding 2019 period were “violence” (-25%), “economic worries” (-13%) and “relationships, family” (-7%).

This can be gleaned from Tables 2a and 2b, and it is illustrated in Figure 2.

These findings suggest that, on average over the lockdown period, “collateral” social strain through domestic violence and tensions within households did not increase relative to more normal times. On the contrary, calls motivated by such problems were down compared to the previous year.

The decline in calls about violence is particularly encouraging, given widespread fears about the effect of stay-at-home policies on domestic violence. The Swiss lockdown was relatively soft, allowing people to move around outside freely. Hence, this pattern probably cannot be explained by victims being unable to call because they are locked in with their aggressors.

The relatively low number of calls for economic reasons may be explained by the fact that the Swiss government acted early and decisively to compensate workers for lockdown-related income losses.

Result 5: Since the onset of the lockdown, the volume of total calls has remained relatively stable.

This can be gleaned from the specifications in Table 1 that feature the variable “Days since 13 March”, and it is illustrated in Figures 3 and 5.

We find no statistically significant linear increase in total calls since the onset of the lockdown. Total calls by gender and age subgroups look similarly stable over time. Overall,

therefore, this analysis implies no indication of a gradual worsening of revealed anxiety over the duration of the lockdown.

Result 6: Over the course of the lockdown, the prevalence of the problem category “fear of infection” has been decreasing.

This can be gleaned from the specifications in Table 2a that feature the variable “Days since 13 March”, and it is illustrated in Figures 4 and 6.

The decreasing trend in the frequency of calls about “fear of infection” is likely due to increasing learning about and familiarity with the pandemic situation.

Result 7: In the first month of the lockdown, the prevalence of the problem category “addiction, suicidality” increased, while the prevalence of the problem category “relationships, family” decreased.

This can be gleaned from the specifications in Table 2b that feature the variable “Days since 13_March”, and it is illustrated in Figures 4 and 6.

Our estimations suggest that in the initial weeks of the lockdown, problems with relationships, addiction and suicidality were increasing. After about one month of lockdown, the prevalence of these problems no longer appears to have increased. The reverse time pattern is observed for problems with relationships and family.

4. Conclusions

Overall, we find that psychological and social strain as measured through calls to the helpline seems to have been remarkably limited during the Covid-19 crisis: total calls grew in line with the long-run trend.

To the extent that calls did increase, this was mainly explained by worries linked directly to the pandemic: callers aged over 65 and calls about fear of infection. Small increases are observed also in calls about loneliness and struggle with everyday life, which can be attributed directly to people having to adjust to life under the lockdown.

Widespread fears about a spike in domestic violence related to the partial lockdown, however, are not borne out by this analysis. On the contrary: calls motivated by acts of violence are both down on the corresponding period of the previous year and falling further as the lockdown is progressing. Also, calls about family and relationship issues decrease in the first weeks of the lockdown and return to 2019 levels by the time the end of the lockdown is announced.

Increases in the initial weeks of the lockdown are observed for calls addiction and suicidality. While the social and psychological strain of the lockdown might not manifest itself in outright violence, these observations suggest that such strain nevertheless existed.

Our analysis mainly focuses on the period since the lockdown and compares it to the corresponding period of 2019. The observed effects on psychological and social strain appear second order to the economic and medical ramifications of the pandemic.

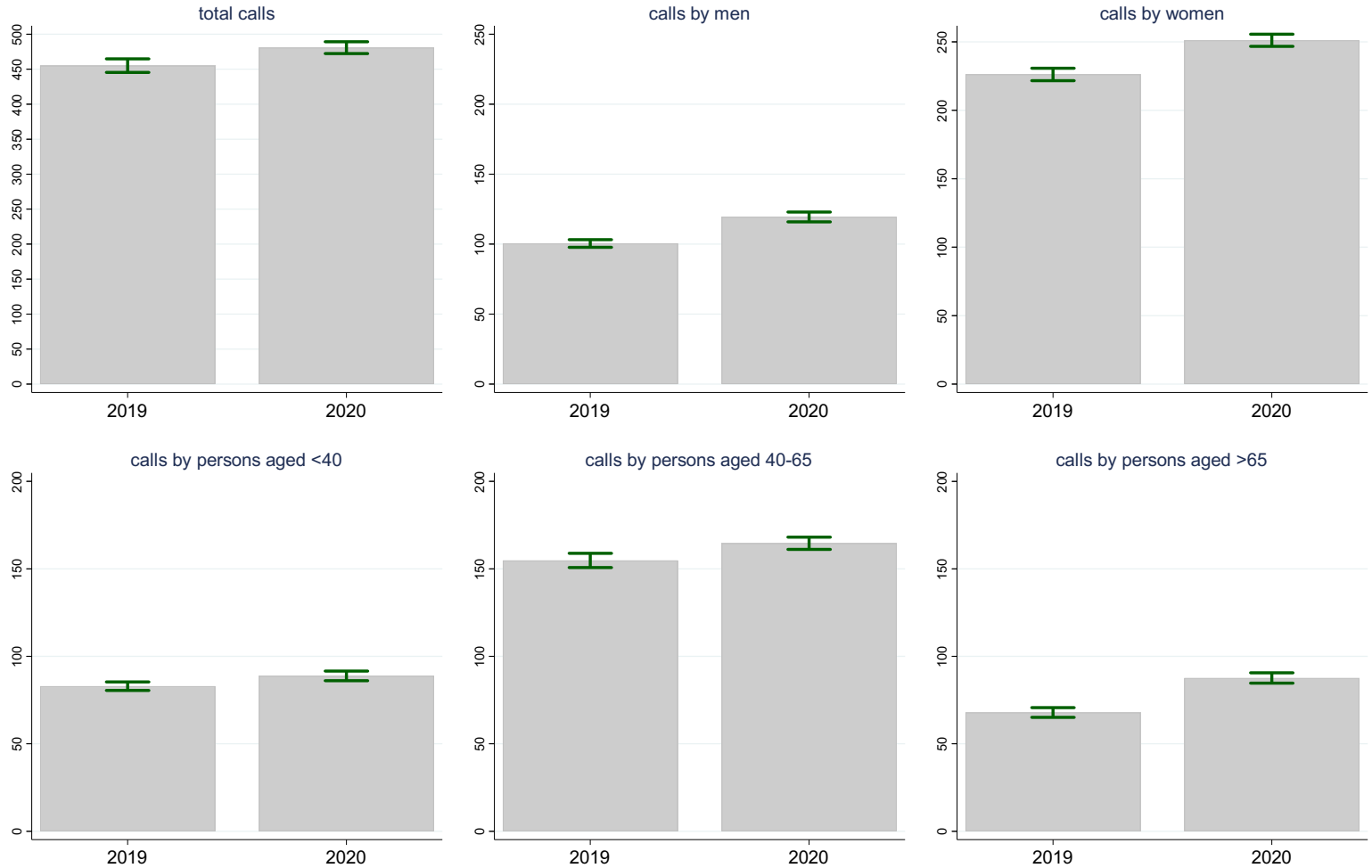
It will be interesting to follow the situation as the lockdown restrictions are lifted further, to validate the findings based on helpline calls by those based on surveys and administrative records such as police reports, and, perhaps most importantly, to compare the Swiss helpline data with those for other countries with different policy responses to the pandemic. More broadly, helpline data could be used to monitor societal suffering also in “normal” times.

References

- Blendon, R. J., DesRoches, C. M., Cetron, M. S., Benson, J. M., Meinhardt, T., & Pollard, W. (2006) Attitudes Toward The Use Of Quarantine In A Public Health Emergency In Four Countries: The experiences of Hong Kong, Singapore, Taiwan, and the United States are instructive in assessing national responses to disease threats. *Health Affairs*, 25 (Suppl1), W15-W25.
- Brooks, S. K., Webster, R. K., Smith, L. E., Woodland, L., Wessely, S., Greenberg, N., & Rubin, G.J. (2020) The Psychological Impact of Quarantine and How to Reduce It: Rapid Review of the Evidence. *The Lancet* .
- Day, T., Park, A., Madras, N., Gumel, A., & Wu, J. (2006) When Is Quarantine a Useful Control Strategy for Emerging Infectious Diseases?. *American Journal of Epidemiology*, 163 (5), 479-485.
- Dayrit, M., & Mendoza, R. U. (2020) Social Cohesion vs COVID-19. *Available at SSRN 3555152*.

Figure 1: Total calls¹⁵⁰

(daily averages for 28 February - 6 May, 95%-confidence intervals)



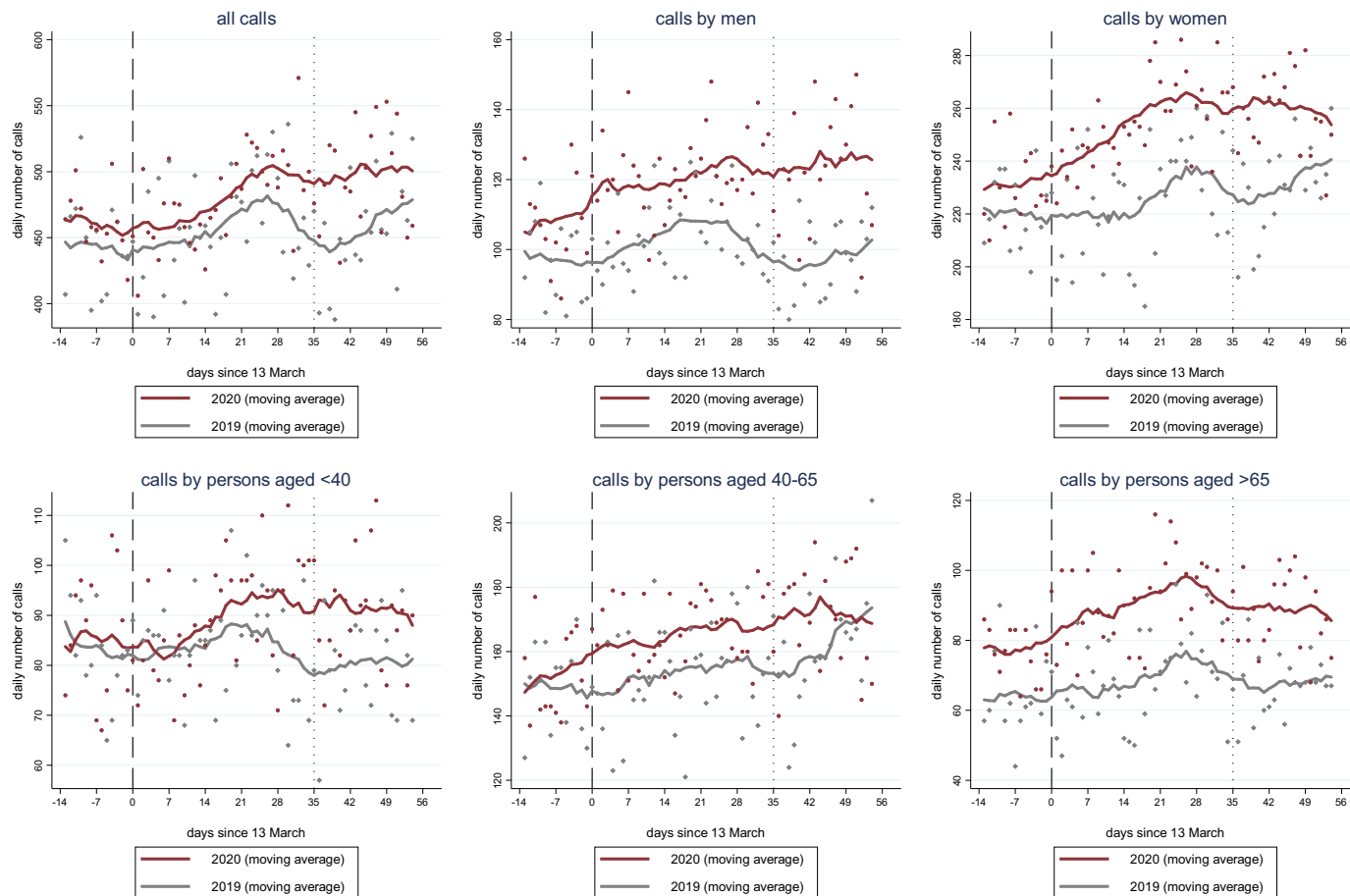
Data from Swiss helpline Die Dargebotene Hand (Tel. 143)

Figure 2: Calls by problem category
(daily averages for 28 February - 6 May, 95%-confidence intervals)



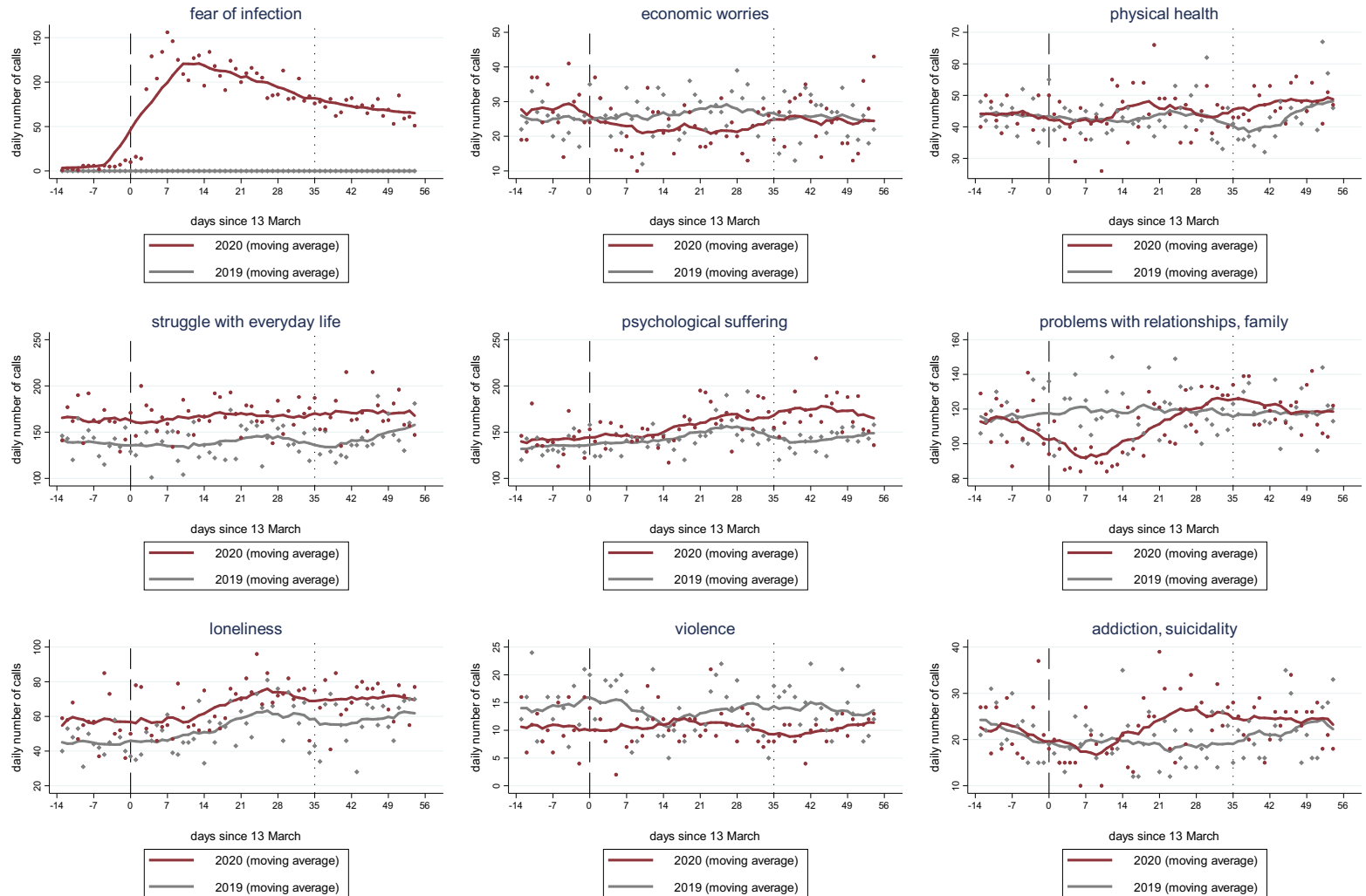
Data from Swiss helpline Die Dargebotene Hand (Tel. 143)

Figure 3: Total calls (with moving average)



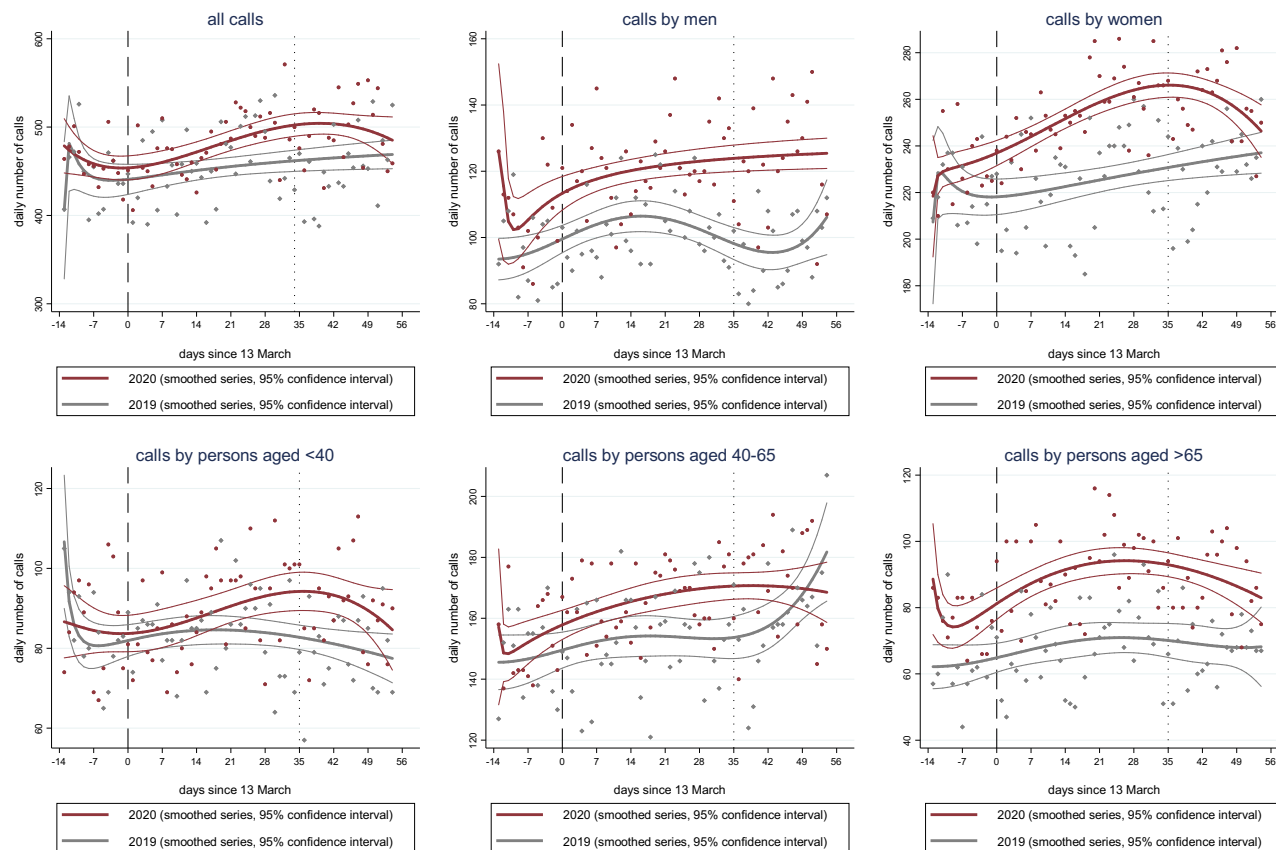
Dashed (dotted) vertical lines: announcement of partial lockdown (first steps of lockdown release); data from Swiss helpline Die Dargebotene Hand (Tel. 143)

Figure 4: Calls by problem Category (with moving average)¹⁵³



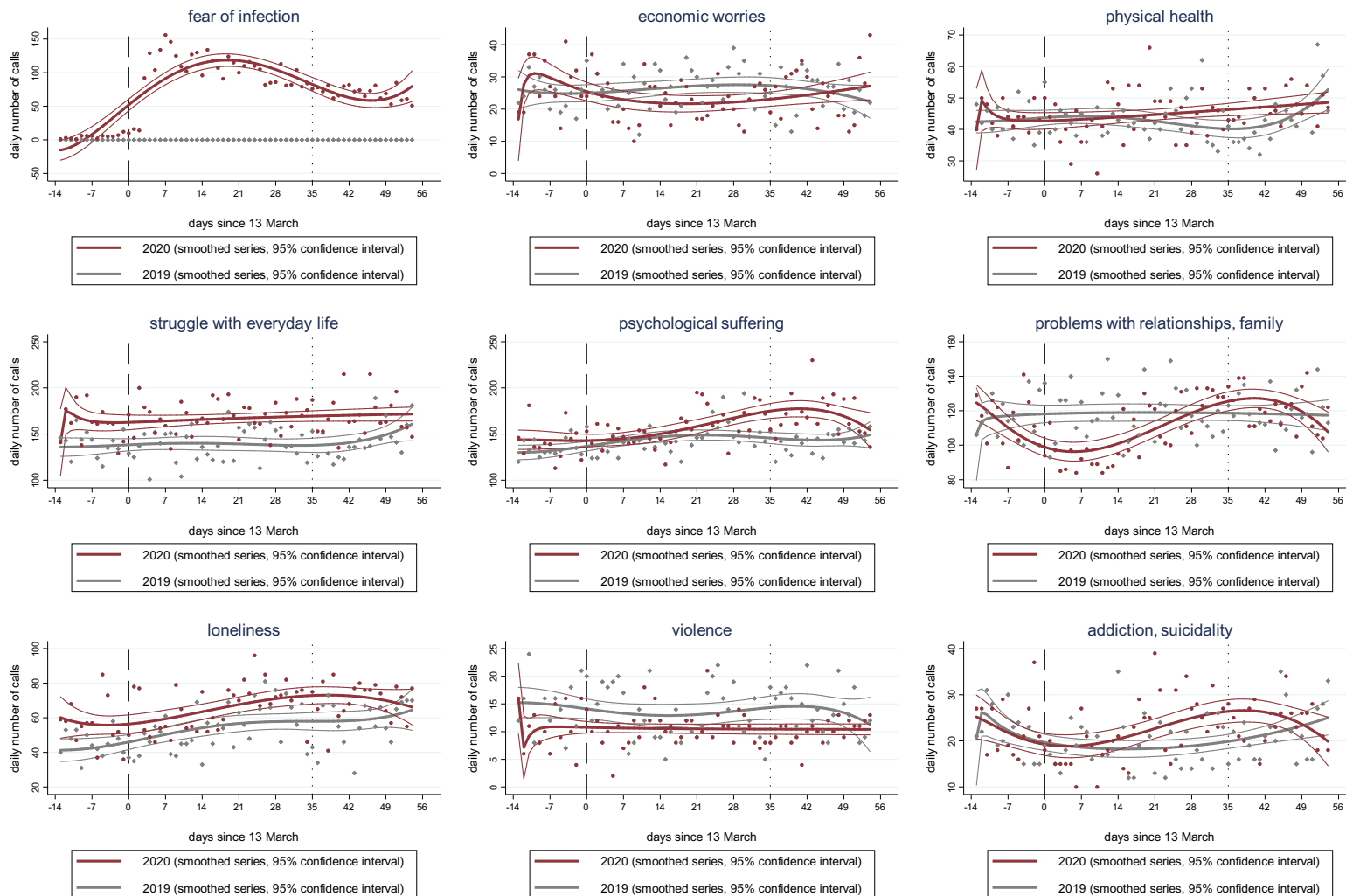
Dashed (dotted) vertical lines: announcement of partial lockdown (first steps of lockdown release); data from Swiss helpline Die Dargebotene Hand (Tel. 143)

Figure 5: Total calls (with polynomial smoothing)



Dashed (dotted) vertical lines: announcement of partial lockdown (first steps of lockdown release); data from Swiss helpline Die Dargebotene Hand (Tel. 143)

Figure 6: Calls by problem category (with polynomial smoothing)



Dashed (dotted) vertical lines: announcement of partial lockdown (first steps of lockdown release); data from Swiss helpline Die Dargebotene Hand (Tel. 143)

Table 1: Total calls

	Dependent variable:																	
	Total calls			Calls by men			Calls by women			Calls by persons aged <40			Calls by persons aged 40-65			Calls by persons aged >65		
2020 dummy	0.04 1.20	0.04 1.25	0.04 1.26	0.11 * 2.49	0.11 * 2.48	0.11 * 2.49	0.04 1.39	0.04 1.45	0.04 1.51	0.03 0.50	0.03 0.51	0.03 0.52	0.02 0.58	0.02 0.60	0.02 0.60	0.17 ** 2.96	0.17 ** 2.96	0.17 ** 2.99
Post-13_March dummy	0.03 1.19	0.001 0.03	-0.02 -0.64	0.06 1.68	0.07 1.72	0.03 0.62	0.03 1.11	-0.02 -0.76	-0.04 -1.20	-0.01 -0.22	0.03 0.64	-0.004 -0.07	0.05 1.84	-0.02 -0.48	-0.01 -0.15	0.06 1.27	0.02 0.36	-0.05 -0.65
2020 dummy x Post-13_March dummy	0.02 0.67	0.002 0.05	-0.02 -0.47	0.08 1.61	0.04 0.65	0.03 0.60	0.09 * 2.56	0.09 * 2.47	0.05 0.99	0.05 0.98	-0.03 -0.51	-0.09 -1.11	0.05 1.30	0.10 * 2.08	0.06 0.98	0.11 1.70	0.15 1.91	0.15 1.49
Weekend dummy	-0.003 -0.21	-0.001 -0.06	-0.001 -0.12	0.03 1.44	0.03 1.42	0.03 1.33	-0.03 -1.90	-0.02 -1.76	-0.02 -1.87	-0.04 -1.54	-0.04 -1.58	-0.04 -1.67	-0.03 -1.78	-0.03 -1.63	-0.03 -1.58	0.07 * 2.56	0.07 * 2.61	0.07 * 2.52
Easter_week dummy	-0.02 -0.94	-0.03 -1.26	-0.05 * -2.14	-0.05 -1.87	-0.05 -1.74	-0.07 * -2.21	-0.004 -0.21	-0.01 -0.74	-0.04 * -2.01	-0.02 -0.68	-0.02 -0.45	-0.05 -1.45	-0.04 -1.69	-0.06 * -2.35	-0.07 * -2.48	0.03 0.78	0.02 0.57	-0.01 -0.33
Days since 13_March		0.001 1.64	0.004 1.50	-0.001 -0.62	0.004 1.06		0.002 ** 2.90	0.004 * 1.71		-0.001 -1.39	0.003 0.62		0.003 *** 3.47	0.002 0.51		0.001 1.13	0.01 1.81	
2020 dummy x Days since 13_March		0.001 0.83	0.003 1.11		0.001 1.05	0.001 0.20	-0.0005 -0.57	0.01 1.68		0.003 * 2.16	0.01 1.76		-0.002 -1.67	0.003 0.72		-0.001 -0.92	-0.0005 -0.07	
Days since 13_March squared			-0.0001 -1.09			-0.0001 -1.24		-0.00004 -0.94			-0.0001 -0.97			0.00002 0.39			-0.0001 -1.55	
2020 dummy x Days since 13_March squared			-0.0001 -0.95			0.00001 0.06		-0.0001 -1.93			-0.0001 -1.27			-0.0001 -1.19			-0.00002 -0.20	
Constant	6.10 *** 269.18	6.10 *** 278.16	6.10 *** 282.76	4.56 *** 145.09	4.56 *** 144.61	4.56 *** 144.95	5.41 *** 260.72	5.40 *** 271.38	5.40 *** 282.50	4.43 *** 122.73	4.43 *** 124.01	4.43 *** 126.68	5.01 *** 188.49	5.01 *** 196.47	5.01 *** 196.22	4.13 *** 99.69	4.13 *** 99.40	4.13 *** 100.63
adjusted R2	0.12 136	0.17 136	0.20 136	0.42 136	0.42 136	0.42 136	0.41 136	0.45 136	0.50 136	0.06 136	0.08 136	0.12 136	0.19 136	0.25 136	0.25 136	0.48 136	0.48 136	0.49 136

Notes: OLS regressions (t-statistics in italics below coefficient estimates). Data from Swiss hotline "Die Dargebotene Hand (143)": daily counts of calls between 29 February and 6 May in 2019 and 2020. Up to three problem categories possible per individual call. 13 March 2020 marks the announcement date of the Corona-lockdown in Switzerland (entry into force: 16 March).

Table 2a: Calls by problem category

	<i>Dependent variable:</i>											
	Problem: fear of infection			Problem: economic worries			Problem: physical health			Problem: struggle with everyday life		
2020 dummy				0.11 <i>1.11</i>	0.11 <i>1.11</i>	0.11 <i>1.11</i>	0.02 <i>0.28</i>	0.02 <i>0.29</i>	0.02 <i>0.29</i>	0.14 ** <i>3.01</i>	0.14 ** <i>3.05</i>	0.14 ** <i>3.04</i>
Post-13_March dummy	3.05 *** <i>17.04</i>	3.11 *** <i>13.98</i>	2.52 *** <i>9.99</i>	0.07 <i>0.94</i>	0.12 <i>1.18</i>	-0.01 <i>-0.05</i>	0.003 <i>0.06</i>	-0.03 <i>-0.52</i>	0.03 <i>0.39</i>	0.01 <i>0.16</i>	-0.05 <i>-1.24</i>	-0.06 <i>-1.05</i>
2020 dummy x Post-13_March dummy				-0.24 * <i>-2.14</i>	-0.33 * <i>-2.40</i>	-0.17 <i>-0.99</i>	0.03 <i>0.53</i>	-0.02 <i>-0.21</i>	-0.12 <i>-1.23</i>	0.05 <i>0.95</i>	0.10 <i>1.59</i>	0.07 <i>0.92</i>
Weekend dummy	-0.21 <i>-1.40</i>	-0.21 <i>-1.41</i>	-0.21 <i>-1.55</i>	-0.26 *** <i>-5.43</i>	-0.26 *** <i>-5.42</i>	-0.27 *** <i>-5.57</i>	0.005 <i>0.38</i>	0.01 <i>0.41</i>	0.01 <i>0.45</i>	-0.04 <i>-1.95</i>	-0.04 * <i>-1.83</i>	-0.04 <i>-1.82</i>
Easter_week dummy	0.13 <i>0.61</i>	0.14 <i>0.62</i>	-0.25 <i>-1.14</i>	-0.15 * <i>-2.16</i>	-0.14 * <i>-2.01</i>	-0.15 * <i>-2.01</i>	-0.11 ** <i>-2.76</i>	-0.12 ** <i>-2.97</i>	-0.12 ** <i>-2.84</i>	-0.05 <i>-1.62</i>	-0.06 * <i>-2.02</i>	-0.07 * <i>-2.17</i>
Days since 13_March		-0.002 <i>-0.50</i>	0.07 *** <i>3.62</i>		-0.002 <i>-0.72</i>	0.01 <i>1.39</i>		0.001 <i>0.98</i>	-0.005 <i>-1.03</i>		0.002 * <i>2.33</i>	0.003 <i>0.69</i>
2020 dummy x Days since 13_March					0.004 <i>1.16</i>	-0.01 <i>-1.23</i>		0.002 <i>1.07</i>	0.01 <i>1.99</i>		-0.002 <i>-1.37</i>	0.001 <i>0.24</i>
Days since 13_March squared			-0.001 *** <i>-3.88</i>			-0.0003 <i>-1.63</i>			0.0001 <i>1.33</i>			-0.00001 <i>-0.11</i>
2020 dummy x Days since 13_March squared						0.0003 <i>1.57</i>			-0.0002 <i>-1.78</i>			-0.0001 <i>-0.62</i>
Constant	1.40 *** <i>9.46</i>	1.40 *** <i>8.42</i>	1.40 *** <i>9.31</i>	3.26 *** <i>45.23</i>	3.26 *** <i>45.11</i>	3.26 *** <i>45.33</i>	3.76 *** <i>90.72</i>	3.76 *** <i>92.53</i>	3.76 *** <i>92.93</i>	4.95 *** <i>150.06</i>	4.95 *** <i>152.08</i>	4.95 *** <i>151.38</i>
adjusted R2	0.82	0.82	0.85	0.22	0.22	0.23	0.04	0.08	0.09	0.37	0.39	0.38
N	68	68	68	136	136	136	136	136	136	136	136	136

Notes: OLS regressions (t-statistics in italics below coefficient estimates). Data from Swiss hotline "Die Dargebotene Hand (143)": daily counts of calls between 29 February and 6 May in 2019 and 2020. Up to three problem categories possible per individual call. 13 March 2020 marks the announcement date of the Corona-lockdown in Switzerland (entry into force: 16 March).

Table 2b: Calls by problem category (continued)

	<i>Dependent variable:</i>														
	Problem: psychological suffering			Problem: relationships, family			Problem: loneliness			Problem: violence			Problem: addiction, suicidality		
2020 dummy	0.04 <i>0.97</i>	0.04 <i>1.02</i>	0.04 <i>1.05</i>	-0.02 <i>-0.36</i>	-0.02 <i>-0.41</i>	-0.02 <i>-0.42</i>	0.20 * <i>2.40</i>	0.20 * <i>2.54</i>	0.20 * <i>2.56</i>	-0.28 * <i>-2.00</i>	-0.28 * <i>-1.98</i>	-0.28 <i>-1.97</i>	0.05 <i>0.50</i>	0.05 <i>0.52</i>	0.05 <i>0.54</i>
Post-13_March dummy	0.07 * <i>2.11</i>	0.05 <i>1.13</i>	-0.01 <i>-0.29</i>	0.01 <i>0.30</i>	0.03 <i>0.58</i>	0.01 <i>0.20</i>	0.18 ** <i>2.64</i>	0.02 <i>0.30</i>	-0.06 <i>-0.61</i>	-0.02 <i>-0.21</i>	-0.002 <i>-0.02</i>	0.10 <i>0.58</i>	-0.11 <i>-1.29</i>	-0.22 * <i>-2.13</i>	-0.11 <i>-0.88</i>
2020 dummy x Post-13_March dummy	0.07 <i>1.39</i>	0.002 <i>0.04</i>	-0.01 <i>-0.11</i>	-0.05 <i>-0.79</i>	-0.22 *** <i>-3.45</i>	-0.32 *** <i>-4.16</i>	-0.004 <i>-0.04</i>	0.04 <i>0.34</i>	0.04 <i>0.27</i>	0.03 <i>0.17</i>	-0.03 <i>-0.13</i>	-0.12 <i>-0.48</i>	0.06 <i>0.48</i>	-0.05 <i>-0.33</i>	-0.36 * <i>-2.04</i>
Weekend dummy	-0.02 <i>-1.14</i>	-0.02 <i>-1.04</i>	-0.02 <i>-1.20</i>	0.04 <i>1.45</i>	0.04 <i>1.77</i>	0.04 <i>1.85</i>	0.10 * <i>2.48</i>	0.11 ** <i>2.86</i>	0.11 ** <i>2.77</i>	0.12 <i>1.70</i>	0.12 <i>1.68</i>	0.12 <i>1.75</i>	0.002 <i>0.04</i>	0.01 <i>0.23</i>	0.02 <i>0.38</i>
Easter_week dummy	-0.03 <i>-1.03</i>	-0.04 * <i>-1.30</i>	-0.07 * <i>-2.40</i>	0.06 <i>1.56</i>	0.06 <i>1.73</i>	0.03 <i>0.76</i>	0.08 <i>1.42</i>	0.05 <i>0.87</i>	0.004 <i>0.07</i>	0.05 <i>0.55</i>	0.06 <i>0.58</i>	0.08 <i>0.77</i>	0.08 <i>1.08</i>	0.06 <i>0.78</i>	0.01 <i>0.18</i>
Days since 13_March		0.001 <i>1.14</i>	0.01 * <i>2.27</i>		-0.0003 <i>-0.33</i>	-0.001 <i>-0.21</i>		0.01 ** <i>3.34</i>	0.02 * <i>2.22</i>		-0.001 <i>-0.26</i>	-0.01 <i>-1.01</i>		0.004 <i>1.77</i>	-0.01 <i>-0.89</i>
2020 dummy x Days since 13_March		0.002 <i>1.87</i>	0.004 <i>0.80</i>		0.01 *** <i>4.55</i>	0.02 *** <i>3.38</i>		-0.01 <i>-0.63</i>	-0.001 <i>-0.11</i>		0.002 <i>0.45</i>	0.01 <i>0.70</i>		0.004 <i>1.23</i>	0.04 ** <i>3.22</i>
Days since 13_March squared			-0.0001 * <i>-2.01</i>			0.00001 <i>0.17</i>			-0.0002 * <i>-1.41</i>			0.0002 <i>0.97</i>			0.00020 <i>1.43</i>
2020 dummy x Days since 13_March squared			-0.00003 <i>-0.36</i>			-0.0002 * <i>-2.28</i>			-0.00001 <i>-0.08</i>			-0.0002 <i>-0.59</i>			-0.0010 ** <i>-3.00</i>
Constant	4.91 *** <i>155.48</i>	4.91 *** <i>163.55</i>	4.91 *** <i>168.14</i>	4.73 *** <i>126.63</i>	4.73 *** <i>142.99</i>	4.73 *** <i>146.56</i>	3.77 *** <i>61.32</i>	3.77 *** <i>64.78</i>	3.77 *** <i>65.26</i>	2.53 *** <i>23.38</i>	2.53 *** <i>23.17</i>	2.53 *** <i>23.59</i>	3.06 *** <i>38.67</i>	3.06 *** <i>40.61</i>	3.06 *** <i>41.76</i>
adjusted R2	0.24	0.31	0.35	0.04	0.25	0.29	0.26	0.34	0.35	0.10	0.09	0.12	0.02	0.11	0.16
N	136	136	136	136	136	136	136	136	136	136	136	136	136	136	136

Notes: OLS regressions (t-statistics in italics below coefficient estimates). Data from Swiss hotline "Die Dargebotene Hand (143)": daily counts of calls between 29 February and 6 May in 2019 and 2020. Up to three problem categories possible per individual call. 13 March 2020 marks the announcement date of the Corona-lockdown in Switzerland (entry into force: 16 March).

Globalization in the time of COVID-19¹

Alessandro Sforza² and Marina Steininger³

Date submitted: 12 May 2020; Date accepted: 13 May 2020

The economic effects of a pandemic crucially depend on the extent to which countries are connected in global production networks. In this paper we incorporate production barriers induced by COVID-19 shock into a Ricardian model with sectoral linkages, trade in intermediate goods and sectoral heterogeneity in production. We use the model to quantify the welfare effect of the disruption in production that started in China and quickly spread across the world. We find that the COVID-19 shock has a considerable impact on most economies in the world, especially when a share of the labor force is quarantined. Moreover, we show that global production linkages have a clear role in magnifying the effect of the production shock. Finally, we show that the economic effects of the COVID-19 shock are heterogeneous across sectors, regions and countries, depending on the geographic distribution of industries in each region and country and their degree of integration in the global production network.

1 We thank Lorenzo Caliendo, Lisandra Flach, Annalisa Loviglio, Luca David Opromolla, Gianmarco Ottaviano, Fernando Parro, Vincenzo Scrutinio, Tommaso Sonno for useful discussion. We thank Matilde Bombardini for sharing the Chinese Census data with us. All errors are ours.

2 Assistant Professor, University of Bologna.

3 Phd Candidate, ifo Institute and LMU.

Copyright: Alessandro Sforza and Marina Steininger

1 Introduction

Globalization allows firms to source intermediate inputs and sell final goods in many different countries. The diffusion of a local shock through input-output linkages and global value chains has been extensively studied (see for example Carvalho et al. (2016)) but little is known on how a pandemic affects global production along with its diffusion.¹

In this paper we study the role of global production linkages in the transmission of a pandemic shock across countries. We exploit an unprecedented disruption in production in the recent world history, namely the global spread of COVID-19 virus disease, to instruct a multi-country, multi-sector Ricardian model with interactions across tradable and non-tradable sectors observed in the input-output tables. We use the model to quantify the trade and welfare effects of a disruption in production that started in China and then quickly spread across the world. The spread of COVID-19 disease provides a unique set-up to understand and study the diffusion of a global production shock along the global value chains for three main reasons. First, it is possibly the biggest production disruption in the recent world history. With around 2.424.419 cases, 166.256 deaths and millions of people in quarantine around the world to date², the spread of COVID-19 disease is the largest pandemic ever experienced in the globalized world.³ Second, the COVID-19 shock is not an economic shock in its nature, hence its origin and diffusion is independent from the fundamentals of the economy. Third, differently from any other non-economic shock experienced before, it is a global shock. Indeed, while the majority of natural disasters or epidemics have a local dimension, the spread of the COVID-19 disease has been confined to the Chinese province of Hubei only for a few weeks, to then spread across the entire world.

Understanding the effects of a global production disruption induced by a pandemic is complex. We build on the work by Caliendo and Parro (2015) who develop a tractable and simple model that allows to decompose and quantify the role that intermediate goods and sectoral linkages have in amplifying or reducing the impact of a change in tariffs. We extend their framework and introduce a role for policy intervention in deterring production. In our set-up, the policy maker can use the instrument of quarantine as a policy response to deter the COVID-19 virus diffusion; moreover, we account for the geographic distribution of industries

¹Huang (2019) studies how diversification in global sourcing improves firm resilience to supply chain disruptions during the SARS epidemics in China. We complement his analysis by studying the effect of an epidemic shock that is not geographically confined to a specific region, but it spreads fast in the entire world

²as of 20th of April 2020

³See Maffioli (2020) for a comparison of COVID-19 with other pandemics in the recent history.

in each region and country and for the labor intensity of each sector of production to have a complete picture of the distribution of the shock across regions and sectors. The policy intervention of quarantine translates into a lockdown, a production barrier that increases the production costs for intermediates and final goods produced for the internal market as well as for the exporting market. We construct a measure of quarantine using two different pillars: first, we use a country level measure for the stringency of the policy intervention of lockdown from Hale (2020). Second, we allow the quarantine to heterogeneously affect each sector in each country using the share of work in a sector that can be performed at home (henceforth *teleworkability*) from Dingel and Neiman (2020).⁴ Crucially, in a model with interrelated sectors the cost of the input bundle depends on wages and on the price of all the composite intermediate goods in the economy, both non-tradable and tradable. In our framework, the policy intervention has a direct effect on the cost of each input as well as an indirect effect via the sectoral linkages.⁵ Moreover, our modeling choice for the shock allows the spread of COVID-19 disease to also have a direct effect on the cost of non-tradable goods in each economy, hence on domestic trade.

We follow Dekle et al. (2008) and Caliendo and Parro (2015) and solve the model in relative changes to identify the welfare effect of the COVID-19 shock. We perform three different exercises: (i) we include the COVID-19 shock in the model and we estimate a *snap-shot* scenario based on the actual number of COVID-19 cases in each country, (ii) we include the quarantine shock in the model and estimate a quarantine scenario, imposing quarantine to a fraction of the labour force in each country, (iii) we decompose the effect into a direct effect from the production shock induced by the COVID-19 quarantine and an indirect effect coming from the global shock affecting the other countries. We perform the three exercises

⁴It is crucial to note that the sectoral heterogeneity in labor intensity as well as teleworkability are time invariant in our set-up, while the number of COVID-19 cases as well as the restrictiveness and duration of the implemented policy measures are in continuous evolution, hence the point estimates of the counterfactual scenarios might change as the spread of the COVID-19 disease affects more countries and more people. Even if the size of the shock changes, the sensitivity and the comparisons across sectors and countries as well as the decomposition of the effects will remain similar. The focus of this paper is to highlight the importance of global production networks in the diffusion of a global shock and on how to use a simple theoretical framework to provide insights on the heterogeneous effects of the COVID-19 shock across countries and across sector under different scenarios, rather than providing the absolute numbers of the drop in real income due to the COVID-19 shock. We will constantly update the results of the paper to account for the new cases as well as for the number of countries in quarantine. The results presented in this version are supposed to provide a first *snap-shot* of the economic effect of the COVID-19 shock. A more complete picture will be available when the full information of COVID-19 cases, quarantined countries and share of people in quarantine is available.

⁵This feature of the model is a key difference compared to one-sector models or multi-sector models without interrelated sectors, as highlighted by Caliendo and Parro (2015).

both in an open economy with the actual tariff and trade cost levels and in a closer economy, where we increase the trade costs by 100 percentage points in each sector-country. The quantitative exercise requires data on bilateral trade flows, production, tariffs, sectoral trade elasticities, employment shares by sector and region and the number of COVID-19 cases in each region or country. We calibrate a 40 countries 50 sectors economy and incorporate the COVID-19 shock to evaluate the welfare effects for each country both in aggregate and at the sectoral level.

We find that the COVID-19 shock has a considerable impact on most economies in the world, especially when a share of the labor force is quarantined. In our quarantine scenario, most of the countries experience a drop in real income up to 14%, with the most pronounced drops for India and Turkey. We further decompose the economic impact of the COVID-19 shock by sectors and find that the income drop is widespread across all sectors. Indeed, contrary to drops in tariffs that affect only a subset of sectors, the COVID-19 shock is a production barrier that affects both home and export production in all sectors of the economy. The observed heterogeneity in the sectoral decrease in value added is partially driven by the geography of production in each country combined with the geographic diffusion of the shock, by the inter-sectoral linkages across countries, but also by the heterogeneity in the degree of *teleworkability* across sectors and countries.

The role of the global production linkages in magnifying the effect of the production shock is clear when we decompose the total income change into a *direct* component due to a domestic production shock and an *indirect* component due to global linkages. We show that linkages between countries account for a substantial share of the total income drop observed. Moreover, we estimate a simple econometric model to better understand the determinants of the observed heterogeneity in the income drop accounted for by the *direct* and the *indirect* effect. We find that the degree of trade openness of a country is a key element in explaining the observed heterogeneity.

Finally, to deeper understand the importance of global production networks in the diffusion of the shock, we investigate what would have been the impact of the COVID-19 shock in a less integrated world. To answer this question, we quantify the real income effect of the COVID-19 shock in a less integrated world scenario, where we increase the current trade barriers in each country and sector by 100 percentage points. First and unsurprisingly, a less integrated world itself implies enormous income losses for the great majority of countries in our sample. Focusing on the economic impact of the COVID-19 shock in a less integrated world compared to a world as of today, we find some interesting results. Indeed, when raising trade costs in all countries, the *indirect* component is lower than in an open economy, but

it still accounts for a relevant share of the drop in the income due to the COVID-19 shock. In our counterfactual exercise, the increase in trade cost mimics a world with higher trade barriers, but not a complete autarky scenario; countries would still trade, use intermediates from abroad and sell final goods in foreign countries. This finding highlights the importance of inter-sectoral linkages in the transmission of the shock: a higher degree of integration in the global production network implies that a shock in one country directly diffuses through the trade linkages to other countries. Trade has two different effects in our model: on the one hand, it smooths the effect of the shock by allowing consumers to purchase and consume goods they wouldn't otherwise be able to consume in a world with production barriers in quarantine. On the other hand, the COVID-19 shock increases production costs of intermediate inputs that are used at home and abroad. Our counterfactual exercise clearly shows that an increase in trade costs would not significantly decrease the impact of the COVID-19 shock across countries. However, increasing trade barriers would imply an additional drop in real income between 14% and 33% across countries.

Our paper is closely related to a growing literature that study the importance of trade in intermediate inputs and global value chains. For example Altomonte and Vicard (2012), Antràs and Chor (2013), Antràs and Chor (2018), Antràs and de Gortari (Forthcoming), Alfaro et al. (2019), Antràs (Forthcoming), Bénassy-Quéré and Khoudour-Casteras (2009), Gortari (2019), Eaton and Romalis (2016), Hummels and Yi (2001), Goldberg and Topalova (2010), Gopinath and Neiman (2013), Halpern and Szeidl (2015)). Our paper is especially close to a branch of this literature that extends the Ricardian trade model of Eaton and Kortum (2002a) to multiple sectors, allowing for linkages between tradable sectors and between tradable and non-tradable.⁶ Indeed, our paper is based on the work of Caliendo and Parro (2015) and adds an additional channel through which a policy intervention could affect welfare at home and in other countries, namely a production barrier induced by the spread of the virus. We use an unprecedented shock affecting simultaneously most of the countries across the world to understand the response of the economy under different production barrier scenarios in free trade and a less integrated world. Moreover, we use the rich structure of the model to show the distribution of the effects of the shock across regions and sectors.

Finally, our paper contributes to the literature evaluating the impact of natural disasters or epidemics on economic activities (see for example the papers by Barrot and Sauvagnat (2016), Boehm et al. (2019), Carvalho et al. (2016), Young (2005) and Huang (2019)). Similar to Boehm et al. (2019), Barrot and Sauvagnat (2016) and Carvalho et al. (2016) and Huang

⁶See for example Dekle et al. (2008), Arkolakis et al. (2012)

(2019) we also study how a natural disaster or an epidemic affects the economy through the input channels. We add to their work by using a shock that is unprecedented both in its nature and in its effect. Indeed, while a natural disaster is a geographically localized shock that can destroy production plants and affects the rest of the economy and other countries only through input linkages, in our set-up the shock induced by COVID-19 is modelled as a policy intervention that constraints production simultaneously in almost all countries in the world. Indeed, in our paper each country is hit by a local shock induced by the spread of the virus at home, and by a foreign shock through the input linkages induced by the spread of corona abroad.⁷

The paper is structured as follows. In section 2 we describe the COVID-19 shock and motivate the rationale of our modeling choice. In section 3 we present the model we use for the quantitative exercise. In section 4 we describe the data used for the quantitative exercise and we present the results. In section 5 we conclude.

2 COVID-19 - A production barrier shock

The new coronavirus (the 2019 novel coronavirus disease COVID-19) was first identified in Wuhan city, Hubei Province, China, on December 8, 2019 and then reported to the public on December 31, 2019 (Maffioli (2020)). As of April 20, 2020, the virus has affected 2.424.419 people in the world, causing 166.256 deaths and forcing millions of people in quarantine for several weeks around the world. The exponential contagion rate of the COVID-19 virus has led many governments to implement a drastic shut-down policy, forcing large shares of the population into quarantine. Because of forced quarantine, there is wide consensus that the economic costs of the pandemic will be considerable, as factories, businesses, schools and country borders have been closed and are going to be closed for several weeks. Moreover, the spread of the COVID-19 disease has followed unpredictable paths, with a marked heterogeneity in the contagion rates across countries and across regions within the same country.

We propose a simple measure that quantifies the intensity of the economic shock, leveraging on the diffusion of COVID-19 across space, the geographical distribution of sectors in each country and the sectoral labor intensity. The virus shock v_i^j can be expressed as

⁷A growing literature in economics extends the SIER model to study the economic consequences of the diffusion of the pandemic under different policy scenarios (see for example Atkeson (2020), Berger (2020), Eichenbaum et al. (2020))

$$v_i^j = \sum_{r=1}^R \left(\frac{cases_{ir}}{\sum_{j=1}^J l_{ijr}} * \frac{l_{ijr}}{\sum_{r=1}^R l_{ijr}} \right) * e^{\gamma_i^j} \quad (1)$$

where l_{ijr} is the total employment of sector j in region r of country i , $cases_{ir}$ is the number of official cases of COVID-19 in region r of country i , γ_i^j is the share of value added of sector j in country i , $\sum_{j=1}^J l_{ijr}$ is the sum of employed individuals across all sectors in a region r of country i , while $\sum_{r=1}^R l_{ijr}$ is the sum of employed individuals in a sector j across all regions r of country i . The first term of the formula is a measure of the impact of the COVID-19 on the regional employment. The second term is a measure of the geographic distribution of production in the country, measuring how much each sector is concentrated in a region compared to the rest of the country. The last term is meant to capture the labor intensity of each sector in a country.

In our counterfactual exercise we substitute the share of COVID-19 cases over total employment in a region $\frac{cases_{ir}}{\sum_{j=1}^J l_{ijr}}$, with a constructed share of people under quarantine ψ_i^j as follows:⁸

$$v_i^j = \sum_{r=1}^R \left(\psi_i^j * \frac{l_{ijr}}{\sum_{r=1}^R l_{ijr}} \right) * e^{\gamma_i^j} \quad (2)$$

and

$$\psi_i^j = IndexClosure_i * (1 - TW_j) * Duration \quad (3)$$

where $IndexClosure_i$ is an index of restrictiveness of government responses ranging from 0 to 100 (see Hale (2020) for a detailed description of the index), where 100 indicates full restrictions. The index is meant to capture the extent of work, school, transportation and public event restrictions in each country. The second term of equation 3, $(1 - TW_j)$ contains a key parameter, namely the degree of *teleworkability* of each occupation. Following Dingel and Neiman (2020) we use the information contained in the Occupational Information Network (O*NET) surveys to construct a measure of feasibility of working from home for each sector. Finally, we account for the average duration of strict quarantine, which to date is a month in the data.⁹

⁸Additional details on the choice of the share of people under quarantine and the data used for the quantitative exercise are provided in section 4.

⁹We refer to strict quarantine as the policy restriction that imposes strict and generalized workplace closures. See Hale (2020) for a detailed time-series of government policy responses to the diffusion of the COVID-19 virus.

Our measure ψ_i^j returns an index of quarantined labor force for each country and sector in our dataset. In fact, it takes into account the extent of the policy restrictions in each country as well as the possibility to work remotely in presence of restrictions for each sector of the economy. Ideally, one would need data on the degree and the duration of the restrictions for each country, region and sector to construct a perfect measure of the quarantine in the counterfactual scenario. However, precise data on the restrictions and duration are only going to be available ex-post; we approximate the quarantine in each country and sector with our measure ψ_i^j that exploits all the information available to date. Finally, it is important to highlight that the modelling of the production barrier shock presented in equation 2 substantially differs from the modelling of a natural disaster. A natural disaster is a geographically localized shock that can lead to the destruction of production plants, to the loss of human lives and to a lock-down of many economic activities in a country or region. These types of shocks affect the rest of the economy and foreign countries through input linkages (see Carvalho et al. (2016)). In our set-up, the shock induced by COVID-19 virus is modeled as a shock to the production cost of both domestic goods and goods for foreign markets. Moreover, the global nature of the shock implies that most countries are simultaneously affected by the shock both directly – through an increase in the production cost of the goods for domestic consumption – and indirectly – through an increase in the cost of intermediates from abroad and through a decrease in demand of goods produced for the foreign markets. Our set-up crucially allows us to quantify both channels and highlights the importance of the direct effect of the shock on domestic production vis a vis the indirect effect coming from the global production linkages.

To conclude, an economic assessment of the COVID-19 shock should take into account the global spread of the disease, the degree of integration among countries through trade in intermediate goods and the heterogeneity in countries' production structure. In the next section we describe the framework used for the analysis and the mechanisms at work.

3 Theoretical Framework

The quantitative model presented in this section follows the theoretical framework of Caliendo and Parro (2015) and we refer to their paper for a more detailed description of the framework and the model solution. We modify the model allowing for the role of a policy intervention that leads to a production barrier of the form described in section 2. There are N countries, indexed by i and n , and J sectors, indexed by j and k . Sectors are either tradable or non-

tradable and labor is the only factor of production. Labor is mobile across sectors and not mobile across countries and all markets are perfectly competitive.

Households. In each country the representative households maximize utility over final goods consumption C_n , which gives rise to the Cobb-Douglas utility function $u(C_n)$ of sectoral final goods with expenditure shares $\alpha_n^j \in (0, 1)$ and $\sum_j \alpha_n^j = 1$.

$$u(C_n) = \prod_{j=1}^J C_n^{\alpha_n^j} \quad (4)$$

Income I_n is generated through wages w_n and lump-sum transfers (i.e. tariffs).

Intermediate Goods. A continuum of intermediates can be used for production of each ω^j and producers differ in the efficiency $z_n^j(\omega^j)$ to produce output. The production technology of a good ω^j is

$$q_n^j(\omega^j) = z_n^j(\omega^j) [l_n^j(\omega^j)]^{\gamma_n^j} \prod_{k=1}^J [m_n^{k,j}(\omega^j)]^{\gamma_n^{k,j}},$$

with labor $l_n^j(\omega^j)$ and composite intermediate goods $m_n^{k,j}(\omega^j)$ from sector k used in the production of the intermediate good ω^j . $\gamma_n^{k,j} \geq 0$ are the share of materials from sector k used in the production of the intermediate good ω^j . The intermediate goods shares $\sum_{k=1}^J \gamma_n^{k,j} = 1 - \gamma_n^j$ and $\gamma_n^j \geq 0$, which is the share of value added vary across sectors and countries.

Due to constant returns to scale and perfect competition, firms price at unit costs,

$$c_n^j = Y_j w_n^{\gamma_n^j} \prod_{k=1}^J p_n^{k,j \gamma_n^{k,j}}, \quad (5)$$

with the constant Y_j , and the price of a composite intermediate good from sector k , $p_n^{k,j \gamma_n^{k,j}}$.

Production Barriers and Trade Costs. Trade can be costly due to tariffs τ_{in}^j and non-tariff barriers d_{ni}^j (i.e. FTA, bureaucratic hurdles, requirements for standards, or other discriminatory measures). Combined, they can be represented as trade costs κ_{ni}^j when selling a product of sector j from country i to n

$$\kappa_{in}^j = \underbrace{(1 + t_{in}^j)}_{\tau_{in}^j} \underbrace{D_{in}^{\rho_j} e^{\delta^j Z_{in}}}_{d_{ni}^j} \quad (6)$$

where $t_{in}^j \geq 0$ denotes ad-valorem tariffs, D_{in} is bilateral distance, and \mathbf{Z}_{in} is a vector collecting trade cost shifters.¹⁰

Additionally, intermediate and final goods are now subject to barriers arising from domestic policy interventions, v_i^j that can potentially deter production. As described in section 2, COVID-19 is modeled as a barrier to production in the affected areas. The key difference when compared to trade costs is that the latter one only directly affects tradable goods, while production barriers can also directly affect non-tradable goods.

Under perfect competition and constant returns to scale, an intermediate or final product (trade and non-tradable) is provided at unit prices, which are subject to v_i^j , κ_{ni}^j and depend on the efficiency parameter $z_i^j(\omega^j)$.

Producers of sectoral composites in country n search for the supplier with the lowest cost such that

$$p_n^j(\omega^j) = \min_i \left\{ \frac{c_i^j \kappa_{ni}^j v_i^j}{z_i^j(\omega^j)} \right\}. \quad (7)$$

Note that v_i is independent of the destination country and thus will also have effects on non-tradeable and domestic sales. In the non-tradeable sector, with $\kappa_{in}^j = \infty$, the price of an intermediate good is $p_n^j(\omega^j) = c_n^j v_n^j / z_i^j(\omega^j)$.

Composite intermediate product price. The price for a composite intermediate good is given by

$$P_n^j = A^j \left(\sum_{i=1}^N \lambda_i^j (c_i^j \kappa_{in}^j v_i^j)^{\frac{-1}{\theta^j}} \right)^{-\theta^j} \quad (8)$$

where $A^j = \Gamma [1 + \theta^j(1 - \eta^j)]^{\frac{1}{1-\eta^j}}$ is a constant. Following Eaton and Kortum (2002b), Ricardian motives to trade are introduced in the model and allow productivity to differ by country and sector.¹¹ Productivity of intermediate goods producers follows a Fréchet distribution with a location parameter $\lambda_n^j \geq 0$ that varies by country and sector (a measure of absolute advantage) and shape parameter θ^j that varies by sector and captures comparative advantage.¹² Equation 8 also provides the price index of non-tradable goods and goods confronted with production barriers, which can affect tradable and non-tradable goods. For non-tradable goods the price index is given by $P_n^j = A^j \lambda_n^{j-1/\theta^j} c_n^j v_n^j$.

¹⁰Iceberg type trade cost in the formulation of Samuelson (1954) are captured by the term \mathbf{Z}_{in}

¹¹see Caliendo and Parro (2015) for more details.

¹²Convergence requires $1 + \theta^j > \eta^j$.

Firm's output price. Due to the interrelation of the sectors across countries, the existence of production barriers v_i^j has also an indirect effect on the other sectors across countries. A firm in country i can supply its output at price,¹³

$$p_{in}^j(\omega^j) = v_i^j \kappa_{in}^j \frac{c_i^j}{z_i^j(\omega^j)} \quad (9)$$

Consumption prices. Under Cobb-Douglas preferences, the consumers can purchase goods at the consumption prices P_n , which are also dependent on production barriers v_i^j . In fact, with perfect competition and constant-returns to scale, an increase in the costs of production of final goods will directly translate into an increase in consumption prices.

$$P_n = \prod_{j=1}^J (P_n^j / a_n^j)^{d_n^j} \quad (10)$$

Expenditure Shares. The total expenditure on goods of sector j from country n is given by $X_n^j = P_n^j Q_n^j$. Country n 's share of expenditure on goods from i is given by $\pi_{ni}^j = X_{ni}^j / X_n^j$, which gives rise to the structural gravity equation.

$$\pi_{in}^j = \frac{\lambda_i^j [c_i^j \kappa_{in}^j v_i^j]^{\frac{-1}{\theta^j}}}{\sum_{i=1}^N \lambda_i^j [c_i^j \kappa_{in}^j v_i^j]^{\frac{-1}{\theta^j}}} \quad (11)$$

The bilateral trade shares are affected by the production barriers v_i^j both directly and indirectly through the input bundle c_i^j from equation 3, which contains all information from the IO-tables.

Total expenditure and Trade Balance. The value of gross production Y_i^j of varieties in sector j has to equal the demand for sectoral varieties from all countries $i = 1, \dots, N$ and hence the total expenditure is the sum of expenditure on composite intermediates and the expenditure of the households.

¹³ c_i^j is the minimum cost of an input bundle (see equation 6), where Y_i^j is a constant, w_i is the wage rate in country i , p_i^k is the price of a composite intermediate good from sector k , which can be affected by production barriers. $\gamma_i^j \geq 0$ is the value added share in sector j in country i , the same parameter we use in equations 2 and 1 when defining the shock v_i^j . $\gamma_i^{k,j}$ denotes the cost share of source sector k in sector j 's intermediate costs, with $\sum_{k=1}^J \gamma_i^{k,j} = 1$.

The goods market clearing condition is given by

$$X_n^j = \sum_{k=1}^J \gamma_n^{j,k} \sum_{i=1}^N X_i^k \frac{\pi_{in}^k}{(1 + \tau_{in}^k)} + \alpha_i^j I_i \quad (12)$$

where national income consists of labor income, tariff rebates R_i and the (exogenous) trade surplus S_i , i.e. $I_i = w_i L_i + R_i - S_i$. X_i^j is country i 's expenditure on sector j goods and $M_n^j = \frac{\pi_{ni}^j}{(1 + \tau_{ni}^j)} X_i^j$ are country n 's imports of sector j good from country i . Thus, the first part on the right-hand side gives demand of sectors k in all countries i for intermediate usage of sector j varieties produced in country n , the second term denotes final demand. Tariff rebates are $R_i = \sum_{j=1}^J X_i^j \left(1 - \sum_{n=1}^N \frac{\pi_{ni}^j}{(1 + \tau_{ni}^j)}\right)$.

The second equilibrium condition requires that, for each country n the value of total imports, domestic demand and the trade surplus has to equal the value of total exports including domestic sales, which is equivalent to total output Y_n :

$$\sum_{j=1}^J \sum_{i=1}^N \frac{\pi_{ni}^j}{(1 + \tau_{ni}^j)} X_n^j + S_n = \sum_{j=1}^J \sum_{i=1}^N \frac{\pi_{in}^j}{(1 + \tau_{in}^j)} X_i^j = \sum_{j=1}^J Y_n^j \equiv Y_n \quad (13)$$

Substituting equation 12 into 13 further implies that the labor market is clear.

Equilibrium in relative changes. We solve for changes in prices and wages after changing the production barriers v to v' . This gives us an equilibrium in relative changes and follows Dekle et al. (2008).

We solve for counterfactual changes in all variables of interest using the following system of equations:

$$\hat{c}_n^j = \hat{w}_n^{j,l} \prod_{k=1}^J P_n^{k,j} \gamma_n^{k,j} \quad (14)$$

$$\hat{p}_n^j = \left(\sum_{i=1}^N \pi_{in}^j [\hat{\kappa}_{in}^j \hat{c}_i^j]^{-1/\theta^j} \right)^{-\theta^j} \quad (15)$$

$$\hat{\pi}_{in}^j = \left(\frac{\hat{c}_i^j}{\hat{p}_n^j} \hat{\kappa}_{in}^j \hat{c}_i^j \right)^{-1/\theta^j} \quad (16)$$

$$X_n^{j'} = \sum_{k=1}^J \gamma_n^{j',k} \sum_{i=1}^N X_i^k \frac{\pi_{in}^{k'}}{(1 + \tau_{in}^{k'})} + \alpha_i^j I_i' \quad (17)$$

$$\frac{1}{B} \sum_{j=1}^J F_n^{j'} X_n^{j'} + s_n = \frac{1}{B} \sum_{j=1}^J \sum_{i=1}^N \frac{\pi_{ni}^{j'}}{1 + \tau_{ni}^{j'}} X_i^{j'} \quad (18)$$

where \hat{w}_n are wage changes, X_n^j are sectoral expenditure levels, $F_n^j \equiv \sum_{i=1}^N \frac{\pi_{ij}^{in}}{(1+t_{in}^j)}$, $I_n' = \hat{w}_n w_n L_n + \sum_{j=1}^J X_n^{j'}(1 - F_n^{j'}) - S_n$, L_n denotes country n 's labor force, and S_n is the (exogenously given) trade surplus. We fix $s_n \equiv S_n/B$, where $B \equiv \sum_n w_n L_n$ is global labor income, to make sure that the system is homogenous of degree zero in prices. The shift in unit costs due to changes in input prices (i.e., wage and intermediate price changes) is laid out in equation (14).

Changes in production barriers \hat{v}_i^j directly affect the sectoral price index p_n^j , and thus translate into changes of the unit costs (see equation 15). The trade shares in equation 16 respond to change in the production costs, unit costs, and prices. The productivity dispersion parameter θ^j governs the intensity of the reaction. Equation 17 ensures goods market clearing in the new equilibrium and the balanced trade condition is given by equation 18.

Solving the model in relative changes allows abstracting from the estimation of some structural parameters of the model, such as total factor productivity or trade costs.¹⁴ In the next sections we describe the data and the set of parameters we use to calibrate the baseline economy as well as the data used to construct the production shock \hat{v}_i^j . Moreover, we provide a description of the counterfactuals exercises we perform together with results.

4 Quantifying the effects of COVID-19

In this section we evaluate the welfare effects from the increase in the production barrier caused by the spread of COVID-19. We use data from different sources to calibrate the model to our base year. To provide a realistic picture of the effect of COVID-19, we maximize the number of countries covered in our sample conditional on having reliable information on tariffs, production and trade flows. Our quantification exercise requires a large number of data, which we gather combining different sources.¹⁵

First, we use the World Input-Output Database (WIOD). It contains information on sectoral production, value added, bilateral trade in final and intermediate goods by sector for 43 countries and a constructed rest of the world (ROW). WIOD allows us to extract bilat-

¹⁴We refer the reader to Caliendo and Parro (2015) for a complete explanation of the hat algebra. Intuitively, the solution method mimics the difference in difference set-up, hence allows to abstract from data on parameters that do not change in response to the shock.

¹⁵A more detailed description of the different data sources can be found in Appendix A.

eral input-output tables and expenditure levels for 56 sectors, which we aggregate into 50 industries. This aggregation concerns mostly services; we keep the sectoral detail in the manufacturing and agricultural industries. Data on bilateral preferential and MFN tariffs stem from the World Integrated Trade Solutions (WITS-TRAINS) and the WTO's Integrated Database (IDB).

Second, a crucial element for the quantification exercise is to measure the intensity of the COVID-19 shock across countries as detailed in equations 1 and 2. For this end, we use information on the number of corona cases ($cases_{it}$) in each country and region from multiple sources. We use the database from the Johns Hopkins Coronavirus Resource Center¹⁶ and we combine it with information from national statistical offices for Italy, Germany, Spain and Portugal. This procedure returns the number of official COVID-19 cases as of April 16th in each of the 43 countries of our dataset, with regional disaggregation for the US, Italy, China, Germany, Spain and Portugal.¹⁷

Third, our measure of the shock as detailed in equations 1 and 2 requires information on employment by country-region and sector. This data is crucial to account for the geographical distribution of sectors across each country as well as for the COVID-19 shares over employment in a country-region. We combine different sources: for the EU, we use the information contained in Eurostat, while for the US we use IPUMSeps to construct employment by state(region) and sector of activity.¹⁸ The construction of employment by sector and province in China required two different data sources: first, we use the information from the National Bureau of Statistic of China for the year 2018 on employment by region and sector¹⁹. However, the information for manufacturing and services provided by the National Bureau of Statistic of China is not disaggregated into sub-sectors. We complement this information with the employment shares by region and sector from the 2000 census to retrieve the employment level of manufacturing and services²⁰. This procedure returns employment shares by region and sector for 50 sectors and each province in China in 2018.²¹

¹⁶For further details, visit the following website: <https://coronavirus.jhu.edu/>

¹⁷We collect regional information on COVID-19 official cases for all the countries that provide it at the date of writing the paper.

¹⁸More information on the construction of the employment matrices is detailed in the appendix.

¹⁹See <http://www.stats.gov.cn/english/> for a general overview of the data collected by the NBSC, and <http://data.stats.gov.cn/english/> for employment data at regional level.

²⁰We thank Matilde Bombardini for kindly providing us the employment shares by region and industry from the 2000 Chinese Census used in the paper Bombardini and Li (2016). More details on the construction of the region-sector employment shares for China is provided in the appendix.

²¹Data on employment at sector-region level are not available for some countries in our sample, and we

Fourth, constructing the quarantine index ψ_i^j requires information on the degree of restriction for each country ($IndexClosure_i$), on the degree of *teleworkability* of each occupation and on the duration of the strict quarantine. We use the index on government responses to the COVID-19 diffusion of the University of Oxford (<https://www.bsg.ox.ac.uk/research/research-projects/coronavirus-government-response-tracker>), where $IndexClosure_i$ is an index of restrictiveness of government responses ranging from 0 to 100 (see Hale (2020) for a detailed description of the index), where 100 indicates full restrictions. The index is meant to capture the extent of work, school, transportation and public event restrictions in each country. Moreover, we follow Dingel and Neiman (2020) and construct a measure of the degree of *teleworkability* of each occupation. We use the information contained in the Occupational Information Network (O*NET) surveys to construct a measure of feasibility of working from home for each sector.²² Finally, using the information contained in the dataset on government responses to the COVID-19 from the University of Oxford, we account for the average duration of strict quarantine, which we estimate to be of one month. We refer to strict quarantine as the policy restriction that imposes strict and generalized workplace closures.²³

We use this extensive set of data to construct our measure for the COVID-19 shock and to instruct the model to perform counterfactual analysis. As described in section 3, we follow Dekle et al. (2008) and Caliendo and Parro (2015) and solve the model in relative changes to identify the welfare effect of the COVID-19 shock. We perform three different exercises: (i) we include the COVID-19 shock in the model as in equation 1 and we estimate a *snap-shot* scenario based on the actual number of COVID-19 cases in each country (*Shock-1* in the tables and figures), (ii) we include the quarantine shock in the model as in equation 2 and estimate a quarantine scenario, imposing quarantine to a fraction of the labour force in each countries (*Shock-2* in the tables and figures), (iii) we decompose the effect into a direct effect from the production shock induced by the COVID-19 quarantine and an indirect effect

construct a simpler version of equation 1, $v_i^j = \frac{c_i}{\sum_{j=1} l_{ij}} * e^{Y_i^j}$. In this case, the formula does not capture the geographical distribution of sectors in the country, but accounts for the sectoral distribution of employment and for their labor intensity. This is the case for Australia, Brazil, Canada, India, Indonesia, Japan, Korea, Mexico, Russia, Taiwan, RoW.

²²Some *sensitive* sectors of the economy are excluded by each government from the restrictive measures. We account for *sensitive* sectors by increasing the share of employment that can be teleworkable to 0.8 in each of the *sensitive* sectors. The list of sensitive sectors includes (ISIC rev 3 sectoral classification): Agriculture (sector 1), Fishing (sector 3), Electricity and gas (sector 23), Water supply (sector 24), Sewage and Waste (sector 25), Postal and courier (sector 34), Human health and social work (sector 49).

²³See Hale (2020) for a detailed time-series of government policy responses to the diffusion of the COVID-19 virus.

coming from the global shock affecting the other countries. We perform the three exercises both in an open economy with the actual tariff and trade cost levels and in a closer economy, where we increase the trade costs by 100 percentage points in each sector-country.

4.1 Open economy

In this section, we present the results of the change in welfare, sectoral value added and trade for each country in our sample for both, the *snap-shot* and the quarantine scenario. The formula for the welfare change is

$$\hat{W}_n = \frac{\hat{I}_n}{\prod_{j=1}^J (\hat{p}_n^j)^{\alpha_n^j}}$$

where \hat{W}_n is the change in welfare of country n , \hat{I}_n is the change in nominal income of country n and $\prod_{j=1}^J (\hat{p}_n^j)^{\alpha_n^j}$ is the change in the price index for country n in each sector j . The aggregated welfare results of the *snap-shot* and the quarantine scenario by country are presented in table 1. In column 2 and 5 we present the real income drops from the *snap-shot* scenario (shock 1), assuming no quarantine for any country in the world.²⁴ In this case, we find real income drops up to almost 2.9% for Spain, with heterogeneous effects depending mainly on the actual COVID-19 cases in each country of our sample. In figure 1 we present graphical evidence on the relation between corona cases and the change in real income across countries in log changes.²⁵

In the quarantine scenario (shock 2) in the open economy in table 1 (columns 3 and 6), we include quarantine as presented in equation 2. Countries have heterogeneous *treatments* depending on the restrictiveness of the policy measures, on the share of workforce employed in each sector of the economy and on the degree of *teleworkability* of each sector. Results in table 1 show that most countries with quarantined labor force experience a drop in real income above 10%, with the only exception of Sweden. Indeed, Sweden did not implement any coercive and generalized restriction to the workforce, unless infected with the COVID-19 virus disease. In tables 2, we further investigate the sectoral distribution of the economic impact of the COVID-19 shock. We find that the drop in the value added (in billion US

²⁴It is important to highlight that this scenario would however imply a tremendous cost in terms of human lives that our model does not account for.

²⁵The size of shock 1 across all countries is shown in Appendix A in figure A4 and zooms into the EU member states in figure A6a.

dollars) is widespread across all sectors, but it is especially pronounced for services, intermediate resource manufacturing and wholesale and retail trade across all countries and both in the *snap-shot* scenario (*Shock-1*) as well as in the quarantine scenario (*Shock-2*). In absolute terms, the strongest drops in value added are experienced in the services sectors, which include services, such as accommodation and food, real estate, and also public services.²⁶ In relative terms, the drops in sectoral value added are the highest in the sectors of textiles and electrical equipment for Italy, pharmaceuticals and motor vehicles for Germany, manufacturing and machinery equipment for the US and textiles and electrical equipment for China (see table A2 in the Appendix).

The impact of the COVID-19 shock on countries' trade is presented in tables 3 and 4. For the case of Italy, we observe a severe decline in exports in billion US Dollars in intermediate resource manufacturing, machinery equipment and textiles. Germany faces a decrease in exports especially marked in the motor vehicle industry, as well as in the intermediate resource manufacturing sector and machinery and equipment. The US has a severe drop in exports in the service sector, followed by the intermediate resource manufacturing and wholesale trade while China experiences the biggest drop in exports in the sectors of electrical equipment, intermediate resource manufacturing and textiles.

All results in tables 2, 3 and 4 present a clear picture of the structure of comparative advantages of each economy, highlighting the importance of accounting for sectoral production linkages and inter-sectoral trade when studying the economic impact of a global shock. Moreover, these results suggest that the production structure of each economy, as well as their centrality in the global value chains might have heterogeneous roles in explaining the size of the observed income drops across the countries.

Decomposition of the Effects

What is the share of the real income drop due to COVID-19 shock that comes from the disruption of production in each country? What is the share that comes from a decrease in trade through global production networks? To decompose the real income changes observed in table 1 we use the structural model and perform a counterfactual exercise in which we shock each country individually. This allows us to isolate the direct production effect of the COVID-19 shock on each country from the indirect effect that each other country experience

²⁶Table 2 provides the results for selected countries and regions and aggregated sectors. See table A3 for the aggregation of the 50 WIOD-sectors. All results for the sectoral value added changes for each of the sectors in all countries can be retrieved from the authors.

through the global production network. We perform the following decomposition:

$$\forall i \neq j : \hat{W}_i = \underbrace{\left(\hat{W}_i^D(v_i) \right)}_{\text{Direct}} + \underbrace{\left(\sum_{j=1}^J \hat{W}_i^I(v_j) \right)}_{\text{Indirect}} \times \underbrace{\left(1 - \hat{W}_i(v_{ALL}) \right)}_{\text{Global}} \quad (19)$$

where $\hat{W}_i^D(v_i)$ is the direct (*D*) change in real income of country *i* when only country *i* is hit by the COVID-19 shock (v_i), $\sum_{j=1}^J \hat{W}_i^I(v_j)$ is the sum of the indirect (*I*) real income changes in country *i* when any other country *j* is treated with the COVID-19 shocks (v_j), $\hat{W}_i(v_{ALL})$ is the total change in real income of country *i* when all countries are affected by the COVID-19 shock (v_{ALL}), and \hat{W}_i is the sum of the three different components from the decomposition. We perform the decomposition with both *Shock-1* and *Shock-2*.

Suppose, for example, that Germany is the only country hit by the COVID-19 virus disease; in this case, the real income of Germany would drop because of the disruption in production that the COVID-19 shock provokes to the German economy, what we call the *direct* effect in our decomposition. Suppose now that Italy is the only country affected by the COVID-19 shock. In this case, we would observe a drop in real income for Germany as well, which is driven by the decrease in trade between Germany and Italy, as well as by the increase in the cost of intermediates that Germany buys from Italy. This is what we call the *indirect* effect. Summing over the *indirect* effects for Germany will provide us the total *indirect* effect, namely the drop in real income that Germany faces when each other country is shocked individually.

The third term of our decomposition is the difference between the sum of the direct and the indirect effects for Germany from the decomposition and the drop in real income observed for Germany in the counterfactual exercise in which we shock all the countries at same time. We call this component the *global* adjustment. Indeed, when we shock all the countries with quarantine at the same time, the observed income drop differs from the sum of the direct and the indirect effect from the decomposition. This points to the importance of using a GE framework with input-output linkages and trade when studying the effect of a global shock to local economies. In fact, when shocked all together, each country keeps the relative importance in the world trade networks, hence the structure of comparative advantages remains the same and the total effect of the shock is smaller for each of them. On the contrary, when only one country is hit by the COVID-19 shock, that country faces an increase in the production costs of the goods produced for the domestic and for the foreign markets and loses its role in the global production networks, thus experiencing an additional

drop in income.

Figures 2 and 3 present a graphical representation of each part of the decomposition for the *snap-shot* scenario (*Shock-1*) as well as for the quarantine scenario (*Shock-2*). Figure 2 and table 5 present the results for the *snap-shot* scenario (*Shock-1*): we observe a marked heterogeneity both in the total size of the income drop, but also in the share of each component of the decomposition. Without quarantine, the total income drop would be between 3% (Spain) and 0.1% (India). Moreover, the share of the total shock that is accounted for by the *indirect* effect varies substantially across countries, accounting for the biggest shares in countries that have a smaller number of COVID-19 cases, thus experiencing a smaller *direct* effect due to disruption in production.

Figure 3 and table 6 show the results of the decomposition for the quarantine scenario (*Shock-2*). In this case, each country is hit by a shock that accounts for the restrictiveness of the policy implemented as explained in section 2. It is straightforward to notice the heterogeneity in the relative importance of the *direct* as well as the *indirect* components of the shock across countries. Moreover, the share of the total drop in real income accounted for by the *indirect* effect is systematically higher for European countries than for the other countries in our sample, with the exceptions of Korea and Taiwan. To better understand the heterogeneities observed in figure 3 and table 6, we construct a simple measure of trade openness as the sum of imports and exports over total income of the country ($\frac{X_i + M_i}{I_i}$). Using the data from the baseline economy and the results of counterfactual economy, we investigate if our measure of openness is correlated with a higher *indirect* effect. We estimate the following model:

$$\sum_{j=1}^J \hat{W}_i^I(v_j) = \beta_0 + \beta_1 \frac{X_i + M_i}{I_i} + \beta_2 \hat{W}_i + \beta_3 HHI_M + \beta_4 HHI_output + I_i + \epsilon_i \quad (20)$$

where $HHI_M = \sum_{n=1}^N \left(\frac{M_{ni}}{\sum_{n=1}^N M_{ni}} \right)^2 \forall i \neq n$ is an Herfindahl index of diversification in trade partners. The fraction shows the imports of country i , M_{ni} from origin country n , over the sum of all Imports of country i ; the higher the number of trading partners and the more diversified its importing sources are, the lower is the HHI of diversification. $HHI_output = \sum_{j=1}^J \left(\frac{output_i^j}{\sum_{j=1}^J output_i^j} \right)^2 \forall i \neq n$ is an index of specialization in production. The fraction within the brackets presents the output in sector j , in country i , over the total output of country i . The higher the HHI of specialization, the lower is the degree of specialization in the country.²⁷

²⁷Similarly, we construct an index of diversification of exports. Results using the index of diversification of exports are similar to the ones using the diversification in imports.

Table 7 presents the results of this exercise for *quarantine* scenario (Shock-2). Indeed, countries with a higher degree of trade openness experience a bigger *indirect* effect (columns 1 to 3 in table 7). This simple exercise confirms that openness is correlated with a higher global production network shock. In fact, countries that rely more on international partners both for intermediate supplies as well as for exporting their goods, experience a higher *indirect* shock. Looking at the degree of specialization in production ($\log(\text{specialization})$), we find that a higher degree of specialization is correlated with a bigger indirect effect of the shock.²⁸ Countries that specialize their production leverage more on their comparative advantages. At the same time, a higher degree of specialization implies a higher dependence on other countries both for the intermediaries as well as for exporting the final goods, but crucially it also implies a higher dependence on trading partners to buy all other goods that are not produced at home.

In columns 4 to 6 of table 7, we show the regressions where the dependent variable is the $\log(|\text{direct}|)$. First, both the degree of openness as well as the degree of specialization in production play a smaller role. The direct effect is mainly driven by the direct production shock that each country experiences due to the policy intervention of the quarantine. In this case, openness smooths the direct effect of the COVID-19 shock, allowing countries to source intermediates or consumption goods when home production is disrupted. On the other hand, a higher degree of specialization in production is correlated with a smaller direct effect. In this case, a higher degree of specialization implies that countries have a higher comparative advantage in a specific sector, hence a lower price compared to their competitors. In our model, the COVID-19 shock is a production barrier that imposes quarantine to a share of the labor force and increases the production cost of the goods produced in each country, proportionally to the share of employment in each sector of activity. An increase in the production cost in a sector will prove to be less severe in a country that has a higher comparative advantage in that specific sector.

It is important to clarify that this exercise compares countries with different degrees of openness conditional on receiving the same drop in real income. However, it does not allow us to answer the following counterfactual question: "what would have happened if the world was less integrated? Would the total drop in real income due to the COVID-19 be smaller in a less integrated world? In the next section, we leverage on our model to answer these questions.

²⁸Note the dependent variable in the regression is $\log(|\text{indirect}|)$ and the HHI index for specialization in production is higher for less specialized countries, while it is lower for more specialized countries. The same applies for the HHI index of diversification in trade partners.

4.2 Less Integrated World

In this section we quantify the real income effect of the COVID-19 shock in a less integrated world scenario, where we increase the trade costs in each country and sector by a 100 percentage points. First and unsurprisingly, a less integrated world itself implies enormous income losses for all countries in our sample. Tables 8 and 9 show the real income changes for all countries in the sample for *shock-1* and *shock-2* in a less integrated world. In both tables, column 2 and 7 present the real income losses stemming from the increase in trade costs by a 100 percentage points. Column 3 and 8 show the real income changes stemming from the COVID-19 shocks in a less integrated economy, while columns 4 and 9 present the welfare effects due to the COVID-19 shocks in the open economy (as in table 1). Finally, columns 5 and 10 (Δ Shock 1 and Δ Shock2) present the difference between the real income drop due to the COVID-19 shocks in a less integrated vs. open economy.

The COVID-19 shock is smaller for all countries in the less integrated economy than in the open economy under both shocks. Indeed, in a less integrated world countries experience an enormous reduction in real income due to the increase in trade costs, hence the additional effect of the global pandemic shock plays a relatively smaller role. Indeed, in tables 10 and 11, we present the results of the decomposition from equation 19 in a less integrated world. Interestingly, when raising trade costs in all countries, the *indirect* component is lower than in the open economy, but it still accounts for a relevant share of the drop in income due to the COVID-19 shock. In our counterfactual exercise, the increase in trade cost mimics a world with higher trade barriers, but not a complete autarky scenario; countries would still trade, use intermediates from abroad and sell final goods in foreign countries.

This finding highlights the importance of inter-sectoral linkages in the transmission of the shock: a higher degree of integration in the global production network implies that a shock in one country directly diffuses through the trade linkages to other countries. Trade has two different effects in our model: on the one hand, it smooths the effect of the shock by allowing consumers to purchase and consume goods they wouldn't otherwise be able to consume in a world with production barriers in quarantine. On the other hand, the COVID-19 shock increases production costs of intermediate inputs that are used at home and abroad. Our counterfactual exercise clearly shows that an increase in trade costs would not significantly decrease the impact of the COVID-19 shock across countries. However, increasing trade barriers implies an additional drop in real income between 14% and 33% across countries.

5 Conclusions

This study uses a general equilibrium framework to evaluate the economic impact of the COVID-19 shock. We model the COVID-19 shock as a production barrier that deters production for home consumption and for exports through a temporary drop in the labor units available in each country. The spread of COVID-19 disease provides a unique set-up to understand and study the diffusion of a global production shock along the global value chains. However, understanding the effects of a global production disruption induced by a pandemic is complex. In this paper, the modelling choice of the shock accounts for the geography of the diffusion of the COVID-19 shock across regions and countries, the geographical distribution of sectors in each country and the labour intensity of each sector of production to return a reliable measure of the impact of the COVID-19 disease as a production barrier. Crucially, in a model with interrelated sectors the cost of the input bundle depends on wages and on the price of all the composite intermediate goods in the economy, both non-tradable and tradable. In our framework, the COVID-19 shock has a direct effect on the cost of each input as well as an indirect effect via the sectoral linkages.

We perform three different exercises: (i) we include the COVID-19 shock in the model and we estimate a *snap-shot* scenario based on the actual number of COVID-19 cases in each country, (ii) we include the quarantine shock and estimate a quarantine scenario, imposing quarantine to a fraction of the labour force in each countries, (iii) we decompose the effect into a direct effect from the production shock induced by the COVID-19 quarantine and an indirect effect coming from the global shock affecting the other countries. We perform the three exercises both in an open economy with the actual tariff and trade cost levels and in a closer economy, where we increase the trade costs by 100 percentage points in each sector-country. The quantitative exercise requires data on bilateral trade flows, production, tariffs, sectoral trade elasticities, employment shares by sector and region and the number of COVID-19 cases in each region or country. We calibrate a 44 countries 50 sector economy and incorporate the COVID-19 shock to evaluate the welfare effects for each country both in aggregate and at the sectoral level.

We show that the shock dramatically reduces real income for all countries in all counterfactual scenarios and that sectoral interrelations and global trade linkages have a crucial role in explaining the transmission of the shock across countries. COVID-19 shock is a pandemic shock, hence it has a contemporaneous effect in many countries and to all sectors of production. We use the model to perform a model-based identification of the effect of COVID-19 shock and provide evidence on the importance of global trade linkages and inter-sectoral

trade when studying the effect of a global shock to production on the welfare of each country. We decompose the COVID-19 total income change into a *direct* component due to the domestic production shock and an *indirect* component due to global linkages. We show that linkages between countries account for a substantial share of the total income drop observed.

Certainly, this model abstracts from many other aspects related to the diffusion of the COVID-19 disease which are the topic of study of epidemiologist, medical doctors and statisticians. Moreover, we do not account for the health consequences of the pandemic itself. We believe that understanding how the COVID-19 virus disease spreads across regions is outside the scope of this paper. In our framework, the spread of COVID-19 disease is modeled an exogenous shock that allows us to study the diffusion of the production disruption along the global value chains and to highlight the importance of modeling and including sectoral interrelations to quantify the economic impact of the COVID-19 shock.

References

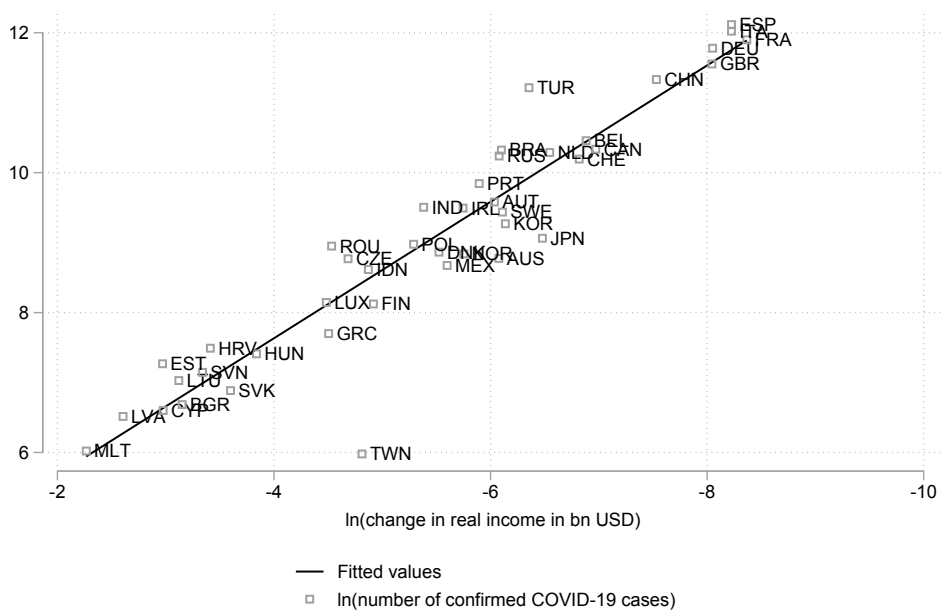
- Alfaro, L., Antràs, P., Chor, D., Conconi, P., 2019. Internalizing global value chains: A firm-level analysis. *Journal of Political Economy* 127 (2), 509–559.
URL <https://www.journals.uchicago.edu/doi/10.1086/700935>
- Altomonte, C, F. D. M. G. O. A. R., Vicard, V., 2012. Global value chains during the great trade collapse: a bullwhip effect? *Firms in the international economy: Firm heterogeneity meets international business*.
- Antràs, P., Forthcoming. Conceptual aspects of global value chains. *World Bank Economic Review*.
- Antràs, P., Chor, D., 2013. Organizing the global value chain. *Econometrica* 81 (6), 2127–2204, from March 2013.
URL <http://onlinelibrary.wiley.com/doi/10.3982/ECTA10813/abstract>
- Antràs, P., Chor, D., 2018. On the Measurement of Upstreamness and Downstreamness in Global Value Chains. *Taylor & Francis Group*, pp. 126–194.
- Antràs, P., de Gortari, A., Forthcoming. On the geography of global value chains.
- Arkolakis, C., Costinot, A., Rodríguez-Clare, A., February 2012. New trade models, same old gains? *American Economic Review* 102 (1), 94–130.
URL <http://www.aeaweb.org/articles?id=10.1257/aer.102.1.94>
- Atkeson, A., March 2020. What will be the economic impact of covid-19 in the us? rough estimates of disease scenarios. Working Paper 26867, National Bureau of Economic Research.
URL <http://www.nber.org/papers/w26867>
- Barrot, J.-N., Sauvagnat, J., 05 2016. Input Specificity and the Propagation of Idiosyncratic Shocks in Production Networks *. *The Quarterly Journal of Economics* 131 (3), 1543–1592.
URL <https://doi.org/10.1093/qje/qjw018>
- Bénassy-Quéré, A, Y. D. L. F., Khoudour-Casteras, D., 2009. Economic crisis and global supply chains. *Mimeo*.
- Berger, D., H. K. M. S., 2020. An seir infectious disease model with testing and conditional quarantine. *Mimeo*.
- Boehm, C. E., Flaaen, A., Pandalai-Nayar, N., 2019. Input linkages and the transmission of shocks: Firm-level evidence from the 2011 tōhoku earthquake. *The Review of Economics and Statistics* 101 (1), 60–75.
- Bombardini, M., Li, B., November 2016. Trade, pollution and mortality in china. Working Paper 22804, National Bureau of Economic Research.
URL <http://www.nber.org/papers/w22804>

- Caliendo, L., Parro, F., 2015. Estimates of the Trade and Welfare Effects of NAFTA. *Review of Economic Studies* 82 (1), 1–44.
- Carvalho, V., Nirei, M., Saito, Y., Tahbaz-Salehi, A., 2016. Supply chain disruptions: Evidence from the great east japan earthquake. Mimeo.
- Dekle, R., Eaton, J., Kortum, S., 2008. Global rebalancing with gravity: Measuring the burden of adjustment. *IMF Economic Review* 55 (3), 511–540.
- Dingel, J. I., Neiman, B., 2020. How many jobs can be done at home? Mimeo.
- Eaton, J., Kortum, S., September 2002a. Technology, Geography, and Trade. *Econometrica* 70 (5), 1741–1779.
- Eaton, J., Kortum, S., 2002b. Technology, geography, and trade. *Econometrica* 70 (5), 1741–1779.
- Eaton, J. S. K. B. N., Romalis, J., 2016. Trade and the global recession. *American Economic Review* 106 (11), 3401–38.
- Eichenbaum, M. S., Rebelo, S., Trabandt, M., March 2020. The macroeconomics of epidemics. Working Paper 26882, National Bureau of Economic Research.
URL <http://www.nber.org/papers/w26882>
- Goldberg, Pinelopi K., A. K. N. P., Topalova, P., 2010. Imported intermediate inputs and domestic product growth: Evidence from india. *Quarterly Journal of Economics* 125 (4), 1727–67.
- Gopinath, G., Neiman, B., 2013. Trade adjustment and productivity in large crises. *American Economic Review* 104 (3), 793–831.
URL <http://dx.doi.org/10.1257/aer.104.3.793>
- Gortari, A. D., 2019. Disentangling global value chains. Mimeo.
- Hale, Thomas, A. P. T. P. S. W., 2020. Variation in government responses to covid-19. Blavatnik School of Government Working Paper.
- Halpern, L., K. M., Szeidl, A., 2015. Imported inputs and productivity. *American Economic Review*.
- Huang, H., 2019. Germs, roads and trade: Theory and evidence on the value of diversification in global sourcing. Mimeo.
- Hummels, D., I. J., Yi, K., 2001. The nature and growth of vertical specialization in world trade. *Journal of International Economics* 54 (1), 75–96.
- Maffioli, E. M., 2020. How is the world responding to the 2019 coronavirus disease compared with the 2014 west african ebola epidemic? the importance of china as a player in the global economy. *The American Journal of Tropical Medicine and Hygiene*.
URL <https://www.ajtmh.org/content/journals/10.4269/ajtmh.20-0135>

- Samuelson, P. A., 1954. The transfer problem and transport costs, ii: Analysis of effects of trade impediments. *The Economic Journal* 64 (254), 264–289.
URL <http://www.jstor.org/stable/2226834>
- Timmer, M., Dietzenbacher, E., Los, B., Stehrer, R., Vries, G., 2015. An Illustrated User Guide to the World Input–Output Database: the Case of Global Automotive Production. *Review of International Economics* 23 (3), 575–605.
- Young, A., 2005. The gift of the dying: The tragedy of aids and the welfare of future african generations. *The Quarterly Journal of Economics* 120 (2), 423–466.
URL <http://www.jstor.org/stable/25098743>

Figures

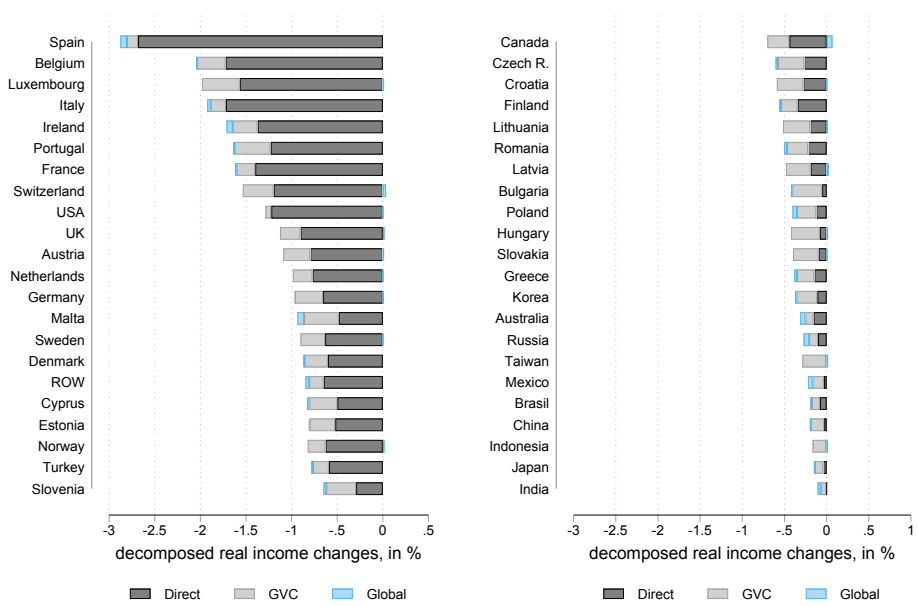
Figure 1: Corona Cases and change in welfare



Note: The figure shows the correlation between the log change in real income across countries over the log number of COVID-19 cases per country.

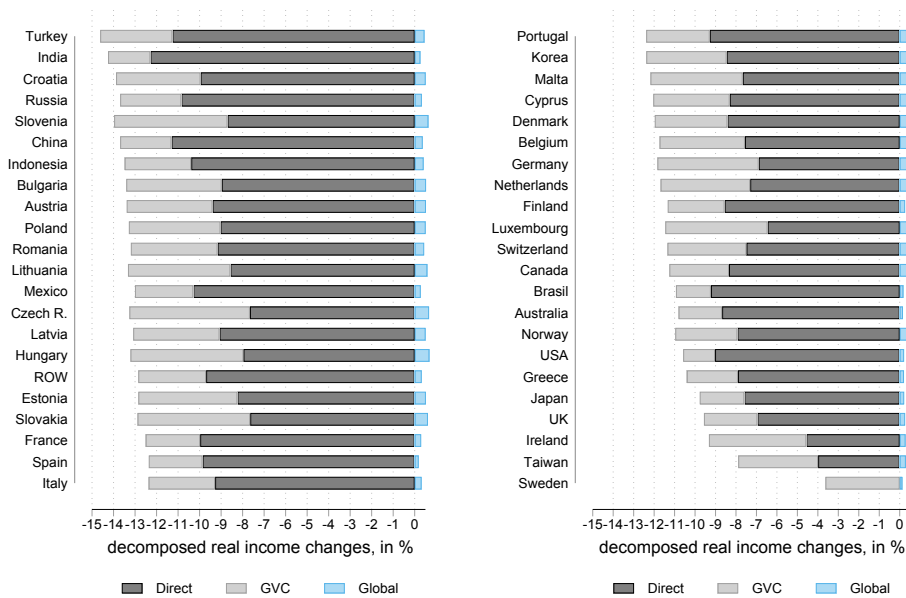
Covid Economics 19, 18 May 2020: 159-210

Figure 2: Decomposition of real income changes - Shock 1 - Open Economy



Covid Economics 19, 18 May 2020: 159-210

Figure 3: Decomposition of real income changes - Shock 2 - Open Economy



Tables

Table 1: Welfare change across countries (in %) - Open Economy

Country	Open Economy		Country	Open Economy	
	(Shock 1) in %	(Shock 2) in %		(Shock 1) in %	(Shock 2) in %
Australia	-0.31	-10.65	India	-0.11	-13.99
Austria	-1.08	-12.87	Indonesia	-0.15	-13.07
Belgium	-2.04	-11.30	Japan	-0.14	-9.55
Brasil	-0.19	-10.76	Luxembourg	-1.97	-10.92
Bulgaria	-0.42	-12.88	Malta	-0.94	-11.82
Canada	-0.63	-10.85	Mexico	-0.22	-12.72
China	-0.19	-13.32	Netherlands	-0.98	-11.19
Croatia	-0.59	-13.37	Norway	-0.81	-10.59
Cyprus	-0.83	-11.65	Poland	-0.40	-12.78
Czech R.	-0.60	-12.59	Portugal	-1.64	-12.03
Denmark	-0.87	-11.54	ROW	-0.85	-12.52
Estonia	-0.81	-12.33	Romania	-0.50	-12.75
Finland	-0.56	-11.07	Russia	-0.27	-13.36
France	-1.62	-12.20	Slovakia	-0.39	-12.27
Germany	-0.96	-11.24	Slovenia	-0.65	-13.34
Greece	-0.38	-10.19	Spain	-2.88	-12.18
Hungary	-0.40	-12.53	Sweden	-0.90	-3.50
Ireland	-1.71	-9.04	Switzerland	-1.50	-10.89
Italy	-1.93	-12.05	Taiwan	-0.27	-7.59
Korea	-0.38	-11.92	Turkey	-0.79	-14.17
Latvia	-0.46	-12.58	UK	-1.11	-9.30
Lithuania	-0.51	-12.74	USA	-1.29	-10.36

Note: The table presents the aggregated real income changes in % for every country. Column 2 and 5 show the real income changes in the snap-shot scenario assuming no quarantine for any country (shock 1) in the open economy. Columns 3 and 6 present the real income changes in % for the quarantine scenario (shock 2) in the open economy. Equation 2 highlights how we included the shock.

Table 2: Change in value added in bn USD - Open Economy

Panel A: Shock 1 - Open Economy						
Sector	Italy bn USD	Germany bn USD	USA bn USD	China bn USD	EU28 bn USD	Rest of World bn USD
Agriculture	-0.85	-0.26	-2.79	-1.50	-3.85	-10.04
Food, Beverages, Tobacco	-0.66	-0.59	-3.08	-0.74	-4.93	-3.10
Mining, Quarrying	-0.17	-0.07	-5.93	-0.87	-1.38	-14.83
Textiles	-0.71	-0.10	-0.33	-0.13	-1.53	-1.23
Electrical Equipment	-0.58	-1.08	-4.23	-0.05	-3.41	-2.49
Machinery, Equipment	-0.99	-1.51	-2.10	-0.69	-5.06	-1.97
Motor Vehicles	-0.22	-1.42	-1.57	-0.58	-2.82	-1.79
Intm. Resources Manufacturing	-2.00	-2.11	-8.01	-1.66	-10.22	-6.67
Manufacturing, nec.	-0.40	-0.47	-2.84	-0.45	-2.54	-1.47
Pharmaceuticals	-0.22	-0.33	-1.21	-0.19	-2.00	-1.00
Chemicals	-0.37	-0.60	-3.52	-0.27	-2.77	-1.34
Electricity, Water, Gas	-1.01	-1.03	-4.12	-0.38	-6.62	-5.94
Construction	-1.89	-1.59	-8.53	-1.33	-12.45	-9.23
Wholesale, Retail Trade	-4.30	-3.25	-27.17	-1.28	-25.47	-18.75
Transport	-2.18	-1.53	-5.81	-0.67	-11.22	-8.22
Accommodation and Food	-1.38	-0.53	-6.26	-0.36	-7.81	-3.07
Real Estate	-5.31	-3.80	-26.49	-1.05	-26.34	-10.58
Public Services	-3.81	-3.90	-37.83	-0.89	-25.37	-12.83
Social Services	-2.45	-2.64	-15.79	-0.36	-17.45	-5.22
Services, nec.	-9.52	-8.57	-55.14	-3.14	-61.37	-30.13
Panel B: Shock 2 - Open Economy						
Sector	Italy bn USD	Germany bn USD	USA bn USD	China bn USD	EU28 bn USD	Rest of World bn USD
Agriculture	-5.18	-2.80	-22.03	-132.75	-31.80	-228.74
Food, Beverages, Tobacco	-4.07	-6.51	-25.11	-55.36	-40.21	-79.95
Mining, Quarrying	-1.00	-0.66	-47.01	-76.51	-12.78	-269.77
Textiles	-3.85	-1.08	-2.98	-35.60	-11.21	-35.28
Electrical Equipment	-3.10	-10.99	-34.56	-61.85	-29.66	-69.01
Machinery, Equipment	-6.90	-17.12	-19.13	-33.98	-47.81	-40.02
Motor Vehicles	-1.80	-17.14	-15.00	-29.62	-30.99	-44.66
Intm. Resources Manufacturing	-12.14	-23.40	-66.55	-138.77	-89.86	-185.15
Manufacturing, nec.	-2.86	-5.76	-25.69	-20.24	-23.62	-33.83
Pharmaceuticals	-1.35	-3.86	-9.99	-10.78	-16.39	-15.97
Chemicals	-1.91	-5.99	-27.53	-30.54	-20.82	-38.87
Electricity, Water, Gas	-6.20	-11.77	-34.00	-32.23	-55.30	-115.63
Construction	-11.78	-18.40	-69.02	-93.81	-103.05	-228.11
Wholesale, Retail Trade	-26.21	-36.11	-218.86	-136.29	-206.58	-466.48
Transport	-13.11	-16.40	-46.44	-61.45	-90.10	-192.99
Accommodation and Food	-8.59	-6.04	-50.55	-26.73	-55.60	-75.05
Real Estate	-32.89	-43.89	-213.44	-78.04	-209.44	-257.97
Public Services	-23.51	-44.49	-305.83	-61.71	-206.75	-329.16
Social Services	-15.23	-31.00	-127.22	-24.96	-142.41	-125.95
Services, nec.	-58.43	-96.33	-444.32	-250.79	-490.24	-680.97

Note: The table presents the sectoral value added changes, in bn USD for selected countries, Italy, Germany, USA, and China. The upper part of the table presents the results for shock 1 in an open economy. The second part presents the results in the case of shock 2 in an open economy. Column 6 reports the value added results for EU28, which are weighted by the initial value added by country. Column 7 shows the value added weighted results for all remaining countries. Further, sectors are aggregated into broader categories (see table A3 in the Appendix).

Table 3: Change of sectoral trade, in bn USD - Shock 1 - Open Economy

Panel A: Shock 1 - Changes of Exports - Open Economy						
Sector	Italy bn USD	Germany bn USD	USA bn USD	China bn USD	EU28 bn USD	Rest of World bn USD
Agriculture	-0.07	-0.15	-0.24	-0.11	-1.40	-2.12
Food, Beverages, Tobacco	-0.16	-0.91	-0.21	-0.54	-3.89	-3.10
Mining, Quarrying	-0.01	-0.10	-0.28	-0.11	-0.97	-10.86
Textiles	-0.37	-0.26	-0.06	-2.74	-1.54	-3.49
Electrical Equipment	-0.34	-1.61	-0.81	-6.59	-4.96	-6.59
Machinery, Equipment	0.21	-1.68	-0.42	-2.53	-3.54	-2.78
Motor Vehicles	0.01	-2.45	-0.26	-0.84	-5.13	-5.95
Intm. Resources Manufacturing	-0.81	-2.71	-1.59	-3.33	-11.08	-10.90
Manufacturing, nec.	0.05	-0.81	-0.93	-2.12	-2.21	-3.50
Pharmaceuticals	-0.07	-0.56	-0.39	-0.30	-2.14	-1.14
Chemicals	-0.31	-1.50	-0.70	-0.72	-5.00	-3.31
Electricity, Water, Gas	-0.04	-0.33	-0.24	-0.05	-1.28	-0.64
Construction	-0.02	-0.03	-0.00	-0.14	-0.59	-0.22
Wholesale, Retail Trade	-0.22	-0.91	-1.75	-1.78	-5.92	-3.83
Transport	-0.14	-0.46	-0.86	-0.88	-4.04	-3.80
Accommodation and Food	-0.00	-0.10	-0.01	-0.09	-0.37	-1.21
Real Estate	-0.02	-0.02	-0.02	0.00	-0.14	-0.07
Public Services	-0.13	-0.18	-0.99	-0.04	-2.64	-2.57
Social Services	-0.01	-0.01	-0.02	-0.01	-0.11	-0.18
Services, nec.	-0.32	-1.46	-3.41	-1.03	-10.22	-5.89
Panel B: Shock 1 - Changes of Imports - Open Economy						
Sector	Italy bn USD	Germany bn USD	USA bn USD	China bn USD	EU28 bn USD	Rest of World bn USD
Agriculture	-0.35	-0.35	-0.74	-0.08	-2.23	-1.00
Food, Beverages, Tobacco	-0.82	-0.58	-1.22	0.11	-5.15	-2.03
Mining, Quarrying	-0.84	-0.52	-3.19	-0.37	-5.25	-3.55
Textiles	-0.75	-0.47	-2.18	0.01	-3.76	-2.40
Electrical Equipment	-0.86	-1.42	-4.77	-0.18	-7.37	-7.05
Machinery, Equipment	-0.76	-0.74	-2.06	0.36	-4.62	-3.14
Motor Vehicles	-0.78	-1.00	-4.17	0.31	-6.00	-2.75
Intm. Resources Manufacturing	-1.94	-2.19	-4.98	-0.11	-13.37	-9.12
Manufacturing, nec.	-0.46	-0.60	-2.06	0.24	-3.94	-3.25
Pharmaceuticals	-0.46	-0.25	-0.68	0.08	-2.61	-0.80
Chemicals	-0.84	-0.95	-1.85	-0.18	-5.48	-2.45
Electricity, Water, Gas	-0.23	-0.20	-0.21	0.00	-1.52	-0.47
Construction	-0.07	-0.10	-0.04	-0.00	-0.56	-0.35
Wholesale, Retail Trade	-0.75	-0.78	-0.88	-0.03	-5.35	-7.02
Transport	-0.50	-0.53	-0.65	-0.04	-4.09	-4.80
Accommodation and Food	-0.09	-0.09	-0.09	-0.01	-0.78	-0.79
Real Estate	-0.02	-0.01	-0.00	-0.00	-0.13	-0.10
Public Services	-0.30	-0.17	-1.56	-0.01	-3.78	-0.89
Social Services	-0.01	-0.01	-0.07	-0.00	-0.14	-0.11
Services, nec.	-0.87	-1.45	-2.23	-0.05	-10.64	-7.63

Note: The table presents the sectoral export and import changes under shock 1 in an open economy. The upper part of the table shows the changes in exports in bn USD for the selected countries and regions, while the lower part of the table shows the sectoral import changes for the same countries and regions under shock 1 in the open economy.

Table 4: Change of sectoral trade, in bn USD - Shock 2 - Open Economy

Panel A: Shock 1 - Changes of Exports - Open Economy						
Sector	Italy bn USD	Germany bn USD	USA bn USD	China bn USD	EU28 bn USD	Rest of World bn USD
Agriculture	-0.87	-1.62	-6.55	-1.61	-14.37	-33.88
Food, Beverages, Tobacco	-3.79	-9.15	-8.83	-5.66	-45.89	-41.28
Mining, Quarrying	-0.17	-1.32	-5.15	-1.47	-11.42	-190.71
Textiles	-6.67	-3.48	-1.58	-33.65	-21.37	-42.29
Electrical Equipment	-4.53	-20.97	-17.58	-85.47	-61.21	-140.49
Machinery, Equipment	-10.79	-29.45	-14.23	-16.91	-72.70	-36.47
Motor Vehicles	-4.29	-38.06	-12.64	-5.50	-80.49	-54.47
Intm. Resources Manufacturing	-13.34	-31.77	-33.45	-36.49	-131.03	-168.76
Manufacturing, nec.	-4.41	-11.66	-20.89	-14.31	-43.06	-40.60
Pharmaceuticals	-2.51	-5.87	-4.98	-1.94	-26.92	-12.53
Chemicals	-3.53	-16.28	-13.89	-11.14	-52.74	-58.57
Electricity, Water, Gas	-0.44	-3.11	-2.44	-0.55	-12.08	-6.02
Construction	-0.29	-0.36	-0.01	-1.74	-6.88	-3.67
Wholesale, Retail Trade	-3.16	-10.54	-25.05	-22.84	-68.81	-53.94
Transport	-2.16	-6.49	-15.29	-10.01	-50.86	-51.04
Accommodation and Food	-0.01	-1.27	-0.20	-1.09	-5.27	-18.56
Real Estate	-0.28	-0.28	-0.33	0.00	-1.61	-0.96
Public Services	-1.33	-1.61	-8.24	-0.43	-23.90	-23.93
Social Services	-0.18	-0.10	-0.24	-0.09	-1.47	-1.98
Services, nec.	-3.77	-17.15	-40.53	-10.47	-116.59	-72.33
Panel B: Shock 2 - Changes of Imports - Open Economy						
Sector	Italy bn USD	Germany bn USD	USA bn USD	China bn USD	EU28 bn USD	Rest of World bn USD
Agriculture	-2.02	-3.87	-5.72	-11.65	-18.55	-23.76
Food, Beverages, Tobacco	-4.36	-6.76	-8.47	-7.92	-41.98	-50.57
Mining, Quarrying	-4.83	-5.60	-24.91	-41.83	-40.43	-104.57
Textiles	-4.03	-5.41	-16.88	-4.79	-29.83	-53.92
Electrical Equipment	-5.09	-15.87	-37.10	-61.14	-68.94	-144.63
Machinery, Equipment	-3.59	-7.85	-12.89	-18.72	-39.44	-71.67
Motor Vehicles	-4.08	-11.08	-27.34	-13.19	-50.92	-66.00
Intm. Resources Manufacturing	-10.81	-24.13	-37.08	-34.67	-116.31	-191.74
Manufacturing, nec.	-2.20	-6.69	-12.50	-13.25	-31.84	-64.76
Pharmaceuticals	-2.63	-3.13	-5.40	-2.73	-21.06	-17.57
Chemicals	-4.85	-10.32	-14.98	-18.43	-46.82	-60.02
Electricity, Water, Gas	-1.27	-2.20	-1.66	-0.62	-11.79	-7.01
Construction	-0.38	-1.15	-0.31	-0.81	-4.72	-6.45
Wholesale, Retail Trade	-4.28	-8.99	-6.86	-7.15	-44.41	-112.22
Transport	-2.82	-5.71	-4.87	-9.71	-33.46	-79.14
Accommodation and Food	-0.50	-0.98	-0.70	-3.36	-6.13	-14.94
Real Estate	-0.14	-0.07	-0.04	-0.02	-1.08	-1.76
Public Services	-1.68	-1.96	-12.05	-1.53	-25.81	-17.11
Social Services	-0.05	-0.10	-0.52	-0.30	-1.05	-1.90
Services, nec.	-4.99	-16.19	-17.42	-15.23	-79.67	-127.60

Note: The table presents the sectoral export and import changes under shock 1 in an open economy. The upper part of the table shows the changes in exports in bn USD for the selected countries and regions, while the lower part of the table shows the sectoral import changes for the same countries and regions under shock 2 in the open economy.

Table 5: Decomposition of real income changes - Shock 1 - Open Economy

Country	Direct Effect in %	GVC Effect in %	GE Effect in %	Country	Direct Effect in %	GVC Effect in %	GE Effect in %
Australia	-0.156	-0.095	-0.062	Korea	-0.110	-0.247	-0.018
Austria	-0.796	-0.296	0.014	Latvia	-0.191	-0.292	0.026
Belgium	-1.724	-0.310	-0.010	Lithuania	-0.195	-0.322	0.009
Brasil	-0.080	-0.094	-0.020	Luxembourg	-1.569	-0.413	0.015
Bulgaria	-0.053	-0.353	-0.015	Malta	-0.483	-0.381	-0.073
Canada	-0.442	-0.261	0.068	Mexico	-0.032	-0.136	-0.055
China	-0.029	-0.161	-0.004	Netherlands	-0.771	-0.215	0.003
Croatia	-0.277	-0.314	0.002	Norway	-0.629	-0.196	0.018
Cyprus	-0.498	-0.306	-0.027	Poland	-0.123	-0.229	-0.052
Czech R.	-0.266	-0.311	-0.027	Portugal	-1.229	-0.396	-0.012
Denmark	-0.602	-0.256	-0.010	ROW	-0.648	-0.160	-0.040
Estonia	-0.522	-0.279	-0.011	Romania	-0.220	-0.250	-0.033
Finland	-0.345	-0.193	-0.023	Russia	-0.102	-0.104	-0.065
France	-1.398	-0.206	-0.014	Slovakia	-0.096	-0.303	0.006
Germany	-0.654	-0.311	0.005	Slovenia	-0.293	-0.326	-0.031
Greece	-0.146	-0.206	-0.033	Spain	-2.684	-0.121	-0.072
Hungary	-0.081	-0.341	0.018	Sweden	-0.632	-0.269	0.003
India	-0.005	-0.065	-0.036	Switzerland	-1.197	-0.338	0.036
Indonesia	-0.008	-0.158	0.013	Taiwan	-0.009	-0.279	0.019
Ireland	-1.373	-0.272	-0.067	Turkey	-0.591	-0.174	-0.020
Italy	-1.720	-0.166	-0.039	UK	-0.903	-0.225	0.018
Japan	-0.040	-0.101	-0.001	USA	-1.223	-0.063	0.000

Note: The table reports the real income changes decomposed into the direct production effect (columns 2 and 6), the indirect global value chains effect (columns 3 and 7) and into the additional GE effect that occurs due to the global nature of the shock and its feedback general equilibrium effects (columns 4 and 8).

Table 6: Decomposition of real income changes - Shock 2 - Open Economy

Country	Direct Effect in %	GVC Effect in %	GE Effect in %	Country	Direct Effect in %	GVC Effect in %	GE Effect in %
Australia	-8.677	-2.127	0.159	Korea	-8.455	-3.928	0.459
Austria	-9.398	-3.994	0.525	Latvia	-9.072	-4.014	0.508
Belgium	-7.564	-4.168	0.435	Lithuania	-8.567	-4.763	0.588
Brasil	-9.225	-1.710	0.179	Luxembourg	-6.454	-5.000	0.534
Bulgaria	-8.970	-4.437	0.531	Malta	-7.671	-4.508	0.359
Canada	-8.341	-2.914	0.402	Mexico	-10.292	-2.714	0.283
China	-11.307	-2.385	0.375	Netherlands	-7.305	-4.377	0.492
Croatia	-9.954	-3.929	0.511	Norway	-7.930	-3.037	0.374
Cyprus	-8.306	-3.736	0.397	Poland	-9.029	-4.260	0.511
Czech R.	-7.661	-5.603	0.671	Portugal	-9.282	-3.106	0.354
Denmark	-8.417	-3.552	0.433	ROW	-9.696	-3.155	0.328
Estonia	-8.241	-4.606	0.522	Romania	-9.165	-4.032	0.443
Finland	-8.556	-2.783	0.268	Russia	-10.849	-2.844	0.335
France	-9.973	-2.531	0.305	Slovakia	-7.646	-5.239	0.616
Germany	-6.890	-4.949	0.599	Slovenia	-8.702	-5.271	0.637
Greece	-7.905	-2.495	0.211	Spain	-9.862	-2.502	0.188
Hungary	-7.960	-5.252	0.685	Sweden	0.000	-3.629	0.129
India	-12.286	-1.970	0.263	Switzerland	-7.487	-3.860	0.454
Indonesia	-10.388	-3.095	0.416	Taiwan	-3.988	-3.905	0.301
Ireland	-4.562	-4.761	0.286	Turkey	-11.263	-3.359	0.455
Italy	-9.279	-3.090	0.322	UK	-6.952	-2.615	0.268
Japan	-7.592	-2.183	0.221	USA	-9.024	-1.556	0.217

Note: The table reports the real income changes decomposed into the direct production effect (columns 2 and 6), the indirect global value chains effect (columns 3 and 7) and into the additional GE effect that occurs due to the global nature of the shock and its feedback general equilibrium effects (columns 4 and 8).

Table 7: Openness, trade diversification and specialization in production

	(1)	(2)	(3)	(4)	(5)	(6)
VARIABLES	log(indirect)	log(indirect)	log(indirect)	log(direct)	log(direct)	log(direct)
log(Openness)	0.639 ^a (0.185)	0.921 ^a (0.118)	0.902 ^a (0.109)	-0.299 ^a (0.070)	-0.383 ^a (0.032)	-0.386 ^a (0.031)
log(Specialization)		-8.380 ^a (1.220)	-7.903 ^a (1.157)		2.661 ^a (0.429)	2.733 ^a (0.384)
log(Diversification)			-0.446 (0.434)			-0.070 (0.136)
Constant	1.155 ^b (0.561)	1.192 ^a (0.377)	1.140 ^a (0.368)	-0.913 ^a (0.275)	-1.036 ^a (0.229)	-1.038 ^a (0.228)
Controls	x	x	x	x	x	x
Observations	44	44	44	43	43	43
Adjusted R ²	0.697	0.839	0.841	0.924	0.958	0.957

Notes: The table reports the regression of the $\log(|\text{direct}|)$ and the $\log(|\text{indirect}|)$ change in real income for all the 44 countries in our sample. In columns from 4 to 6, the number of observation is 43 because Sweden did not implement any policy restriction that imposed quarantine to the population, so it is not included in the regression. The explanatory variables are $\log(\text{openness}) = \log(\frac{X_i + M_i}{Y_i})$, $\log(\text{diversification}) = \log(\text{HHI_M})$, $\log(\text{specialization}) = \text{HHI_output}$. Note that an increase in the HHI indexes implies a reduction in diversification(specialization). Controls include $\log(\text{initial} - \text{income})$ and $\log(\text{total} - \text{income} - \text{change})$ Robust standard errors in parenthesis, ^a<0.01, ^b<0.05, ^c<0.10.

Table 8: Real income changes (in %) - Shock 1 - Less integrated vs. Open Economy

Country	Less integrated Economy		Open Economy	Δ	Country	Less integrated Economy		Open Economy	Δ
	Trade Costs	Shock 1				Shock 1	Shock 1		
Australia	-18.36	-0.27	-0.31	0.04	Korea	-21.77	-0.32	-0.38	0.06
Austria	-22.59	-0.84	-1.08	0.24	Latvia	-30.80	-0.32	-0.46	0.14
Belgium	-27.05	-1.49	-2.04	0.56	Lithuania	-30.00	-0.37	-0.51	0.14
Brasil	-13.98	-0.18	-0.19	0.01	Luxembourg	-29.65	-1.43	-1.97	0.53
Bulgaria	-33.50	-0.29	-0.42	0.14	Malta	-34.43	-0.62	-0.94	0.32
Canada	-20.02	-0.51	-0.63	0.12	Mexico	-17.38	-0.20	-0.22	0.03
China	-17.12	-0.20	-0.19	-0.00	Netherlands	-19.99	-0.81	-0.98	0.17
Croatia	-27.89	-0.43	-0.59	0.16	Norway	-19.55	-0.66	-0.81	0.15
Cyprus	-31.14	-0.58	-0.83	0.25	Poland	-23.09	-0.32	-0.40	0.08
Czech R.	-21.68	-0.49	-0.60	0.11	Portugal	-24.12	-1.23	-1.64	0.40
Denmark	-19.91	-0.71	-0.87	0.16	ROW	-29.33	-0.60	-0.85	0.25
Estonia	-31.87	-0.56	-0.81	0.26	Romania	-27.35	-0.38	-0.50	0.13
Finland	-22.12	-0.44	-0.56	0.12	Russia	-20.91	-0.23	-0.27	0.04
France	-18.87	-1.31	-1.62	0.31	Slovakia	-25.90	-0.31	-0.39	0.08
Germany	-19.44	-0.79	-0.96	0.17	Slovenia	-26.58	-0.49	-0.65	0.16
Greece	-24.02	-0.31	-0.38	0.08	Spain	-18.31	-2.32	-2.88	0.56
Hungary	-22.13	-0.33	-0.40	0.07	Sweden	-22.61	-0.70	-0.90	0.20
India	-13.84	-0.10	-0.11	0.00	Switzerland	-19.72	-1.22	-1.50	0.28
Indonesia	-18.60	-0.14	-0.15	0.01	Taiwan	-24.39	-0.22	-0.27	0.05
Ireland	-21.57	-1.37	-1.71	0.34	Turkey	-18.55	-0.64	-0.79	0.14
Italy	-16.61	-1.60	-1.93	0.33	UK	-20.38	-0.88	-1.11	0.22
Japan	-14.63	-0.14	-0.14	0.00	USA	-13.06	-1.11	-1.29	0.17

Note: The table presents the aggregated real income changes in % for every country. Column 2 and 6 show the real income changes solely driven by the increase in trade costs by 100 percentage points. Column 3 and 7 present the real income changes in % driven by the COVID-19 shock under a Less integrated economy. Column 4 and 8 present the shock i under an open economy (similar to table 1). Column 5 and 9 present the difference between the shock under an open vs. a Less integrated economy. Equation 2 highlights how we included the shock.

Table 9: Real income changes (in %) - Shock 2 - Less integrated vs. Open Economy

Country	Less integrated Economy		Open Economy	Δ	Country	Less integrated Economy		Open Economy	Δ
	Trade Costs	Shock 2				Trade Costs	Shock 2		
Australia	-18.36	-8.70	-10.65	1.94	Korea	-21.77	-9.26	-11.92	2.66
Austria	-22.59	-9.96	-12.87	2.90	Latvia	-30.80	-8.71	-12.58	3.87
Belgium	-27.05	-8.25	-11.30	3.05	Lithuania	-30.00	-8.97	-12.74	3.77
Brasil	-13.98	-9.30	-10.76	1.45	Luxembourg	-29.65	-7.76	-10.92	3.16
Bulgaria	-33.50	-8.56	-12.88	4.32	Malta	-34.43	-7.76	-11.82	4.06
Canada	-20.02	-8.68	-10.85	2.17	Mexico	-17.38	-10.53	-12.72	2.20
China	-17.12	-10.90	-13.32	2.42	Netherlands	-19.99	-8.92	-11.19	2.27
Croatia	-27.89	-9.66	-13.37	3.71	Norway	-19.55	-8.51	-10.59	2.08
Cyprus	-31.14	-8.04	-11.65	3.61	Poland	-23.09	-9.81	-12.78	2.97
Czech R.	-21.68	-9.85	-12.59	2.74	Portugal	-24.12	-9.14	-12.03	2.89
Denmark	-19.91	-9.24	-11.54	2.29	ROW	-29.33	-8.82	-12.52	3.70
Estonia	-31.87	-8.41	-12.33	3.92	Romania	-27.35	-9.31	-12.75	3.44
Finland	-22.12	-8.63	-11.07	2.44	Russia	-20.91	-10.55	-13.36	2.81
France	-18.87	-9.89	-12.20	2.31	Slovakia	-25.90	-9.07	-12.27	3.20
Germany	-19.44	-9.03	-11.24	2.21	Slovenia	-26.58	-9.78	-13.34	3.55
Greece	-24.02	-7.80	-10.19	2.39	Spain	-18.31	-9.94	-12.18	2.24
Hungary	-22.13	-9.75	-12.53	2.78	Sweden	-22.61	-2.82	-3.50	0.68
India	-13.84	-12.01	-13.99	1.98	Switzerland	-19.72	-8.77	-10.89	2.13
Indonesia	-18.60	-10.69	-13.07	2.38	Taiwan	-24.39	-5.80	-7.59	1.79
Ireland	-21.57	-7.10	-9.04	1.94	Turkey	-18.55	-11.52	-14.17	2.64
Italy	-16.61	-10.03	-12.05	2.02	UK	-20.38	-7.45	-9.30	1.85
Japan	-14.63	-8.21	-9.55	1.35	USA	-13.06	-9.04	-10.36	1.32

Note: The table presents the aggregated real income changes in % for every country. Column 2 and 6 show the real income changes solely driven by the increase in trade costs by 100 percentage points. Column 3 and 7 present the real income changes in % driven by the COVID-19 shock under a Less integrated economy. Column 4 and 8 present the shock Δ under an open economy (similar to table 1). Column 5 and 9 present the difference between the shock under an open vs. a Less integrated economy. Equation 2 highlights how we included the shock.

Table 10: Decomposition of the real income changes economy - Shock 1 - Less integrated Economy

Country	Shock 1				Country	Shock 1			
	Direct	Indirect	GE	Trade Costs		Direct	Indirect	GE	Trade Costs
Australia	-0.124	-0.124	-0.021	-18.361	Korea	-0.082	-0.285	0.048	-21.767
Austria	-0.608	-0.221	-0.011	-22.586	Latvia	-0.127	-0.187	-0.007	-30.795
Belgium	-1.243	-0.255	0.012	-27.053	Lithuania	-0.135	-0.253	0.022	-29.996
Brasil	-0.068	-0.113	-0.004	-13.982	Luxembourg	-1.134	-0.301	0.000	-29.646
Bulgaria	-0.035	-0.245	-0.006	-33.503	Malta	-0.312	-0.311	0.008	-34.429
Canada	-0.343	-0.097	-0.070	-20.019	Mexico	-0.028	-0.140	-0.029	-17.380
China	-0.023	-0.160	-0.011	-17.123	Netherlands	-0.619	-0.194	0.003	-19.994
Croatia	-0.195	-0.237	0.004	-27.888	Norway	-0.501	-0.162	0.004	-19.545
Cyprus	-0.337	-0.250	0.006	-31.143	Poland	-0.092	-0.227	-0.005	-23.089
Czech R.	-0.210	-0.268	-0.014	-21.684	Portugal	-0.915	-0.322	0.003	-24.121
Denmark	-0.479	-0.255	0.027	-19.907	ROW	-0.445	-0.113	-0.037	-29.326
Estonia	-0.350	-0.198	-0.009	-31.869	Romania	-0.155	-0.229	0.007	-27.346
Finland	-0.263	-0.175	-0.006	-22.117	Russia	-0.083	-0.221	0.074	-20.908
France	-1.117	-0.170	-0.021	-18.866	Slovakia	-0.069	-0.265	0.026	-25.896
Germany	-0.538	-0.263	0.011	-19.443	Slovenia	-0.212	-0.263	-0.017	-26.575
Greece	-0.109	-0.170	-0.030	-24.020	Spain	-2.150	-0.182	0.014	-18.312
Hungary	-0.065	-0.305	0.035	-22.134	Sweden	-0.483	-0.210	-0.009	-22.607
India	-0.001	-0.015	-0.085	-13.838	Switzerland	-0.963	-0.283	0.029	-19.719
Indonesia	-0.007	-0.118	-0.015	-18.603	Taiwan	-0.003	-0.194	-0.021	-24.390
Ireland	-1.096	-0.254	-0.025	-21.573	Turkey	-0.477	-0.168	0.004	-18.546
Italy	-1.414	-0.213	0.031	-16.612	UK	-0.704	-0.173	-0.008	-20.375
Japan	-0.033	-0.101	-0.003	-14.631	USA	-1.048	-0.027	-0.037	-13.055

Note: This table decomposes the real income changes under shock 1, in the less integrated world, into its four components: direct, indirect, GE and trade cost effect.

Table 11: Decomposition of the real income changes economy - Shock 2 - Less integrated Economy

Country	Shock 2				Country	Shock 2			
	Direct	Indirect	GE	Trade Costs		Direct	Indirect	GE	Trade Costs
Australia	-6.986	-1.896	0.177	-18.361	Korea	-6.355	-3.386	0.481	-21.767
Austria	-7.175	-3.172	0.383	-22.586	Latvia	-6.174	-2.862	0.328	-30.795
Belgium	-5.442	-3.150	0.346	-27.053	Lithuania	-5.904	-3.507	0.442	-29.996
Brasil	-7.751	-1.769	0.217	-13.982	Luxembourg	-4.614	-3.499	0.350	-29.646
Bulgaria	-5.806	-3.117	0.366	-33.503	Malta	-4.955	-3.133	0.329	-34.429
Canada	-6.561	-2.271	0.147	-20.019	Mexico	-8.336	-2.516	0.325	-17.380
China	-8.885	-2.354	0.338	-17.123	Netherlands	-5.866	-3.443	0.386	-19.994
Croatia	-7.055	-2.989	0.379	-27.888	Norway	-6.325	-2.461	0.272	-19.545
Cyprus	-5.649	-2.694	0.304	-31.143	Poland	-6.825	-3.406	0.420	-23.089
Czech R.	-6.019	-4.337	0.505	-21.684	Portugal	-6.901	-2.525	0.288	-24.121
Denmark	-6.701	-2.930	0.388	-19.907	ROW	-6.688	-2.324	0.193	-29.326
Estonia	-5.522	-3.244	0.361	-31.869	Romania	-6.473	-3.263	0.427	-27.346
Finland	-6.539	-2.350	0.256	-22.117	Russia	-8.439	-2.535	0.426	-20.908
France	-7.954	-2.173	0.234	-18.866	Slovakia	-5.555	-4.012	0.499	-25.896
Germany	-5.645	-3.837	0.455	-19.443	Slovenia	-6.271	-3.984	0.472	-26.575
Greece	-5.914	-2.048	0.161	-24.020	Spain	-7.900	-2.347	0.309	-18.312
Hungary	-6.166	-4.129	0.545	-22.134	Sweden	0.000	-2.915	0.091	-22.607
India	-10.366	-1.795	0.152	-13.838	Switzerland	-6.029	-3.120	0.383	-19.719
Indonesia	-8.299	-2.705	0.315	-18.603	Taiwan	-2.919	-3.073	0.191	-24.390
Ireland	-3.630	-3.744	0.275	-21.573	Turkey	-9.064	-2.859	0.398	-18.546
Italy	-7.610	-2.805	0.384	-16.612	UK	-5.448	-2.210	0.207	-20.375
Japan	-6.345	-2.066	0.205	-14.631	USA	-7.722	-1.426	0.108	-13.055

Note: This table decomposes the real income changes under shock 2, in the less integrated world, into its four components: direct, indirect, GE and trade cost effect.

A Appendix: Data Sources and Description

This section describes the data sources used for the construction of the COVID-19 shocks and for the counterfactual simulations.

Data needed for the simulation. We use data from World Input-Output database (WIOD) as our main data source for the simulations. It provides information on bilateral intermediate and final trade, sectoral output and value-added information, consumer and producer prices. With this data, one can construct bilateral input-output tables, intermediate consumption and expenditure levels for 43 countries and a rest of the world aggregate (RoW) (Timmer et al., 2015). In total each country consists of 56 sectors, which we aggregate into 50 industries (see table A4) in the Appendix. This aggregation concerns mostly services; we keep the sectoral detail in the manufacturing and agricultural industries. Data on bilateral preferential and MFN tariffs stem from the World Integrated Trade Solutions (WITS-TRAINS) and the WTO's Integrated Database (IDB). The parameter for the productivity dispersion, hence the trade cost elasticity is taken from Caliendo and Parro (2015).

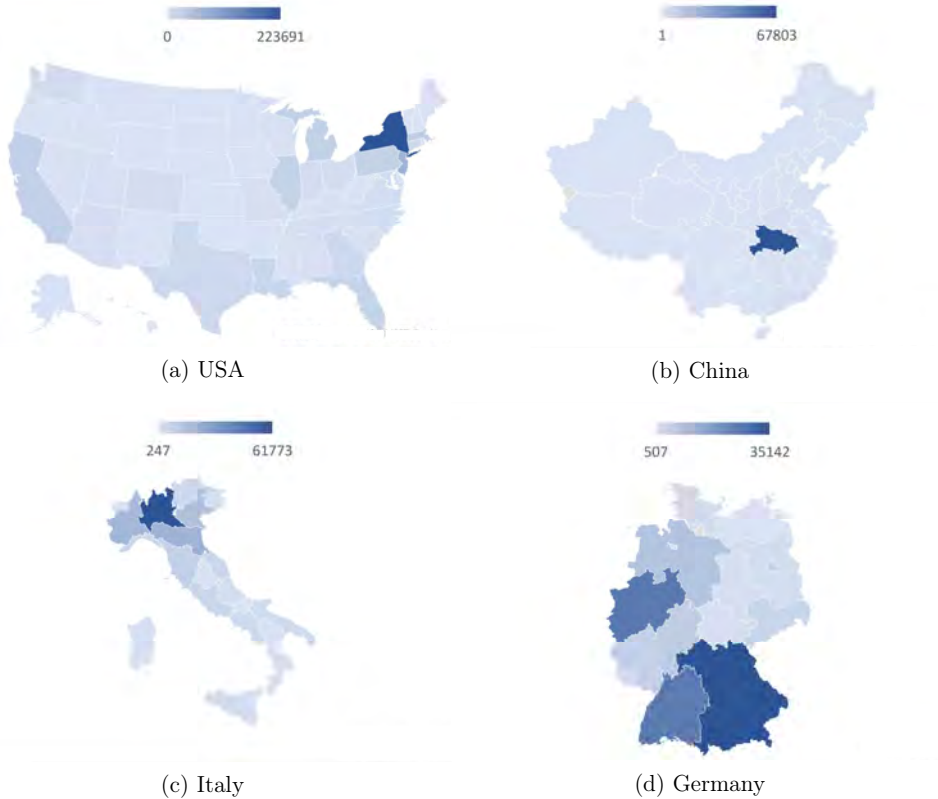
To construct the shocks, as detailed in equation 1 and 2, we need the following data:

COVID-19 cases. We exploit information on the number of corona cases in each country c_i and region from multiple sources. We use data from the Johns Hopkins Coronavirus Resource Center and combine them with information from national statistical offices for Italy, Germany, Spain and Portugal. This provides us with COVID-19 cases as of April 16th in each of the 43 countries of our data set, with regional disaggregation for the US, Italy, China, Germany, Spain and Portugal.²⁹ Figure A1 shows 4 selected country maps with regional variation in the number of COVID-19 cases. The data of COVID-19 cases on regional level is then merged with the regional, sector level employment data. This way, we can construct a measure that accounts for the severity with which a sector is hit by the COVID-19 pandemic. Concrete, the severity of the effect in a sector depends on the geographical distribution of the sector across regions, on the share of employment affected in each region and on the labor intensity of each sector.

Employment Data. Information on employment by country-region and sector is crucial to account for the geographical distribution of sectors across each country as well as for the

²⁹The regional dimension will be updated for every country as soon as this information becomes available.

Figure A1: COVID-cases by region in selected countries



Note: The maps show the number of COVID-19 cases by region for the US (A1a), China (A1b), Italy (A1c), and Germany (A1d) until the 16th of April 2020. We chose this date to coincide with the data of the simulations. Since COVID-19 pandemics is still ongoing, we will update the data of COVID-cases in future versions of this paper.

COVID-19 shares over employment in a country-region.³⁰

For the *EU*, we use the information contained in Eurostat. For the *US* we use IPUMScps to construct employment by state(region) and sector of activity. To construct the employment shares across regions and sectors for *China*, we use two data sources: first, we use data

³⁰Data on employment at sector-region level are not available for some countries in the sample, we therefore construct a simpler version of equation 1. In this case, the formula does not capture the geographical distribution of sectors in the country, but accounts for the sectoral distribution of employment and for their labor intensity. This is the case for Australia, Brazil, Canada, India, Indonesia, Japan, Korea, Mexico, Russia, Taiwan, RoW.

from the National Bureau of Statistic of China for the year 2018 on employment by region and sector.³¹ The second data source comes from the 2000 census. The National Bureau of Statistic of China provides the sector information for 19 sectors and 31 regions. Sectors consist of one agricultural sector, one mining sector, one manufacturing sector and 16 services sectors, hence a more aggregated sector level than provided in the paper. We therefore complement the available data with the employment shares by prefectures and sector from the 2000 census to construct the regional employment level for each of the WIOD sectors. The census data is used to retrieve the employment shares in each Chinese region and sector. We now have information for China divided into 340 prefectures and 151 sectors (SIC industry code), which is then aggregated to 31 Chinese regions and the 50 WIOD sectors.³² We then redistribute the most recent available number of employment from the National Bureau of Statistic of China according to the shares from the 2000 census data (see figure A2).³³ This returns regional employment shares for each WIOD sector and region in China.

Quarantine Restrictiveness. For the construction of the quarantine index ψ_i^j we require information on the degree of restriction for each country ($IndexClosure_i$).

We use the index on government responses to the COVID-19 diffusion of the University of Oxford, where $IndexClosure_i$ is an index of restrictiveness of government responses ranging from 0 to 100 (see Hale (2020) for a detailed description of the index), where 100 indicates full restrictions. The index is meant to capture the extent of work, school, transportation and public event restrictions in each country. Further, using the information contained in the data-set on government responses to the COVID-19 from the University of Oxford, we account for the average duration of strict quarantine, which we estimate to be of one month. COVID-pandemics is still ongoing, which is why we do not have the final number of quarantine days across countries. Figure A3 presents a graphical representation of the index from Hale (2020) for our set of countries.

Teleworkability. We follow Dingel and Neiman (2020) to construct a measure of the degree of *teleworkability* of each occupation. The information contained in the Occupa-

³¹See <http://www.stats.gov.cn/english/> for a general overview of the data collected by the NBSC, and <http://data.stats.gov.cn/english/> for employment data at regional level.

³²The concordance of SIC industry codes to WIOD can be retrieved from the authors. We aggregate the 340 Chinese prefectures to 31 regions, because the COVID-19 data is only available at the more aggregated, regional level.

³³The correlation of the employment shares across regions of the census 2000 data and the data from the National Bureau of Statistics is 0.93.

Figure A2: Employment shares across Chinese regions

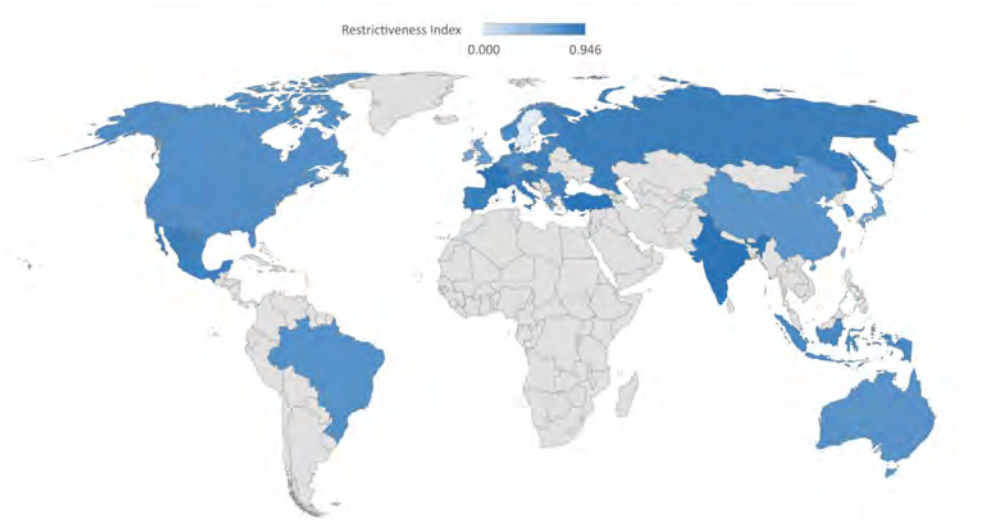


Note: The map shows the regional employment over total Chinese employment, which is crucial to construct the geographical distribution of the extent of the shock. We further have data on the within regional sector distribution needed to construct the shock 1.

tional Information Network (O*NET) surveys is used to construct a measure of feasibility of working from home for each sector. The information on O*NET is provided as NAICS classification, for which we provide a concordance to match the WIOD sector classification (see table A1). The policy interventions implemented due to COVID-19 explicitly exempt the sensitive sectors from all restrictive measures, which is the reason why we increase the share of teleworkable employment for such sensitive sectors to 0.8. Precisely, the sensitive sectors are still producing their goods and services without a complete shutdown. The list of sensitive sectors includes (ISIC rev 3 sectoral classification): Agriculture (sector 1), Fishing (sector 3), Electricity and gas (sector 23), Water supply (sector 24), Sewage and Waste (sector 25), Postal and courier (sector 34), Human health and social work (sector 49).

Construction of the shocks. Using all the data described above we can construct the two shocks (see equations 1 and 1). Figures A4 and A5 show maps of the two shocks for all countries of the sample. Figure A6 zooms into the EU and shows the size of the two shocks for the EU countries.

Figure A3: Restrictiveness Index across countries



Note: The map reports the restrictiveness index for all countries in our sample. An index equal to zero means no restrictions (i.e. in Sweden), while an index equal 100 means that the entire economy is set under a complete shutdown (i.e. France it is 0.97). No information is available for countries shaded in gray.

B Additional results

In this subsection, we present different scenarios in which we gradually increase trade costs in each economy. In practice, we increase trade costs from 10 percentage points to 100 percentage points in each sector-country.³⁴ For both shocks, the additional increases in trade costs by 10 percentage points on average decreases the size of the real income drops by 0.02 for Germany and China, 0.18 for Italy, 0.013 for the USA, and by 0.03 across all countries. Figure A7 shows the real income changes for Italy, Germany, USA, and China and for an aggregate EU28 and the RoW. At the point 0, the real income changes are identical to the changes of shock 1 shown in table 1. 100 is identical to our less integrated economy scenario shown in the main body. The black solid lines indicate the decrease in real income due to the increase in trade costs plus the shock (1) under different degrees of openness of the economy. The grey dashed line shows the drop in real income that solely comes from the trade cost increases. The blue bars show the decrease in real income due to the shock (2).

³⁴The main body of the text presents the results for a less integrated world with an increase of trade costs by a hundred percentage points.

Table A1: Teleworkability by sector

NAICS sec-id	WIOD sec-id	Sector Description	sec-id	Teleworkability sec-id	NAICS Description	WIOD	Sector
11	1	Crops, Animals	0.08	23	26	Construction	0.19
11	2	Forestry, Logging	0.08	42	27	Trade, Repair of Motor Vehicles	0.52
11	3	Fishing, Aquaculture	0.08	42	28	Wholesale Trade	0.52
21	4	Mining, Quarrying	0.25	44-45	29	Retail Trade	0.14
11	5	Food, Beverages, Tobacco	0.08	48-49	30	Land Transport	0.19
31-33	6	Textiles, Apparel,Leather	0.22	48-49	31	Water Transport	0.19
31-33	7	Wood, Cork	0.22	48-49	32	Air Transport	0.19
31-33	8	Paper	0.22	48-49	33	Aux. Transportation Services	0.19
31-33	9	Recorded Media Reproduction	0.22	48-49	34	Postal and Courier	0.19
31-33	10	Coke, Refined Petroleum	0.22	72	35	Accommodation and Food	0.04
31-33	11	Chemicals	0.22	51	36	Publishing	0.72
31-33	12	Pharmaceuticals	0.22	51	37	Media Services	0.72
31-33	13	Rubber, Plastics	0.22	51	38	Telecommunications	0.72
31-33	14	Other non-Metallic Mineral	0.22	55	39	Computer, Information Services	0.79
31-33	15	Basic Metals	0.22	52	40	Financial Services	0.76
31-33	16	Fabricated Metal	0.22	52	41	Insurance	0.76
31-33	17	Electronics, Optical Products	0.22	53	42	Real Estate	0.42
31-33	18	Electrical Equipment	0.22	54	43	Legal and Accounting	0.80
31-33	19	Machinery, Equipment	0.22	54	44	Business Services	0.80
31-33	20	Motor Vehicles	0.22	54	45	Research and Development	0.80
31-33	21	Other Transport Equipment	0.22	56	46	Admin., Support Services	0.31
31-33	22	Furniture, Other Manufacturing	0.22	99	47	Public, Social Services	0.41
22	23	Electricity, Gas	0.37	61	48	Education	0.83
22	24	Water Supply	0.37	62	49	Human Health and Social Work	0.25
22	25	Sewerage, Waste	0.37	71	50	Other Services, Households	0.30

Note: The table shows the degree of teleworkability of each WIOD sector. Zero would indicate that work cannot be done from home, while teleworkability equal to 1 indicates that the entire work is independent of the location.

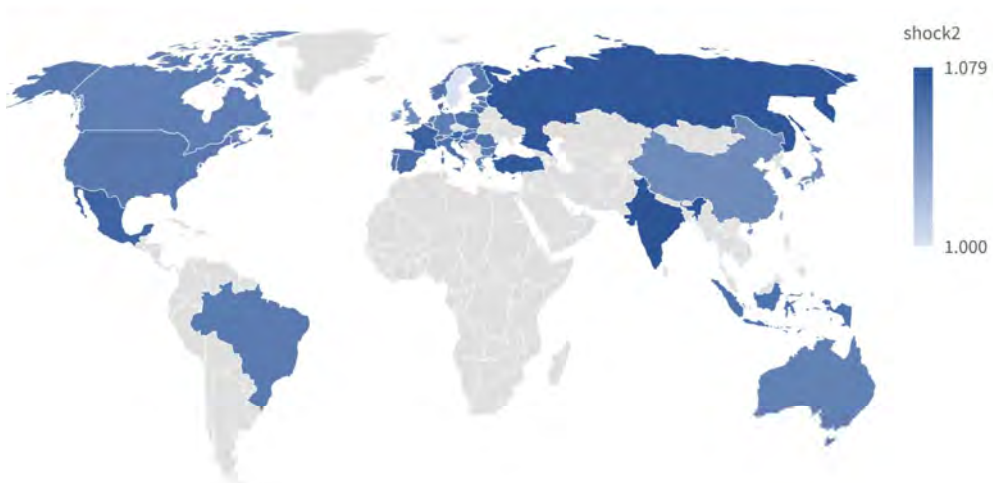
The green bar (at x-axis 0 - no trade costs) shows the decrease in real income that stems from the shock. It is identical to the decreases shown in table 1.

Figure A4: Shock 1 across all countries



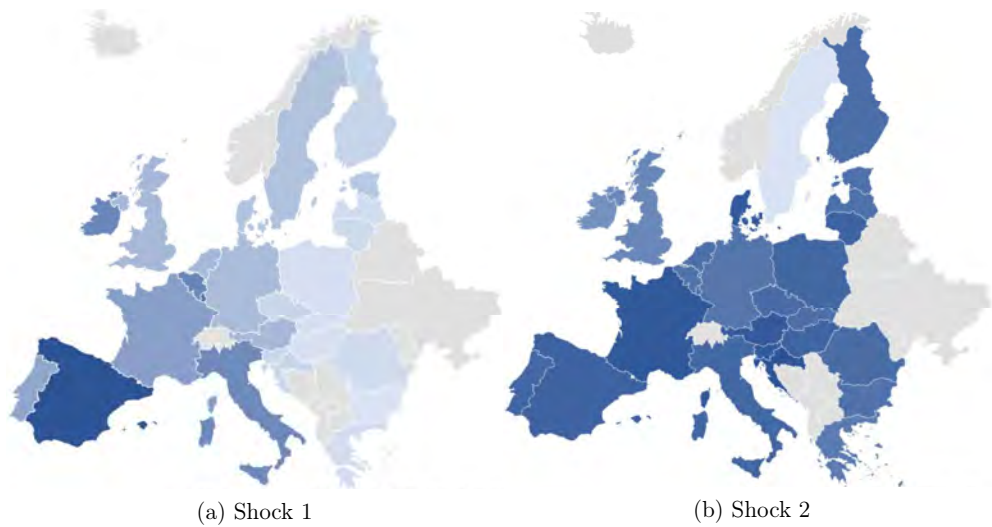
Note: The map reports the intensity of the snap-shot shocks (1) imputed into the model for all countries in our sample. A shock equal to 1 means no changes from the baseline, while a shock of 2 would imply an increase in the production barrier by a hundred percent. See equation 1 for the precise construction of the shock.

Figure A5: Shock 2 across all countries



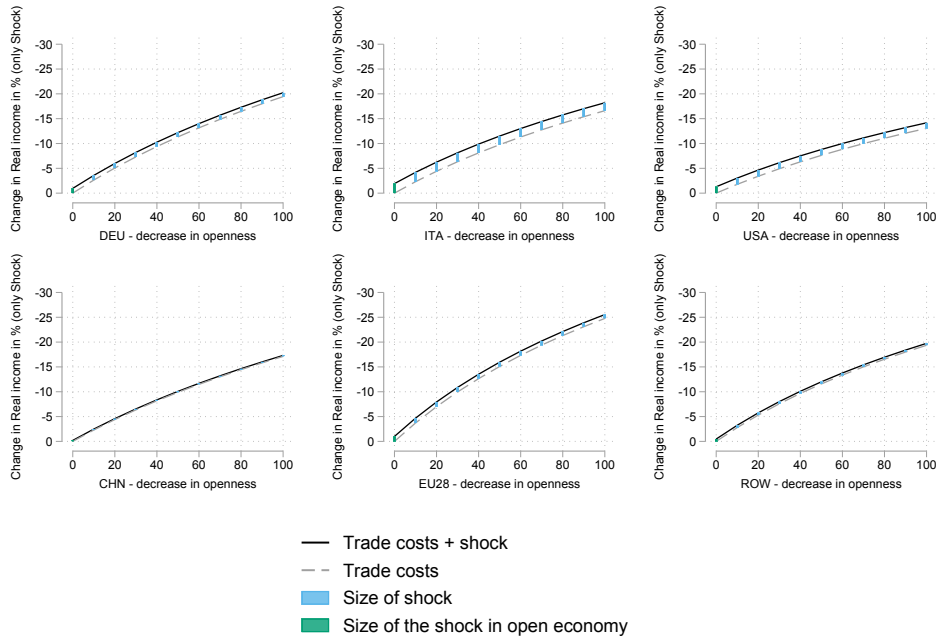
Note: The map reports the size of the quarantine shocks (2) imputed into the model for all countries in our sample. A shock equal to 1 means no changes from the baseline, while a shock of 2 would imply an increase in the production barrier by a hundred percent. See equation 2 for the precise construction of the shock.

Figure A6: Size of the Shocks across EU28 member states



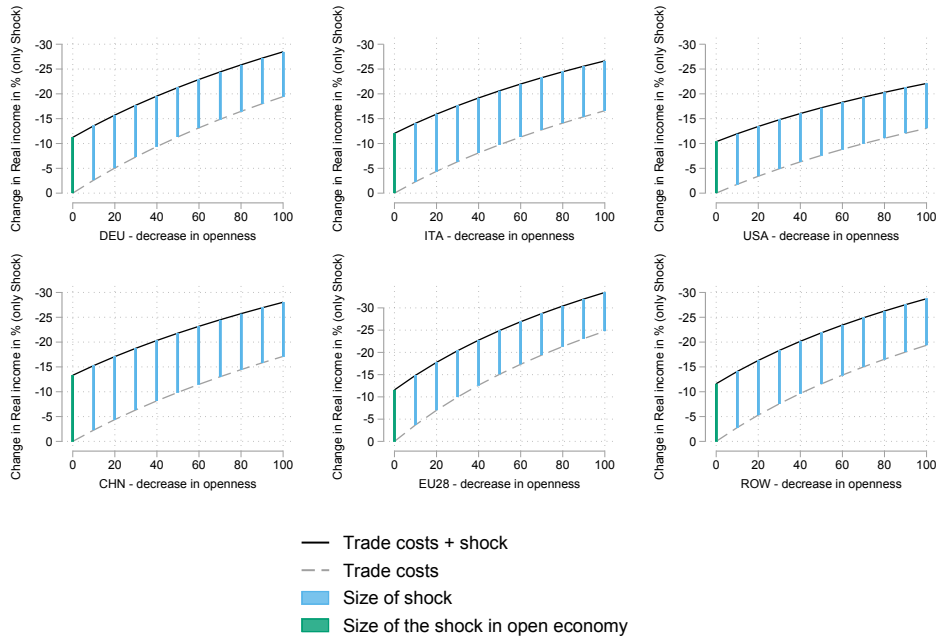
Note: The maps show the size of the snap-shot shocks (1) and the quarantine shock (2), which are imputed into the model for the EU28 member states. A shock equal to 1 means no changes from the baseline, while a shock of 2 would imply an increase in the production barrier by a hundred percent for an entire year. See equations 1 and 2 for the precise construction of the shock. The darker the shade of blue, the higher is the size of the effect. The scale of subfigure A6a goes from 1 (e.g. Bulgaria) to 1.018 (Spain). The scale of subfigure A6b goes from 1, the least restrictive country (Sweden) to 1.072, the most restrictive country (i.e. France).

Figure A7: Real Income Changes with different openness degrees of the economy - Shock 1



Note: The 6 sub-figures show the real income changes for the four selected countries, Italy, Germany, USA, and China and the regions EU28, ROW. The x-axis presents the scenarios with different trade cost increases. At the point 0, the real income changes are identical to the changes of shock 1 shown in table 1. 50 equals the increase in trade costs for every country by 50 percentage points. 100 is identical to our less integrated economy scenario shown in the main body. The black solid line indicates the decrease in real income due to the increase in trade costs plus the shock 1 under different degrees of openness of the economy. The grey dashed line shows the drop in real income that solely comes from the trade cost increases. The blue bars show the decrease in real income due to the shock 1. The green bar (at x-axis 0 - no trade costs) shows the decrease in real income that stems from the shock. It is identical to the decreases shown in table 1.

Figure A8: Real Income Changes with different openness degrees of the economy - Shock 2



Note: The six figures show the real income changes for the four selected countries, Italy, Germany, USA, and China and the regions EU28, RoW. The x-axis presents the scenarios with different trade cost increases. At the point 0, the real income changes are identical to the changes of shock 2 shown in table 1. 50 equals the increase in trade costs for every country by 50 percentage points. 100 is identical to our less integrated economy scenario shown in the main body. The black solid line indicates the decrease in real income due to the increase in trade costs plus the shock (2) under different degrees of openness of the economy. The grey dashed line shows the drop in real income that solely comes from the trade cost increases. The blue bars show the decrease in real income due to the shock (2). The green bar (at x-axis 0 - no trade costs) shows the decrease in real income that stems from the shock. It is identical to the decreases shown in table 1.

Table A2: Change in value added (in %) - Open Economy

Panel B: Shock 1 - Open Economy						
Sector	Italy in %	Germany in %	USA in %	China in %	EU28 in %	Rest of World in %
Agriculture	-1.98	-0.98	-1.30	-0.15	-1.38	-0.55
Food, Beverages, Tobacco	-1.93	-0.99	-1.26	-0.18	-1.37	-0.46
Mining, Quarrying	-2.10	-1.05	-1.30	-0.15	-1.13	-0.67
Textiles	-2.28	-0.98	-1.21	-0.05	-1.63	-0.45
Electrical Equipment	-2.29	-1.01	-1.31	-0.01	-1.22	-0.40
Machinery, Equipment	-1.71	-1.01	-1.20	-0.26	-1.22	-0.57
Motor Vehicles	-1.53	-0.97	-1.11	-0.25	-1.05	-0.46
Intm. Resources Manufacturing	-2.00	-0.98	-1.26	-0.16	-1.28	-0.43
Manufacturing, nec.	-1.67	-0.95	-1.21	-0.29	-1.23	-0.50
Pharmaceuticals	-1.89	-1.05	-1.27	-0.24	-1.39	-0.69
Chemicals	-2.39	-0.99	-1.32	-0.12	-1.42	-0.41
Electricity, Water, Gas	-1.97	-0.97	-1.27	-0.16	-1.33	-0.62
Construction	-1.94	-0.97	-1.28	-0.19	-1.34	-0.48
Wholesale, Retail Trade	-1.98	-0.99	-1.28	-0.13	-1.37	-0.48
Transport	-2.01	-1.00	-1.29	-0.15	-1.37	-0.52
Accommodation and Food	-1.93	-0.98	-1.28	-0.18	-1.58	-0.47
Real Estate	-1.94	-0.97	-1.29	-0.18	-1.40	-0.47
Public Services	-1.95	-0.97	-1.28	-0.19	-1.36	-0.46
Social Services	-1.94	-0.96	-1.29	-0.19	-1.35	-0.46
Services, nec.	-1.97	-0.98	-1.29	-0.17	-1.36	-0.51
Panel B: Shock 2 - Open Economy						
Sector	Italy in %	Germany in %	USA in %	China in %	EU28 in %	Rest of World in %
Agriculture	-12.08	-10.69	-10.23	-13.55	-11.42	-12.61
Food, Beverages, Tobacco	-11.90	-10.91	-10.32	-13.47	-11.21	-11.82
Mining, Quarrying	-12.10	-9.69	-10.32	-13.47	-10.49	-12.27
Textiles	-12.36	-10.25	-10.75	-14.02	-11.92	-12.77
Electrical Equipment	-12.34	-10.27	-10.68	-13.99	-10.62	-10.97
Machinery, Equipment	-11.95	-11.45	-10.93	-12.89	-11.57	-11.52
Motor Vehicles	-12.24	-11.72	-10.62	-12.98	-11.49	-11.61
Intm. Resources Manufacturing	-12.11	-10.93	-10.47	-13.44	-11.23	-11.83
Manufacturing, nec.	-11.81	-11.63	-11.00	-13.22	-11.50	-11.65
Pharmaceuticals	-11.42	-12.16	-10.47	-13.24	-11.38	-10.96
Chemicals	-12.30	-9.90	-10.31	-13.63	-10.67	-12.03
Electricity, Water, Gas	-12.06	-11.03	-10.45	-13.46	-11.15	-12.04
Construction	-12.05	-11.19	-10.37	-13.33	-11.07	-11.83
Wholesale, Retail Trade	-12.05	-10.96	-10.35	-13.57	-11.08	-11.90
Transport	-12.06	-10.74	-10.33	-13.52	-11.00	-12.11
Accommodation and Food	-12.06	-11.10	-10.37	-13.38	-11.27	-11.57
Real Estate	-12.06	-11.17	-10.37	-13.37	-11.15	-11.35
Public Services	-12.04	-11.11	-10.37	-13.32	-11.12	-11.76
Social Services	-12.05	-11.24	-10.37	-13.32	-10.99	-11.15
Services, nec.	-12.06	-11.04	-10.36	-13.40	-10.89	-11.63

Note: The table shows the sectoral value added changes, in % for selected countries, Italy, Germany, USA, and China. The upper part of the table presents the results for shock 1 in an open economy. The second part presents the results in the case of shock 2 in an open economy. Column 6 presents the value added results (in %) for EU28, which are weighted by the initial value added by country. Column 7 shows the value added weighted results for all remaining countries. Further, sectors are aggregated into broader categories (see table A3 in the Appendix).

Table A3: WIOD Sector Aggregation

WIOD sec-id	Sector Description	WIOD sec-id	Sector Description
	Agriculture	23	Electricity, Gas
2	Forestry, Logging	24	Water Supply
1	Crops, Animals		Construction
3	Fishing, Aquaculture	26	Construction
	Food, Beverages, Tobacco		Wholesale and Retail Trade
5	Food, Beverages, Tobacco	29	Retail Trade
	Mining, Quarrying	28	Wholesale Trade
4	Mining, Quarrying	27	Trade, Repair of Motor Vehicles
	Textiles		Transport
6	Textiles, Apparel, Leather	30	Land Transport
	Electrical Equipment	33	Aux. Transportation Services
18	Electrical Equipment		Transport
17	Electronics, Optical Products	32	Air Transport
	Machinery, Equipment	31	Water Transport
19	Machinery, Equipment		Accommodation and Food
	Motor Vehicles	35	Accommodation and Food
20	Motor Vehicles		Real Estate
	Intm. Resources Manufacturing	42	Real Estate
9	Recorded Media Reproduction		Public Services
8	Paper	46	Admin., Support Services
10	Coke, Refined Petroleum	47	Public, Social Services
16	Fabricated Metal		Social Services
13	Rubber, Plastics	49	Human Health and Social Work
7	Wood, Cork		Services, nec.
15	Basic Metals	37	Media Services
14	Other non-Metallic Mineral	40	Financial Services
	Manufacturing, nec.	36	Publishing
22	Furniture, Other Manufacturing	45	Research and Development
21	Other Transport Equipment	50	Other Services, Households
	Pharmaceuticals	44	Business Services
12	Pharmaceuticals	48	Education
	Chemicals	38	Telecommunications
11	Chemicals	34	Postal and Courier
	Electricity, Water, Gas	41	Insurance
25	Sewerage, Waste	43	Legal and Accounting
		39	Computer, Information Services

Note: The sectors written in bold indicate the broad categories each WIOD sector belongs to.

Table A4: Concordance WIOD Sectors - ISIC Rev. 4

WIOD		ISIC Rev. 4	WIOD		ISIC Rev. 4
ID	Description		ID	Description	
1	Crops & Animals	A01	26	Construction	F
2	Forestry & Logging	A02	27	Trade & Repair of Motor Vehicles	G45
3	Fishing & Aquaculture	A03	28	Wholesale Trade	G46
4	Mining & Quarrying	B	29	Retail Trade	G47
5	Food, Beverages & Tobacco	C10-C12	30	Land Transport	H49
6	Textiles, Apparel, Leather	C13-C15	31	Water Transport	H50
7	Wood & Cork	C16	32	Air Transport	H51
8	Paper	C17	33	Aux. Transportation Services	H52
9	Recorded Media Reproduction	C18	34	Postal and Courier	H53
10	Coke, Refined Petroleum	C19	35	Accommodation and Food	I
11	Chemicals	C20	36	Publishing	J58
12	Pharmaceuticals	C21	37	Media Services	J59_J60
13	Rubber & Plastics	C22	38	Telecommunications	J61
14	Other non-Metallic Mineral	C23	39	Computer & Information Services	J62_J63
15	Basic Metals	C24	40	Financial Services	K64
16	Fabricated Metal	C25	41	Insurance	K65_K66
17	Electronics & Optical Products	C26	42	Real Estate	L68
18	Electrical Equipment	C27	43	Legal and Accounting	M69_M70
19	Machinery & Equipment	C28,C33	44	Business Services	M71,M73-M75
20	Motor Vehicles	C29	45	Research and Development	M72
21	Other Transport Equipment	C30	46	Admin. & Support Services	N
22	Furniture & Other Manufacturing	C31_C32	47	Public & Social Services	O84
23	Electricity & Gas	D35	48	Education	P85
24	Water Supply	E36	49	Human Health and Social Work	Q
25	Sewerage & Waste	E37-E39	50	Other Services, Households	R-U

Jobs' amenability to working from home: Evidence from skills surveys for 53 countries¹

Maho Hatayama,² Mariana Viollaz³ and Hernan Winkler⁴

Date submitted: 11 May 2020; Date accepted: 11 May 2020

The spread of COVID-19 and implementation of “social distancing” policies around the world have raised the question of how many jobs can be done at home. This paper uses skills surveys from 53 countries at varying levels of economic development to estimate jobs’ amenability to working from home. The paper considers jobs’ characteristics and uses internet access at home as an important determinant of working from home. The findings indicate that the amenability of jobs to working from home increases with the level of economic development of the country. This is driven by jobs in poor countries being more intensive in physical/manual tasks, using less information and communications technology, and having poorer internet connectivity at home. Women, college graduates, and salaried and formal workers have jobs that are more amenable to working from home than the average worker. The opposite holds for workers in hotels and restaurants, construction, agriculture, and commerce. The paper finds that the crisis may exacerbate inequities between and within countries. It also finds that occupations explain less than half of the variability in the working-from-home indexes within countries, which highlights the importance of using individual-level data to assess jobs’ amenability to working from home.

1 The findings, interpretations, and conclusions in this paper are entirely those of the authors. They do not necessarily represent the view of the World Bank Group, its Executive Directors, or the countries they represent. The empirical results for the Middle East and North Africa region are part of a background paper for the report “Economic Transformation and Jobs: Making markets work for people in the MENA region” of the World Bank MNA Chief Economist Office.

2 Junior Professional Officer, The World Bank, Jobs Group.

3 Senior Researcher, CEDLAS-FCE-UNLP.

4 Senior Economist, The World Bank, Jobs Group.

Copyright: Maho Hatayama, Mariana Viollaz and Hernan Winkler

1. Introduction

The spread of COVID-19 and the implementation of “social distancing” policies around the world have raised the question of how many jobs can be done at home. Most of the existing efforts to estimate these figures rely on US-based measures of the type of tasks required by different occupations (Dingel & Neiman, 2020a; Avdiu & Nayyar, 2020; Mongey, Pilossoph, & Weinberg, 2020; Leibovici, Santacreu, & Famiglietti, 2020).¹ However, the task content of jobs exhibits substantial variation across countries (Lo Bello, Sanchez-Puerta, & Winkler, 2019; Hardy, Lewandowski, Park, & Yang, 2018). Differences in the organization of production or in the level of technology adoption across countries imply that the same occupation may be more intensive in face-to-face interactions or in physical tasks in poorer economies. As a result, using US-based measures to estimate the amenability to *working from home* (WFH) in developing countries may lead to biased conclusions.

To overcome this challenge, this paper uses skill and household surveys from 53 countries at different levels of economic development with rich information on the type of tasks carried out by people at work. We estimate indexes of the task content of jobs to rank them by their vulnerability to social distancing measures according to their amenability to a remote setup. In addition, given that the task data vary at the individual-level—and not by occupation, as in the Occupational Information Network (O*NET) classification—we show how the likelihood of being able to work from home correlates with other characteristics of the individual and his or her job.

We build on the literature by estimating jobs’ amenability to WFH, as opposed to estimating the fraction of jobs that can be done at home. Estimating the latter is challenging since choosing the tasks that determine whether a person can work from home is largely arbitrary, specifically if one does not have a model linking such tasks to the probability of WFH during a pandemic. Dingel & Neiman (2020b) and Saltiel (2020) consider that an occupation cannot be performed from home if at least one of several conditions holds. For instance, in the Dingel & Neiman (2020b) study, some of categories that are sufficient to consider that an occupation cannot be done at home include “Performing for or Working Directly with the Public is very important”, “Handling and Moving Objects is very important” or “Repairing and Maintaining Electronic Equipment is very important.” However, occupational requirements can change during exceptional conditions. For example, while for professionals in communications or in law it is very important to have contact with the public, they can still carry out some (but not all) of their tasks using ICT (Information and Communication Technologies); craft workers for whom handling and moving objects is crucial may still be able to sell their products through e-commerce; individuals repairing equipment can still work on portable objects at home, to name a few examples. More generally, occupations comprise a bundle of tasks, and while

¹ An exception is Saltiel (2020), who uses STEP surveys.

it may be optimal to work at a specific location and in *face-to-face* (F2F) contact with the public or co-workers, suboptimal work arrangements are also feasible for some occupations, particularly during a pandemic.²

Another caveat of using criteria where at least one sufficient condition has to be satisfied to categorize jobs is that it is not clear how to choose the number of conditions to consider when several alternatives are available. If only one condition needs to be satisfied to classify an occupation as not being able to be done at home, then the more conditions that the researcher adds to the list, the higher are the chances that at least one of them will be satisfied by a given job. For example, one of the data sets used in this paper includes a battery of questions to measure F2F contact. Two of these questions are “How often does your job usually involve sharing work-related information with co-workers?” and “How often does your job usually involve instructing, training or teaching people, individually or in groups?” A priori, both are valid proxy variables for F2F work, but while almost 100 percent of people respond “very often” to the first question in most countries, there is substantially more variation in the responses to the latter. More generally, the more questions we consider to measure F2F, the higher the fraction of workers that would be classified as having an F2F-intensive job. Discarding questions and data based on this empirical observation is somewhat arbitrary.

There are two studies that are exceptions to the one-sufficient-condition criteria. Mongey et al. (2020) construct WFH and physical proximity measures for the United States using O*NET data. For the WFH measure, they use the same set of task variables as Dingel & Neiman (2020a, 2020b), but instead of defining binary indicators, they allow both the WFH and physical proximity measures to vary between 0 and 1. Leibovici, Santacreu, & Famiglietti (2020) construct a contact-intensity measure for the United States using occupation-level information from O*NET and aggregating the possible scores for the question about performing tasks in close physical proximity to other people. The final measure can take a value from 0 to 100.

To measure jobs’ amenability to WFH, we exploit all the variables available in the data that describe job tasks related to home-based work. Instead of using a criterion based on satisfying at least one sufficient condition to classify occupations, we argue that the more (less) the conditions that are satisfied, the lower (higher) the amenability of a given job to be carried out at home. For example, according to our criteria, a job that satisfies three conditions would be less amenable to home-based-work than one that satisfies only one or two of those conditions. Accordingly, we also exploit categorical variables describing the intensity of different tasks, instead of transforming them into binary outcomes. While this approach still relies on the assumption that all

² As a robustness check, we construct an index following a methodology more similar to that of Dingel and Neiman (2020a, 2020b) and Saltiel (2020) where only one condition needs to be satisfied in order for a job not to be amenable to WFH and find that it is highly correlated with our WFH measures (see Figure A 3).

characteristics related to the probability of working from home have the same weight, it exploits more information than a binary approach.

We use four groups of tasks to assess jobs' amenability to WFH. First, we use measures of physical intensity and manual work to capture tasks that are more likely to be location-specific—because they require handling large items or use specific equipment, for example—and cannot be done at home. Second, we use measures of F2F-intensive tasks such as those that involve supervision or contact with the public. Third, we create an index of ICT use at work, to reflect the fact that while some jobs may require substantial F2F intensity, some of such tasks can be carried out using ICT and do not necessarily have to be done in-person. Finally, and in contrast to existing studies, we also exploit information on having an internet connection at home as an important factor to determine the likelihood of a remote setup. This is important since workers in developing countries who may use ICT and have internet connectivity at the workplace, do not necessarily have access to the same resources at home. Another reason why we estimate the amenability—and not the fraction—of jobs that can be performed remotely for such a large set of countries is that several of the surveys were collected circa 2012, when internet connectivity was significantly lower than today. However, under the assumption that relative connectivity across countries or types of workers remained stable, our estimates can still be used to compare the WFH measures across these categories.³

We find that the social distancing measures associated with COVID-19 may exacerbate the jobs divide that preceded the crisis. The jobs intensive in tasks that are amenable to WFH are more prevalent in richer countries, and among workers with high levels of education, in salaried employment and with access to social insurance. Low-income, self-employed, and informal workers are not only less likely to do their jobs when WFH is the only option, but also less likely to have access to income protection schemes if these are channeled through the existing social security infrastructure.

Our findings highlight the importance of social protection programs to safeguard the most vulnerable during the crisis. Efforts to reach informal workers are crucial since they are less likely to have access to existing social insurance benefits, and also to additional programs launched in response to the crisis through the social security or tax administration infrastructures. Our results also show the importance of fostering technology adoption to protect jobs while respecting social distancing measures. To a large extent, the between and within country divide in WFH amenability is driven by unequal access to ICT. These benefits of digital technologies should be considered by governments in developing countries when investing in broadband infrastructure.

³ In fact, the coefficient of correlation between the share of internet users by country in 2012 vs 2017 is 0.94 (own estimates based on data from World Development Indicators, WDI).

Finally, it is important to mention that this paper does not consider the role of essential sectors or workers (whose jobs are not affected by social distancing measures) since there is substantial heterogeneity in these policies between and within countries that cannot be fully accounted for in this paper.⁴ Our individual-level measures of WFH amenability, however, can be used to assess the potential impacts of essential work policies.

The rest of this paper is structured as follows. Section 2 describes the data and the main features of the methodology. Section 3 describes the results and Section 4 concludes. The paper includes an Appendix with more detailed information on the methodology, and the estimated indexes by detailed socioeconomic group and country.

2. Data

We use three data sets covering 53 countries at different levels of development to estimate our WFH measure (see Table 1). First, we use the Surveys of Adult Skills of PIAAC (Programme for the International Assessment of Adult Competencies) for 35 countries. This survey collects information about working-age individuals and covers both rural and urban areas. Second, we use the STEP (Skills Towards Employability and Productivity) surveys for 15 developing countries.⁵ The surveys are representative of urban areas (except Sri Lanka and the Lao People's Democratic Republic, which included both urban and rural areas) and collect information about working-age individuals. Finally, we use the Labor Market Panel Surveys (LMPS) for three countries in the Middle East and North Africa (MENA) region, namely the Arab Republic of Egypt, Jordan and Tunisia. These are standard labor force surveys that, in addition to the typical labor market information, also collect data about specific tasks carried out at work. Our final sample for all three data sets includes employed individuals ages 16 to 64 years.

⁴ Garrote Sanchez, Gomez Parra, Ozden, & Rijkers (2020) consider the role of essential workers in their assessment of WFH measures in the European Union.

⁵ We exclude China since the data are only representative of Yunnan province. There is no STEP survey for El Salvador, thereby we use instead a skills survey that includes a similar questionnaire.

Table 1. List of skills surveys

Dataset	Countries	Year
PIAAC	Austria, Belgium (Flanders), Canada, Czech Republic, Denmark, Estonia, Finland, France, Germany, Ireland, Italy, Japan, Korea, Netherlands, Norway, Poland, Russian Federation, Slovak Republic, Spain, Sweden, United Kingdom (England and Northern Ireland), United States	2011/2012
	Chile, Greece, Israel, Lithuania, New Zealand, Singapore, Slovenia, Turkey	2014/2015
	Ecuador, Hungary, Kazakhstan, Mexico, Peru	2017
STEP	Bolivia, Colombia, Lao PDR, Sri Lanka, Vietnam	2012
	Armenia, El Salvador, Georgia, Ghana, Kenya, North Macedonia, Ukraine	2013
	Serbia	2015/2016
	Kosovo, Philippines	2015
LMPS	Tunisia	2014
	Jordan	2016
	Egypt	2018

Table 2 shows the types of tasks used to estimate the WFH index, Appendix 1 describes the rationale for choosing these tasks, and Table A 1 in Appendix 2 shows the complete list of variables. Such variables are slightly different across the three data sets. For example, while STEP has information on whether the job requires contact with customers, such information is not collected in the LMPS for Jordan and Tunisia. Thereby, while the indexes can be compared across countries within the STEP, PIAAC and LMPS data sets, comparisons are not possible across them.

Table 2. Description of the task indexes

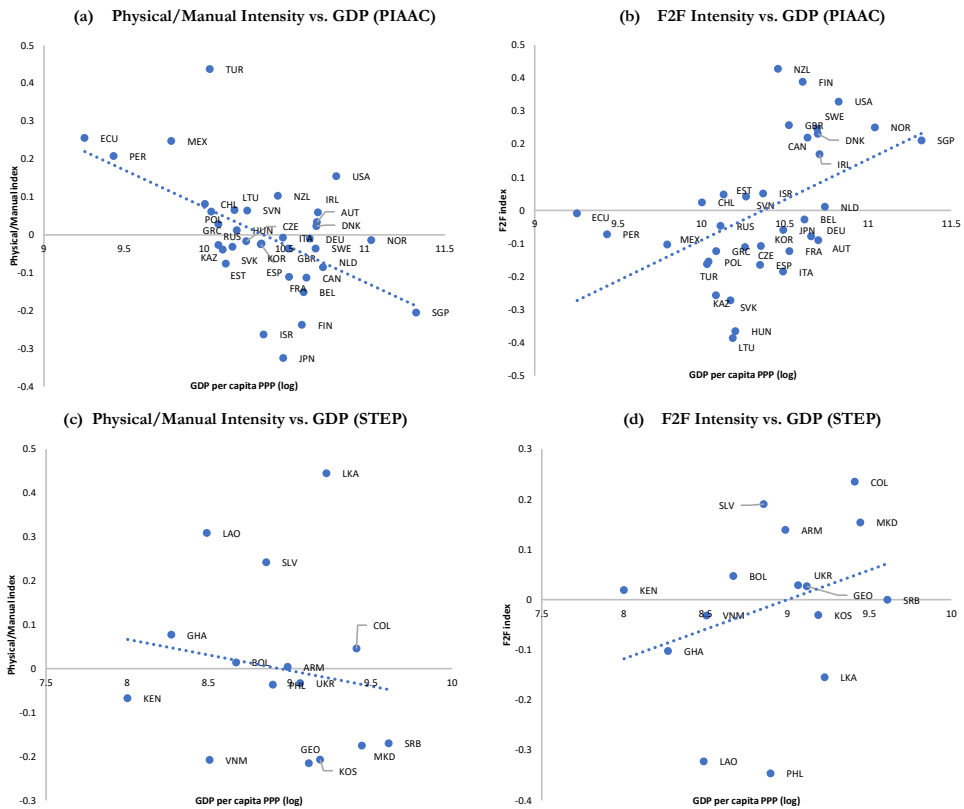
Task index	Tasks
a) Physical and manual (a higher value indicates more physical/manual intensity)	Job is physically intensive Repairing equipment Operating heavy machinery
b) Face-to-Face (F2F) (a higher value indicates more F2F intensity)	Supervising others Contact with customers, public, students
c) Low ICT use at work (a higher value indicates lower ICT use at work)	Low or no computer use at work Low or no cell phone use at work
d) Low ICT at home (based on a dummy variable equal to one if the home has no internet connection)	No internet connection at home
e) WFH (a higher value indicated higher WFH amenability)	Combination of Physical/Manual, F2F, Low ICT use at work, multiplied by -1
f) WFH adjusted (a higher value indicated higher WFH amenability)	Combination of Physical/Manual, F2F, Low ICT use at work, Low ICT at home, multiplied by -1

3. Results

3.1 Cross-country results

Figure 1 shows the correlation between the physical/manual and F2F task indexes and GDP per capita. The magnitude of the indexes is equivalent to the number of standard deviations above/below the average worker among all the countries in the sample. For example, a physical/manual index equal to 0.45 in the case of Turkey (Figure 1, panel (a)) means that jobs in Turkey are on average 0.45 standard deviations above that of the average worker among PIAAC countries in terms of physical/manual intensity. Richer countries have jobs less intensive in physical/manual skills (Figure 1, panels (a) and (c)). This factor would tend to reduce the amenability of jobs to be done at home disproportionately among poorer countries, given that their jobs would tend to be more location or equipment-specific according to this measure. In contrast, the intensity of jobs in F2F tasks tends to increase with economic development (Figure 1, panels (b) and (d)). This is driven by jobs intensive in non-routine interpersonal tasks, whose duties require more supervision or contact with the public.

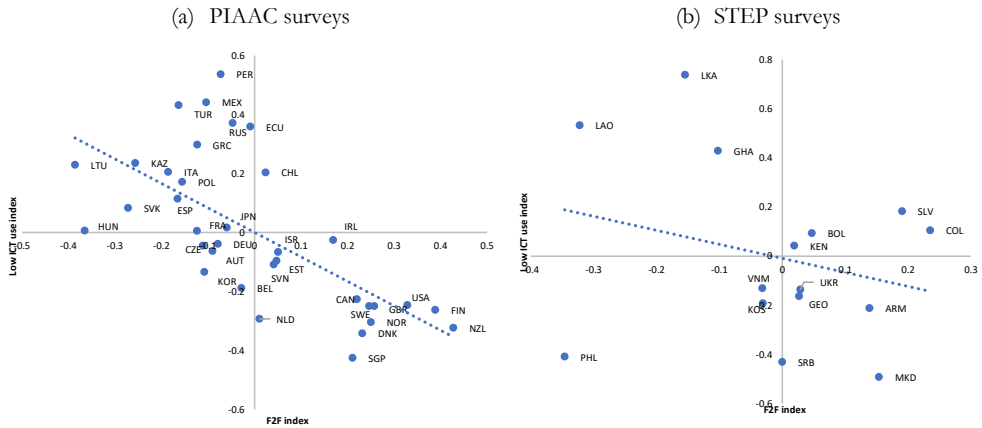
Figure 1. Physical/Manual and F2F intensity, by GDP per capita



Note: The vertical axis measures the corresponding task index, in standard deviations from the mean for all PIAAC/STEP countries. GDP per capita PPP comes from the World Development Indicators (WDI) and corresponds to the same year of the respective PIAAC and STEP surveys.

The fact that the intensity of jobs on physical/manual tasks tends to decline with economic development, and that the intensity on F2F tasks shows the opposite pattern suggests that two opposing forces are at play when shaping the relationship between WFH measures and GDP per capita. However, F2F occupations also tend to be more intensive in ICT use. As seen in Figure 2, countries such as Singapore or the United States that have jobs more intensive in F2F tasks also use more ICT at work than countries such as Lithuania or Kazakhstan. That is, several of the tasks embedded in such occupations are more prone to be performed remotely. In other words, ICT use at work would tend to weaken the effect of F2F intensity on WFH measures. This correlation between F2F tasks and ICT use at work can also be observed within countries (see Figure A 1 in Appendix 2).

Figure 2. ICT use and F2F intensity across countries

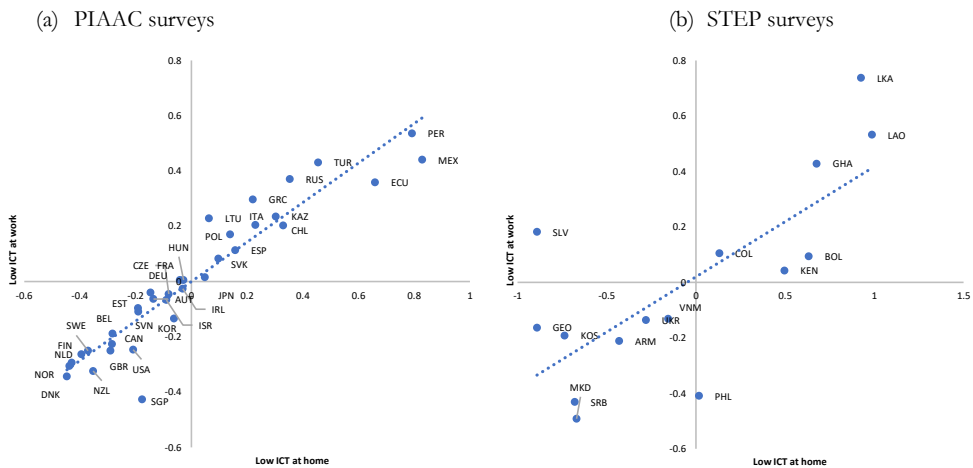


Note: The vertical axis measures the Low ICT use index (a higher value means lower ICT use at work), while the horizontal axis measures F2F contact index (a higher value means more intense F2F contact). Both indexes in standard deviations from the mean for all PIAAC/STEP countries.

Figure 3 illustrates the importance of distinguishing between ICT use at work and the availability of an internet connection at home. While both variables are highly correlated—i.e. countries where people use more ICT at work also have higher internet connectivity at home—there are some differences, particularly among less developed countries.⁶ For instance, Peru, Mexico and Ecuador are closer to the average with respect to ICT use at work, but are lagging more with respect to internet access at home. Accordingly, while the Philippines ranks relatively high in terms of ICT use at work, it has relatively low levels of internet connectivity at home (Figure 3 (b)). Thereby, while their jobs could be amenable to telecommuting based on a tasks approach, poor internet connectivity implies that many workers may not be able to do their jobs at home.

⁶ While El Salvador stands out as an outlier, this could be driven by the fact that the variable to measure internet access at home is not available in its STEP survey so we use a different approach, combining two questions on having a computer and fixed telephone access at home.

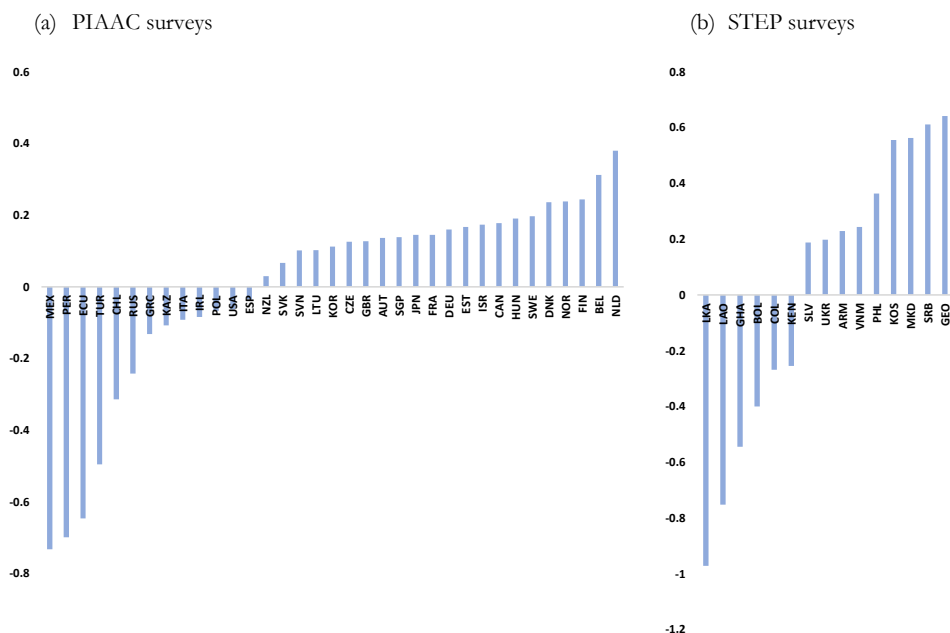
Figure 3. ICT use at work and at home



Note: The vertical axis measures the Low ICT use index (a higher value means lower ICT use at work), while the horizontal axis measures the Low ICT at home index (a higher value means poorer internet access at home). The variable to measure internet connectivity at home is not available for El Salvador, thereby we use a different approach for this country. We consider that households have internet access at home if they have a computer and fixed telephone access.

When combining the four indexes, we find substantial cross-country variation in the amenability of jobs to working from home. As seen in Figure 4, the most vulnerable countries in the PIAAC sample are Turkey and those from the LAC region. In the STEP sample, countries from the ECA region have jobs more amenable to working from home, while the opposite is true for Sri Lanka, Lao PDR, and Ghana. In contrast to Dingel & Neiman (2020a), we find that the United States ranks lower than most OECD countries in terms of its jobs' amenability to working from home. Our findings are consistent with Hardy et al. (2018), who use the PIAAC surveys and find that the United States has more jobs that are more manually intensive than most other countries.

Figure 4. WFH amenability index across countries.



Note: Each bar shows the number of standard deviations below/above the mean. A higher value indicates a greater amenability of jobs to working from home. The magnitude of the estimates is not comparable between the PIAAC and STEP datasets.

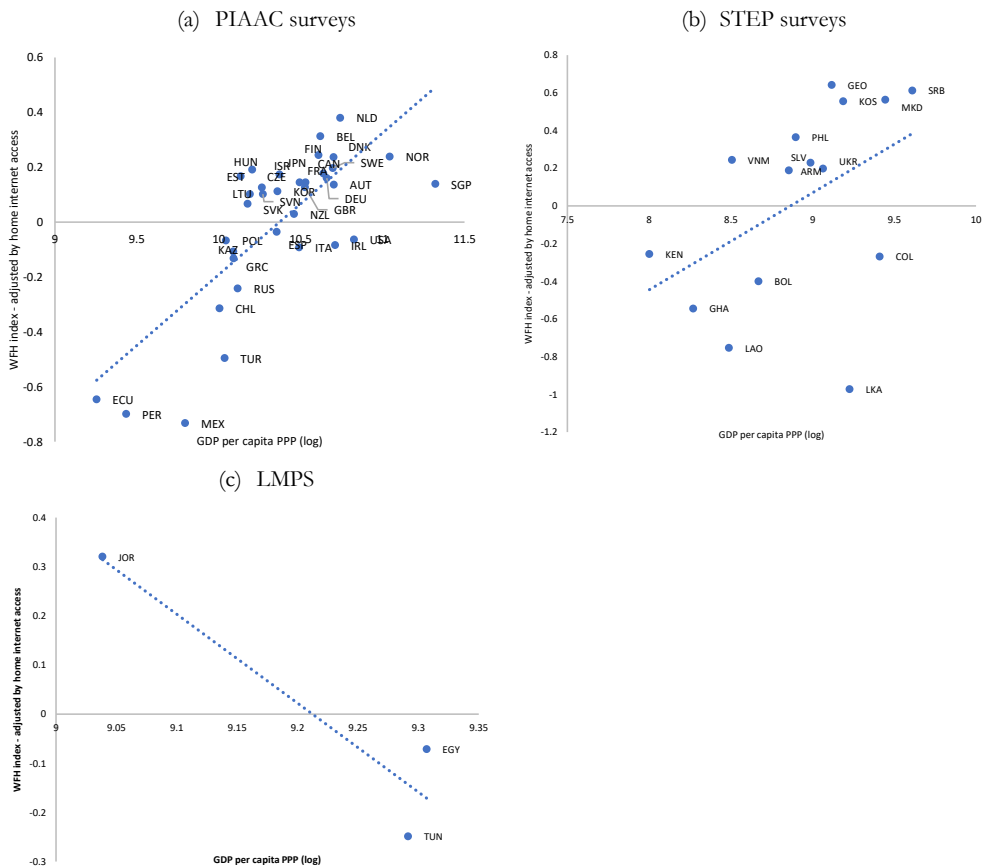
The difference between our results and those of Dingel & Neiman (2020a) seems to be driven by the fact that while the United States has a higher share of jobs in occupations that are more amenable to working from home than other countries, the tasks associated with these occupations are different across countries and tend to be less favorable to working from home in the United States. Figure A 2 in Appendix 2 illustrates this issue using Norway, the United States and Spain as examples. The United States has 61 percent of its jobs in the four occupational categories that are more amenable to WFH, a figure higher than for Norway (55 percent) and Spain (59 percent). If we imputed the US WFH measures to each occupation of these other two countries (as in Dingel & Neiman, 2020a), we would conclude that jobs are more amenable to WFH in the United States. However, when comparing the same occupations across countries, we find that most occupations in the United States are less amenable to WFH than in Norway and Spain. For example, the US WFH index for technicians is far lower than that for Norway and Spain. In other words, these findings illustrate the importance of using measures of tasks that vary across occupations and countries, since occupations are not associated with the same tasks in different economies.

Our findings also shed light on the importance of using task measures that vary at the individual level instead of at the occupation level. A simple decomposition shows that less than half of the variation in the WFH index is explained by variation between 4-digit ISCO occupations (see Table A 2 in the appendix). Most of the variation in the tasks related to WFH takes place within narrowly defined occupations.

The correlation between economic development and the amenability of jobs to working from home is positive within the PIAAC and STEP datasets. When we also consider the availability of internet access at home, the relative ranking of countries does not change significantly. That is, poorer countries have a lower share of jobs that are amenable to be done at home (Figure 5). For example, the Netherlands is 0.38 standard deviations above the average PIAAC country in terms of its jobs' amenability to working from home, while Ecuador and Turkey are 0.65 and 0.5 standard deviations below the average, respectively. In the PIAAC sample, other countries whose jobs are also more amenable to WFH are Belgium and the Nordic countries. In contrast, Peru, Mexico, and Chile have jobs that are more vulnerable in this regard. The correlation between GDP per capita and the WFH measure is negative for the LMPS countries, as Jordan ranks higher in terms of WFH amenability despite having a lower level of GDP per capita. However, this may be explained by Jordan having higher internet penetration than Egypt and Tunisia.⁷

⁷ According to data from the World Development Indicators, the share of internet users in the corresponding survey year was 62.3 percent in Jordan, and 46.9 and 46.1 in Egypt and Tunisia, respectively.

Figure 5. WFH amenability and GDP per capita



Note: The vertical axis measures the corresponding task index, in standard deviations from the mean of the (A) PIAAC, (B) STEP and (C) LMPS samples. A higher value indicates that jobs are more amenable to WFH.

3.2 Within-country findings

There are large disparities in terms of jobs' amenability to working from home within countries. Figure 6 shows differences with respect to the average worker for the whole PIAAC, STEP and LMPS data sets.⁸

Across most countries, women are more likely to have jobs more amenable to WFH. This is because they are less likely to have jobs intensive in physical/manual work than men. Educational attainment is strongly linked

⁸ Tables showing country-level findings are available in the Online Appendix (http://www.hernanwinkler.com/uploads/5/5/1/1/5511764/appendix_jobs_amenability_to_wfh_v13.xlsx).

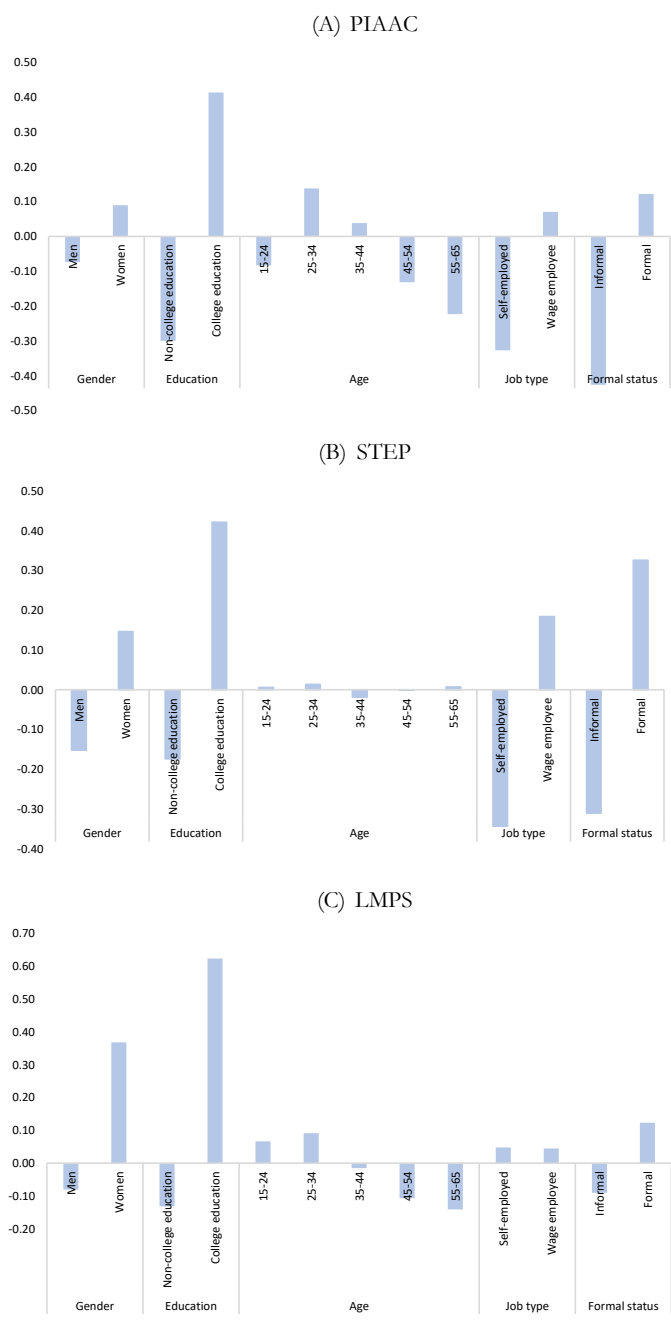
to WFH amenability, since college graduates in all 53 countries have jobs more amenable to WFH than their less educated peers.

Older workers are less likely to have jobs' amenable to WFH in most countries, and this is due to a combination of counteracting forces. On the one hand, the F2F intensity increases and ICT use declines with age, which tends to reduce older workers' jobs amenability to WFH. On the other hand, the physical/manual intensity declines with age, making jobs of older workers more amenable to WFH. However, the latter is not strong enough to counteract the role of F2F and ICT tasks for older workers.

Self-employment is associated with lower amenability to WFH in most countries. Their jobs require more physical/manual intensity and require more F2F interaction. On the other hand, they are more likely to use ICT at work than salaried workers, but this factor does not affect their WFH measure to a large extent.

Workers with a formal job—either because they have a contract (PIAAC) or social security contributions (STEP and LMPS)—are more likely to have jobs amenable to WFH than their informal counterparts. This is because informal workers have more physical/manual intensive jobs and lower ICT use at work. This is important because informal workers are less likely to be protected against important risks. For example, subsidies and other forms of assistance during the COVID-19 crisis are easier to implement when using the social insurance infrastructure, which often only includes formal workers.

Figure 6. WFH (adjusted for home internet access), by individual characteristics.

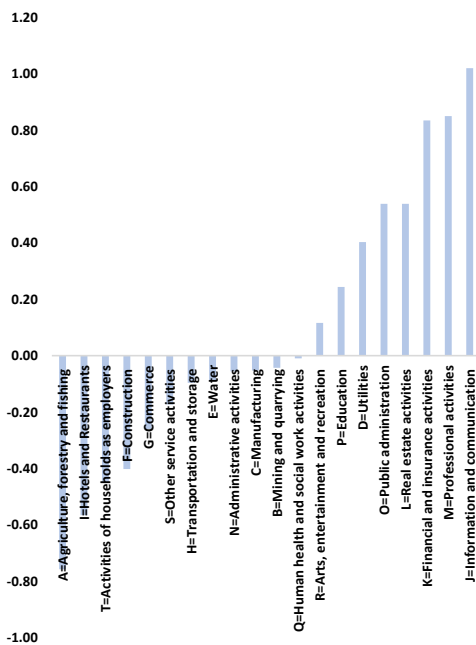


Covid Economics 19, 18 May 2020: 211-240

Note: The vertical axis measures the WFH index adjusted by internet access at home, in standard deviations from the mean of the (A) PIAAC, (B) STEP and (C) LMPS samples. A higher value indicates that jobs are more amenable to WFH.

The sectors that emerge as more amenable to WFH tend to be the same across most countries in the PIAAC and LMPS data sets. These sectors include ICT, professional services, the public sector, and finance (Figure 7). In contrast, jobs in hotels and restaurants, agriculture, construction, and commerce are the least amenable to WFH.

Figure 7. WFH index by sector of economic activity, PIAAC sample



Note: The vertical axis measures the WFH index adjusted by internet access at home, in standard deviations from the mean of the PIAAC sample. A higher value indicates that jobs are more amenable to WFH.

Finally, we regress the WFH index for each data set on individual and job characteristics and confirm that even after controlling for observable characteristics, women, college graduates and salaried workers are more likely to have jobs amenable to WFH than men, lower educated, and self-employed workers (Table 3).⁹

⁹ Tables showing country-level findings are available in the Online Appendix (http://www.hernanwinkler.com/uploads/5/5/1/1/5511764/appendix_jobs_amenability_to_wfh_v13.xlsx).

Differences in educational attainment predict large gaps in WFH measures: the jobs of college graduates are 0.70 standard deviation more amenable to WFH than those of their less educated counterparts in the PIAAC sample. That figure for the MNA region is 0.61. In all three samples, workers aged 25 and older have jobs less amenable to WFH than those 24 years or younger. In PIAAC countries, the relationship between amenability to WFH and age has an inverted U-shaped pattern, where those aged 25 to 34 years have the jobs most amenable to WFH, while those younger than 25 and older than 55 are at the opposite end. Among countries in the STEP and LMPS data sets, workers in the youngest age bracket have the jobs most amenable to WFH, but there are little differences by age among those aged 25 to 65.

Table 3. OLS regression of the WFH index (adjusted for home internet access)

	PIAAC	STEP	LMPS
Women	0.0611 [0.00613]***	0.282 [0.0118] ***	0.38 [0.0167]***
College education	0.702 [0.00642]***	0.429 [0.0136] ***	0.615 [0.0173]***
25-34	0.305 [0.0141]***	-0.117 [0.0182] ***	-0.0788 [0.0213]***
35-44	0.302 [0.0121]***	-0.146 [0.0190] ***	-0.144 [0.0215]***
45-54	0.224 [0.0119]***	-0.157 [0.0196] ***	-0.162 [0.0229]***
55-65	0.0747 [0.0122]***	-0.138 [0.0232] ***	-0.139 [0.0292]***
Wage employee	0.204 [0.00870]***	0.117 [0.0138] ***	0.0471 [0.0155]***
Constant	-1.045 [0.0264]***	-0.220 [0.0192] ***	-0.297 [0.0240]***
Observations	138,954	20,259	22,088
R-squared	0.21	0.320	0.148

Notes: All models include country fixed effects. Robust standard errors in brackets. *** $p < 0.01$, ** $p < 0.05$, * $p < 0.1$

4. Concluding Remarks

This paper provides new evidence on which countries and types of workers have jobs that are less amenable to working from home. Using data from 53 countries on the types of tasks that each person does at work—as

opposed to occupation-level measures from the United States—it finds that poorer countries and workers who are male, with lower levels of education, self-employed, and with informal jobs are more vulnerable to social distancing policies, since the nature of their jobs makes them less amenable to working from home. These findings highlight the importance of income protection policies for workers who are not in the formal sector and thereby are less likely to be reached by social protection programs channeled through formal mechanisms. At the same time, it highlights the importance of accelerating ICT adoption to facilitate home-based work when working on-location is not an option. Finally, it shows that using individual information on the tasks that people do at work is important, since occupations capture only half or less of the types of tasks that workers do on-the-job.

REFERENCES

- Avdiu, B., & Nayyar, G. (2020). When face-to-face interactions become an occupational hazard: Jobs in the time of COVID-19. Retrieved April 22, 2020, from <https://www.brookings.edu/blog/future-development/2020/03/30/when-face-to-face-interactions-become-an-occupational-hazard-jobs-in-the-time-of-covid-19/#cancel>
- Dingel, J., & Neiman, B. (2020a). *How many jobs can be done at home?* Retrieved from University of Chicago website: https://bfi.uchicago.edu/wp-content/uploads/BFI_White-Paper_Dingel_Neiman_3.2020.pdf
- Dingel, J., & Neiman, B. (2020b). How Many Jobs Can be Done at Home? *Centre for Economic Policy Research*. Retrieved from https://cepr.org/active/publications/discussion_papers/dp.php?dpno=14584
- Garrote Sanchez, D., Gomez Parra, N., Ozden, C., & Rijkers, B. (2020). *Which jobs are most vulnerable to COVID-19? Analysis of the European Union*.
- Hardy, W., Lewandowski, P., Park, A., & Yang, D. (2018). *THE GLOBAL DISTRIBUTION OF ROUTINE AND NON-ROUTINE WORK*.
- Leibovici, F., Santacreu, A. M., & Famiglietti, M. (2020). Social distancing and contact-intensive occupations. *On the Economy, St. Louis FED*.
- Lo Bello, S., Sanchez-Puerta, L., & Winkler, H. (2019). *From Ghana to America The Skill Content of Jobs and Economic Development*. Retrieved from <http://www.worldbank.org/research>.
- Mongey, S., Pilosoph, L., & Weinberg, A. (2020). Which Workers Bear the Burden of Social Distancing Policies? *University of Chicago, Becker Friedman Institute for Economics Working Paper*, (2020–51).
- Saltiel, F. (2020). *Who Can Work From Home in Developing Countries?* 1–15.

Appendix 1. Measuring the amenability of jobs to working from home

If data constraints did not exist, we argue that the probability that a job can be done at home during the COVID-19 can be modeled as:

$$\Pr(WFH = 1) = F(x, z, \varepsilon)$$

Where WFH is a dummy variable equal to 1 if the job cannot be done at home, and zero otherwise; x and z are vectors of observable and unobservable variables summarizing characteristics of the job, and ε is a random term. The observable characteristics of the job may include the extent to which it requires special equipment, supervision of others, etc. Unobservable characteristics include whether the job is considered essential by local authorities, whether the employer can financially support remote operations, etc. These variables can be summarized in a latent variable y^* :

$$y^* = x'\beta + z'\gamma + \varepsilon$$

Where

$$WFH = 1 \text{ if } y^* > 0,$$

$$WFH = 0 \text{ if } y^* \leq 0,$$

The vectors of parameters β and γ can be thought of as weights. For example, lifting heavy items at work may be a more important factor to determine the probability to WFH than having to repair equipment.

If we observed WFH during the COVID-19 crisis and had information on the job's characteristics x before the crisis, the vector of parameters β could be estimated using a standard binary choice model. However, since data on WFH are not available, we only have data on x to rank jobs by their likelihood to be done remotely. Thereby, we need to make assumptions about the values of the weights β .

We construct four indices that can be interpreted as latent variables for the probability of not working from home during COVID-19:

- (1) Physical/Manual: $PH = f(p)$
- (2) Face-to-face: $F2F = f(f)$
- (3) Low ICT use at work: $Low\ ICT\ work = f(iw)$
- (4) Low ICT at home: $Low\ ICT\ home = f(ih)$

Where p, f, iw and ih are vectors of tasks. The Physical/Manual index reflects the fact that some jobs are intensive in tasks that are location-specific and cannot be performed remotely. Examples include low-skilled

jobs in mining, cleaning or in a capital-intensive manufacturing, middle-skilled jobs in equipment repairs, and high-skilled jobs that require specialized equipment such as in laboratory research. The F2F index measures the extent to which jobs require in-person interactions, that is those where the worker must be in the same place as his or her co-worker(s), supervisor, subordinate, customer, public or students.

To distinguish between face-to-face interactions that must be carried out in-person as opposed to those that can be done remotely, we construct a third index to reflect the fact that some of these face-to-face interactions can be done using Information and Communication Technologies (ICT), i.e. the low ICT at work index. Finally, we create a fourth index to capture the availability of an internet connection at home (low ICT at home index).

The *WFH* index is a combination of the physical/manual task index, the F2F index, the low ICT at work index and the low ICT at home index. The later captures the lack of internet connectivity at home. This is important since many workers may carry out activities that can be easily done at home, but the lack of connectivity could make it impossible.

A limitation of the data is that ICT use increased dramatically since the time that several of the surveys were collected. Assuming that the share of ICT users remained stable is not consistent with reality, since the share of internet users increased by about 65 percent in low and middle-income countries since 2012, the year of the oldest survey of our dataset.¹⁰ Thereby, this is another reason for which is not possible to estimate the fraction of jobs that can be conducted currently using ICT. However, under the weaker assumption that the relative use of ICT across countries, types of jobs or workers remained stable over time, we provide new insights on what type of workers and jobs are more vulnerable to social distancing measures.

The components of each vector, for each dataset, are listed in **Table A 1**. We first standardize each variable within each vector with mean zero and variance one. We then proceed to sum up all the variables within each vector and normalize the sum again to have mean zero and variance one. As mentioned above, each component within tasks receives the same weight. All four indexes are constructed so that higher values indicate a lower amenability to WFH. For example, a higher value of the physical/manual index contributes to reduce the amenability to WFH.

Then, we proceed to estimate the WFH index using the standardize indexes PH, F2F, Low ICT work and Low ICT home. We multiply the sum of the four subindexes by -1 so that a higher value of WFH indicates a higher amenability to WFH. Each of these four components are also given equal weights. That is, an increase in one standard deviation in either of the four tasks measures has the same impact on the WFH index. All the

¹⁰ According to data from the World Development Indicators (WDI), the share of internet users in low and middle income countries increased from 26 to 43 percentage points between 2010 and 2017 (<https://data.worldbank.org/indicator/IT.NET.USER.ZS?locations=XO>).

standardizations are done within the PIAAC, STEP and LPMS datasets, by pooling the surveys for all the countries, to allow for cross-country comparisons.

Appendix 2. Additional tables and figures

Table A 1. Variables capturing tasks for each dataset

A. PIAAC Surveys

Task Index	Variables	Type of variable
Physical & Manual index	How often does your job usually involve working physically for a long period?	Frequency
	How often does your job usually involve using skill or accuracy with your hands or fingers?	Frequency
Face-to-face index	How often does your job usually involve sharing work-related information with co-workers?	Frequency
	How often does your job usually involve instructing, training or teaching people, individually or in groups?	Frequency
	How often does your job usually involve making speeches or giving presentations in front of five or more people?	Frequency
	How often does your job usually involve selling a product or selling a service?	Frequency
	How often does your job usually involve advising people?	Frequency
	How often does your job usually involve persuading or influencing people?	Frequency
	How often does your job usually involve negotiating with people either inside or outside your firm or organisation?	Frequency
Low ICT at work index	Do you use a computer in your job? This includes cellphones and other hand-held electronic devices that are used to connect to the internet, check e-mails etc.	Yes/No
	In your job, how often do you usually use email?	Frequency
	In your job, how often do you usually use the internet in order to better understand issues related to your work?	Frequency
	In your job, how often do you usually conduct transactions on the internet, for example buying or selling products or services, or banking?	Frequency
	In your job, how often do you usually use spreadsheet software, for example Excel?	Frequency
	In your job, how often do you usually use a word processor, for example Word?	Frequency
	In your job, how often do you usually use a programming language to program or write computer code?	Frequency
Low ICT at home index	In your job, how often do you usually participate in real-time discussions on the internet, for example online conferences, or chat groups?	Frequency
	In everyday life, how often do you usually use email?	Frequency
	In everyday life, how often do you usually use the internet in order to better understand issues related to, for example, your health or illnesses, financial matters, or environmental issues?	Frequency
	In everyday life, how often do you usually Conduct transactions on the internet, for example buying or selling products or services, or banking?	Frequency
	In everyday life, how often do you participate in real-time discussions on the internet, for example online conferences or chat groups?	Frequency
	In everyday life, how often do you use spreadsheet software, for example Excel?	Frequency
	In everyday life, how often do you use a word processor, for example Word?	Frequency
WFH adjusted index	In everyday life, how often do you use a programming language to program or write computer code?	Frequency
	Physical & Manual index	
	Face-to-face index	
	Low ICT at work index	
	Low ICT at home index	
	(multiplied by -1)	

Note: PIAAC surveys also collect information on whether a person manage or supervise other workers and about the proportion of time cooperating or collaborating with coworkers. The supervision variable only applies to self-employed people. The cooperation/collaboration variable has several missing values in all countries. We decided not to include any of these two variables in the F2F index.

B. STEP Surveys

Task Index	Variables	Type of variable
Physical & Manual index	As part of this work do you regularly have to lift or pull anything weighing at least 50 lbs?	Yes/No
	What number would you use to rate how physically demanding your work is?	Frequency
	As part of this work do you repair / maintain electronic equipment?	Yes/No
	As part of this work do you operate or work with any heavy machines or industrial equipment?	Yes/No
Face-to-face index	As part of this work, do you have any contact with people other than co-workers, for example with customers, clients, students, or the public?	Yes/No
	As a normal part of this work do you direct and check the work of other workers (supervise)?	Yes/No
	Using any number from 1 to 10, where 1 is little involvement or short routine involvements, and 10 means much of the work involves meeting or interacting for at least 10-15 minutes at a time with a customer, client, student or the public, what number would you use to rate this work?	Frequency
Low ICT at work index	As part of this work do you (did you) regularly use a telephone, mobile phone, pager or other communication device?	Yes/No
	As part of your work do you(did you) use a computer?	Yes/No
	How often do you (did you) use a computer at work?	Frequency
Low ICT at home index	Does anybody in the household own (in working condition) any internet connection/internet access?	Yes/No (all countries except EL Salvador)
	Does anybody in the household own (in working condition) a computer?	Yes/No (El Salvador)
	Does anybody in the household own (in working condition) a fixed telephone line?	Yes/No (El Salvador)
WFH adjusted index	Physical & Manual index	
	Face-to-face index	
	Low ICT at work index	
	Low ICT at home index	
	(multiplied by -1)	

C. LMPS

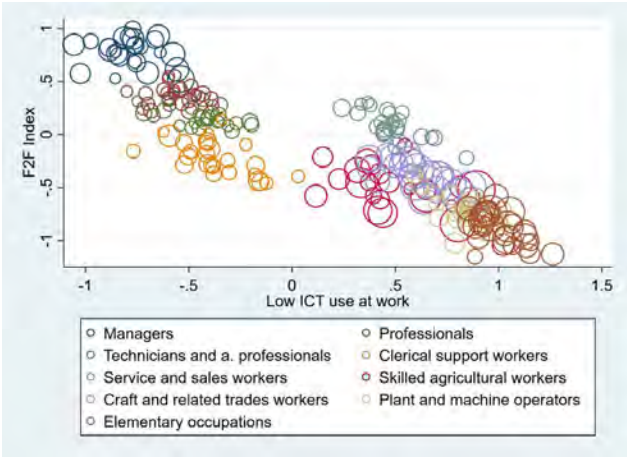
Task Index	Variables	Type of variable
Physical & Manual index	Are you exposed to bending for a long time?	Yes/No
	Does your job require physical fitness?	Yes/No
	Is the individual engaged in a craft-related job?	Yes/No
Face-to-face index	Does your job require supervising others?	Yes/No
Low ICT at work index	Do you use a computer in your work?	Yes/No
	If so, is this computer connected to the internet?	Yes/No
Low ICT at home index	Do you have access to internet at home?	Yes/No
	Does your family have internet connection?	Yes/No
	Does your family own a wireless internet router?	Yes/No
WFH adjusted index	Physical & Manual index	
	Face-to-face index	
	Low ICT at work index	
	Low ICT at home index	
	(multiplied by -1)	

Table A 2. Between-within occupations variance decomposition of task indexes

	Peru	UK
Physical-manual		
Explained variance	1098.1	2470.79
Unexplained variance	3192.94	3103.47
Total	4291.04	5574.27
Explained %	26%	44%
Unexplained %	74%	56%
ICT Reverse		
Explained variance	3165.28	1723.52
Unexplained variance	2922.33	2241.61
Total	6087.61	3965.13
Explained %	52%	43%
Unexplained %	48%	57%
Face-to-face		
Explained variance	1947.61	1854.37
Unexplained variance	3080.34	3175.28
Total	5027.95	5029.65
Explained %	39%	37%
Unexplained %	61%	63%
Work-from-home		
Explained variance	2187.99	2191.44
Unexplained variance	3246.55	2636.51
Total	5434.54	4827.94
Explained %	40%	45%
Unexplained %	60%	55%

Note: Estimated using an OLS regression of each task index on a set of 4-digit ISCO dummy variables. The Between-occupations component is the share explained by the model, while the Within-occupations component is the unexplained variance (the residuals).

Figure A 1. F2F intensity and ICT use at work, variation across occupations and countries



Note: PIAAC sample. Each bubble shows the average F2F and Low ICT use at work index for each 1-digit ISCO occupation and country. The size of the bubble is proportional to the employment share of each occupation in the country. The task indexes are residuals of a regression on country fixed effects, to net out average cross-country differences.

Figure A 2. WFH index and occupational shares in Norway, US and Spain

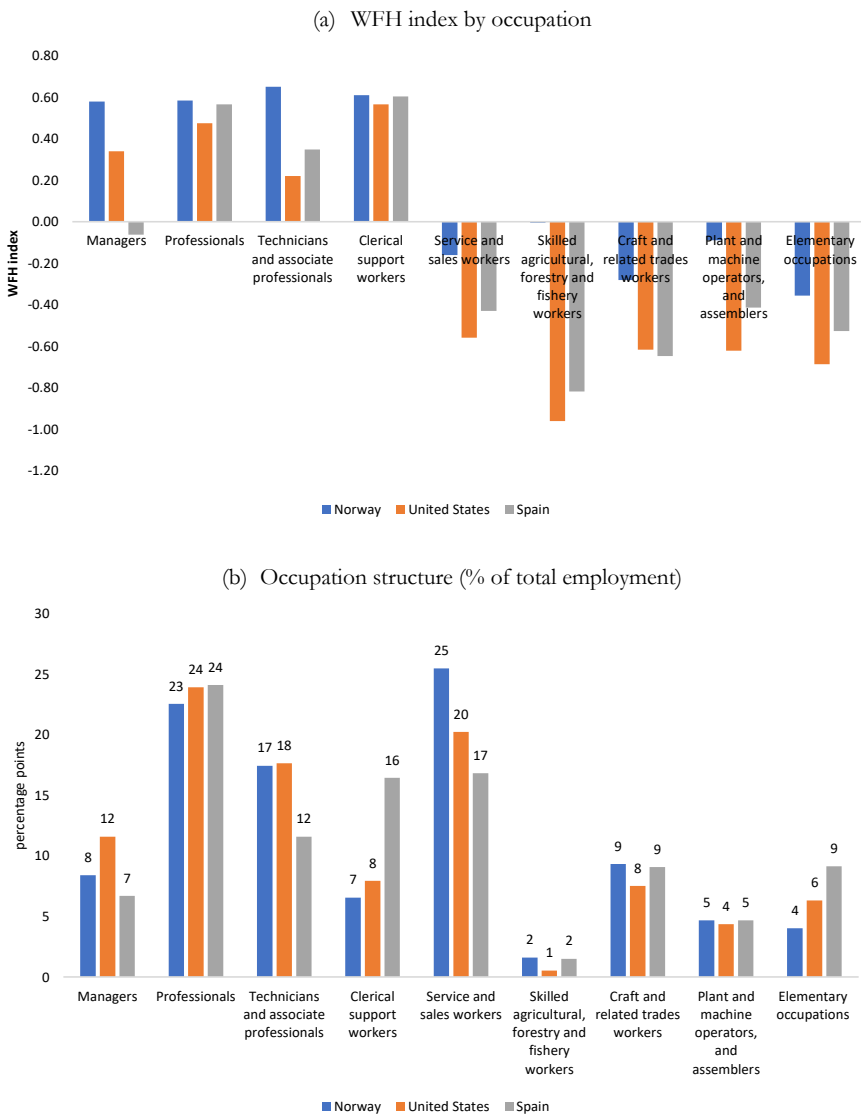
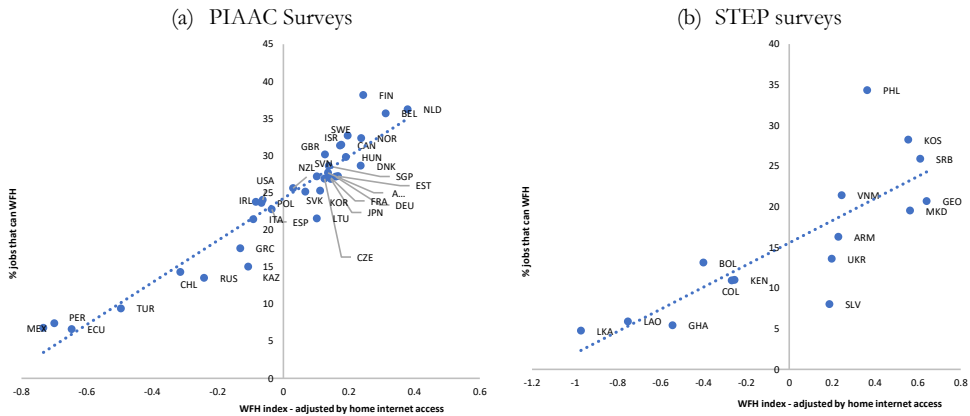


Figure A 3. Correlation with Dingel and Neiman-like measures



Note: The vertical axis measures the share of jobs that can be done from home, following a methodology similar to Dingel & Neiman (2020a, 2020b). We restrict the set of task variables to those closer to the ones used by Dingel & Neiman (2020b). For the PIAAC sample, we define a job as unable to be done from home if at least one of the following conditions is met: (i) the job requires working physically for a long period at least once a week, (ii) the frequency of email use is less than once a month, (iii) the job involves selling products or services at least once a week. Using this definition, we obtained values very close to those reported by Dingel & Neiman (2020a) in Figure 2. For the STEP sample, we use the calculations obtained by Saltiel (2020).

Covid: Not a great equaliser¹

Vincenzo Galasso²

Date submitted: 10 May 2020; Date accepted: 11 May 2020

Coronavirus has been portrayed as the “great equalizer”. None seems immune to the virus and to the economic consequences of the lockdown measures imposed to contain its diffusion. We exploit novel data from two real time surveys to study the early impact on the labor market of the lockdown in Italy – one of the two countries, with China, hit hard and early. COVID was not a “great economic equalizer.” Quite on the contrary. Low-educated workers, blue collars and low-income service workers were more likely to have stopped working both three-week and six-week after the lockdown. Low-educated workers were less likely to work from home. Blue collars worked more from their regular workplace, but not from home. Low-income service workers were instead less likely to work from the regular workplace. For both blue collars and low-income service workers, the monthly labor income dropped already in March. Not surprisingly, they were less in agreement with the public policy measures that required the closing of (non-essential) business and activities. Some positive adjustments took place between the third and the sixth week from the lockdown: the share of idle workers dropped, as the proportion of individuals working at home and from their regular workplace increased. However, these adjustments benefitted mostly highly educated workers and white collars. Overall, low-income individuals faced worse labor market outcomes and suffered higher psychological costs.

1 Nicola Barileto and Marco Lo Faso provided excellent research assistance. Financial Support from Unicredit Foundation is gratefully acknowledged. Survey Data from the project Attitudes on COVID-19: A comparative Study chaired by Sylvain Brouard and Martial Foucault (Sciences Po).

2 Department of Social and Political Sciences, Bocconi University.

Copyright: Vincenzo Galasso

Introduction

As none is immune to it, the coronavirus has been portrayed as the “great equalizer”². Yet, early medical records have soon shown that mortality and vulnerability to COVID largely differ across gender and age (Zhou et al., 2020). The coronavirus takes a higher toll on men, elderly people and individuals with health preconditions, who are more likely to require ICU treatments and less likely to survive. Besides the direct harm of the coronavirus on public health worldwide, the lockdown measures introduced to stop the diffusion of the contagion have imposed huge economic costs (Baldwin and di Mauro, 2020). In many countries, several non-essential sectors of the economy have been shut down and put on hold for long weeks (or months), with workers remaining idle or unemployed (Boeri et al., 2020, Coibion et al., 2020, Dingel and Neiman, 2020, Kore and Peto, 2020; Ban- not et al., 2020). In some sectors, the global supply chain has been slowed down or interrupted. In other sectors, the strict lockdown implemented in some countries has completely collapsed the demand of goods and services. None seems immune to this economic tragedy. Is the coronavirus the “great economic equalizer”?

To provide an answer to this question,³ we study the early impact on the labor market of the restrictive measures introduced in response to the Coronavirus in Italy – one of the two countries, with China, hit hard and early by COVID. In less than three weeks from the first known case of coronavirus, on March 9th Italy moved to a complete lockdown, with only essential sectors of the economy been allowed to run. We exploit novel data from two real time surveys conducted in Italy at the end of March and in mid-April – hence, three-week and six-week into the lock-down, which provides information on the early dynamics of the Italian labor market. The complete lockdown came quite abruptly – particularly in its extension to the entire national territory. Its length was set to 4 weeks, but a large uncertainty continued to linger on several details and its effective duration. Hosting the third large COVID outbreak after China and Korea, Italy had no neighboring country to learn from. The first wave of our survey, launched on March 27-30, allows us to analyze the very initial phase of the economic shock, in which workers and firms had little time to adjust. Smart working from home represented the only early option. However, this was not feasible for all jobs and workers. In fact, while 35% of the workers moved to smart working and 18% remained in the workplace, 47% had to stop. With a further tightening of the restrictive measures on March 22nd, it became apparent that the lockdown was to last longer than the four weeks initially announced. More substantial adjustments had to occur in the labor market. Our second survey, fielded on April 15-17, captures a later stage of this adjustment process. By mid-April, smart working had been adopted by 41% of the workers, 25% were working outside, but 34% were still idle.

The empirical evidence from these two surveys provides a clear picture of the initial response of the Italian labor market to this sudden stop. COVID was not a “great economic equalizer.” Quite on the contrary. Low-educated workers, blue collars and low-income service workers were more likely to be idle both three-week and six-week after the lockdown. Low-educated workers were less likely to work from home. Blue collars were overrepresented among the workers remaining in their regular

² In a Instagram video, the rock star Madonna called Coronavirus “the great equalizer,” since it “doesn’t care about how rich you are, how famous you are, how funny you are, how smart you are, where you live, how old you are, what amazing stories you can tell.”

³ Some studies argued that COVID-19 will likely increase income inequality, due to a stronger negative effect on more vulnerable categories of individuals, such as young (Bell et al., 2020), women (Alon et., 2020), low educated (Adams-Prassl et al., 2020), Gig economy workers (Stabile et al., 2020).

workplace, but almost absent among those working from home. Low-income service workers were instead less likely to work from the regular workplace. For both blue collars and low-income service workers, the monthly labor income dropped already in March. Not surprisingly, they were less in agreement with the public policy measures that required the closing of (non-essential) business and activities. Overall, low-income individuals fared worse in the labor market and suffered higher psychological costs too. Future studies (a third survey will be launched in June) will further analyze the dynamics of this unequal labor market response to the initial shut-down induced by COVID. However, the current analyze has the opportunity to isolate the response to the initial shock, while the future evolution will largely depend on the timing and the magnitude of the diffusion, of the lockdown measures and of the economic policies introduced to cope with the economic crisis.

Background and Real-time Survey Data

On March 9th, with the official count of COVID-positive individuals at 7985 and of deaths from COVID at 463, Italy entered into a comprehensive, nation-wide lockdown. Containment measures were further tightened on March 22nd, when a Prime Minister's Decree mandated the shut-down of any unessential productive activity, de facto bringing to a halt a large chunk of the Italian economy. The aim of the lockdown was to contain the spread of the coronavirus, to limit pressure on its national health system and, of course, to reduce the death counts. These measures proved successful in the province of Hubei in China. However, the lockdown causes also economic and psychological harms for the restrained individuals (Brooks et al., 2020) and has large economic consequences (see Baldwin and di Mauro, 2020, for a review). On April 14th, the IMF reported estimates of a 9.1% reduction in the Italian GDP for 2020, and a corresponding increase in the unemployment rate from 10.0% in 2019 to 12.7% in 2020.

We use real time survey data from the project REPEAT (REpresentations, PErceptions and ATtitudes on the COVID-19), which allows also a comparison of the labor market responses in other countries, albeit at different stages of the diffusion of the coronavirus – and thus featuring different public policy restraining measures.

The first wave of our survey was launched on March 27-30 by IPSOS on a representative sample of 1000 Italian citizens. The second wave was launched on April 15-17, again on a representative sample of 1000 Italian citizens, of whom around 650 had participated to the first wave. This survey is part of the more comprehensive REPEAT project (REpresentations, PErceptions and ATtitudes on the COVID-19), which collects information on perceptions and individual behavior related to COVID-19 and to public health measures in several countries (Austria, Canada, France, Germany, Italy, New Zealand, UK and USA). Here, we consider the information on the current labor market status of the respondents, on their attitudes towards the restraining measures adopted in Italy, on their satisfaction with the government action during the crisis and on their level of psychological distress.

More specifically, in both waves, our labor market information includes whether an individual has stopped working or continues to work in the usual workplace or from home. From the second wave, we know whether the labor income of the respondents in March has decreased, increased or remained constant, with respect to its usual level, and we have a self-assessment of their future income perspectives. The survey provides also individual information on gender, age, education, in-

come groups, geographical location, employment status (full time or part time worker, self-employed, unemployed or out of the labor force), type of occupation (blue collar, service, white collar, no occupation).

The overall picture that emerges for the Italian labor market is bleak. In our survey, the employment rate prior to the coronavirus was 57% (thus in line with official data). Of these employed individuals, 47% had stopped working three weeks after the lockdown; 35% were working from home and only 18% were still working in their usual workplace. Hence, only 53% of the employed individuals were still actively working three-week into the lock-down. However, whether in their regular place or from home, they were mostly working full time – in fact 34% reports to be working more than usual and only 21% less than usual (45% same as usual).

The REPEAT project allows comparing these outcomes with those of other countries in the surveys, as shown in Table 1. Partially due to the different timing and diffusion of the coronavirus and to the different timing in the introduction (and magnitude) of the restraining measures, Italy appears to have the worse overall labor market outlook. In Germany, where the survey was launched on March 20-21, 53% of the employed respondents were still working in their usual workplace, 24% at home and only 23% had stopped. In France, data from March 31-April 2 shows that 28% had stopped, 34% were working from home and 38% in their usual workplace. In the UK, where the survey was launched on March 25-26, 22% of the employed respondents were still working in their usual workplace, 46% from home and 32% had stopped.

Six-week after the lockdown, the labor market situation in Italy had slightly changed. The share of individuals working from home increased to 41% and of those working outside to 25%, but 34% of the workers were still idle. However, the economic cost of the initial lock-down measures were substantial, as 34% of the individuals reported a lower month income in March (38% among the employed individuals). Moreover, 36% of the respondents were pessimistic about their future labor market outcomes.

Perhaps in response to the economic costs of the lockdown, the support for the main restraining measures changed between the two waves. After three-week of lockdown, two respondents out of three agreed with the public policy measures of closing (non-essential) business and economic activities. After six weeks, the support had decreased to one respondent in two. Instead, the general satisfaction with the action of the government and of the prime minister remained relatively constant around respectively 56% and 42%.

The data from the second wave allows assessing the psychological costs of the lockdown. Individuals were in fact asked a set of questions on social isolation (whether they felt isolated, excluded or missed something) and on mental health (feeling down, without energy, lack of sleep, lack of interest, difficulty in concentrating, etc). Six-week into the lockdown, almost one respondent out of three felt socially isolated and almost one of two experienced mental distress.

COVID: a Great economic (un)equalizer

Data from our survey suggests that, besides the public health problem, six-week into the lockdown many Italians had serious economic and psychological issues. To assess the distributional aspects of

these effects, we use data from the two waves to analyze how the labor market outcomes depend on the pre-existing socio-economic, demographic and occupational characteristics of the respondents. For both waves, our labor market outcomes of interests are whether an individual has stopped working, whether she works from home or whether she works from the usual work place. We run OLS regressions of these outcomes on gender, age groups (young are aged 18-35, adults 36-49, fifties 50-59 and elderly 60+), education (no high school, high school, college or more), income groups (low, medium and high, corresponding to the three terciles of the family income distribution), occupation (blue collars, white collars and service workers, corresponding respectively to 6-9, 1-2 and 3-5 in the 1-digit ISCO classification), working conditions (full time, part time, self-employed, inactive), self-assessed health condition, geographical location (macro regions: north-east, north-west, center, south, islands) and city density (low, medium and high). Standard errors are clustered at province level.

The results, reported in Tables 2 and 3, show several clear patterns of raising inequality in the labor market.

Low educated individuals are more likely to stop working and less likely to work from home. After 3-week of lockdown, the difference in the percentage of idle workers between no high school and college graduate was 0.25, almost entirely driven by the difference in working at home (-0.21). Three weeks later, i.e., 6-week into the lockdown, the difference in idle workers had increased to 0.29 and in working from home had become -0.34. Also the difference in stop working and working from home between high school and college graduate is (statistically and economically) significant and increased between the two surveys. Since the absolute share of idle workers decreased from the end of March to mid-April, while the share of individuals working from home increased, our results suggest that this (positive) adjustment from the initial situation was mostly favored college graduates.

Large differences emerge also with respect to the type of occupation. Compared with white collars, after 3-week of lockdown, blue collars were less likely to work from home (-0.16), more likely to work from the regular workplace (0.08) and overall more likely to be idle (0.08). Three weeks later, these differences had doubled. The difference in idle workers between blue and white collars had increased to 0.16, as the result of an increase to -0.33 of the difference in working from home, only partially compensated by the contemporaneous increase to 0.16 of the difference in working from the workplace. Since the share of idle workers decreased between the two surveys, these results suggest that the positive adjustment come mostly – albeit not exclusively – from white collars.

Also low (family) income workers suffered more in the labor market. After three weeks of lockdown, they were more likely than high (family) income to be idle (0.11), as they were less likely to work from home (-0.13). The difference in idle workers can largely be attributed to low income service workers. As shown in columns 4 to 6 in Table 2, low income service workers are much more likely to be idle, mostly because they were less likely to continue working from their regular workplace. The same pattern for low income service workers is confirmed after 6-week of lockdown (see columns 4 to 6 in Table 3).

Finally, full time workers were initially less likely (than self-employed) to remain idle, mostly because they were more likely to continue working in their regular workplace. The same pattern does not

emerge 6-weeks into the lockdown, due to a stronger adjustment by the self-employed, among whom the share of idle workers dropped from 38% to 26%.

Overall, these results suggest that the initial effect of the lockdown fall disproportionately on the more fragile individuals in the labor market: low educated, blue collars, low income service workers. Some adjustments took place between the third and the sixth week from the lockdown (corresponding to the first and second wave of our survey). Overall, the share of idle workers dropped, as the proportion of individuals working at home and from their regular workplace increased. However, also these positive adjustments had strong differential effects, since they benefitted mostly highly educated workers and white collars.

Data from the second wave allows us to assess the early effect of the lockdown measures on the individuals' current income and on their expectations regarding their future income. Table 4 presents the results from two qualitative questions, which asked respectively whether the respondent's income had dropped in March (relatively to January) and how optimistic or pessimistic the respondent was with respect to the future family income. Consistently with the previous results, the March monthly income was more likely to drop for low income individuals, blue collars and service workers, but less for full time workers. For employed individuals, these reductions were not due to layoffs, which were blocked for two months on March 17, but more likely to the use of alternative instruments (such as unused maternal leaves, extraordinary redundancy fund), which were associated with a drop in the worker's income. Interestingly, the drop in monthly income was less likely among elderly individuals – mostly retirees – since pension benefits were unaffected. When asked about their future income, the elderly remained less pessimistic, perhaps as they do not expect reduction in future pension benefits. Also full time workers, who were less likely to be idle in March, were less pessimistic. Instead, low income individuals (and low income workers, see columns 4 and 5 in Table 4) were substantially more pessimistic about their future income prospects than high income ones.

Does the differential impact of these lockdown measures on the individuals' labor market experience affect their agreement with these public policy measures and their satisfaction with the government action? In both waves of the surveys, questions were asked on the agreement with closing (non essential) business and with closing activities and institutions, as well as on individual satisfaction with the prime minister's action and with the government's action. Results are reported in Tables 5 and 6, respectively for the first (27-30 March) and for second wave (15-17 April). Among the regressors, we add the political ideology of the respondent (left, center, right).

Opposition to the lockdown measures concerning economic activities emerged among the main labor market losers: blue collars, service workers and low income individuals. For these individuals, the disagreement is stronger earlier on. The general agreement with these restrictive policies largely drops from the third to the sixth week into the lockdown: from two individuals out of three to less than one out of two. This reduction is more pronounced among white collars and high income individuals. Satisfaction for the actions of the (left leaning) government and of the prime minister is strongly related to the political orientation of the respondents – and remained relatively constant over time, above 40% for the prime minister and above 55% for the government. Among the main labor market losers, low educated individuals show a consistently low support for the actions of the prime minister and of the government.

The lockdown measures carry also important negative psychological effects (Brooks et al., 2020). Questions posed in the second wave allow us to measure the degree of isolation, exclusion and loss felt by the respondents. We averaged the answers to these questions to construct an exclusion index. Moreover, respondents were asked about their current feelings and behavior: whether they lost interest in doing things, felt depressed, had hard time sleeping, had no energy, were no hungry (or too hungry), felt bad about themselves or their family, had hard time concentrating on reading the newspaper or watching TV, moved too slowly (or too much), had suicidal thoughts. We averaged the answers to all these questions to construct a distress index. Finally, individuals were asked in their opinion how much longer the lockdown should last. Exclusion and distress may depend on the impact of the lockdown measures on the individuals' labor market conditions, but also on their housing conditions and family composition. We thus add to the socio-economic and demographic regressors used earlier information on the respondent family composition (single, with family or living with others) and on their housing conditions (homeownership, room per person, lack of an open space). Not surprisingly, being confined at home, but with the family and more space at disposal, reduces both feelings of exclusion and distress, while having no open space (such a garden or a terrace) increases the sense of distress. The feeling of distress is stronger for women and young individuals, and lower among elderly individuals and people in good health. As expected, low income individuals display more distress and feeling of exclusion, even after controlling for housing, occupational and family characteristics.

Discussion

The picture emerging from two snapshots of the Italian labor market taken three-week and six-week into the lock-down is clear. The initial shock was massive, leading to a halt for almost half of the workers. Among those who were able to continue, two out of three worked from home and only one in three from the regular workplace. On impact, COVID hit much harder the more fragile individuals on the labor market – low educated, blue collars, low income service workers – who were more likely to stop working and to suffer immediate income losses. Not surprisingly, they were less in agreement with the public health measures mandating the closure of non-essential business and activities.

However, some adjustment took place in the labor market after the sudden halt. Six-week into the lockdown, the share of idle workers had dropped to 34%, due to an increase in the use of smart working from home and to some workers returning to their usual workplace. However, also these positive adjustments were uneven, as they mostly affected highly educated workers and white collars.

Hence, after six-week of lockdown, the dis-equalizing effects of the Coronavirus are still strongly visible in the Italian labor market. And they show no sign of going away. Low income individuals are more likely to face psychological problems, such as having feeling of exclusion and distress, and are more pessimistic about their future income prospects.

Economic measures to support low income individuals are thus immediately needed, but also their medium term perspectives look bleak, if effective policies are not implemented to ensure the coexistence of social distancing and on-the-workplace production. In fact, since less affluent individuals

are more likely to work from the regular workplace than from home, these more fragile individuals are more exposed to both health and economic risks.

Reference

Adams-Prassl A., T. Boneva, M. Golin and C. Rauh (2020). Inequality in the Impact of the Corona-virus Shock: Evidence from Real Time Surveys

Alon T., M. Doepke, J. Olmstead-Rumsey and M. Tertilt (2020). The impact of the coronavirus pandemic on gender equality. Covid Economics Vetted and Real-Time Papers, Issue 4

Bell B., N. Bloom, J. Blundell and L. Pistaferri (2020). Prepare for large wage cuts if you are younger and work in a small firm. VoxEU.org 06/04/2020.

Baldwin, R and B Weder di Mauro (2020), Economics in the Time of COVID-19, a VoxEU.org eBook, CEPR Press.

Barrot, J-N., B. Grassi, and J. Sauvagnat (2020) Sectoral effects of social distancing Covid Economics Vetted and Real-Time Papers, Issue 3

Boeri T., A. Caiumi and M. Paccagnella (2020). Mitigating the work-security trade-off while rebooting the economy. Covid Economics Vetted and Real-Time Papers, Issue 2

Brooks, S. K., Webster, R. K., Smith, L. E., Woodland, L., Wessely, S., Greenberg, N., & Rubin, G. J. (2020). The psychological impact of quarantine and how to reduce it: rapid review of the evidence. The Lancet.

Coibion, O, Y Gorodnichenko and M Weber (2020a), "Labor Markets During the Covid 19 Crisis: A Preliminary View," Working Paper.

Dingel J. and B. Neiman (2020). Who can work at home? Covid Economics Vetted and Real-Time Papers, Issue 2

Koren M. and R. Peto (2020) Business disruptions from social distancing. Covid Economics Vetted and Real-Time Papers, Issue 2

Stabile M., B. Apouey and I. Solal (2020). Covid-19, inequality and gig economy workers. VoxEU.org 01/04/2020.

Zhou, F., Yu, T., Du, R., Fan, G., Liu, Y., Liu, Z., Xiang, J., Wang, Y., Song, B., Gu, X. and Guan, L., 2020. Clinical course and risk factors for mortality of adult inpatients with COVID-19 in Wuhan, China: a retrospective cohort study. The lancet.

Table 1: Labor Market Outcomes

	Working from		Stopped	Date of the	Date of the
	Home	Usual Work Place	Working	Survey	Lockdown
Austria	38%	33%	29%	24-26 March	16March
France	34%	38%	28%	31 Mar-2 Apr	17 March
Germany	24%	53%	23%	20-21 March	17 March
Italy	36%	18%	46%	27-30 March	9 March
UK	46%	22%	32%	25-26 March	23 March
USA	34%	28%	38%	26-27 March	--

Author’s calculation using Survey Data from Attitudes on COVID-19: A comparative Study

Table 2: Labor Market after 3-week of Lockdown

VARIABLES	(1)	(2)	(3)	(4)	(5)	(6)
	Stopped Working	Work from Home	Work Outside	Stopped Working	Work from Home	Work Outside
female	0.002 [0.046]	0.007 [0.037]	-0.008 [0.034]	0.006 [0.047]	0.005 [0.038]	-0.011 [0.035]
young	-0.027 [0.066]	0.008 [0.057]	0.019 [0.051]	-0.020 [0.064]	0.007 [0.056]	0.013 [0.050]
fifty	-0.030 [0.058]	0.005 [0.051]	0.025 [0.058]	-0.029 [0.058]	0.005 [0.051]	0.023 [0.058]
elderly	0.036 [0.059]	0.032 [0.053]	-0.068 [0.045]	0.036 [0.059]	0.034 [0.054]	-0.069 [0.045]
No high school	0.248** [0.115]	-0.218*** [0.082]	-0.031 [0.093]	0.265** [0.116]	-0.222*** [0.082]	-0.043 [0.095]
High school	0.094* [0.051]	-0.128** [0.051]	0.034 [0.040]	0.081 [0.051]	-0.124** [0.052]	0.043 [0.040]
Low income	0.115** [0.054]	-0.133** [0.053]	0.018 [0.051]	-0.014 [0.084]	-0.107 [0.067]	0.121 [0.076]
Medium income	0.051 [0.057]	-0.060 [0.057]	0.009 [0.055]	-0.008 [0.092]	-0.040 [0.071]	0.048 [0.088]
Income no answer	-0.054 [0.064]	0.053 [0.066]	0.002 [0.055]	-0.104 [0.107]	0.047 [0.096]	0.057 [0.090]
Service worker	0.012 [0.062]	0.010 [0.065]	-0.023 [0.041]	-0.080 [0.085]	0.029 [0.080]	0.052 [0.055]
Blue collar	0.075 [0.073]	-0.159** [0.069]	0.083* [0.045]	0.104 [0.073]	-0.165** [0.071]	0.061 [0.049]
Low income Service W				0.284** [0.116]	-0.057 [0.108]	-0.227** [0.087]
Med income Service W				0.111 [0.113]	-0.039 [0.104]	-0.073 [0.099]
No Answer Service W				0.083 [0.146]	0.019 [0.134]	-0.102 [0.123]
Full time worker	-0.125** [0.056]	0.027 [0.056]	0.098** [0.046]	-0.125** [0.055]	0.026 [0.056]	0.099** [0.046]
Part time worker	0.100 [0.074]	-0.088 [0.067]	-0.012 [0.054]	0.100 [0.074]	-0.089 [0.067]	-0.011 [0.054]
Good health	-0.005 [0.048]	0.047 [0.042]	-0.042 [0.038]	0.002 [0.049]	0.045 [0.043]	-0.047 [0.038]
Low density area	0.074 [0.054]	-0.094** [0.047]	0.019 [0.049]	0.078 [0.053]	-0.095** [0.047]	0.017 [0.049]
Middle density area	0.074 [0.047]	-0.041 [0.046]	-0.033 [0.046]	0.082* [0.047]	-0.042 [0.046]	-0.040 [0.045]
Constant	0.344*** [0.085]	0.522*** [0.077]	0.134 [0.082]	0.375*** [0.099]	0.516*** [0.079]	0.109 [0.094]
Observations	535	535	535	535	535	535
R-squared	0.112	0.141	0.054	0.123	0.141	0.066
Region FE	YES	YES	YES	YES	YES	YES

Table 3: Labor Market after 6-week of Lockdown

VARIABLES	(1)	(2)	(3)	(4)	(5)	(6)
	Stopped Working	Work from Home	Work Outside	Stopped Working	Work from Home	Work Outside
female	0.069 [0.046]	0.010 [0.053]	-0.079 [0.051]	0.069 [0.046]	0.011 [0.054]	-0.080 [0.049]
young	0.071 [0.063]	0.012 [0.060]	-0.083 [0.054]	0.087 [0.061]	0.006 [0.061]	-0.093* [0.054]
fifty	-0.099 [0.078]	0.029 [0.060]	0.069 [0.078]	-0.078 [0.078]	0.017 [0.063]	0.060 [0.079]
elderly	-0.090 [0.073]	0.057 [0.068]	0.034 [0.067]	-0.080 [0.072]	0.053 [0.068]	0.027 [0.069]
No high school	0.289*** [0.089]	-0.343*** [0.064]	0.054 [0.092]	0.277*** [0.097]	-0.331*** [0.066]	0.054 [0.092]
High school	0.165*** [0.050]	-0.167*** [0.054]	0.002 [0.052]	0.153*** [0.050]	-0.160*** [0.054]	0.008 [0.049]
Low income	0.024 [0.065]	-0.045 [0.052]	0.021 [0.059]	-0.167* [0.094]	0.014 [0.066]	0.153 [0.094]
Medium income	0.081 [0.063]	-0.097 [0.058]	0.016 [0.063]	0.106 [0.097]	-0.132* [0.079]	0.026 [0.097]
Income no answer	0.126** [0.059]	-0.035 [0.070]	-0.091 [0.067]	0.013 [0.087]	0.079 [0.079]	-0.092 [0.085]
Service worker	0.018 [0.056]	-0.048 [0.076]	0.030 [0.056]	-0.060 [0.069]	-0.020 [0.094]	0.080 [0.077]
Blue collar	0.165** [0.073]	-0.333*** [0.083]	0.167*** [0.063]	0.228*** [0.076]	-0.358*** [0.081]	0.130** [0.063]
Low income Service W				0.435*** [0.113]	-0.130 [0.103]	-0.305*** [0.114]
Med income Service W				-0.040 [0.106]	0.066 [0.130]	-0.025 [0.124]
No Answer Service W				0.216 [0.140]	-0.224 [0.149]	0.008 [0.131]
Full time worker	0.031 [0.060]	-0.071 [0.070]	0.040 [0.056]	0.023 [0.059]	-0.071 [0.070]	0.048 [0.056]
Part time worker	0.112 [0.085]	-0.152** [0.072]	0.040 [0.080]	0.120 [0.087]	-0.162** [0.074]	0.042 [0.078]
Good health	-0.034 [0.052]	0.005 [0.045]	0.029 [0.052]	-0.026 [0.050]	0.006 [0.047]	0.020 [0.051]
Low density area	0.024 [0.056]	0.030 [0.058]	-0.054 [0.054]	0.008 [0.052]	0.036 [0.055]	-0.043 [0.055]
Middle density area	0.035 [0.046]	-0.023 [0.042]	-0.012 [0.047]	0.029 [0.045]	-0.025 [0.040]	-0.005 [0.048]
Constant	0.070 [0.093]	0.747*** [0.093]	0.183* [0.097]	0.092 [0.097]	0.737*** [0.093]	0.172* [0.099]
Observations	411	411	411	411	411	411
R-squared	0.150	0.243	0.103	0.186	0.252	0.122
Region FE	YES	YES	YES	YES	YES	YES

Table 4: Current (March) & Future Income Reductions

VARIABLES	(1) Income Drop	(2) Income Drop	(3) Income Drop	(4) Future Income Drop	(5) Future Income Drop	(6) Future Income Drop
Female	-0.001 [0.032]	0.069 [0.051]	0.069 [0.052]	-0.012 [0.032]	-0.012 [0.050]	-0.011 [0.050]
Young	-0.017 [0.038]	0.010 [0.055]	0.012 [0.054]	-0.096** [0.040]	-0.102 [0.062]	-0.102 [0.062]
Fifty	-0.024 [0.051]	-0.006 [0.070]	-0.003 [0.070]	0.016 [0.049]	-0.086 [0.077]	-0.086 [0.079]
Elderly	-0.181*** [0.044]	-0.055 [0.069]	-0.053 [0.069]	-0.136*** [0.044]	-0.116 [0.073]	-0.116 [0.074]
No high school	-0.059 [0.052]	0.127 [0.099]	0.120 [0.097]	0.017 [0.055]	0.184* [0.106]	0.191* [0.107]
High school	0.028 [0.037]	0.067 [0.057]	0.064 [0.058]	0.008 [0.034]	0.032 [0.044]	0.036 [0.045]
Low income	0.151*** [0.036]	0.112* [0.059]	0.087 [0.092]	0.125*** [0.040]	0.101* [0.060]	0.114 [0.092]
Medium income	0.049 [0.042]	0.035 [0.054]	0.030 [0.089]	-0.002 [0.034]	0.001 [0.049]	0.026 [0.084]
Income no answer	0.082* [0.046]	-0.058 [0.078]	-0.112 [0.117]	0.052 [0.044]	0.079 [0.073]	0.135 [0.128]
Service worker	0.117** [0.058]	0.094 [0.069]	0.071 [0.087]	0.022 [0.065]	-0.010 [0.073]	0.020 [0.100]
Blue collar	0.204*** [0.074]	0.149* [0.084]	0.158* [0.081]	0.072 [0.082]	-0.002 [0.083]	-0.006 [0.080]
White collar	0.069 [0.066]			0.043 [0.062]		
Low income Service W			0.054 [0.130]			-0.026 [0.132]
Med income Service W			0.010 [0.133]			-0.051 [0.122]
No Answer Service W			0.109 [0.162]			-0.112 [0.165]
Full time worker	-0.193*** [0.055]	-0.297*** [0.067]	-0.296*** [0.068]	-0.171*** [0.056]	-0.215*** [0.072]	-0.217*** [0.072]
Part time worker	0.034 [0.072]	-0.120 [0.086]	-0.116 [0.088]	0.019 [0.072]	-0.029 [0.100]	-0.033 [0.101]
Good health	-0.003 [0.030]	0.039 [0.058]	0.039 [0.059]	-0.058* [0.030]	-0.034 [0.055]	-0.034 [0.056]
Low density area	0.001 [0.041]	-0.058 [0.072]	-0.059 [0.073]	-0.050 [0.038]	-0.100 [0.068]	-0.102 [0.069]
Middle density area	-0.041 [0.031]	-0.112** [0.047]	-0.110** [0.047]	-0.033 [0.029]	-0.078 [0.051]	-0.082 [0.051]
Constant	0.335*** [0.062]	0.392*** [0.085]	0.402*** [0.090]	0.437*** [0.066]	0.513*** [0.110]	0.499*** [0.118]
Observations	997	411	411	997	411	411
R-squared	0.096	0.140	0.141	0.070	0.107	0.109
Region FE	YES	YES	YES	YES	YES	YES

Table 5: Individual Perceptions after 3-week of Lockdown

	(1)	(2)	(3)	(4)
	Agree with		Satisfaction with	
VARIABLES	Closed Business	Closed Activity	Prime Minister	Government
Female	0.136*** [0.036]	0.108*** [0.030]	0.047 [0.035]	0.048 [0.036]
Young	0.036 [0.044]	-0.003 [0.046]	-0.002 [0.047]	0.038 [0.039]
Fifty	-0.024 [0.052]	-0.032 [0.045]	-0.081 [0.052]	-0.053 [0.053]
Elderly	-0.012 [0.041]	-0.022 [0.038]	-0.023 [0.047]	-0.039 [0.037]
No high school	0.072 [0.070]	0.072 [0.069]	-0.129** [0.057]	-0.140* [0.072]
High school	0.077* [0.039]	0.025 [0.033]	-0.074** [0.037]	-0.068* [0.041]
Low income	-0.101** [0.044]	-0.088** [0.039]	-0.068* [0.038]	-0.032 [0.037]
Medium income	-0.051 [0.045]	-0.051 [0.045]	-0.013 [0.039]	0.008 [0.043]
Income no answer	0.048 [0.055]	-0.015 [0.041]	-0.076 [0.053]	-0.089* [0.053]
Service worker	-0.143** [0.063]	-0.182*** [0.057]	0.046 [0.058]	-0.047 [0.061]
Blue collar	-0.165** [0.064]	-0.240*** [0.059]	-0.034 [0.068]	-0.076 [0.062]
White collar	-0.036 [0.069]	-0.087 [0.071]	-0.065 [0.078]	-0.078 [0.057]
Full time worker	0.063 [0.068]	0.077 [0.067]	-0.006 [0.048]	0.032 [0.053]
Part time worker	0.088 [0.065]	0.118* [0.061]	-0.032 [0.060]	0.030 [0.068]
Good health	0.036 [0.029]	0.059* [0.034]	-0.010 [0.032]	0.031 [0.030]
Low density area	0.058 [0.046]	0.073* [0.039]	0.049 [0.036]	0.018 [0.038]
Middle density area	0.045 [0.044]	0.042 [0.040]	0.060* [0.031]	0.065** [0.030]
Left Ideology	0.033 [0.050]	-0.018 [0.048]	0.335*** [0.052]	0.257*** [0.058]
Center Ideology	-0.048 [0.043]	-0.065 [0.044]	0.169*** [0.038]	0.106** [0.049]
Right Ideology	-0.014 [0.053]	-0.072 [0.052]	-0.057 [0.050]	-0.185*** [0.056]
Constant	0.541*** [0.087]	0.652*** [0.069]	0.381*** [0.083]	0.565*** [0.094]
Observations	1,000	1,000	1,000	1,000
R-squared	0.059	0.052	0.139	0.159
Region FE	YES	YES	YES	YES

Table 6: Individual Perceptions after 6-week of Lockdown

	(1)	(2)	(3)	(4)
	Agree with		Satisfaction with	
VARIABLES	Closed Business	Closed Activity	Prime Minister	Government
Female	0.091** [0.038]	0.085*** [0.032]	0.040 [0.030]	0.063* [0.033]
Young	0.003 [0.056]	-0.015 [0.053]	0.046 [0.040]	0.043 [0.039]
Fifty	-0.020 [0.055]	0.005 [0.063]	-0.055 [0.045]	-0.013 [0.039]
Elderly	-0.029 [0.045]	-0.101** [0.047]	0.010 [0.043]	-0.007 [0.037]
No high school	0.005 [0.057]	-0.015 [0.070]	-0.169*** [0.050]	-0.166*** [0.056]
High school	0.001 [0.040]	0.011 [0.036]	-0.091** [0.035]	-0.100*** [0.034]
Low income	-0.008 [0.055]	-0.024 [0.051]	-0.009 [0.042]	0.015 [0.038]
Medium income	-0.047 [0.045]	-0.055 [0.044]	-0.041 [0.044]	0.001 [0.039]
Income no answer	0.006 [0.066]	-0.006 [0.058]	-0.041 [0.050]	-0.018 [0.044]
Service worker	-0.177*** [0.056]	-0.170*** [0.060]	0.093* [0.048]	0.066 [0.058]
Blue collar	-0.101 [0.071]	-0.070 [0.068]	0.049 [0.053]	-0.041 [0.055]
White collar	-0.117* [0.066]	-0.155** [0.071]	-0.020 [0.060]	-0.040 [0.067]
Full time worker	0.102* [0.053]	0.108* [0.060]	-0.005 [0.045]	-0.007 [0.057]
Part time worker	0.080 [0.063]	0.118* [0.068]	0.043 [0.057]	-0.036 [0.062]
Good health	-0.027 [0.033]	-0.056* [0.032]	0.059** [0.030]	0.057** [0.028]
Low density area	-0.027 [0.046]	-0.026 [0.040]	0.011 [0.036]	0.029 [0.041]
Middle density area	-0.010 [0.036]	-0.046 [0.037]	0.011 [0.032]	-0.001 [0.028]
Left Ideology	-0.000 [0.062]	0.070 [0.054]	0.385*** [0.056]	0.251*** [0.055]
Center Ideology	-0.105* [0.057]	-0.068 [0.055]	0.154*** [0.053]	0.066 [0.055]
Right Ideology	-0.119* [0.065]	-0.066 [0.059]	-0.019 [0.049]	-0.188*** [0.057]
Constant	0.595*** [0.099]	0.641*** [0.089]	0.213*** [0.076]	0.454*** [0.087]
Observations	997	997	997	997
R-squared	0.039	0.050	0.178	0.174
Region FE	YES	YES	YES	YES

Table 7: Psychological Costs after 6-week of Lockdown

VARIABLES	Exclusion Index	Distress Index	Lockdown Duration
Female	0.019	0.098***	-0.150
	[0.022]	[0.021]	[0.317]
Young	0.051	0.075**	-0.566
	[0.035]	[0.034]	[0.373]
Fifty	0.016	-0.015	-0.252
	[0.042]	[0.041]	[0.444]
Elderly	-0.011	-0.077***	0.425
	[0.027]	[0.028]	[0.424]
No high school	0.030	-0.050	-0.069
	[0.044]	[0.034]	[0.505]
High school	0.025	-0.013	0.030
	[0.028]	[0.023]	[0.343]
No open space	0.036	0.044**	0.159
	[0.025]	[0.022]	[0.316]
Homeowner	0.008	-0.028	0.091
	[0.032]	[0.024]	[0.372]
Room per people	-0.021**	-0.024***	-0.248**
	[0.010]	[0.009]	[0.106]
Single	0.064	0.051	-0.462
	[0.039]	[0.035]	[0.554]
With family	-0.074**	-0.042*	0.230
	[0.029]	[0.025]	[0.432]
Low income	0.059*	0.056**	0.746*
	[0.034]	[0.027]	[0.448]
Medium income	0.019	0.040	-0.132
	[0.039]	[0.029]	[0.482]
Income no answer	0.008	-0.010	0.373
	[0.040]	[0.028]	[0.479]
Service worker	-0.037	-0.032	-0.817*
	[0.046]	[0.037]	[0.468]
Blue collar	-0.072	-0.021	-0.171
	[0.053]	[0.037]	[0.503]
White collar	0.046	0.054	0.312
	[0.053]	[0.051]	[0.582]
Full time worker	0.076	0.053	0.178
	[0.047]	[0.036]	[0.384]
Part time worker	0.078	0.090**	0.815
	[0.055]	[0.041]	[0.493]
Good health	-0.046	-0.133***	-0.991***
	[0.029]	[0.022]	[0.303]
Low density area	-0.010	-0.059*	-0.309
	[0.034]	[0.033]	[0.422]
Medium density area	0.010	-0.020	-0.410
	[0.027]	[0.026]	[0.351]
Constant	0.286***	0.525***	6.765***
	[0.051]	[0.055]	[0.611]
Observations	997	997	997
R-squared	0.055	0.143	0.057
Region FE	YES	YES	YES